

# **The Golem tokamak for Fusion Education**

**The smallest and oldest tokamak with the biggest control room in the world**

A Final Report to the FUSENET WP7

”An Improvement of An Existing Teaching Hardware.”

version 3.00 (September 2013 status)

Vojtěch Svoboda<sup>1</sup>, Jana Brotánková<sup>1</sup>, Gergo Pokol<sup>2</sup>, Laszlo Horvath<sup>2</sup>, Csaba Buday<sup>2</sup>, Dániel Imre Réfy<sup>2</sup>, Attila Bencze<sup>5</sup>, Jan Stöckel<sup>3</sup>, Ondřej Grover<sup>1</sup>, Michal Odstrčil<sup>1</sup>, Tomáš Odstrčil<sup>1</sup>, Ondřej Pluhař<sup>4</sup>, Jiri Zara<sup>4</sup>, and Gabriel Vondrášek<sup>1</sup>

<sup>1</sup>Faculty of Nuclear Sciences and Physical Engineering, Czech Technical University, Prague, Czech Republic

<sup>2</sup>Budapest University of Technology and Economics, Hungary

<sup>3</sup>Faculty of Electrical Engineering, Czech Technical University, Prague, Czech Republic

<sup>4</sup>Institute of Plasma Physics, Czech Academy of Sciences, Prague, Czech Republic

<sup>5</sup>Wigner Research Center for Physics, Hungarian Academy of Sciences, Hungary





# Contents

<b>1</b>	<b>Introduction</b>	<b>5</b>
<b>2</b>	<b>Proposal</b>	<b>7</b>
<b>3</b>	<b>Report</b>	<b>9</b>
3.1	Virtual Model of the Tokamak and Infrastructure rooms . . . . .	9
3.2	Virtual Control Room (blue banner) . . . . .	9
3.3	Real Remote Control Room (red banner) . . . . .	9
3.3.1	Remote Control . . . . .	11
3.3.2	Remote Data Access . . . . .	11
3.3.3	Methods of Data Evaluation . . . . .	14
3.4	Experiment Menu . . . . .	15
3.4.1	Basic Measurements . . . . .	15
3.4.2	Magnetic Measurements . . . . .	19
3.4.3	Probe Measurements . . . . .	23
3.4.4	Tomographic reconstruction . . . . .	25
3.4.5	Plasma MHD Activity Observations via Magnetic Diagnostics . . . . .	25
3.4.6	Other possible exercises . . . . .	31
3.5	Golem wiki (documentation repository) . . . . .	32
<b>4</b>	<b>Education Events and Presentations</b>	<b>33</b>
4.1	2009 . . . . .	33
4.2	2010 . . . . .	33
4.3	2011 . . . . .	34
4.4	2012 . . . . .	34
4.5	2013 . . . . .	36
4.6	GOMTRAIC 2013 (Flagship of the project) . . . . .	37
4.6.1	Proposal . . . . .	37
4.6.2	Concept . . . . .	38
4.6.3	Participants . . . . .	39
4.6.4	Production and supervision . . . . .	40
4.6.5	Schedule . . . . .	40
4.6.6	Quotes . . . . .	40
4.6.7	Conclusions (lessons learned) . . . . .	42
4.7	Czech students from CTU Prague involved in the project . . . . .	43
4.8	Presentations with educational accent . . . . .	43
4.9	First remote experiments and lessons learned . . . . .	44
4.10	Event Outlook 2013/2014 . . . . .	50
<b>A</b>	<b>Photo Gallery</b>	<b>51</b>
A.1	SUMTRAICs . . . . .	51
A.2	GOMTRAIC 2013 . . . . .	53
A.3	Other . . . . .	55

<b>B</b>	<b>Press coverage</b>	<b>59</b>
B.1	12/10 Launch of the world's first global tokamak experiment. ITER news . . . . .	60
B.2	03/12 Students command 100 plasma pulses, remotely. ITER news . . . . .	61
B.3	05/12 A global fusion experiment, EFDA website, picture of the week . . . . .	62
B.4	06/12 The tokamak experiment near you, EFDA newsletters . . . . .	63
B.5	07/13 Tokamak Golem in Prague remotely operated during the lecture Introduction to Plasma Physics. Ruhr-Universität Bochum News . . . . .	64
<b>C</b>	<b>An example of instruction material and student's report (BME Budapest University, Hungary 14.1.2010)</b>	<b>67</b>
<b>D</b>	<b>GOMTRAIC 2013 reports</b>	<b>77</b>
	MHD group . . . . .	77
	Rake probe group . . . . .	86
	Tomography group . . . . .	89
	HXR group . . . . .	92
<b>E</b>	<b>Slide repository for oral presentations</b>	<b>95</b>
	The GOLEM tour . . . . .	95
	The GOLEM experimental setup . . . . .	102
	The GOLEM diagnostics . . . . .	105
	The GOLEM data access . . . . .	109
	The GOLEM physical quantities . . . . .	113
	The MHD activity . . . . .	115
<b>F</b>	<b>Acknowledgement</b>	<b>121</b>

# Chapter 1

## Introduction

GOLEM is a limiter tokamak with circular poloidal cross-section and with an iron transformer core. It has 18 diagnostic ports and it is equipped with basic controls and diagnostics. Main parameters are as follows:

- Major radius  $R = 0.4$  m
- Minor radius (vacuum vessel)  $r = 0.1$  m
- Plasma radius (limiter radius)  $a = 0.085$  m
- Toroidal magnetic field  $B_t < 0.6$  T
- Plasma current  $I_p < 8$  kA
- Length of the discharge  $< 20$  ms
- Central electron temperature  $T_e < 100$  eV
- Liner material: Bellows Stainless Steel
- Diagnostic Ports: 6x3

It is a device with full remote control capability and being operated mainly for an educational purpose.

The experiment is composed from the following principal parts (see Fig. 1.2):

- Circuit for generation of a toroidal magnetic field consisting of a capacitor bank ( $C_B = 24.3$  mF) charged up to  $U_{C_B} = 2$  kV, which is triggered by PC controlled thyristor into a set of 28 magnetic field coils to generate a toroidal magnetic field up to  $B_t \approx 0.8$  T.
- Circuit for generation of a toroidal electric field is composed of two capacitor banks. The first one is used for breakdown of the working gas ( $C_{BD} = 2.7$  mF,  $U_{C_{BD}} = 400$  V). The second bank is used for ohmic current drive and heating ( $C_{CD} = 10.8$  mF,  $U_{C_{CD}} = 400$  V). Both banks are triggered by PC controlled thyristors into two primary windings of the transformer. The time delay with respect to the magnetic field ( $\tau_{BD}$  and  $\tau_{CD}$ ) can be independently selected. The commutation switch can change the mutual orientation of the toroidal magnetic field and plasma current. Additional inductance ( $L = 5.9$  mH) can be included in the “CD” circuit to modify the plasma current ramp-up.
- Circuit for generation of an equilibrium magnetic field, consisting of a set of capacitors charged up to  $U_{C_B} = 1$  kV, which is triggered by a PC controlled thyristor into a dynamic stabilization coil with time delayed pulse with respect to a magnetic field generation  $\tau_{DS}$ .
- Pre-ionization of the working gas is performed by an electron gun.
- Vacuum system, which allows reaching the background pressure  $\approx 0.5$  mPa.
- Gas handling system (again computer controlled) to control the pressure of the working gas (hydrogen) in the vessel in the range of  $p_{H_2} \approx 10 - 200$  mPa.
- System for baking of the tokamak vessel and for glow discharge cleaning.

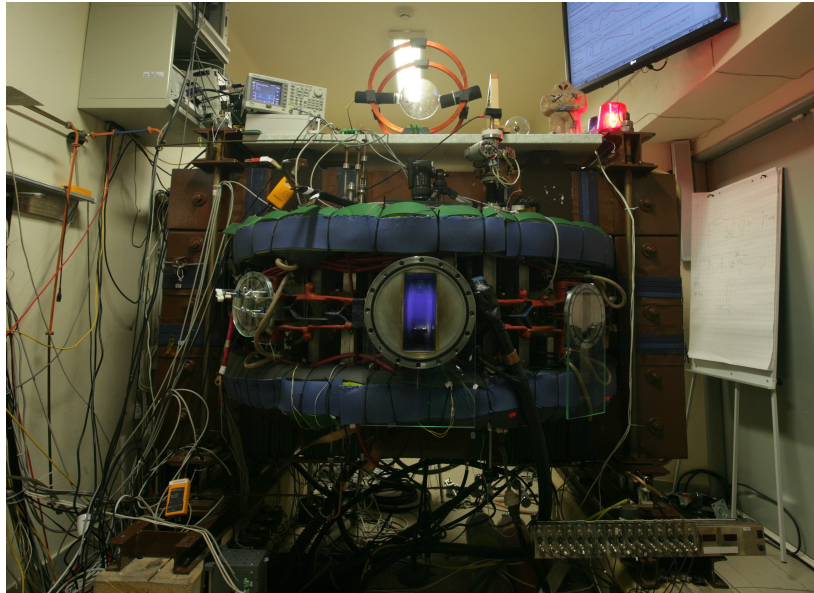


Figure 1.1: Tokamak GOLEM "in action"

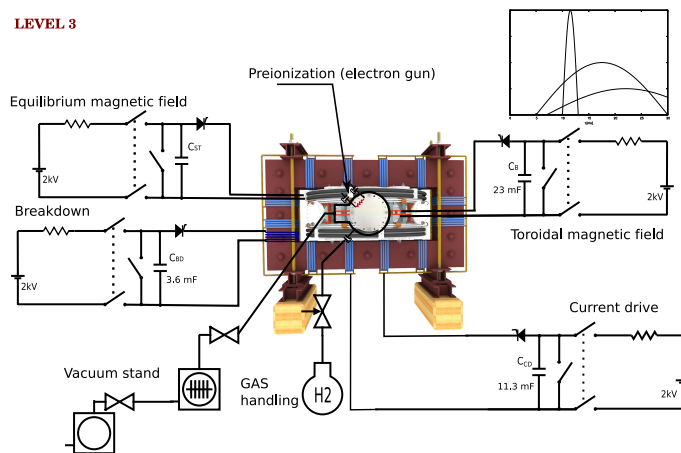


Figure 1.2: Engineering setup of the experiment.

# Chapter 2

# Proposal

## Goals of the practicum

- Learn basic principles of tokamak operation.
- Learn basic instrumentation related to tokamak operation and diagnostics.
- Provide hands-on experience at an integrated tokamak facility, including planning, tokamak control, data acquisition and processing, finalization and presentation of experimental results.
- Provide experience in areas of modern data processing methods, commonly used in today's fusion plasma experiments, in real-life situations.
- Perform several well defined physics experiments addressing basic plasma phenomena occurring in high temperature tokamak plasmas.

## Level of the practicum: M.Sc., Ph.D.

## Description of the practicum

GOLEM (<http://golem.fjfi.cvut.cz>) is a small tokamak with a circular poloidal cross-section. Presently it is equipped with 4 basic diagnostics: measurement of loop voltage, plasma current, toroidal magnetic field and plasma radiation in the visible part of the spectrum. Students can measure basic tokamak plasma characteristics on their own. Optional remote control via Internet is available.

## Training programmes

Methodical material and manuals covering specific fields of tokamak physics, technology and operation have been created providing the necessary basic tokamak-operator training and include a wide range of tasks with increasing levels of complexity, e.g.:

- Determination of vacuum chamber parameters: chamber resistivity  $R_{ch}$  and inductance  $L_{ch}$ , that can be deduced from “vacuum shots”.
- Basic plasma analysis based on raw data from acquisition systems: loop voltage  $U_{loop}$ , time derivative of magnetic field  $\frac{dB_t}{dt}$ , time derivative of both the chamber and plasma current  $\frac{dI_{pl+ch}}{dt}$ , determining plasma time length  $\Delta T_{pl}$ , magnetic field  $B_t$  and plasma current  $I_{pl}$ .
- Evaluation of basic plasma parameters: central electron temperature  $T_e$ , edge safety factor  $q_e$  and plasma heating power  $P_{OH}$ .
- Various types of plasma breakdown studies can be performed:
  1. w/o preionization jet
  2. effect of parallel or antiparallel orientation of the toroidal magnetic field  $B_t$  with respect to the toroidal electric field  $E_t$

3. effect of short ( $\approx 3$  ms) breakdown  $E_{BD}$  pulse on plasma formation
  4. optimization of plasma formation through  $\tau_{BD}$  (breakdown) and  $\tau_{CD}$  (current drive) trigger delays
  5. effect of working gas pressure  $p_{H_2}$  (Paschen's law)
- Plasma position studies with the help of a set of Mirnov coils and a linear set of 20 AXUV bolometers.
  - Plasma position stabilisation with an equilibrium magnetic field generated in the vertical magnetic field coils.

Besides the tokamak plasma, studies of low temperature plasma of the glow discharge are possible. These can be created using  $H_2$  or  $He$  gas in the tokamak chamber.

Advanced mode with the help of the X11 protocol offers the possibility to fully control all the technological aspects of tokamak operation (under appropriate supervision and within pre-programmed specific limits):

- Vacuum management: independent control of all the vacuum valves, rotary and turbomolecular pumps from the “cold” start to the end of the day.
- Gas fuelling management: setting up working gas pressure in an arbitrary manner.
- Chamber conditioning: cleaning the vessel with the help of baking and glow discharge.
- Full control of tokamak energetics: opportunity to control and generate the electric and magnetic fields separately and thus investigate the behaviour of particular diagnostics within specific conditions.
- Data processing management modification: for alternative data processing and presentation.

## Target audience

The practicum is designed for groups of up to 10 students which can participate in in-situ or remote online/offline mode. Many of the students come from the Czech Republic, however, the facility has already several years of experience with Summer school students and special one-time visits. Remote worldwide participation is possible for foreign students. Communication between remote participants and the device is performed after logging into a system, under supervision of an in-situ technician and within pre-described limits, via the following methods:

- WWW interface based on HTTP protocol, see figure 3.4.
- Basic online command line method using the SSH protocol, platform independent (openSSH on Linux or Putty on Windows).
- Command line method allows instruction looping.
- It is also possible to create a batch script with a set of a shot instructions for offline processing.

## Future plans

Further upgrade of GOLEM is envisioned in the near future - an increase of  $B_t$ ,  $I_p$  and the discharge duration. Plasma position stabilization is under consideration and investigation. Basic diagnostics will be supplemented with plasma density measurement (microwave interferometer),  $H_\alpha$  and X-ray radiation measurement will be installed in the near future. The investigation of plasma edge physics with the help of various probe measurements is planned. The previous version of the GOLEM tokamak, the CASTOR was internationally renowned in this field and the team running the present version can use this long and extensive experience for new setups and experiments.

Besides this programme there exists a plan to enhance especially the diagnostic system with a compact mass spectrometer, fast camera and other additional diagnostic techniques. Moreover, a new capacitor bank is planned to greatly prolong the plasma duration. These plans are not currently covered by any application.

# Chapter 3

## Report

### 3.1 Virtual Model of the Tokamak and Infrastructure rooms

In order to present the GOLEM tokamak via the Internet to distant users, an interactive 3D virtual model has been created. It consists of several parts assembled together - the tokamak itself, power supply infrastructure, rooms and access paths. In addition to objects representing real environment, various virtual objects have been added to ease interaction/control and to provide extended information via textual legend and animations. The virtual model offers several ways to

- visit all rooms and corridors around the tokamak (Fig. 3.1 upper left). A user can freely walk through the environment (controlling movement using a mouse) or can navigate along four pre-computed animated walk-throughs. This helps students to get familiar with the overall spatial layout and to imagine dimensions of the real equipment.
- study components of the tokamak by clicking on various virtual parts. A selected part is then activated and presented to a visitor in various ways including simple animation, highlighting related components, showing short text annotation in free virtual space, opening web pages with detailed description, and possibly playing an audio clip. To make access to inner parts easier, arbitrary components can be turned invisible via a virtual control panel (Fig. 3.1 bottom left ) called HUD (Head-Up Display).
- visualize processes inside the tokamak. A user is properly scaled-down and teleported into the chamber having a possibility to see and “feel” an animated magnetic field (Fig.3.1 bottom right). This unusual way of interior presentation makes a novel and unforgettable experience for students.
- control selected processes of the real tokamak via a web browser. This functionality is currently very limited due to security reasons and the final decision has not been made yet. The virtual model can be utilized in several ways - to simulate reactions to user’s requests only (without any connection to real tokamak), to visualize real state and operation of the GOLEM tokamak (read-only mode), and to allow direct control of the GOLEM tokamak through interaction with its virtual model (read-write mode).

### 3.2 Virtual Control Room (blue banner)

Students have the opportunity to learn the basics of operating the GOLEM tokamak in advance through the virtual interface (see Fig. 3.2) where they can set up the parameters in the same way as in the real operation (see Fig. 3.4). The only difference is that virtual operation is inspired and results are generated from the real discharge database of the previous GOLEM tokamak operation (a discharge from the database is selected to have setup parameters as close as possible to the parameters chosen by the student).

### 3.3 Real Remote Control Room (red banner)

Since the GOLEM tokamak is an educational device, it is necessary to uncover the complexity of the experiment “step by step”. This is demonstrated in the Fig. 3.3 where from left (the most simple setup to produce plasma) to



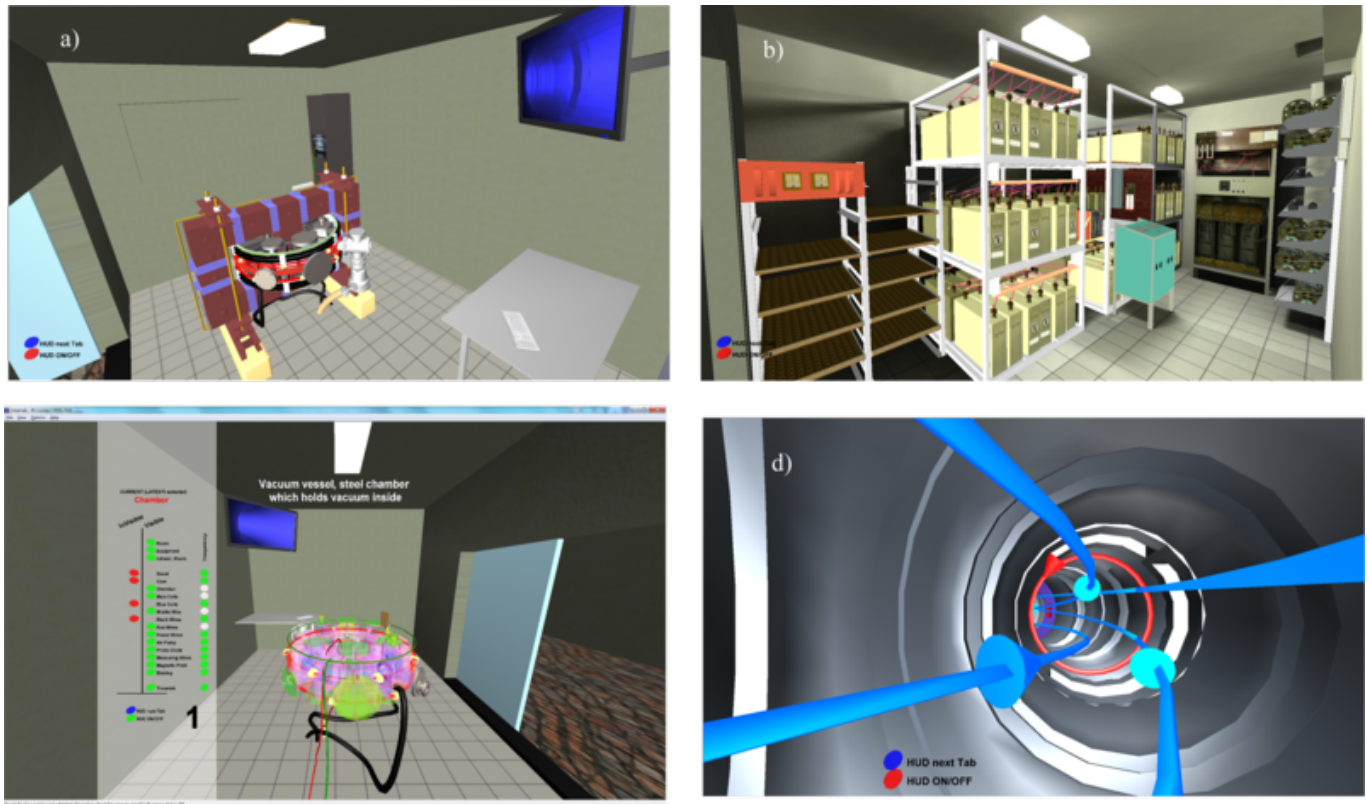


Figure 3.1: An overview of the virtual tokamak model

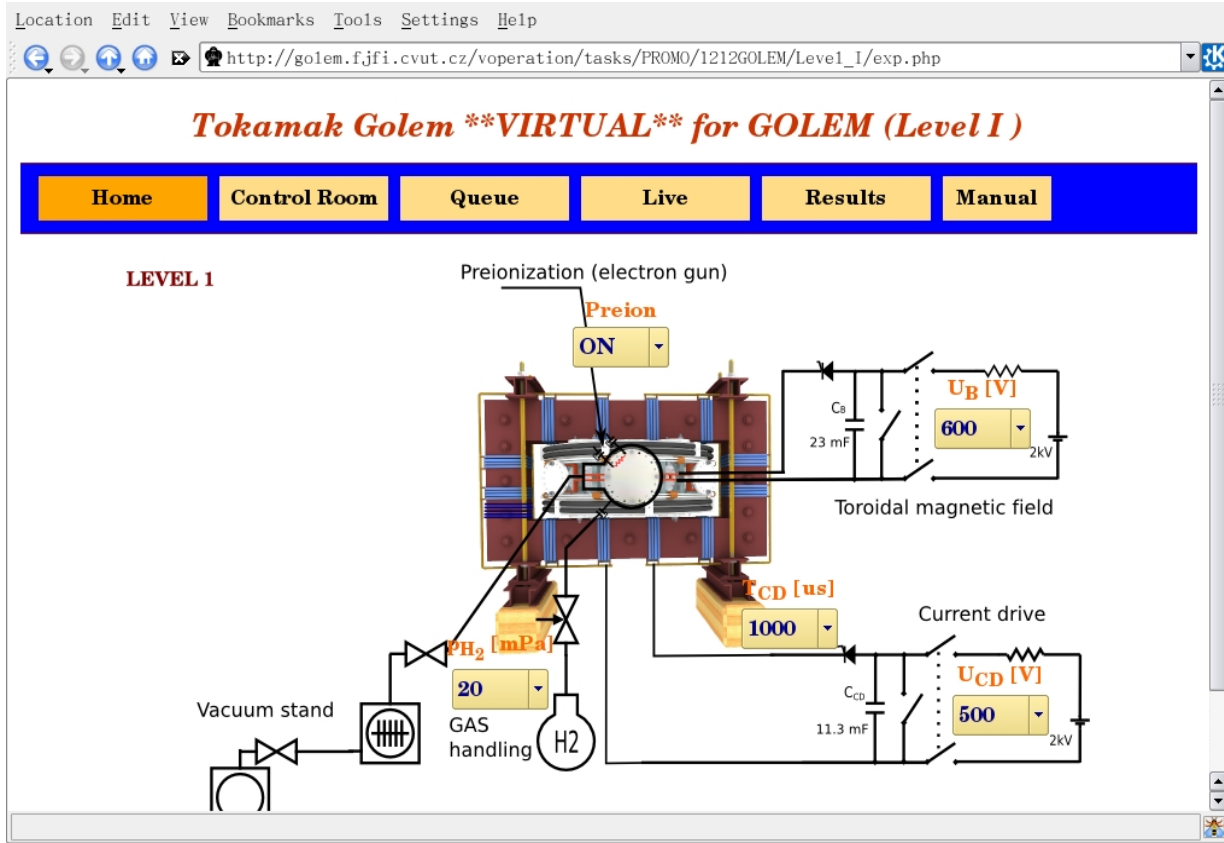


Figure 3.2: Virtual control room

right (the setup with breakdown and equilibrium fields) additional components are added to the system.

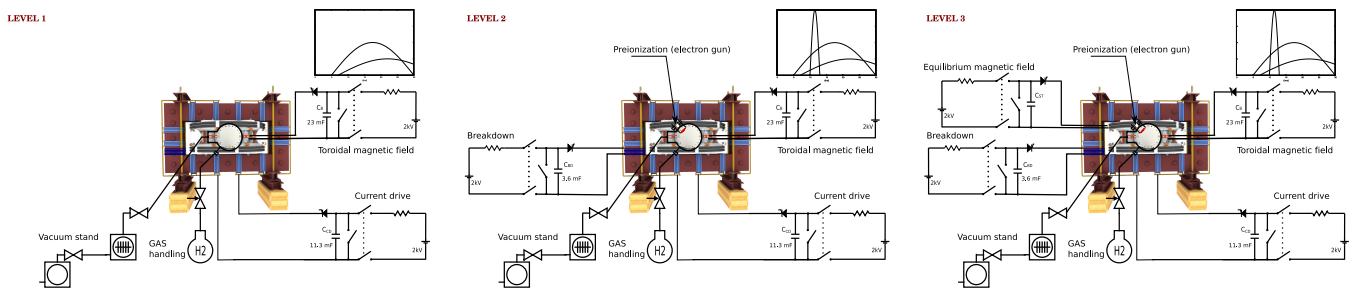


Figure 3.3: Experimental setup from level I to level III.

### 3.3.1 Remote Control

Measurements are to be set up and discharges (often referred to as “shots”) initiated using the web interface of GOLEM tokamak which can be seen on figure 3.4. The exact url address of it is provided by a tokamak operator at the beginning of a session.

### 3.3.2 Remote Data Access

All the recorded data and the parameters of each discharge are available via a shot homepage (see Fig. 3.5) at the GOLEM website. The root directory for the files is:

<http://golem.fjfi.cvut.cz/operation/shots/<shotnumber>/>

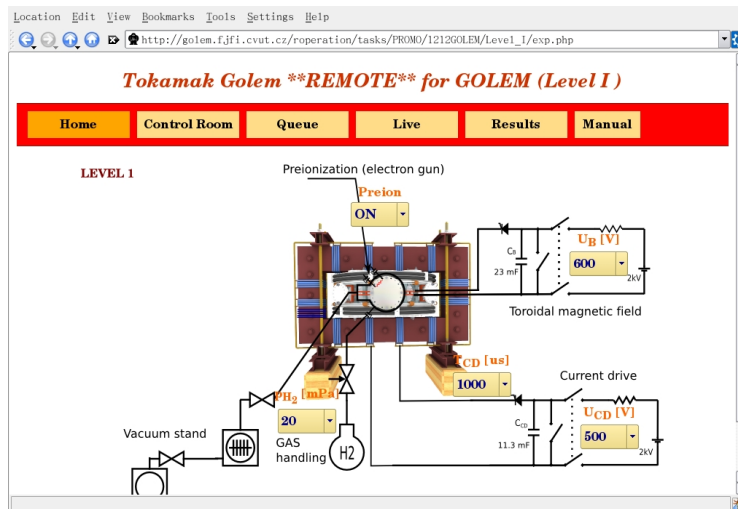


Figure 3.4: Remote control interface of the GOLEM tokamak - level I.

Basic data of the present shot series is collected at a page to be reached at:

<http://golem.fjfi.cvut.cz/operation/currentsession/>

### Accessing data (Matlab oriented)

In order to facilitate the procedure of data analysis, a MATLAB package is available for basic data processing (this package is also compatible with the OCTAVE freeware software). The task is to build a proper work flow using these building blocks. It should be noted that these routines do not cover the whole procedure, some additional programs are supposed to be written by the students. The routines are listed in the table below:

File name	Input parameters	Description
GOLEM_get_data.m	shot_nr	Loads raw data from database into the MATLAB workspace
GOLEM_plot_rawdata.m	shot_nr	Makes plots of the time varying raw data
GOLEM_offset_correction.m	raw_signal, time_vector, t1,t2	Makes offset correction for raw data
GOLEM_cut_data.m	raw_signal, time_vector, t1,t2	Crop the given signal
GOLEM_integrate.m	time_vec, signal	Integrates the given signal
GOLEM_chamber_current.m	time_vec, $I_t$ , $U_l$ , $R_{ch}$ , $L_{ch}$	Calculates chamber current integrating equation (3.1)
GOLEM_diff.m	$x$ , $y$	Calculates $dx/dy$

**GOLEM\_get\_data.m** The return value of GOLEM\_get\_data.m contains then a **rawdata** structure with the following elements:

- **nr:** shotnumber
- **timedata:** structure, contains vectors of time signals
  - **U.l:** loop voltage measurement raw signal vector in [V]
  - **dB.t:** toroidal filed coil raw signal vector in [V]
  - **dI.t:** Rogowski coil raw signal vector in [V]
  - **Photo:** photodiode raw signal vector in [V]
- **N:** number of data points

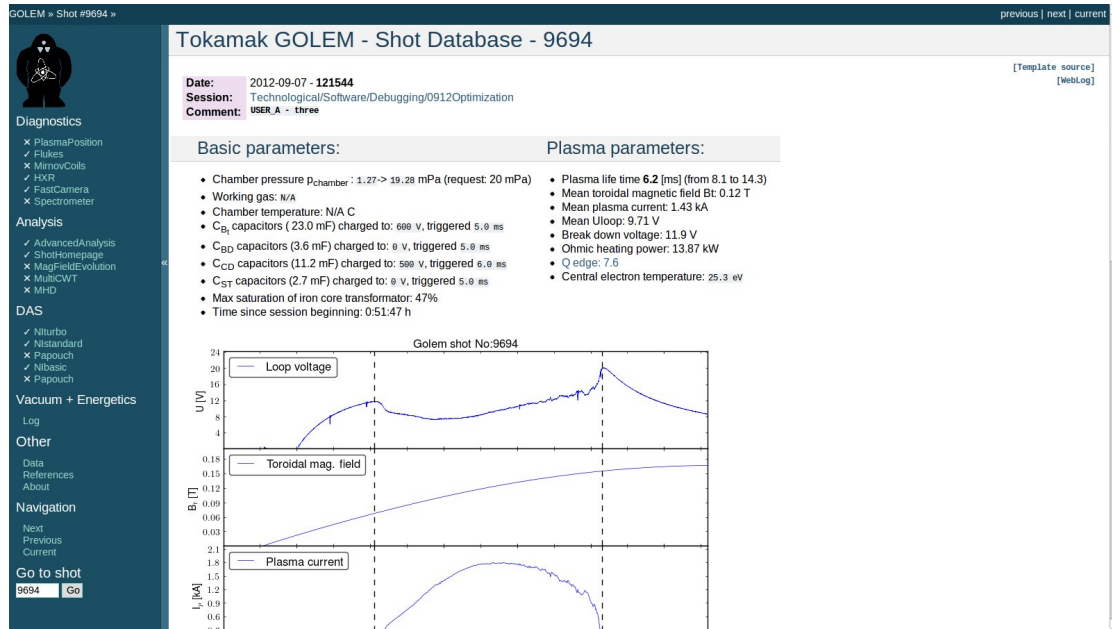


Figure 3.5: An example of a shot homepage.

- **samplerate:** samplerate of the measurements in [Hz]
- **pressure:** pressure of vacuum chamber in [mPa]
- **T\_ch:** temperature of the chamber in [K]
- **trigger:** time delay between starting diagnostics and toroidal magnetic field drive in [s]
- **time\_delay:** time delay between toroidal field and inductive current drive in [s]
- **Bt\_calibration:** calibration factor of toroidal magnetic field diagnostic in [T/Vs]
- **Rogowski\_calibration:** calibration factor of plasma current diagnostics in [A/Vs]
- **U\_loop\_calibration:** calibration factor of loop voltage diagnostic [V/V]

Elements of structures can be referenced as e.g. **rawdata.timedata.U<sub>l</sub>**. Measured signals are saved in the *timedata* structure, but these are raw signals needing further processing to produce the physical quantities measured! Signal processing steps are described in the next section.

### Accessing data (Python oriented)

Under construction, see section E (Documentation collection/Data access)

### Accessing data (Mathematica oriented)

Under construction, see section E (Documentation collection/Data access)

### Accessing data (IDL oriented)

Under construction, see section E (Documentation collection/Data access)

### 3.3.3 Methods of Data Evaluation

This section starts with a short description on how to reconstruct the measured plasma parameters from the raw signals returned by `GOLEM_get_data.m`. Measurement tasks are detailed in the later subsections.

The sampling rate of the time resolved measurements (`samplerate`), time delay between starting diagnostics and toroidal magnetic field drive (`trigger`) and time delay between toroidal field and inductive current drive (`time_delay`) are returned by `GOLEM_get_data.m`, and these are to be used whenever needed instead of the examples provide in this description.

The simplest signal to be reconstructed is the loop voltage ( $U_l$ ). The measurement loop of the loop voltage is connected to a voltage divider, therefore the signal must be multiplied by a calibration factor (`U_loop_calibration`) as plotted in Figure 3.6.

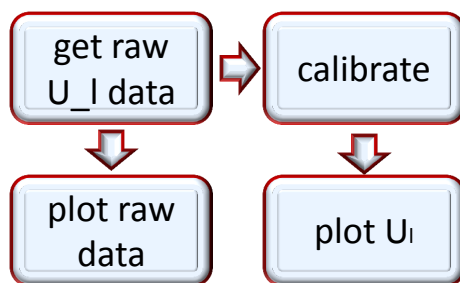


Figure 3.6: Block diagram showing the steps of data processing for loop voltage measurement.

The toroidal magnetic field ( $B_t$ ) and the total current ( $I_{tot}$ ) raw signals must be integrated before multiplying by calibration factors (`Bt_calibration` and `Rogowski_calibration`). The reason for this is that the voltage measured is induced in these diagnostic loops and coils by the changing of the toroidal and poloidal magnetic field respectively.

Integrated magnetic measurements are very sensitive to the DC bias of the measurement circuit, which needs to be corrected for. If the sampling rate is 1 MHz, and the shot starts at 5 ms, we have 5000 samples from the background noise. It is better to exclude a few samples around the swithing time point. This is important, because these samples measure the bias, and we can correct the integrated values with this factor.

Figure 3.7 shows the block diagram for the necessary steps of processing of the toroidal magnetic field signal. Routines for all the steps are ready, they should just be parametrized and linked.

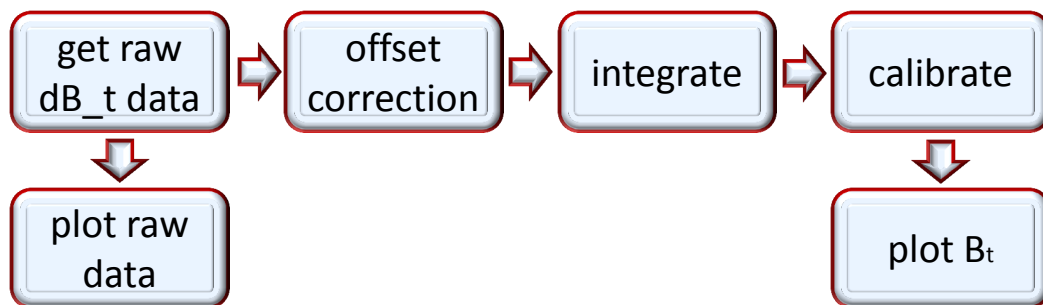


Figure 3.7: Block diagram showing the steps of data processing for toroidal magnetic field measurement.

The block diagram for the total current measured by the Rogowski coils is only slightly more complicated: Switching the toroidal magnetic field on causes an offset in the toroidal current measurement, which has to be corrected by subtracting the average value measured in the  $\tau_{OH}$  long interval before switching on the toroidal electrical field from the integrated current value.

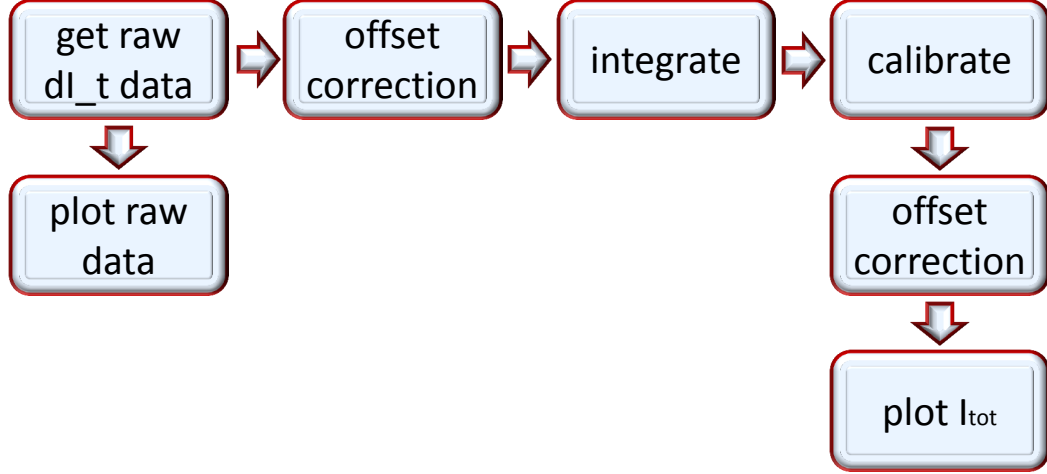


Figure 3.8: Block diagram showing the steps of data processing for total plasma current measurement.

## 3.4 Experiment Menu

### 3.4.1 Basic Measurements

#### Determination of vacuum chamber parameters

In GOLEM, part of the toroidal current always flows in the vacuum vessel, which has to be taken into account during the interpretation of experimental results. In a vacuum shot, when no plasma is formed, it is possible to determine the resistance of the vacuum vessel: all the current measured by the Rogowski-coil flows in the vessel. This is an important parameter for further evaluations.

Let us denote the loop voltage with  $U_l$ , the resistance of the chamber by  $R_{ch}$ , the total current (which is the chamber current ( $I_{ch}$ ) in this case) with  $I_{tot}$  and the inductance of the chamber by  $L_{ch}$ .

The circuit equation is then

$$U_l(t) = R_{ch} \cdot I_{tot}(t) + L_{ch} \frac{dI_{tot}}{dt}. \quad (3.1)$$

Using the loop voltage measurement and the Rogowski coil, we have both  $U_l$ ,  $I_{tot}$  and  $dI_{tot}/dt$  measured, so  $R_{ch}$  and  $L_{ch}$  can be determined.

A simple method is the following: Just after switching on the toroidal electric field, the toroidal current is still close to zero ( $I_{tot} \approx 0$ ), so  $U_l \approx L_{ch} dI_{tot}/dt$ , so  $L_{ch}$  can be determined. On the other hand, at the flat top of the current curve ( $dI_{tot}/dt \approx 0$ ) equation (3.1) simplifies to  $U_l \approx R_{ch} \cdot I_{tot}$ , so  $R_{ch}$  can be estimated.

A more sophisticated method is a 2D least squares linear fit making use of all data points ( $U_l, I_{tot}, dI_{tot}/dt$ ). Since we have only two independent parameters  $R_{ch}$  and  $L_{ch}$ , the fitted plane has to pass through the origin. If we divide equation (3.1) by  $I_{tot}$ , we can simplify the task to a 1D least squares linear fit, which can be easily implemented in MATLAB (OCTAVE), using *polyfit* function.

Values of  $R_{ch}$  and  $L_{ch}$  should be calculated for about 5 discharges having different parameters, and the results should be compiled to a single best estimate for both parameters. Estimation should be performed by both methods described above, and the results of the method giving the more precise estimates should be used in the further steps.

#### Plasma breakdown

After measuring the vacuum chamber properties, we can make the next step towards creating tokamak plasma: we can let  $H_2$  gas into the chamber before initiation of the toroidal electric field. The  $p_{H_2}$  value, which can be set as a discharge parameter, is a control parameter for the inlet valve. The actual value of the pre-discharge gas pressure is measured by a vacuummeter  $p_{ch}$ .

As we will see, letting  $H_2$  gas into the chamber is not always sufficient to produce a plasma. The toroidal electric field must also reach a critical value for mass ionization, in other words plasma breakdown.

The task is to plot the  $p_{ch}$  against the maximum of the loop voltage spikes in the beginning of the discharge for several discharges, and indicate the plasma breakdown by the shape of the symbols. Shots should be concentrated

around the critical line separating breakdown and non-breakdown shots. Detailed scan should be performed for a given magnetic field and the effect of the magnetic field should be studied with a few discharges. During this exercise the pre-ionization should be turned on to produce more reproducible results, but the effect of turning it off could also be studied. About a total of **30** discharges are available for this exercise.

### Estimation of main plasma parameters

If plasma breakdown occurs, plasma parameters can be determined - with different accuracy - from the measured parameters. The aim of this task is to investigate the effect of different parameters on the performance of the discharge, and reach discharges with the highest central temperature, plasma energy or energy confinement time. This task should result in about 25 discharges.

#### Plasma current

A simple electrical model for the inductive current drive is a time-varying voltage source ( $U_l(t)$ ) connected to the plasma and the vacuum chamber in parallel can be seen on Figure 3.9. Both the vacuum chamber and the plasma are modeled by LR circuits. The main difference is, that while the internal inductance and resistance of the chamber are constant, and thus they can be measured separately, the parameters of the plasma differ in each discharge.

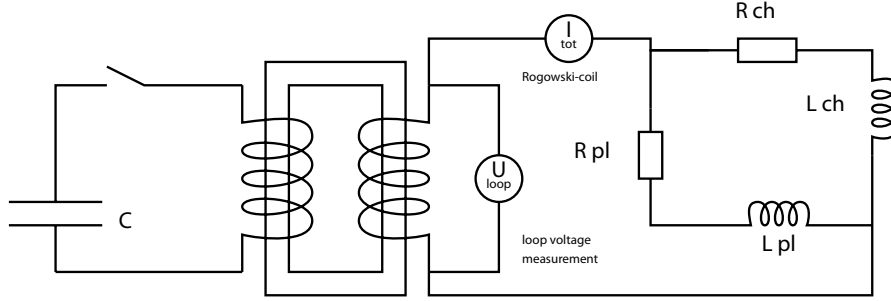


Figure 3.9: Model of the inductive current drive circuit

The basic circuit equations are:

$$U_l(t) = R_{ch} \cdot I_{ch}(t) + L_{ch} \frac{dI_{ch}(t)}{dt} \quad (3.2)$$

$$U_l(t) = R_{pl}(t) \cdot I_{pl}(t) + L_{pl} \frac{dI_{pl}(t)}{dt} \quad (3.3)$$

$$I_{tot}(t) = I_{pl}(t) + I_{ch}(t) \quad (3.4)$$

The chamber parameters have already been determined according to the part 3.4.1. Integration of the (3.2) circuit equation using the initial condition  $I_{tot}(t=0) = I_{ch}(t=0)$  is implemented in the routine `GOLEM_chamber_current.m` to arrive to  $I_{ch}(t)$ . This can then be used to determine the plasma current, as  $I_{pl}(t) = I_{tot}(t) - I_{ch}(t)$  as shown in Figure 3.10. Plasma resistivity can be determined in turn from equation (3.3).

Having calculated the plasma current, a threshold can be defined significantly exceeding the calculation accuracy to safely determine the beginning and end of the plasma discharge. Using this threshold in the "find" function, one can cut the time signals to the extent of the discharge for further processing. Time duration of the discharge is also an important parameter.

It can be attempted to investigate the effect of the  $L_{pl} \approx 0$  H approximation by a more careful integration of choosing  $L_{pl} \approx L_{ch}$  in the time region with plasma. If significant differences are found, this latter approximation has to be implemented for all further data processing.

A suitable threshold in plasma current can be used to determine the discharge duration and cut out the interval of the measured signals relevant for plasma diagnostics.

Plasma current has to be calculated for all discharges with plasma and the maximum value and the discharge duration have to be included in the shot summary table.

#### Plasma heating power



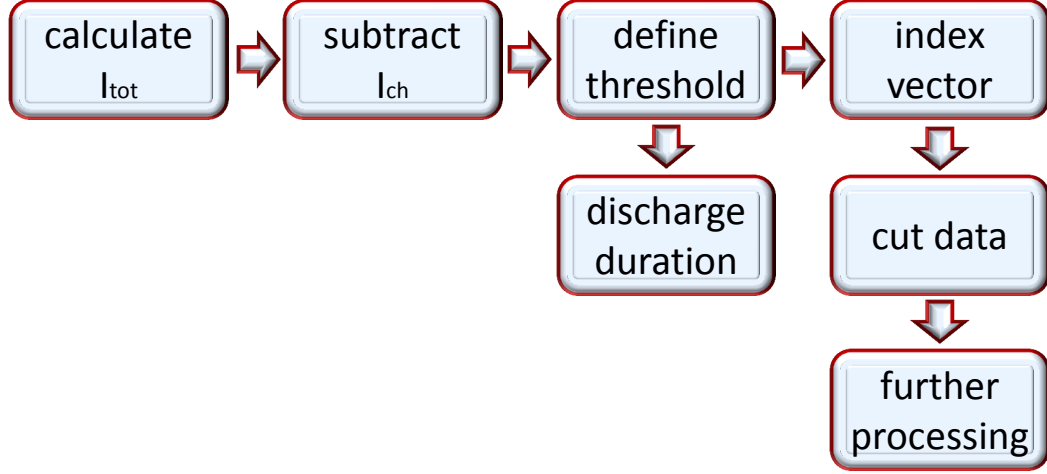


Figure 3.10: Block diagram showing the steps of data processing for the plasma current measurement.

In the GOLEM tokamak the only heating mechanism of the plasma is ohmic heating resulting from current flowing in a conductor with finite resistivity. The ohmic heating power can be calculated as:

$$P_{OH}(t) = R_{pl}(t) \cdot I_{pl}^2(t) \quad (3.5)$$

Ohmic heating power has to be calculated for all discharges with plasma and the maximum value has to be included in the shot summary table.

#### Central electron temperature

Specific resistivity of a fully ionized plasma only depends on its electron temperature ( $T_e$ ) and effective charge number ( $Z_{eff}$ ). This dependence is quantified by the Spitzer formula [2]. It has to be noted that the ion temperature can be very different from electron temperature. The effective charge number is determined by the amount, composition and state of impurities in the  $H_2$  plasma, and we can take value  $Z_{eff} \approx 2.5$  for GOLEM plasmas.

Center of the plasma has higher temperature, and lower resistivity with higher current density, which makes the estimation of the electron temperature ambiguous from an integrated value of resistivity ( $R_{pl}(t)$ ). However, if we use an equilibrium temperature profile (3.6) (Figure 3.11), measured in more detailed measurements [4], we can estimate one parameter of the profile, which is in this case the central electron temperature ( $T_{e0}(t)$ ):

$$T_e(r, t) = T_{e0}(t) \left(1 - \frac{r^2}{a^2}\right)^2 \quad (3.6)$$

The central electron temperature ( $T_{e0}$ ) is then calculated from equation (3.20) of [4], which itself is based on Spitzer's resistivity formula:

$$T_{e0}(t) = \left( \frac{R_0}{a^2} \frac{8Z_{eff}}{1544} \frac{1}{R_{pl}(t)} \right)^{2/3}, \quad (3.7)$$

where  $R_{pl}(t)$  is in Ohms, distances are in meters and we get  $T_{e0}(t)$  in electronvolts.

It has to be noted that plasma in the GOLEM tokamak is only fully ionized in the central region,  $Z_{eff}$  can be estimated with large uncertainty and even the  $a$  plasma small radius might change in an unmonitored way due to the lack of plasma stabilization. All these factors make the estimation of the central electron temperature quite uncertain.

Nevertheless, central electron temperature has to be calculated for all discharges with plasma and the maximum value has to be included in the shot summary table.

#### Electron density

In its current state, the GOLEM tokamak does not have any density measurements. However, as electron density is needed for further calculations, we estimate its order of magnitude from the state law of ideal gases.

For the average density it is assumed, that it is constant during the discharge, apart from the dissociation of the hydrogen gas. There is a 30 second delay between the gas filling and the actual shot, which is enough for the gas



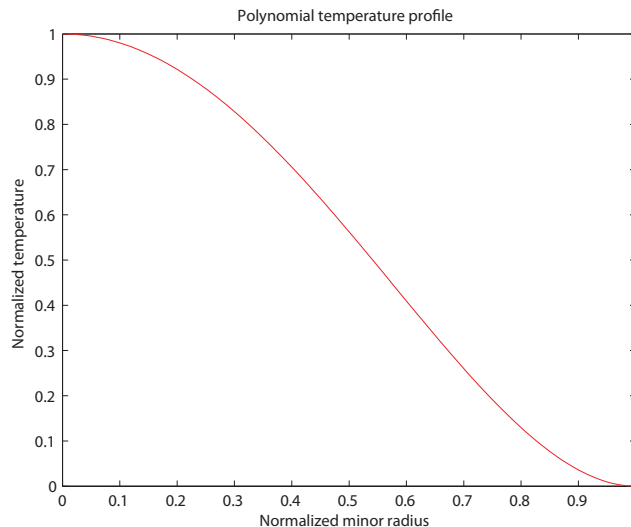


Figure 3.11: Equilibrium temperature profile used in the estimation of central plasma temperature.

to reach thermal equilibrium with the chamber wall. Chamber temperature is monitored with respect to the room temperature, and the difference would normally be zero, but it should be checked. (If chamber temperature is not measured, room temperature can be used instead.) The ideal gas law is used to give an order of magnitude estimate of the electron density (in particle/ $m^3$ ):

$$n_{avr} = \frac{2p_{ch}}{k_B T_{ch}}. \quad (3.8)$$

We have to note that this is a very rough estimate basically for two reasons:

1. Plasma in the GOLEM tokamak is not fully ionized, which makes us overestimate the electron density.
2. Due to the plasma-wall interaction, adsorbed gases are released from the surface of plasma facing components during the discharge. These atoms enter the plasma and can be ionized, thus making us underestimate the electron density.

The order of magnitude estimate of the average electron density has to be calculated for all discharges with plasma and included in the shot summary table.

#### Plasma energy

The total energy content can be simply calculated from the temperature, density and volume ( $V$ ), based on the ideal gas law, taking into account the assumed (3.6) temperature profile:

$$W_{pl}(t) = V \frac{n_{avr} k_B T_{e0}(t)}{3}. \quad (3.9)$$

The information that the magnetic field reduces the degrees of freedom of the particles to two has been used to derive this formula.

Uncertainty of this formula is dominated by the uncertainty of our density estimate, which makes it good only for an order of magnitude estimate. Qualitative time trace reflects that of the electron temperature and thus is more reliable.

Nevertheless, plasma energy has to be calculated for all discharges with plasma and the maximum value has to be included in the shot summary table.

#### Energy confinement time

An important concept regarding the energy balance of the tokamak fusion reactor is the energy confinement time ( $\tau_E$ ). It is the characteristic time of energy loss:

$$P_{loss} = \frac{W_{pl}}{\tau_E}, \quad (3.10)$$

where  $P_{loss}$  is the power lost and  $W_{pl}$  is the total plasma energy. The energy confinement time is a global parameter of the confined plasma, and reaching higher values is of central interest of tokamak research.

Having an estimate for the plasma energy, the energy confinement time can be estimated. The loss power can be estimated from the energy balance:

$$P_{loss}(t) = P_{OH}(t) - \frac{dW_{pl}}{dt} \quad (3.11)$$

We then have to just substitute it into the definition (3.10) of the energy confinement time:

$$\tau_E(t) = \frac{W_{pl}(t)}{P_{loss}(t)}. \quad (3.12)$$

Given the uncertainty of the input parameters, maximum value for the energy confinement time should be taken with care. Nevertheless, its maximum should be included in the shot summary table.

### $q = 2$ disruptions

When the plasma current grows so strong that the edge safety factor, defined by (3.16), reaches the value of 2, a plasma instability resonant to the  $q = 2$  rational surface destabilizes, and a discharge terminating disruption occurs. This limit of operation is to be attempted to be reached in this task using about **5** dedicated shots.

We can calculate the poloidal field at the edge (for large aspect ratio circular tokamaks) using Ampère's law, as the enclosed current is the total plasma current:

$$B_p(a, t) = \frac{\mu_0}{2\pi} \frac{I_{pl}(t)}{a}, \quad (3.13)$$

where  $a$  is the plasma minor radius. Substituting this expression into formula (3.16), the safety factor at the edge can be estimated as:

$$q(a, t) = \frac{a^2}{R_0} \frac{2B_t(t)\pi}{\mu_0 I_{pl}(t)}. \quad (3.14)$$

Discharges aiming to reach a low  $q(a, t)$  need as large plasma current as possible. As we have very limited control over the evolution of plasma current in GOLEM, we can also set the  $\tau_{OH}$  time delay to set up a discharge at the declining phase of the toroidal magnetic field, which will constantly decrease the edge safety factor.

In order to monitor the success of our efforts, the evolution of the discharges should be plotted on the Hugill diagram. The Hugill diagram positions a discharge on the plane of two parameters:

- Inverse edge safety factor:  $\frac{1}{q(a, t)}$
- Murakami parameter (normalized density):  $\frac{n_{avg} R_0}{B_t(t)}$

The Hugill diagram serves as an operation envelope for tokamaks. If either the Murakami parameter is too high or the inverse edge safety factor reaches the value of 0.5, the plasma disrupts.

First, the temporal evolution of the dedicated shots aiming  $q = 2$  disruptions should be plotted on the Hugill diagram. Afterwards, all previous shots could be plotted to check that none reach the region  $1/q > 0.5$ .

## 3.4.2 Magnetic Measurements

### Introduction

A standard method for measuring the changes of magnetic field inside the plasma is a magnetic coil. Turn a piece of wire into a loop and you obtain the simplest coil for measurement of magnetic field. By increasing the number of turns of the coil, or making a larger loop higher sensitivity can be reached. Magnetic pick-up coils are small coils designed for the measurement of a component (typically poloidal or radial) of the local magnetic field.

Coils measure changes of the magnetic field and not the magnetic field directly. As a result, the voltage changes measured on the coils have to be integrated in time to be proportional to the magnetic field. In the case of fluctuation measurements it is not necessary to perform the integration, one can also study the fluctuation of the time derivative of the magnetic field.

### Magnetic pick-up coils on GOLEM

On GOLEM two sets of Mirnov coils - pick-up coils measuring the poloidal magnetic field component - are available. The first system consists of 4 magnetic coils placed inside the chamber in the distance of 93 cm from the magnetic axis as seen on figure 3.12. The effective area of each coil is  $3,8 \cdot 10^{-3} \text{ m}^2$ . Ideally, their axes are perpendicular to the toroidal magnetic field, but actually they are slightly tilted and sensitive to the variations in the toroidal field, too.

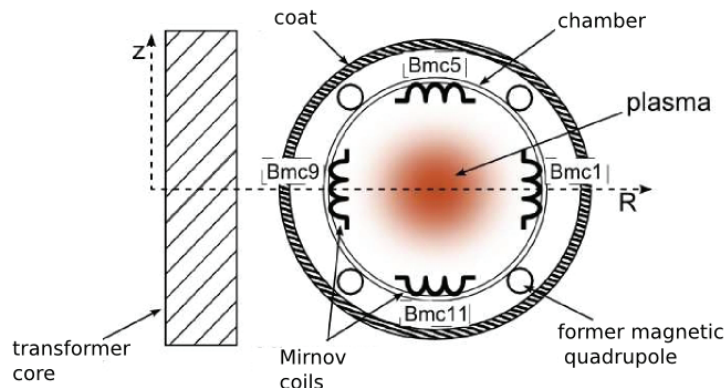


Figure 3.12: Poloidal cross-section of the tokamak with the places of the 4 Mirnov coils.

Recently a new system with 16 Mirnov coils (see figure 3.13) has been installed on GOLEM. This sensor array massively enhances possibilities of detection of large scale plasma wave activity in the tokamak.



Figure 3.13: New set of local magnetic field sensors: 16 Mirnov coils circling the plasma column.

### Plasma position monitoring

The determination of the plasma position is one of the basic tasks during the tokamak operation. Plasma tends to expand in the direction of the major radius and move in random directions influenced by various electric and magnetic fields, which are created during the discharge. The Mirnov coils are used for the determination of the plasma position on GOLEM. Present exercise aims to characterize the movement of plasma in various discharges. About a total of **15** discharges are available for this exercise.

#### The straight conductor approximation

It is hard to express the magnetic field analytically in a toroidal plasma geometry, therefore we take the approximation of an infinite long straight plasma column. From Ampere's law ( $\nabla \times B = \mu_0 j$ ) it follows that the generated poloidal magnetic field decreases with distance from the column's axis as  $1/r$ . If we measure the poloidal field on the two opposite sides of the column, its displacement can be expressed as

$$\Delta = \frac{B_{\theta=0} - B_{\theta=\pi}}{B_{\theta=0} + B_{\theta=\pi}} \cdot b, \quad (3.15)$$

where  $2b$  is the distance between the opposite measurement positions. This approximation is simple, but of sufficient accuracy for demonstration purposes.

The plasma movement is to be reconstructed in all the discharges in both the vertical and horizontal directions. Most frequent directions of movement and dependence on plasma parameters are to be studied.

#### Estimation of the edge safety factor

The tokamak magnetic field consists of such nested magnetic surfaces, each surface characterized by a safety factor ( $q$ ). On large aspect ratio circular tokamaks (like GOLEM), where the major radius ( $R$ ) is much larger than the minor radius ( $r_0$ ), it can be approximated by:

$$q(r, t) = \frac{r}{R} \frac{B_t(t)}{B_p(r, t)}, \quad (3.16)$$

where  $R$  is the major radius of the magnetic axis and  $r$  is the distance of the magnetic surface from the magnetic axis.

In the *Basic tokamak operation laboratory exercise*, the edge safety factor has been already investigated. In that case the radius of the limiter was used instead of the real, time-dependent minor radius of the plasma ( $r = r_0(t)$ ). Using the position of the plasma center, the minor radius of the plasma and the edge safety factor can be calculated considering that the plasma is bounded by the limiter. Discharge evolution is to be visualized on Hugill diagrams with the corrected edge safety factor for every discharge. Most interesting discharges are to be analyzed in detail.

#### MHD mode measurement

Although several tokamaks rely on magnetic pick-up coils for plasma position measurements, their most typical application is to characterize large-scale plasma fluctuations. Due to their finite size and distance from the plasma, pick-up coils are most sensitive to the current variation of macroscopic plasma fluctuations with spatial structure comparable to the size of the machine. Fluctuations in this order of magnitude are most often described by the magneto-hydrodynamic (MHD) theory - treating the plasma as a single conductive fluid.

MHD waves are typically localized around specific magnetic surfaces, but extend to the whole of the tokamak in the toroidal and poloidal directions. In the poloidal and toroidal directions the plasma has periodic boundary conditions, which allows waves with discrete spatial spectrum in these directions characterized by the appropriate mode numbers. The excursion vector  $\xi(r, \Theta^*, \phi, t)$  of an MHD eigenmode is described by the following formula:

$$\xi(r, \Theta^*, \phi, t) = \xi(r, \Theta^*) \exp [i(m\Theta^* - n\phi - \omega t)], \quad (3.17)$$

where  $\Theta^*$  is an appropriately chosen poloidal angle and  $\phi$  is the toroidal angle coordinated,  $\xi(r, \Theta^*)$  is the amplitude, which can change sign only as function of  $r$ ;  $m$  and  $n$  are the poloidal and toroidal mode numbers, respectively, and  $\omega$  is the mode frequency. Positive or negative sign of  $m$  and  $n$  mode numbers determines the direction of propagation (or rotation) of the mode.

There is no fail-safe procedure to excite strong MHD eigenmodes at GOLEM, but they tend to appear in several plasma parameter regimes. 15 discharges are available for this purpose, while time intervals with strong fluctuation are to be selected by looking at the Mirnov coil raw signals in sufficient detail.

#### Determination of the mode numbers

Mirnov coils measure the magnetic field fluctuation at their location, but the currents inducing the magnetic field can be at arbitrary location, which makes it a non-localized measurement. However, the current perturbation gives a magnetic response decaying with the distance, so the current perturbation can be assumed to be near the point of the magnetic surface closest to the Mirnov coil. This way, we can associate a toroidal and a poloidal coordinate to the coils. Localization in the radial direction is usually not possible.

During the course of the present exercise, we are going to approximate  $\Theta^*$  as the geometrical poloidal angle of the probes with respect to the axis of the vacuum chamber. This approach neglects the movement of the magnetic axis and the deformation of the mode structure due to the gradient of the magnetic field, but is still sufficient to see the structure of the MHD eigenmodes.

If we plot signals from a time interval with strong fluctuations with a time axis that allows us to see the periodic changes, we can realize that there is a fixed phase between the oscillation in the different channels. By plotting the signal amplitude on the color scale on the poloidal angle - time plane, we see inclined ridges of maxima and minima (see e.g. Figure 3.14). By counting the maxima in the poloidal direction at a given time point, one can determine the poloidal mode number. The goal is to find at least 5 cases, where a mode number can be determined by this procedure. Aim is to study a variety of frequencies and mode numbers.

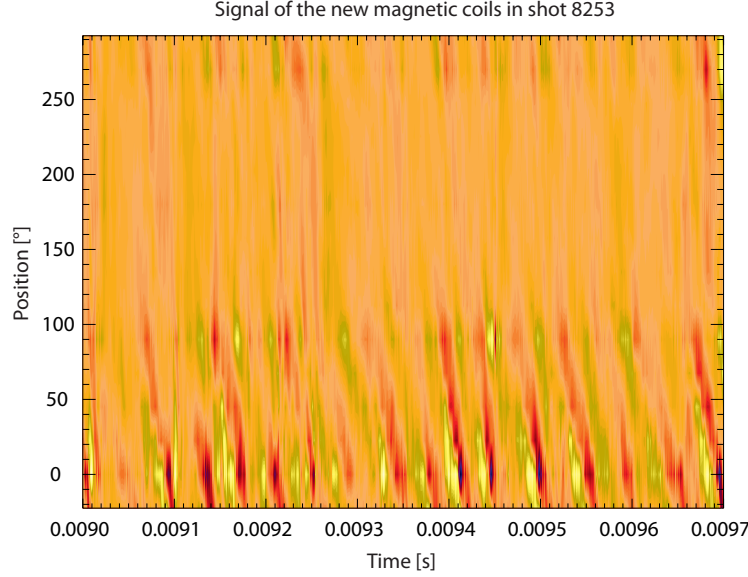


Figure 3.14: Raw signal of magnetic field sensors in shot 8253 [6].

#### Analysis in the frequency domain

MHD modes are often studied in the time domain - as above -, but having discrete frequency fluctuations it is quite natural to transfer the problem into the frequency domain. This transform is traditionally done by taking the Fourier transform of a quasi-stationary time interval. Fourier transform is implemented in discrete signal processing by the FFT algorithm. By taking the absolute value squared of the FFT, we get a spectral power density with the frequency axis going from negative to positive Nyquist frequency (half of sampling frequency). For real signals - like in our case - the spectrum is symmetrical with respect to the zero frequency axis, so we shall only plot the positive frequencies. The first task in frequency domain analysis is to produce the spectrum for a suitable time interval and identify the mode frequency or frequencies.

By producing the power spectra we have dropped the phase information in the signals, which is, however, extremely useful for the identification of fixed phase relations between signals measured by detectors in different spatial locations, and therefore to identify the spatial structure of the magnetic perturbations. At GOLEM we have a poloidal array of Mirnov coils, which makes it possible to determine of the  $m$  poloidal mode number of expression 3.17. Relative phases ( $\xi$ ) between signals can be calculated as the complex phase of their cross-transforms defined by expression 3.18.

$$\xi_{x,y}(\omega) = \arg(Fx(\omega)Fy^*(\omega)), \quad (3.18)$$

where  $Fx(\omega)$  and  $Fy(\omega)$  denote the Fourier transforms of signals  $x(t)$  and  $y(t)$  and  $*$  marks the conjugate.

The only difficulty working these phases is that they are undetermined by a factor of  $2\pi k$ , where  $k$  is an integer. A way to overcome this problem is to arrange the phases with  $2\pi k$  shifts to show monotonic increasing or decreasing trend as a function of the angular position of the corresponding Mirnov coil with respect to a reference probe. The last probe of such arrangement should be the reference probe itself with the corresponding  $2\pi$  relative position. The poloidal mode number is determined by the  $2\pi m$  shift of the reference probe. This method gives a positive and a negative mode number for every frequency depending on our selection of the increasing or decreasing trend, respectively. This is regardless of having a mode at the given frequency or not. If the method with different reference probe selection gives the same mode number, it is a good indication that the mode is really there. Also, mode numbers must be significantly smaller than the number of probes in the array used.

Figure 3.15 shows such a mode number reconstruction for the Wendelstein 7-AS stellarator: black curves connect the phases arranged in monotonically increasing order by adequate  $2\pi$  shifts for different choices of reference probes, blue curve shows the ideal trend for an  $m = 3$  mode if the probe positions were exactly given in the  $\Theta^*$  coordinate of the MHD mode (see formula 3.17 and the red curve is the result of a modeling in real magnetic geometry. It can be concluded that the deviation from the ideal phase curve is due to the deviation of the magnetic  $\Theta^*$  coordinate from the geometric poloidal coordinate of the Mirnov coils. A similar deviation is expected at GOLEM.

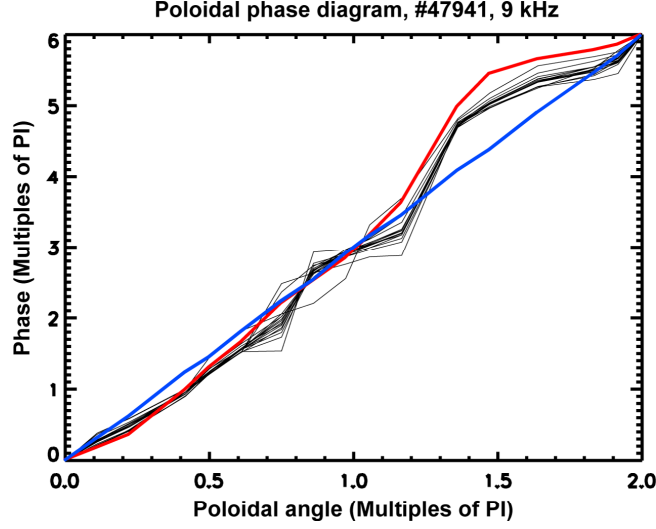


Figure 3.15: Example of determination of mode number from cross-spectrum phases. ( $m = 3$  in Wendelstein 7-AS shot #47941 at 9 kHz) [8]

The task is to plot the relative phases between probes arranged in appropriate monotonic trend for the peaks identified in the spectrograms. Mode numbers should be attempted to be identified and compared to the ones determined from the time-domain analysis.

### 3.4.3 Probe Measurements

#### Basics of the diagnostic

Langmuir probes can be considered as the simplest plasma diagnostic tool. It basically consists of a short and picked piece of metal which is usually biased to some voltage. By a Langmuir probe measurement we mean the measurement of the electric current flowing through the probe - this current can eventually be zero. The simplicity of the hardware can be somewhat misleading since it does not imply the simplicity of the theoretical interpretation of the measurement.

It is a general fact that any piece of material inserted into a quasi-neutral plasma in thermal equilibrium ( $T_e \approx T_i$ ,  $n_e \approx n_i$ ) gets negatively charged due to the large electron mobility. Around this piece of material (let's call it *probe*) a potential barrier (Debye-sheath) is formed which repels electrons and drags ions. The width of this sheath is in the order of Debye-length  $\lambda_D = \sqrt{\frac{\epsilon_0 T_e}{e^2 n_\infty}}$ . Formation of such Debye-sheath implies that the potential of the probe drops from the plasma potential until the electron current is totally compensated by the ion current. The probe potential that corresponds to zero total current is called *floating potential* ( $V_{fl}$ ).

Figure 3.4.3 shows the current-voltage characteristics of a Langmuir-probe. Let us start the qualitative interpretation of the I-V curve by imagining that we apply a voltage biasing to our probe equal to the plasma potential ( $V_p$ ). In this case the probe will collect mainly electrons with flux  $\Gamma_e = \frac{1}{4} n_e \cdot \langle v_e \rangle$ . Increasing the biasing potential above  $V_p$ , the probe current will not increase without limit since we collect all the available electrons per unit area and unit time - this current is called *electron saturation current* ( $I_{es}$ ). We have to note that the probe usually cannot be operated in this regime due to high heat load. From the practical point of view of the real measurements more important is the other limit when the biasing potential is lower than the surrounding plasma potential  $V_p$ . In this case a potential barrier builds up for electrons, therefore the current flowing throughout the probe dramatically drops until becomes zero at the floating potential ( $V_{fl}$ ). Decreasing further the biasing potential the current changes sign indicating the dominance of ion current. This ion current will also saturate but at much lower level than  $I_{es}$ , this is called *ion saturation current* ( $I_{is}$ ). The ion saturation current can be calculated solving in self-consistent way the Poisson equation together with the equation of motion. The I-V curve in the regime of  $V_{bias} \lesssim V_p$  reads:

$$I(V) = I_{is} \left[ 1 - e^{\frac{e(V - V_{fl})}{T_e}} \right], \quad (3.19)$$

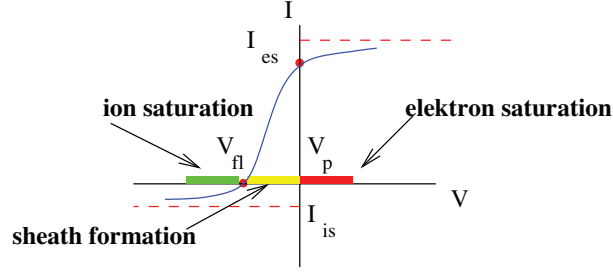


Figure 3.16: The I-V characteristic of a Langmuir probe immersed in hot plasma.

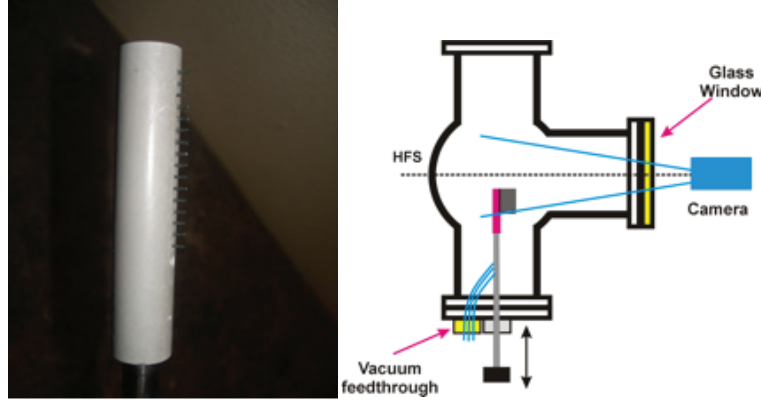


Figure 3.17: Present measurement arrangement at GOLEM.

where

$$I_{is} = -Aen_{\infty}e^{-1/2}\sqrt{\frac{T_e}{m_i}}.$$

Equation (3.19) consists the basis of the Langmuir probe measurements. The I-V characteristic of a given Langmuir probe can be measured using voltage-sweep measurements. If the measurement data are reliably fitted by the Eq. (3.19), important plasma parameters can be determined as the electron density ( $I_{sat} \propto n_{\infty}$ ), the electron temperature ( $T_e$ ) and the plasma potential ( $V_f \propto V_p$ ).

### Langmuir probe array used on GOLEM

GOLEM tokamak is equipped with an array of 16 Langmuir-probe tips measuring signals at different radial positions of the tokamak vessel. This probe array, called the *rake probe*, is inserted into the tokamak from bottom, as it is seen in Fig. 3.4.3.

The probe head can be moved in vertical direction on the shot-to-shot basis. It is also viewed by the fast camera through the corresponding vertical port. Such arrangement allows the observation of probe-plasma interaction at temporal resolution of 0.8 ms. The probe head is composed of 16 tips spaced radially by 2.5 mm. Picture in Fig. 3.4.3 shows the probe head used in the measurement.

The tips are made of Molybdenum wire of thickness 0.7 mm. The length of the tip is 2 mm. The orientation of tips with respect to the magnetic field line can be changed in between shots. In the current experiments, the tips are perpendicular to the magnetic field lines and turned towards the low-field side of the torus. Signals collected by the probe tips are digitized with sampling frequency of 1 MHz. Presently, only 11 ADC channels are available in the DAS system. The 150 kHz bandwidth measuring circuit is schematically shown in Fig. 3.4.3.

### Measurement tasks

1. Measurement of the radial electric field profile in different GOLEM discharges: density scan, comparison of hydrogen and helium plasmas. Calculation of the poloidal component of the  $\mathbb{E} \times \mathbb{B}$  rotation as a function of

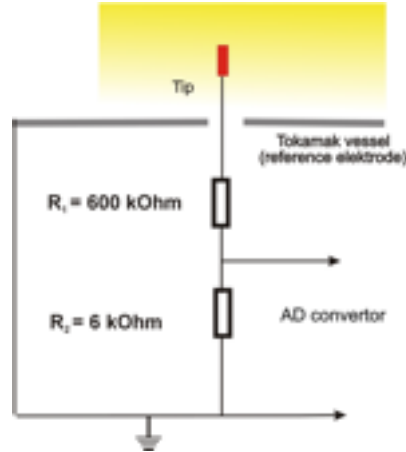


Figure 3.18: Measurement circuit of a given Langmuir probe.

radial position. Hint: let's assume that the plasma potential can be estimated by the floating potential. To what extent can this approximation be correct?

2. Measurement of the floating potential fluctuations. Calculate the amplitude distribution and first 4 statistical moments of the floating potential fluctuation and compare them with the same quantities in the radial electric field fluctuations. Examine the gaussianity of the signal. Determine the auto-correlation time for  $\tilde{V}_{fl}$  and  $\tilde{E}_r$ . Calculate the distribution of cross-correlations along the radial direction, estimate the radial correlation length of the structures.
3. Measurement of plasma ion saturation current (not yet ready for measurement). Applying appropriate biasing voltage (between -100 and -300 V) to the probe it can be driven to ion saturation current regime. Estimate the radial electron density profile. Calculate the amplitude distribution and first 4 statistical moments of the  $\tilde{I}_{is}$  fluctuations. Examine the gaussianity of the signal. Determine the auto-correlation times and the distribution of cross-correlations along the radial direction, estimate the radial correlation length of the structures.
4. Estimate the statistical properties (PDF, moments, correlations) of the radial turbulent particle flux  $\Gamma_r = \langle \tilde{n}_e \cdot \tilde{v}_r \rangle$ .

### 3.4.4 Tomographic reconstruction

The ultimate aim is to perform a good tomographic reconstruction from the two crossed cameras. However, firstly the most basic methods will be introduced to you (Back-filtering, Algebraic Reconstruction Technique, Abel transformation) and later even the state of the art methods that are used for reconstruction in large tokamaks.

Moreover, during this task you will have a chance to develop or improve algorithms to remove reflections from chamber (currently based on PCA), detect and correct slight shifts in cameras position and reach perfect synchronization of both cameras and the rest of tokamak diagnostics.

Some alpha versions of the scripts are already prepared but you should improve reliability/speed/accuracy algorithms for previously mentioned issues and if possible so rewrite them to Python. Moreover, you can try to add the results as a standard GOLEM diagnostics.

*In this task you can reach very interesting results and no previous knowledge of the mathematical algorithms is needed. Moreover, this task is very variable so the level can be setup according to your knowledge and abilities.*

### 3.4.5 Plasma MHD Activity Observations via Magnetic Diagnostics

#### Motivation

Measurement of magnetic fields is one of the most widespread means to study behavior of magnetically confined plasma (surprisingly). Not only magnetic diagnostics provide global plasma parameters such as plasma current ( $I_P$ ), poloidal and toroidal magnetic field flux ( $\psi$  and  $\chi$  respectively), flux surface and plasma position reconstruction (including real-time reconstruction for feedback control), plasma diamagnetism (representing energy deposited in plasma) etc.,



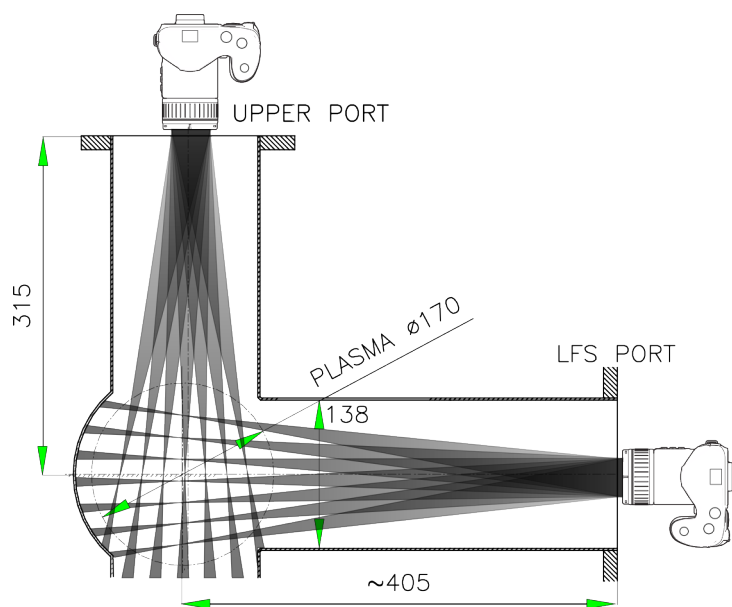


Figure 3.19: Experimental setup

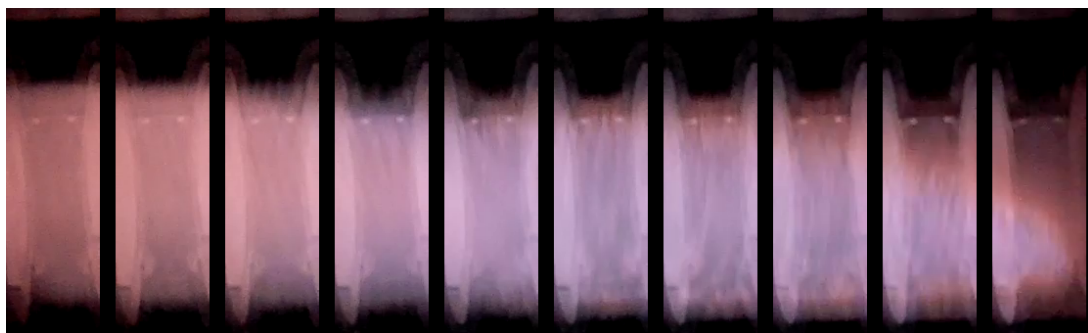


Figure 3.20: Fig 1: An example of nine frames movie of shot connected to time evolution thanks to the “rolling shutter effect”

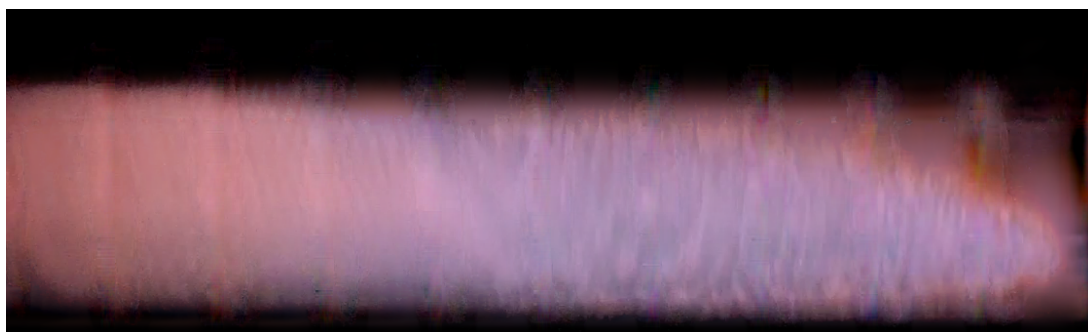


Figure 3.21: Fig 2: An example the same frames with application of some image processing. Background reflections are significantly suppressed and missing stripes are “interpolated”. Note that the camera is not precisely perpendicular to the plasma.

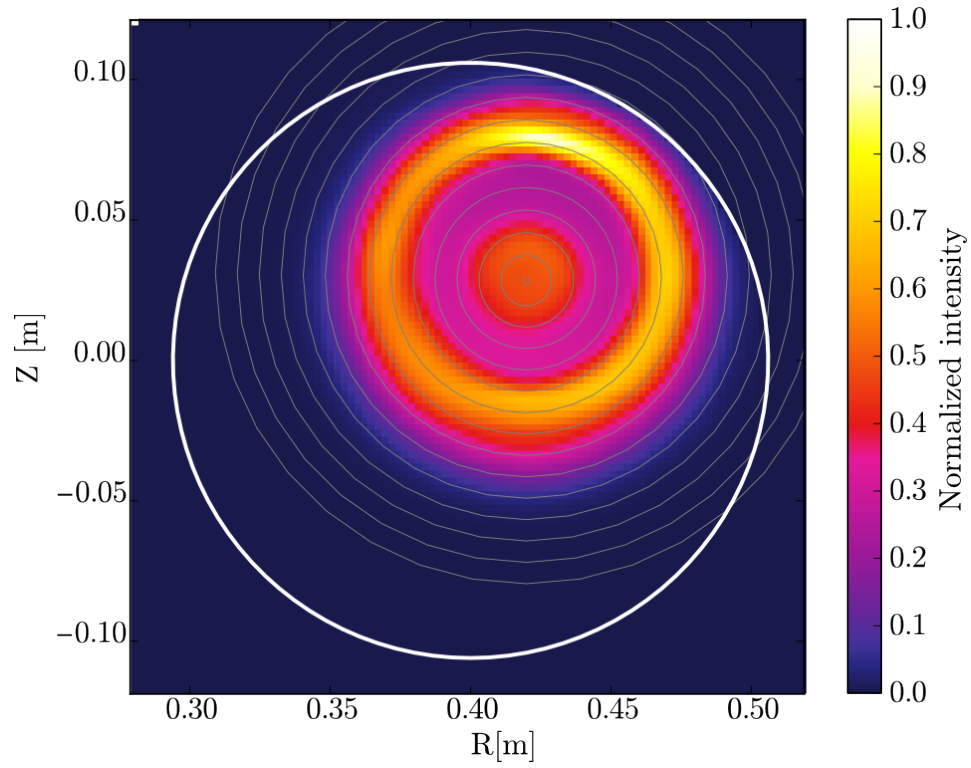


Figure 3.22: An example of tomographic reconstruction.

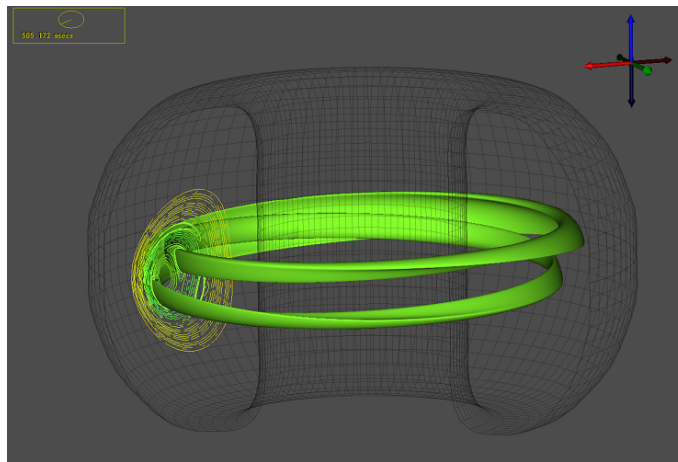


Figure 3.23: 3D model of  $m/n = 2/1$  magnetic island.

Source: [http://www.vacet.org/gallery/images\\_video/NIMROD\\_87009\\_23\\_Surface1.png](http://www.vacet.org/gallery/images_video/NIMROD_87009_23_Surface1.png)

but also enable us to detect local structures presented as inhomogeneities in current distribution. The latter case is characteristic of magnetic islands, which represent perturbation of nested  $\psi$  flux surfaces. Their growth and rotational slowing down has serious consequences for plasma confinement (i.e. leads to disruption). Therefore, control of low mode number magnetic islands, especially by electron cyclotron resonant wave heating - ECRH, is presently hot topic among fusion community. There are two most widespread methods on how to detect and locate these structures in tokamak plasma, so that they might be mitigated by localized heating. One is by SXR tomography and second is by measurement of local and global magnetic fields induced by plasma. Within scope of this task, measurement of local and global magnetic fields will be exploited to study and characterize magnetic islands present during tokamak GOLEM discharges.

### Theoretical Introduction

It is advised to look into ref. [1], or literature of similar character to get some more detailed information on following terms. Seventh chapter (partially the sixth one as well) of publication [1] provides both basic and in-depth insight into character of tokamak instabilities, especially Mirnov instabilities and tearing modes are relevant.

Magnetic islands emerge on flux surfaces, where  $q$  safety factor (inverse rotational transform) is of low-order  $m/n$  value - most common  $2/1$ ,  $3/1$ ,  $3/2$ ,  $4/1$ . For GOLEM plasma,  $q$  increases with radius from plasma center  $r$ . It can be shown that this dependency may be:

$$q(r, \nu) = \frac{2\pi B_T}{R\mu_0 I_P} \frac{r^2}{1 - (1 - \frac{r^2}{a^2})^{\nu+1}}$$

It is evident that radius of say,  $q = 2/1$  depends on global discharge parameters of GOLEM -  $B_T$  toroidal field and  $I_P$  plasma current. Both of these change during the experiment and thus are necessary to be measured. See below.

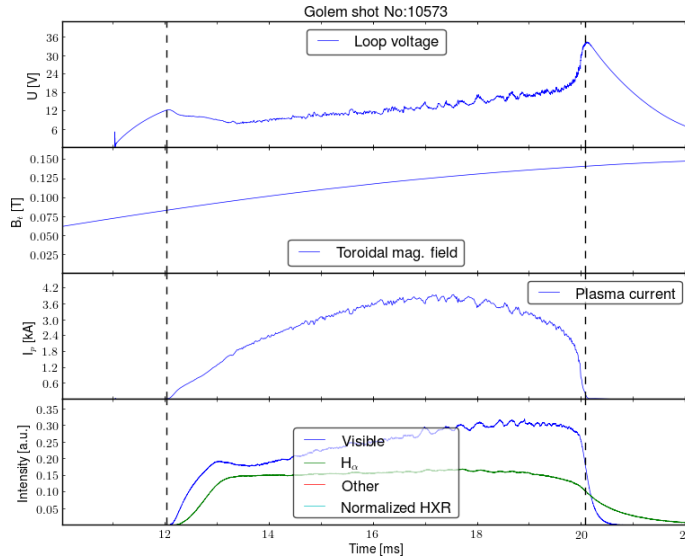


Figure 3.24

This is done by magnetic diagnostics as well and will be thus in the scope of this task. Using previous relation will enable to specify radius of island occurrence - upon specification of  $m/n$ , using  $q(r) = m/n$  condition will yield  $r$ .

$m$  of the island (it is safe to assume that on GOLEM only  $n = 1$  islands emerge), can be specified from its structure i.e. how it behaves on magnetics signal - most typical is as 1-20 kHz oscillation of poloidal magnetic field, see figure below.

When such oscillation is observed, it is safe to assume that it is due to a magnetic island. Such oscillations are best visible when island is on radius close to plasma edge. Explanations above imply that this is for specific values of  $B_T$  and  $I_P$ , ergo for specific time of discharge. Spectrogram below shows that island is present between 16th and 19th ms.

Doing fast-fourier transform (FFT) over this time (see below) will yield that frequency of this oscillation is around 3 kHz.

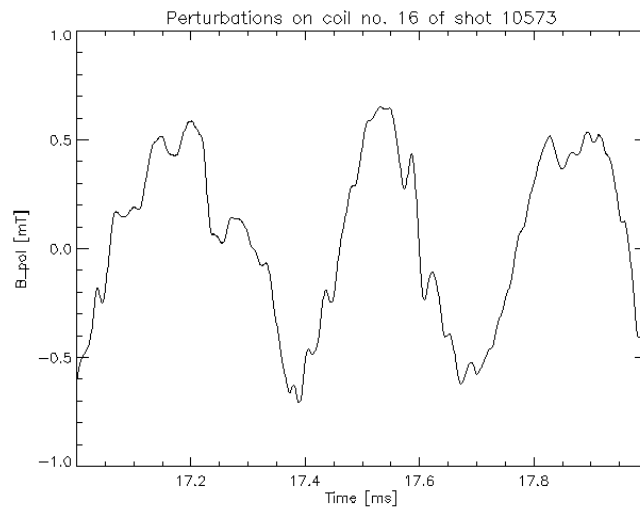


Figure 3.25

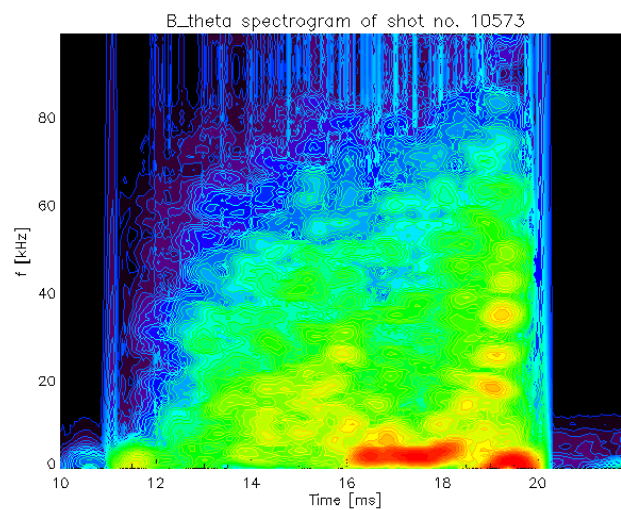


Figure 3.26

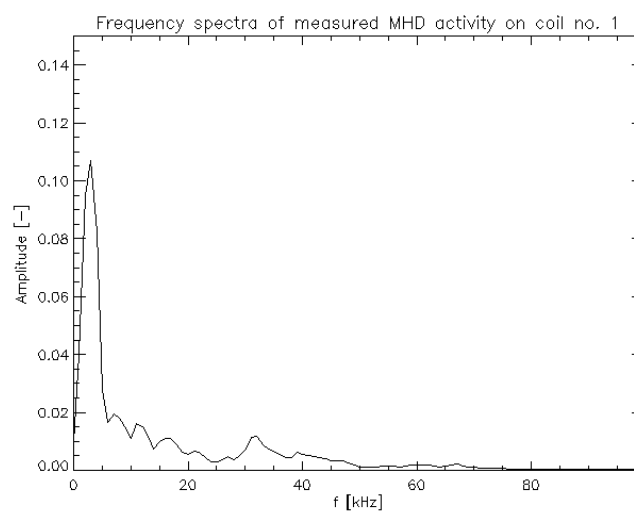


Figure 3.27

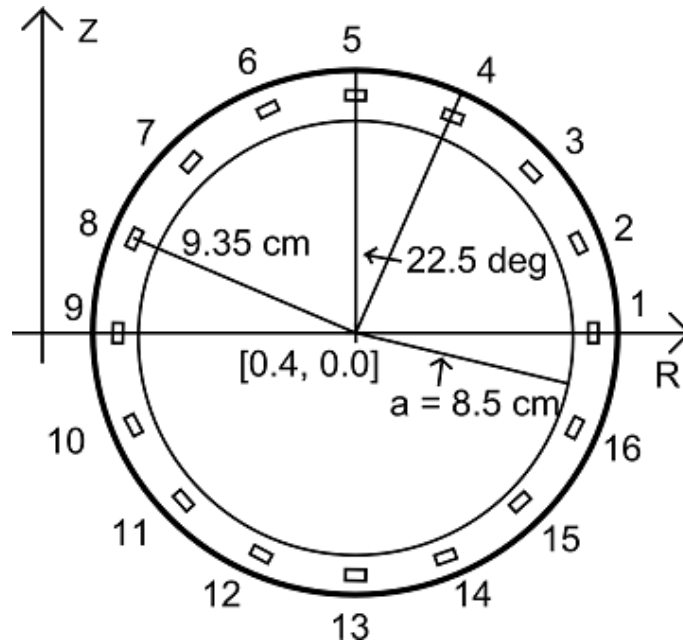


Figure 3.28

If signal is measured on distribution of local magnetic field sensors as shown below:

then the phase of oscillations will be shifted between the different sensors, due to structure of island shown in figure on the top of this page. Number of oscillation maxima for given time moment is equal to  $m$  mode number that is sought. This can be specified by taking window of signal from all the sensors simultaneously and make cross-correlation analysis. How this is done will be covered in course. The result for this specific island is shown below:

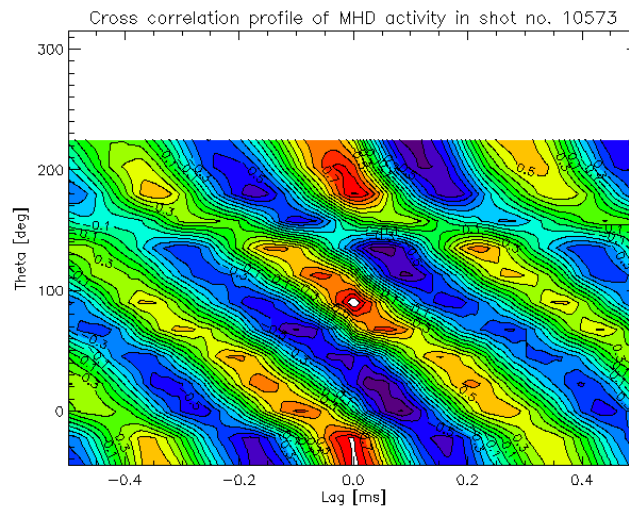


Figure 3.29

This yields  $m = 3$  and thus island rotates with frequency  $f = 3/m = 1$  kHz (taking FFT analysis from above into account). Using the equation for  $q(r)$  would give that island is almost at the edge of plasma, hence the nice signal.

### Equipment

Poloidal flux loop, Rogowski coils, 4 Mirnov coils for local  $B_{\theta}$  measurement and set of 16 Mirnov coils for the same purpose on the fig. below.

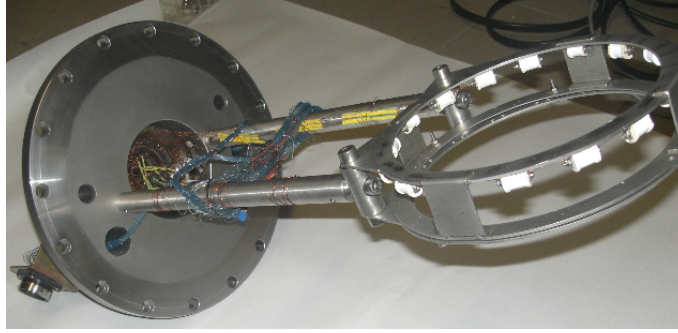


Figure 3.30

### 3.4.6 Other possible exercises

These exercises will need further careful planning, some background calculations and lots of trial measurements before they are considered complete.

#### Runaway Electrons

In tokamak GOLEM, there is a scintillation counter installed to detect hard x-rays. Gamma rays with a wavelength in the range from 0.1 nm to 0.01 nm are detected, this corresponds to energies from 12 keV to 120 keV. The goal is to detect electrons with high energy.

Each electron is affected by the electric field and by collisions. The force of the electric field accelerates the electrons, whereas the friction force decelerates them. When the force of the electric field tops the friction force, the electron is accelerated. The cross section of collisions falls and the electron achieves almost a speed of light. As the electron is accelerated the radius of its trajectory increases. The electron emits photons due to synchrotron radiation, bremsstrahlung, collisions with the vessel (most electrons hit the limiter) The lower energy bounds of HXR can be used for detection of high-Z materials. Lines of heavy impurities in the H-like ionization state produce distinct peaks in the x-ray spectrum at given energies.

#### Breakdown studies

The probability of plasma breakdown (creation of plasma) can be investigated using learning machines algorithms i.e. Support Vector Machine with different setups of tokamak parameters. Mainly the role of the working gas and its pressure, toroidal electric field orientation and breakdown electric field will be investigated. The physical background is rather known but application of learning machines can help to extract more interesting information.

#### Comparison of tokamak discharges in $H_2$ and He working gas

Differences between discharges in H and He as working gas can be analyzed and explained. Which plasma parameters are influenced by higher mass of the main species particles and which are influenced by much higher ionization energy of He can be also investigated.

#### First wall conditioning – baking of the vessel and glow discharge influence on plasma performance

Plasma properties are degraded by flow of neutrals from the walls. Therefore, clear high temperature plasma can be achieved only with pure vessel walls. The cleanness of the walls can be influenced by baking of the tokamak chamber and also by glow discharge in hydrogen or helium. The goal is to find the best cleaning strategy to achieve the best plasma.

#### Role of external magnetic fields on plasma performance

The purpose of the task is to try to characterize the influence of external magnetic fields on plasma behavior. Due to plasma current in toroidal direction, presence of magnetic field external to plasma of either vertical or horizontal direction should result in Lorentz force action on plasma column as a whole, which should shift plasma either vertically or horizontally. Such a field is generated by external sets of coils and is irreplaceable in plasma position control. Of

the two possible major directions of generated field, the vertical direction is of more merit due to the fact that outward (e.g. horizontal) motion of plasma column is always present due to action of hoop force on the plasma column.

To carry out the task successfully, it will be necessary to understand the issues of external magnetic field generation and quantification of the effect of this field on plasma, as a function of coil location and coil current magnitude and direction. This implies that development of appropriate model of magnetic field will be crucial, as well as collaboration with groups working on magnetic diagnostics – in order to obtain experimental means to scan relevant plasma parameters under different discharge regimes and different currents in stabilization windings.

### Spectroscopy studies

The spectra from a spectrometer can be analyzed, the dependency of the observed lines on plasma conditions can be checked and time evolution of the lines investigated.

## 3.5 Golem wiki (documentation repository)

A documentation project inspired by the Wikipedia project has been developed. Screenshot of the one particular page describing a special GOLEM diagnostics tool - the rake probe as an example is at the Fig. 3.31.

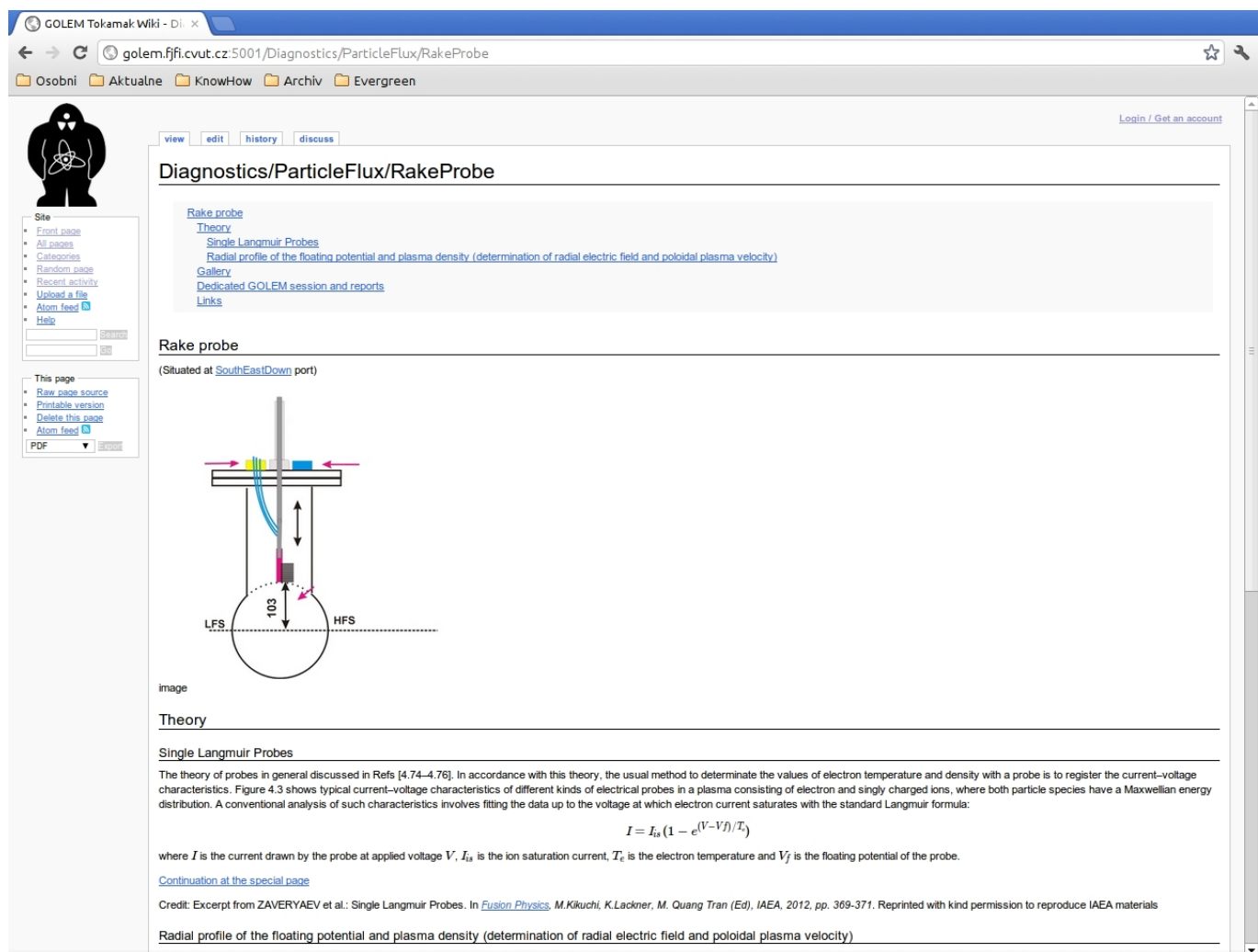


Figure 3.31: GOLEM wiki



## Chapter 4

# Education Events and Presentations

### 4.1 2009

#### August: SUMTRAIC, Prague] Summer Training Course

Introductory session, more than 100 discharges performed by 17 students from 7 European countries. Link: <http://golem.fjfi.cvut.cz/wiki/TrainingCourses/SUMTRAIC/9/index>

### 4.2 2010

#### March: HUNTRAIC, remote practica for BME, Hungary

Introductory session, more than 70 discharges performed by 3 students.

*First of all, we would like to express our gratitude for this remarkable opportunity. To perform a remote measurement on a tokamak, and to be part of such an international operation for the first time in our life, is way beyond our earlier expectations as physics students. We wish you luck for the future, and lots of plasma :)*

Andras Karman, Gergely Klujber, Mate Ferenczy and Peter Nemetvarga (BME Hungary)

Link: <http://golem.fjfi.cvut.cz/wiki/TrainingCourses/HUNTRAIC/10/index>

#### August: SUMTRAIC, Prague] Summer Training Course

Introductory session, more than 100 discharges performed by 17 students from 7 European countries. Link: <http://golem.fjfi.cvut.cz/wiki/TrainingCourses/SUMTRAIC/10/index>

#### December: Global Tokamak Experiment

In a special event called the Global Tokamak Experiment [7], [3] using a web based system, in over 4 hours 38 participants from 10 different countries carried out 83 plasma discharges. Due to the global nature of this experiment a security access keys (also referred to as tokens) were distributed to limit the usage of the tokamak. A login based system identified between participanta, and experiment manager. Thus the machine was based in the Czech Republic, the experiment manager in the UK, and the participants in many other countries.

*It was great! .. Many thanks to Billy for the excellent site design and to Vojtech Svoboda and his team for the interesting experiment. I hope that it will ever happen again. I and another student has already been discussed the results of shots yesterday the whole evening and today, a good idea to make the discussion more global=D.*

*GTE participant*

Link: [http://golem.fjfi.cvut.cz:5001/Links/1210\\_GTE](http://golem.fjfi.cvut.cz:5001/Links/1210_GTE)



### 4.3 2011

#### June: The Science Week for high school students from Czech republic.

3 groups performed more than 50 discharges.

- 2 sessions: Monday, Tuesday.
- Reports (in Czech language): Breakdown studies, Plasma position studies using Mirnov coils, Basic plasma characteristics,

Link: <http://golem.fjfi.cvut.cz/wiki/TrainingCourses/SCIWEEK/11/index>

#### August: SUMTRAIC, Prague] Summer Training Course

Introductory session, more than 100 discharges performed by SUMTRAIC participants. Link: <http://golem.fjfi.cvut.cz/wiki/TrainingCourses/SUMTRAIC/11/index>

### 4.4 2012

#### February: French fusion masters training course

A whole-week event in Cadarache:

- Tuesday: Lecture “Introduction to tokamak operation” and a demonstration session (3 remote shots made by a tutor)
- Wednesday: Introductory training session (8 remote shots made by tutor and students)
- Thursday: experimental session I (68 remote shots made by students)
- Friday: Experimental session II (20 remote shots I & II made by students)

*I just wanted to thank you for coming in Cadarache to introduce us to the amazing work you’ve done with the GOLEM tokamak. It is fascinating to be able to work on such a device, and we’re really enjoying the possibility to make our very first discharges .. From all of us, thank you again.*

*FUMTRAIC 2012 participants*

*Just returning from Cadarache, where last Friday I heard the presentations given by the students in particular on that GOLEM experiments, I confirm it was really a great success !*

*Gerard Bonhomme, mail correspondence*

Link: <http://golem.fjfi.cvut.cz/wiki/TrainingCourses/FUMTRAIC/12/index>

#### May: 2<sup>nd</sup> Remote practica for Budapest University BUTE , Hungary.

Introductory session, more than 90 discharges performed by 3 students.

*Thanks for the operation! The lab exercise went perfectly well, and the students were really enjoying it.*

*Gergo Pokol (teacher)*

*As it turned out already in 2009 for us, GOLEM is a great possibility for student education purposes. Since that time we (Budapest University of Technology and Economics – Department of Nuclear Techniques) organize remote measurements in each year which is the first (and yet only) tokamak experiment for the students at our university. The simplicity and the remote control abilities of the device fits perfectly to the needs of such practical lab exercise.*

*Dániel Imre Réfy (student, supervisor and coordinator)*

**Session link:** [http://golem.fjfi.cvut.cz/operation/tasks/TrainingCourses/HUNTRAIC/October2012/011012\\_0853/](http://golem.fjfi.cvut.cz/operation/tasks/TrainingCourses/HUNTRAIC/October2012/011012_0853/)

#### **April-June: GOMTRAIC**

GOMTRAIC stands for Golem reMote TRAIning Course and is offered by the Faculty of Nuclear Sciences and Physical Engineering, at the Czech Technical University in Prague. The faculty's small tokamak GOLEM can be fully operated remotely via the Internet. It has been used for many face-to-face experimental fusion summer schools over the past years, and now the faculty is using this experience to pioneer a remote training course. GOMTRAIC aims at Masters and PhD students with an interest in experimental tokamak physics. Within three months, they learn how to conduct tokamak experiments and how to operate the diagnostic systems that measure the plasma. The first course started in March 2012 and was advertised through personal contacts and through FUSENET, a European fusion education network. Almost fifty participants registered from all over the world, including India, Croatia, UK, South Korea, Romania, Holland, USA, Hungary, Ukraine, Italy, Mexico, Belgium, Poland, Slovakia, Spain, Bulgaria and the Czech Republic, altogether 17 countries from 3 continents. They were split into nine groups and each student was assigned to one task according to his or her preference and was guided by an experienced supervisor. A remote kick-off meeting introduced the participants to technical aspects of the measurements. An internet based GOLEM simulator programme helped them learn about the operation of the machine. Although the group never met in person, they communicated via email and videoconference to jointly design the experiments. They met in the virtual control room to perform the plasma measurements, evaluate the data and present a report on their experimental results. The performed discharges were displayed on the website from where the students could download their experimental data. Tasks:

- Breakdown studies
- Comparison of tokamak discharges in H and He working gas
- Determination of plasma resistance and electron temperature, variation with different discharge regimes
- First wall conditioning. Baking of the vessel and glow discharge influence on plasma performance.
- Generation of runaway electrons in different discharge regimes by means of hard X-ray radiation.
- Plasma MHD activity observations via magnetic diagnostics
- Plasma position studies
- Radial profile of the floating potential and plasma density (determination of radial electric field and poloidal plasma velocity)
- Role of external magnetic fields on plasma performance
- Spectroscopy studies
- Video processing and analysis

Link: <https://sites.google.com/site/gomtraic/>

#### **June: The Science Week for high school students from the Czech Republic**

4 groups performed more than 70 discharges.

- 2 sessions: Monday, Tuesday.
- Reports (in Czech language): Spectroscopic studies at the GOLEM tokamak, Plasma position studies using fast camera, Vertical plasma position studies using Mirnov coils, HXR studies at the tokamak GOLEM.

Link: <http://golem.fjfi.cvut.cz/wiki/TrainingCourses/SCIWEEK/12/index>

#### **June: the 5<sup>th</sup> International Workshop & Summer School on Plasma Physics. Kiten, Bulgaria**

Introductory session, more than 80 discharges performed by 21 students from 5 European countries.

*I have been present at a remote participation on GOLEM (during the KITEN workshop), and I can confirm that the students are very enthusiastic about this.*

*Jean-Marie Noterdaeme*

Link: [http://golem.fjfi.cvut.cz/tasks/Promotion/2012/0612Kiten/270612\\_1412/](http://golem.fjfi.cvut.cz/tasks/Promotion/2012/0612Kiten/270612_1412/)

### August: SUMTRAIC, Prague] Summer Training Course

Introductory session, more than 100 discharges performed by 17 students from 7 European countries.

Link: <http://golem.fjfi.cvut.cz/wiki/TrainingCourses/SUMTRAIC/12/index>

## 4.5 2013

### February: Cadarache Winter Event 2013

A whole-week event in Cadarache:

- Monday: Lecture "Introduction to tokamak operation" and demonstration session (1 remote shot made by a tutor)
- Tuesday: experimental session I ( 75 remote shots made by students)
- Wednesday: experimental session II ( 14 remote shots made by tutor and students)

*My feeling is that this event was a success. With an extra day of work compared to last year, the students have had time to go more in depth into the analysis. The new diagnostics (rake probe and magnetics) and the spectroscopy data analysis have also proven invaluable. The oral examination .. were quite good.*

*Remy Guirlet, FUMTRAIC 2013 tutor*

Link: <http://golem.fjfi.cvut.cz:5001/TrainingCourses/FUMTRAIC/13/index>

### June: The Science Week for high school students from the Czech Republic

4 groups performed more than 150 discharges.

- 2 sessions: Monday, Tuesday.
- Reports (in Czech language): Spectroscopic studies at the GOLEM tokamak, Plasma position studies using fast camera, Vertical plasma position studies using Mirnov coils, HXR studies at the tokamak GOLEM.

Link: <http://golem.fjfi.cvut.cz/wiki/TrainingCourses/SCIWEEK/12/index>

### July: Tokamak Operation Demonstration for Bochum students

The participants of the "Introduction to Plasma Physics" (held by Jun. Prof. Jan Benedikt) had the possibility to operate the GOLEM Tokamak remotely during the lecture and got familiar with its operation principle. First, the 3D model of the tokamak was presented, with the possibility to virtually visit the control room with the tokamak, to see all the essential parts in detail and even to see the plasma chamber from inside from "plasma perspective" with highlighted magnetic fields. Afterwards, the effect of different plasma parameters such as pressure, magnetic field and preconditioning of the reactor chamber with glow discharge were tested. Two internet cameras enabled to follow the experiments in real time.

*Thanks to the GOLEM team, lead by Dr. Vojtěch Svoboda, the physic students at RUB will have now the opportunity to operate the Golem Tokamak also in the following years. Moreover, the organization of a remote practica, Bachelor theses or even short training visits in Prague is now being prepared.*

*Jan Benedikt, organizer*

Link: [http://golem.fjfi.cvut.cz/tasks/Promotion/0713Bochum/070713\\_1850/](http://golem.fjfi.cvut.cz/tasks/Promotion/0713Bochum/070713_1850/)

More info at Ruhr www news, see [B.5]

**August:** GOLEM day at SUMTRAIC - standard production. More than 70 discharges.

**September:** Golem at Prague Museum Night - 7 excursions. More than 100 visitors.

**September:** HUNTRAIC III, remote practica for Hungarian students. More than 50 remote discharges. Standard production.

## 4.6 GOMTRAIC 2013 (Flagship of the project)

### 4.6.1 Proposal

#### The tokamak GOLEM practical training course GOMTRAIC 2013

An application to the FUSENET WP7 programme

”Further use of the hardware that was set up with FUSENET financial support”

#### Abstract

The GOLEM tokamak at the Czech Technical University in Prague (former CASTOR) became a training facility for local as well as for foreign students. A unique feature of this tokamak is the possibility of a full remote participation and control through internet access. Basic remote control of any planned experiment is possible either in the online mode via WWW or SSH interface or in the offline mode with the batch processing code, allowing to adjust the necessary discharge parameters and to run the discharge. The remote participation of several foreign universities in Hungary, Belgium, Poland, France and Costa Rica was successfully performed and is documented on the web page of the department of physics (<http://golem.fjfi.cvut.cz>). The aim of the proposal is to organize the GOMTRAIC 2013 course.

#### Contact data of person responsible for the application

Vojtech Svoboda, Faculty of Nuclear Sciences and Physical Engineering, Czech Technical University in Prague (FNSPE CTU Prague), Brehova 7, CZ 115 19, Prague 1, Czech Republic. Email: [svoboda@fjfi.cvut.cz](mailto:svoboda@fjfi.cvut.cz), tel: +420 2243 58296, fax: +420 22232 0861

#### GOMTRAIC ..

... stands for Golem reMote TRAIning Course and is offered by the Faculty of Nuclear Sciences and Physical Engineering, at the Czech Technical University in Prague. The faculty’s small tokamak Golem can be fully operated remotely via the internet. It has been used for many faceto face experimental fusion summer schools over the past years, and now the faculty is using this experience to pioneer a remote training course. GOMTRAIC aims at Masters and PhD students with an interest in experimental tokamak physics. Within three months, they learn how to conduct tokamak experiments and how to operate the diagnostic systems that measure the plasma. The first course started in March 2012 and was advertised through personal contacts and through FUSENET, a European fusion education network. Almost fifty participants registered from all over the world, including India, Croatia, UK, South Korea, Romania, Holland, USA, Hungary, Ukraine, Italy, Mexico, Belgium, Poland, Slovakia, Spain, Bulgaria and Czech republic, altogether 17 countries from 3 continents. They were split into nine groups and each student was assigned to one task according to his or her preference and was guided by an experienced supervisor. A remote kickoff meeting introduced the participants to technical aspects of the measurements. An internet based GOLEM simulator programme helped them learn about the operation of the machine. Although the group never met in person, they communicated via email and videoconference to jointly design the experiments. They met in the virtual control room to perform the plasma measurements, evaluate the data and present a report on their experimental results. The performed discharges were displayed on the website from where the students could download their experimental data.

Frankly saying, this event was not absolutely successful because it coincidence with the examination time at universities and students could not concentrate fully for this event.

#### GOMTRAIC 2013

The second year of the course is going to be enriched with the kick-off in-situ week meeting in Prague, that will certainly help to increase the impact of event. The main goals of the meeting are as follows:

- To learn basic principles of tokamak operation.
- To learn basic instrumentation related to tokamak operation and diagnostics.
- To provide working experience with an integrated tokamak facility, including planning, tokamak control, data acquisition and processing, finalization and presentation of experimental results.
- To provide experience with modern data processing methods, commonly used in today's fusion plasma experiments, in real-life situations.
- To perform several well defined physics experiments addressing basic plasma phenomena occurring in high temperature tokamak plasmas.

Then the second part of the GOMTRAIC course will be carried on in remote mode, where students will have opportunity to continue with their projects started in the kick-off week.

### Basic data

**Planned start of the event:** February.

**Level of the practicum:** M.Sc. and Ph.D.

**Number of participants:** up to 20 students.

**Special condition:** students will be from at least 3 different foreign universities.

### 4.6.2 Concept

The Golem reMote TRAIning Course (GOMTRAIC) is an education and training course focuses on basic understanding of experimental tokamak physics and control. It is meant for undergraduate and postgraduate students who want to get experience with operating of a fusion device. GOMTRAIC 2013 was the second year of the event, the

first one was held in 2012. The project started on April 4th 2013 by a warm-up day (remotely). The participants had the opportunity to get in touch with the organizers and try first few shots. The second significant part was the kick-off week. Kick-off week was organized in Prague, in-situ. Students were given presentations on the tokamak, data acquisition systems, basics of programming data access and basics of tokamak operation and began to execute real measurements on the tokamak related to the 7 tasks:

- Basic tokamak measurements.
- Plasma MHD Activity Observations via Magnetic Diagnostics.
- Electrostatic probes.
- Generation of runaway electrons in different discharge regimes and their registration by means of HXR radiation.
- Breakdown studies.
- Tokamak plasma tomography.
- Electron density measurement via a microwave interferometer.

The students who were not able to come to Prague were following the presentations on-line. The kick-off week ended by presentations of the first results, obtained during the week, and conclusions about the next steps in the investigation. During the following months students were collecting data in on-line sessions.

#### 4.6.3 Participants

- In-situ (students)
  - Mauricio Rodríguez - University of Seville, Seville, Spain
  - Fabien Marguet - Ghent University, Ghent, Belgium
  - Daniel Hernandez Arriaga - Instituto Politécnico Nacional, Santiago de Querétaro, Querétaro, México
  - Miguel Gomez - Instituto Superior Técnico, Lisbon, Portugal
  - Fredrik Ostyn - Ghent University, Ghent, Belgium
  - Lukas Matena - Czech Technical University in Prague, Prague, Czech Republic
- Remote participants (students)
  - Costa Rica group - Technological Institute of Costa Rica, Cartago, Costa Rica
    - \* William Jimenez Vasques
    - \* Luiz Miguel Esquivel Sancho
    - \* Rolando Esquivel
    - \* Denis Josué Luna Acuña
  - Pravesh Dhyani Institute for Plasma Research, Gandhinagar, India
  - Marco Martinez - Universidad Nacional Autónoma de México (UNAM), Mexico City, Mexico
- Participants - supervisors
  - Tomas Markovic (PhD. student) - - Czech Academy of Science, Prague, Czech Republic
  - Michal Odstrcil (PhD. student)- Czech Technical University in Prague, Prague, Czech Republic
  - Tomas Odstrcil (PhD. student)- Czech Technical University in Prague, Prague, Czech Republic
  - Ondrej Grover (Bc. student)- Czech Technical University in Prague, Prague, Czech Republic
  - Jindrich Kocman (MSc. student)- Czech Technical University in Prague, Prague, Czech Republic
  - Tereza Ruzickova (Bc. student)- Czech Technical University in Prague, Prague, Czech Republic
  - Daniel Refy (MSc. student) - Hungarian Academy of Sciences, Budapest, Hungary

#### 4.6.4 Production and supervision

- Dr. Jana Brotánková - Czech Technical University in Prague, Prague, Czech Republic
- Dr. Jan Stöckel - Czech Academy of Sciences, Prague, Czech Republic
- Dr. Vojtěch Svoboda - Czech Technical University in Prague, Prague, Czech Republic
- Dr. Selso Ribeiro - Technological Institute of Costa Rica, Cartago, Costa Rica

#### 4.6.5 Schedule

- Starter: Before the kick-off week, participants were practicing on our virtual simulator which is a special interface simulating the control room. The students could choose the parameters as during a real operation, and the system will find shots performed in the past with parameters close to the selected ones. The students could trigger an unlimited number of shots and get an idea of how the device works.
- Warm-up day: After the starter, there was a Warm-up day on 4th April 2013, organized in order to get in touch via Skype. Those who were interested could perform first shots via remote access.
- The Kick-off week: The kick-off week was held in the week April 8th - April 12th 2013. Three groups performed their tasks and concluded their results in presentations at the end of the meeting. During this time participants performed nearly 100 discharges. Kick-off week programme:
  - Monday:
    - \* 10 a.m. Welcoming address and introductory lecture about tokamak GOLEM for remote participants (via Skype)
    - \* 1 p.m. Welcoming address and introductory lecture about tokamak GOLEM for in-situ participants (live)
    - \* 4 p.m. Golem data processing course (for all participants)
    - \* 6 p.m. Welcome party (for in-situ participants) (from now all activities common for remote and in-situ participants as well)
  - Tuesday
    - \* 9 a.m. Virtual operation of the tokamak GOLEM here
    - \* 11 a.m. Introduction to real operation of tokamak GOLEM
    - \* 1 p.m. Lunch
    - \* 2 p.m. Performing given tasks
  - Wednesday
    - \* whole day: Data analysis, performing tasks
    - \* evening: Social programme (in-situ participants)
  - Thursday
    - \* whole day: Data analysis, performing tasks, preparing reports and presentations
  - Friday
    - \* 9 a.m. Presentations
    - \* 1 p.m. End of the kick-off week

#### 4.6.6 Quotes

We really enjoy both sessions. Thanks again for all the efforts and also to be willing for conducting further sessions.

Celso Ribeiro (Costa Rica supervisor)

\*Kick-off week: I think it was very useful for me, serving as a solid introduction on applying algorithms for data analysis. I really enjoyed my stay. \*Remote part: Good to do additional experiments, however I think a strict deadline before 1st of June (when examinations take place) to finish all reports would be better. If the Gomtraic is closed earlier, there is less risk of losing contact after the examination period ended.

Frederik Ostyn (participant)

From the perspective of a co-supervisor of task 'Plasma MHD Activity Observations via Magnetic Diagnostics' (with Daniel Refy being the other supervisor), I must say that this year's GOMTRAIC was exceptionally fruitful. Implementation of kick-off week was critical to its success, as it gave the whole course a much-needed drive, that was from the most part lacking in previous GOMTRAIC. Although a week-long intensive course is still too short to fully cover application of statistical methods to characterize tearing modes in plasma (judging from my experience with Sumtraic and Emtraic courses of similar character), it is still sufficient to cover the basics and get first results, so that the rest can be finished remotely.

Participants of MHD task learned basics of tokamak physics with relevance to tearing modes, such as identification of radial location of magnetic island resonant surface, using assumption of specific plasma current density peaking factor and m/n structure of the island (which they obtained experimentally). The task naturally required to understand and apply the theory of inductive magnetic diagnostics, which participants coepd very well with.

To be more specific, there were 3 participants in the task in total. Frederik Ostyn from Ghent University (Belgium), Mauricio Rodriguez from University of Seville (Spain) and Daniel Hernandez Arriaga from Instituto Politecnico Nacional (Mexico). Each of the participants was creative in different way, and also each was far above the standard. Frederik was well versed in plasma physics and data analysis. It was he, who wrote the main algorithms for magnetic island analysis. He also managed to characterize not only location of resonant surfaces, but also rotation velocities of islands therein, which is why he was considered to be the brain and 'theorist' of the group. Mauricio wrote a full 30 (!) page report of activities of the group during kick-off week, and was in charge of final presentation (which was of exceptionally good quality) for kick-off week, which is why I saw him as 'main author'. Daniel constructed, calibrated and installed a brand new diagnostics for tokamak GOLEM (second Mirnov coil array), which enabled second experimental session to take place and to obtain large amounts of megabytes of nice data. I know from my own experience that construction of such a large diagnostics array is very hard task to do, which is why I saw him as an 'experimentalist' of the group.

Personally, I am glad that I had the opportunity to get to know the guys and to work together with them in the ever-rewarding field of magnetic diagnostics.

Tomas Markovic (participant-supervisor)

GOMTRAIC is an unique project that allows international students to get interesting experiences from tokamak science. From my experience, fusion master students are missing practical experiences in data processing and evaluation. Especially, lack of basic programming skills and experiences in processing of noisy and damaged data seems to be a critical issue. The advantage of tokamak GOLEM is fully opensource environment that allows students to continue in their projects even from home and therefore students have enough time to understand the problem and prepare their results.

Michal Odstreil (remote participant - supervisor)

The GOMTRAIC summer course is an outstanding event, where the inquiring students can improve their acquaintances. This is the first occasion for most of the participants, where they learn how experimental work is carried out. They can see and touch the machine itself, see how the diagnostics built up, on the other hand, the experimental data is delivered for them, as long as the diagnostics and the data



acquisition system is working automated, they don't have to go too much into technical details. This way, their work can be more focused on the data evaluation, and the understanding of physical processes. The participants have to go through the whole process of scientific experimental work, from the basics of the hardware down to the physical interpretation of the processed data, and at the end of the kick off week, they have to give a presentation of their results, which is extremely useful for their future work.

The work was carried on through the following months after the kick off week, the participants could make further shot sessions where they could apply their experiences, and go for more detailed results.

Dániel Imre Réfy (in-situ supervisor of MHD studies)

#### 4.6.7 Conclusions (lessons learned)

- The kick-off week was a very intense and fruitful event.
- It is extremely interesting to "employ" more experienced Czech student GOLEM staff (including Daniel Refy from Budapest) as supervisors for individual GOMTRAIC tasks. We have a very positive experience with such a role for some GOMTRAIC participants having supervisor role.
- In comparison with last year, the kick-off week pushed the participants significantly.
- During the kick-off week, the students kept high focus on the topics and produced most of the results.
- It is difficult for the students to come in April, mainly because of the approaching end of the semester.
- During the remote part, the MHD group and the electrostatic probe group were going on with more analysis and results. The Basic tokamak measurement group from Costa Rica failed to continue in the task. The Electron density measurement via a microwave interferometer group consisted of one student from IPR, India who did not communicate properly and never performed any discharge or produced any result.
- The improvement on the second year of the GOMTRAIC was significant. There were a few factors which contributed. The main difference was made by organizing the kick-off week, which appeared to be a very efficient way of starting the campaign. Especially the students who came to this event were more serious, more devoted, and thus more successful in achieving results and learning.
- There were a few items which can be improved. The main problem was that the GOMTRAIC interfered with the end of the semester and the exam period - thus, a number of students were short in time to work more extensively. The kick-off week was very efficient, but it is not that easy to keep the remote part going especially in a wrong part of the semester.
- Some of the students were not very serious, this should be filtered out by better communication with the supervisors and teachers. The date was coliding with the exam period of the students, which added to this factor.
- It is worth noticing that the financial support for covering the living costs for the kick-off week was very useful and enabled the students to come. On the other hand, they found it difficult to get funds for the travel from their universities which prevented another few students to arrive for the kick-off week.

#### Recommendations:

- Term: February would be more wise as it matches more with the schedules of the students. It is an interesting idea to arrange the GOMTRAIC in August, just before SUMTRAIC (the training course at the Compass tokamak). The students can stay longer and participate in both the summer schools.
- The advertisement should be more in advance, at least 3 months.
- Include a lecture on data evaluation on the GOLEM tokamak.
- Ask the students in advance about their preferred system (IDL, Octave, Gnuplot, Matlab, etc.).

- Better communication with university supervisors (teachers) of the students.
- Better encouraging of the students to go on with the work.

The progress of GOMTRAIC was reported at the EPS conference in Espoo [5] in a scope of a poster presentation and a proceedings paper. Overall, the unique concept of GOMTRAIC again proved the capacity of the GOLEM tokamak to offer training in tokamak fusion physics to students from all over the world. The quality of GOMTRAIC has a positive trend and still some space to improve.

For reports from the event, see Appendix D.

## 4.7 Czech students from CTU Prague involved in the project

**Tomas Markovic** Magnetic field configurations and their measurement on the tokamak GOLEM.

**Jindrich Kocman** Plasma position stabilization on the tokamak GOLEM.

**Ondrej Grover** Interferometric plasma density measurement in the Golem tokamak. HTS experiments.

**Ondrej Vrba** Photodiode diagnostics on the tokamak GOLEM.

**Tomas Odstrcil** Spectroscopic studies on tokamak GOLEM

**Michal Odstrcil** Breakdown studies on the tokamak GOLEM

**Tereza Ruzickova** High Temperature Superconductor implementation on the tokamak GOLEM

## 4.8 Presentations with educational accent

**June 2010** Former Tokamak CASTOR becomes remotely controllable GOLEM at the Czech Technical University in Prague. 37th EPS Conference on Plasma Physics Dublin. Poster presentation. [[11]]

**September 2010** Multimode Remote Participation on the GOLEM Tokamak. 26th Symposium on Fusion Technology Porto. Poster presentation. [[10]]

**July 2011** The GOLEM Tokamak for Fusion Education. The 38th EPS Conference on Plasma Physics Strasbourg. Poster presentation. [[3]]

**July 2011** Remote control and virtual instrumentation of the GOLEM tokamak for educational purposes. 8th REV Remote Engineering & Virtual Instrumentation Conference Brasov, Romania. Oral presentation.

**September 2011** Tokamak GOLEM Remotely for Worldwide Fusion Education. Presentation at the 7. International Conference on Physics Teaching in Engineering Education. Mannheim. [12]

**July 2012** Recent results from GOLEM tokamak. 'Indeed, you can teach an old dog some new tricks.' The 39th EPS Conference on Plasma Physics and 16th International Congress on Plasma Physics Stockholm. Poster presentation. [[9]]

**July 2013** Tokamak GOLEM for fusion education - chapter 4 The 40th EPS Conference on Plasma Physics Helsinki. Poster presentation. [[5]]

## 4.9 First remote experiments and lessons learned

*Remote participation over the Internet has been successfully performed with several foreign universities in Hungary, Belgium, Costa Rica and with a summer school in Kudowa, Poland. Real experimental sessions have been performed online as well as offline with the Budapest University of Technology and Economics. The Advanced operation mode was successfully tested with the Winter Plasma School in Marianska, Czech Republic.*

*Remote practices performed on GOLEM were overwhelmingly successful and popular among students. However, they have already taught some lessons and marked some directions for the development. The most important lesson was that for measurement experience, online measurements are very much preferred over offline measurements. The reason for this is quite clear: remote participants should really have the feeling of operating a device and take decisions based on their understanding of the previous results. In order to be able to schedule an online practice for students, reliable (and/or redundant) Internet connection has high priority. During the practices, it also became clear that in this rapidly changing phase of the GOLEM experiment supervision by a fusion scientist at the students' site is clearly required to help with the interpretation. It was also concluded that programming help should be provided to students in processing raw data so that they can concentrate on online data processing and discussion of the results.*

*This demonstrated the ability to make a tokamak globally accessible and one way in which multiple participants can collaborate on a single tokamak, without the need for specialized software whilst maintaining security. Security also can be achieved using the standard HTTP/S proxy and firewall methods when using web based systems. Participants were presented with a live control panel which self refreshed, constantly informing people of the experiment status. The result of each plasma discharge was available on the system shortly after it took place.*

*Advanced mode with the help of X11 protocol showed satisfactory fast respond over the internet even with the connection speed slightly below the standard.*

From Fusion Eng. and Des., 86, 2011 [[10]]

*During the remote part of the GOMTRAIC event, the most challenging is to keep the students motivated. Usually, the students are do projects in their free time without motivation of extra credits. Therefore, it was necessary to select only the interesting tasks that can keep the participants interested. It is not easy to find the right balance between too boring and too difficult tasks especially when each student has different skills. Therefore, I separated my project into small subtasks and tailored them for each student. Next time I would like to focus on better cooperation between students in the group, however it is sometimes problematic due too different time zones where the students live.*

Tomas Odstrcil (private communication)

# Report on the development of student measurements on the GOLEM tokamak

Dr. Gergo Pokol<sup>(1)</sup>

<sup>(1)</sup> *Department of Nuclear Techniques, Budapest University of Technology and Economics, Association  
EURATOM, Műgyetem rkp. 3-9., H-1111 Budapest, Hungary*

Last update: October 8, 2012

## Abstract

GOLEM is a small tokamak dedicated for education purposes at the Faculty of Physical and Nuclear Engineering of the Czech Technical University (CTU). The development of GOLEM hardware and connected student exercises has benefited from the support of a FUSENET WP7 Grant. This report aims to summarize the work done developing student exercises and the lessons learned from the first student measurements.

# 1 Introduction

GOLEM is a small size (major radius:  $R_0 = 0.4$  m, minor plasma radius:  $a = 0.085$  m), fully operational tokamak hosted at the Faculty of Physical and Nuclear Engineering of the Czech Technical University, which is fully available to educational purposes from anywhere around the world through complete remote operation. The GOLEM tokamak is only equipped with basic controls and diagnostics, which results in easy and robust operation.

After decades of physics research applications under the names of TM-1 and CASTOR, in the end of 2007 the device was transferred to the Faculty of Physical and Nuclear Engineering of the Czech Technical University (CTU) and renamed to GOLEM. Work on the renewed operation started on the 14th of July 2008 with limited capabilities, and improvements are still underway. The present setup can be viewed on Figure 1.

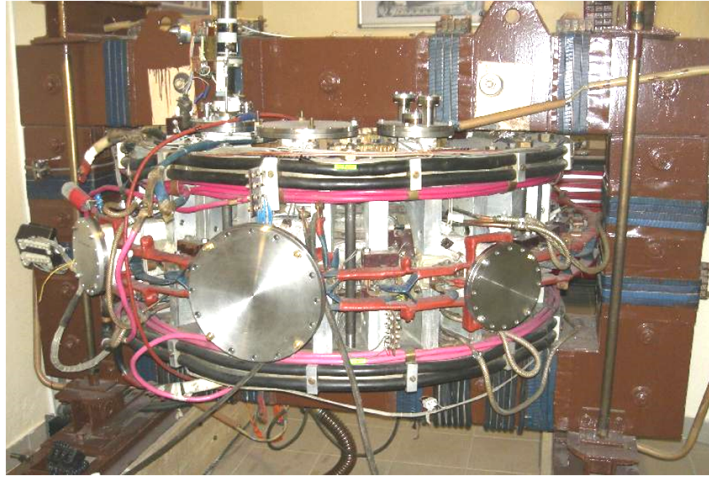


Figure 1: Photo of the GOLEM tokamak

The first remote measurement on GOLEM from Budapest University of Technology and Economics was carried out 14 January, 2010, and methodology development of remote practicums has continued since then. With the support of the FUSENET WP7 Grant student exercises and instructions have been developed aiming the introduction of three subject areas. Characteristics of all of these exercises is that they utilize only the most basic measurement techniques needed to demonstrate their specific subject.

The first of these areas is a general introduction to tokamak measurements from the aspect of thermonuclear fusion as the final goal. The exercise also introduces the basics of magnetics measurements and gives estimates of critical discharge control parameters plotted in all "main parameters" plots in tokamak machines. Estimating quantities in the fusion triple product allows students to properly place GOLEM on the fusion roadmap, and plotting Hugill diagrams allows the introduction of the most important operational limits.

The second area explored is that of MHD equilibrium and MHD eigenmodes. While this instructions lacks both a full taxonomy and the first principles modeling of MHD modes, it gives an introduction to the methodology of characterization of MHD equilibrium and MHD modes in both time and Fourier domain. Experience gained during this exercise should be enough for a student to understand recent advanced signal analysis methods and relate the theory of MHD modes to measurement methods.

The third exercise is the study of plasma turbulence by Langmuir probes. Due to the low plasma temperature, the set of Langmuir probes installed on GOLEM allows the demonstration of the full quantitative characterization of long-wavelength plasma turbulence.

All three instructions can either be executed as single 6-8 hours duration laboratory exercises, or they can be divided into shorter occasions as an alternative. The exercises are designed to promote group work of 2-4 students. Evaluation of student performance is based on class work and on the logbook of the measurement to be submitted by the measuring student group.

## 2 General introduction to tokamak measurements

This exercise is intended not only for students specializing in fusion, but it can also be taken by students of general physics or engineering background even in the BSc education. This case, the goal is to give a glimpse into the methodology of fusion research, and gain experience with the key parameters marking the progress towards fusion energy production. Advanced fusion students can also benefit by gaining hands-on experience with basic tokamak operation and measurements.

The exercise requires basic tokamak operation setting only the following discharge parameters: voltage of the toroidal field capacitor bank, voltage of the capacitor bank for the current drive, time delay between triggers of the toroidal magnetic field and the current drive and hydrogen gas pressure. The diagnostics used are a basic set of loops and coils: a coil for measuring the toroidal magnetic field, the Rogowski coil and a loop for the loop voltage, along with the measurement of some technology parameters, like chamber pressure before the discharge.

Using only these basic diagnostics, an estimate is calculated for plasma current, plasma resistivity, heating power, central electron temperature edge safety factor, and - by using a rough estimate for the plasma density - plasma energy and energy confinement time.

The students are instructed to produce the plasma parameters from the raw signals themselves making use a set of building blocks designed to eliminate the time-consuming searches for the right syntax. This way, students get a direct experience of the evaluation of magnetic measurements and the necessary corrections to the raw measurements. The exercise is designed so that part of the group can develop the signal processing routines, while the other part is conducting a study on the breakdown conditions. The two groups are then pressed to work together in a search for the highest performance plasma and the last task in trying to achieve edge safety factor as low as 2.

Calculating quantities like energy confinement time and plotting discharge evolution on a Hugill diagram gives plenty of occasions to discuss related issues from other tokamaks and thus to put the GOLEM measurements into a wider perspective.

## 3 An introduction to MHD equilibrium and MHD modes

While still accessible for most physics and engineer students, this exercise builds on the knowledge of the universal physics of the development of eigenmodes and basics of Fourier analysis. It is recommended for students in the MSc education in a field related to fusion.

Being a circular tokamak, one aspect of MHD equilibrium is easy to demonstrate and that is plasma position. Students are to determine the time evolution of the vertical and horizontal plasma position based on signals from a poloidal Mirnov coil array in discharges with no position feed-back control. Results are then used to refine the estimation of the edge safety factor.

Description of the MHD mode measurement avoids giving the theoretical background of any particular type of mode, only a general formula for the spatio-temporal variation is given along with

an argument for such solutions in a toroidal system. GOLEM exhibits a reproducible magnetic perturbation of such structure, which can be well measured by the same poloidal Mirnov coil array used to track plasma position. Both time domain and Fourier domain analysis of such perturbations is demonstrated, which forms a good basis for understanding the more sophisticated analysis methods.

## 4 Introducing plasma turbulence

Positioning of this exercise is similar to the one with MHD equilibrium and MHD modes, however, having some basic fusion theory background is highly recommended, which is also necessary to appreciate the central importance of the topic.

Low plasma temperature makes GOLEM ideal for Langmuir probe measurement. This exercise features the measurement of both equilibrium quantities, like electron density and radial electric field profiles, and their fluctuation characteristics. This opens the way to calculate quantitatively characterize turbulence by calculating parameters like ExB rotation speed, correlation length and radial turbulent particle flux. As there are the key parameters in modern turbulent transport theory and transport barriers, most recent advances in the field can be discussed.

## 5 Lessons learned

The instructions on the "General introduction to tokamak measurements" has been tested several times first on voluntary groups of students with fusion background and then on groups of students attending the Nuclear technology track of the Physics MSc program at BME with no particular fusion interest and limited fusion theory background.

All of the student groups have found running a tokamak as a remote experiment was very exciting. Learning outcomes evaluated by on-the-spot questioning and by correcting the logbook revealed a conception of the basic ideas of tokamak operation and magnetics data processing. Specific parameters for discharges were to be set by the students, to promote experiment planning. Supervisor intervention was only necessary in a few cases. Besides the physics-related competences, students have gained experience in group work in international environment, experiment planning and English language professional communication.

Most of the lessons learned have been formulated into proposals and implemented into the remote control system and the aids provided for the practicums. Examples include providing an easy-to set web-based control surface, which remembers the parameters set for the latest shot facilitating parameter scans; providing real-time feedback on the technical preparation for the shots, and providing a set of processing building blocks that cuts the time needed for preparing the signal access and signal processing programs.

Instructions on the MHD mode and the turbulence measurements were designed based on real-life experience with the measurement equipment, but are still to be tested on student groups.

## 6 Conclusions

Three sets of laboratory exercises have been developed that key cover topics of tokamak plasma research starting from the very basics and arriving to still unresolved research problems. With a local supervisor expert in magnetic confinement fusion these exercises can be used to give hands-on experience in tokamak operation and explore the most up-to-date research fields. The total credit

value is between 2 and 3 depending on supervision and exact course requirements, and the three exercises can easily be modified to be carried out in 2-3 hours-long regular classes.

## **7 Human resources involved in development from Hungary**

- Dr. Gergo Pokol (responsible person): associate professor at Department of Nuclear Techniques, Budapest University of Technology and Economics
- Dr. Attila Bencze: senior researcher at Wigner Research Center for Physics, Hungarian Academy of Sciences
- Laszlo Horvath: student at Budapest University of Technology and Economics
- Csaba Buday : student at Budapest University of Technology and Economics
- Daniel Imre Refy: student at Budapest University of Technology and Economics
- 17 students in 5 groups taking part in measurement from Budapest University of Technology and Economics



## 4.10 Event Outlook 2013/2014

**October 2013** HUNTRAIC III - 2nd training course for Hungarian students.

**Autumn 2013** - 2 high school students in the "Junior Tech University" project.

**February 2014** FUMTRAIC III - training course for French master students, Cadarache.

**June 2014** SCIWTRAIC IV - simple short training course for Czech high school students.

**July or August 2014** GOMTRAIC III.

**August 2014** SUMTRAIC GOLEM day VI.

... and other occasional events.

# Appendix A

## Photo Gallery

### A.1 SUMTRAICs

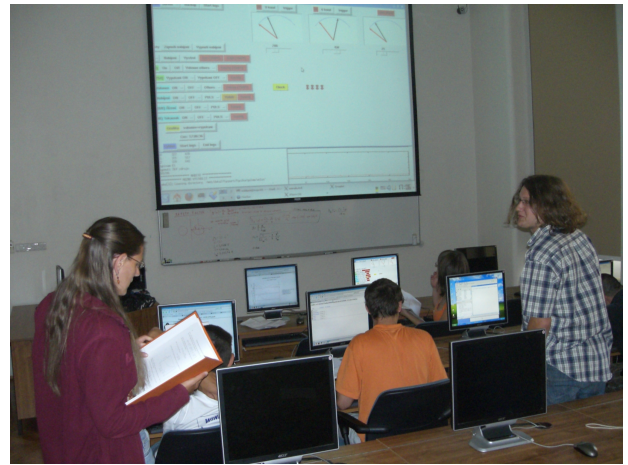


Figure A.1: SUMTRAIC 2009 - A group of participants during the introductory lecture and later on analysing data at the PC room.



Figure A.2: SUMTRAIC 2010 - A group of participants listening the introductory lecture and later on analysing data at the PC room.





Figure A.3: SUMTRAIC 2011 - A group of students in front of the tokamak and later on analysing data at the PC room.



Figure A.4: SUMTRAIC 2012 - 2 groups of students performing their discharges from the "outdoor" control room.



Figure A.5: SUMTRAIC 2013 - Students performing discharges under supervision and presenting results



## A.2 GOMTRAIC 2013



Figure A.6: Introductory lectures

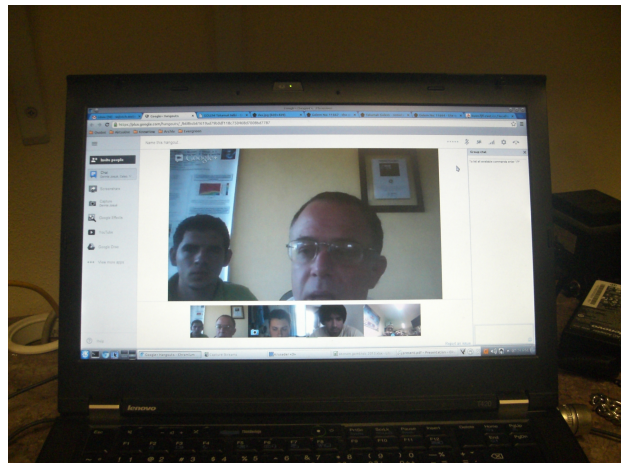
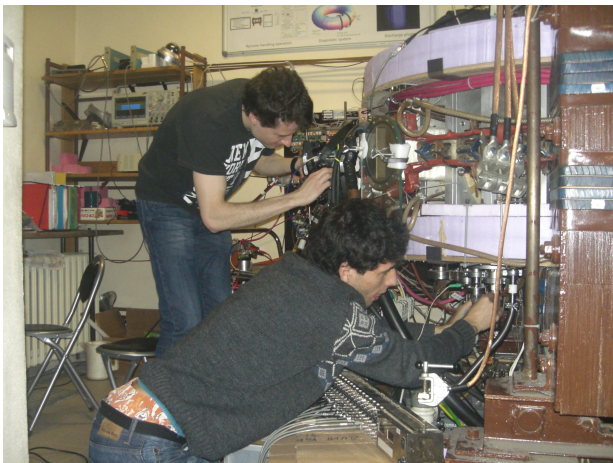


Figure A.7: In-situ (left) and remote (right) participants in action



Figure A.8: Participants at the COMPASS tokamak

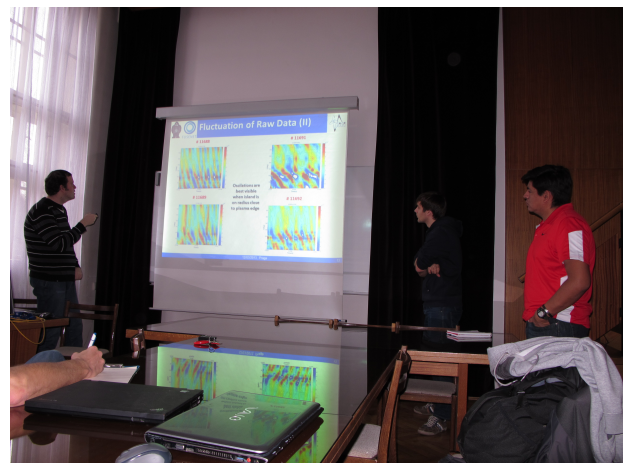


Figure A.9: Final presentations



## A.3 Other

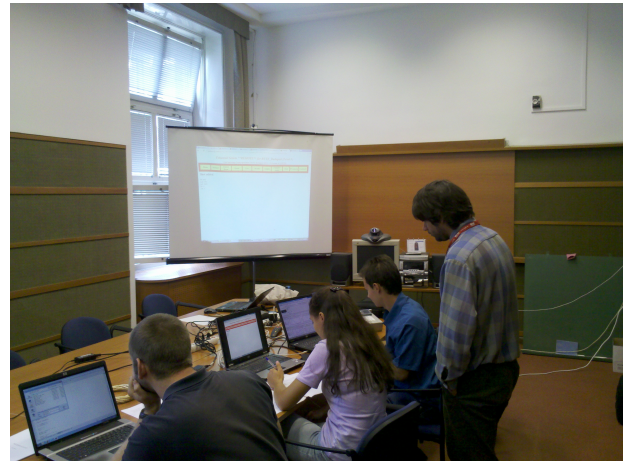
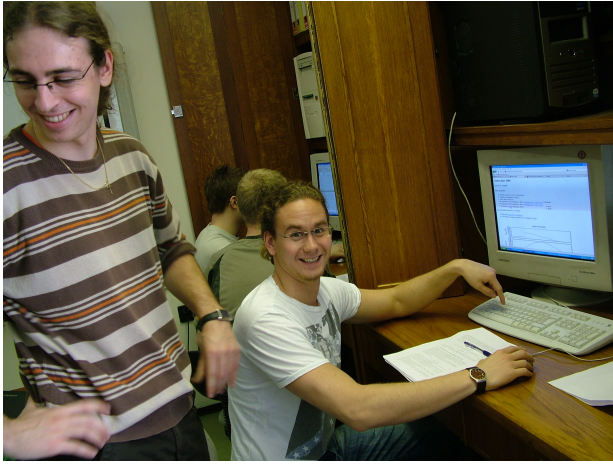


Figure A.10: Control room  $\approx 350$  km away from the device. Introductory course from Budapest. Left March 2010, Right September 2012.



Figure A.11: Science week. Left 2011, right 2012.



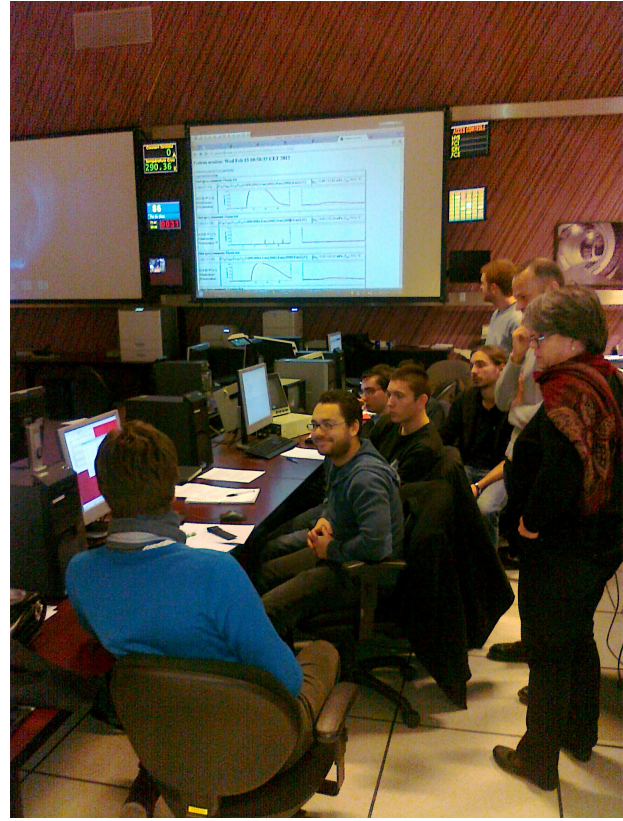
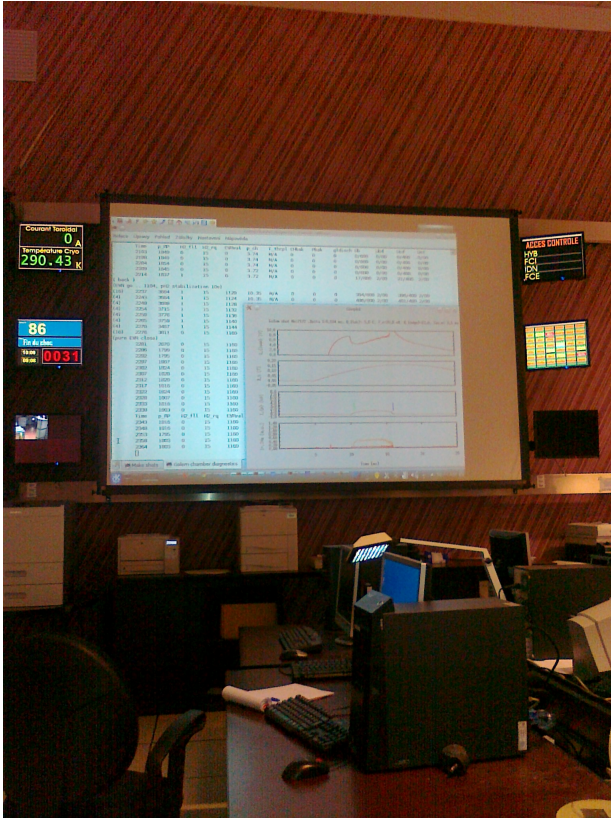


Figure A.12: FUMTRAIC 2012 - a) Performing remote GOLEM discharges from the Tore Supra control room, b) participants with their tutors.

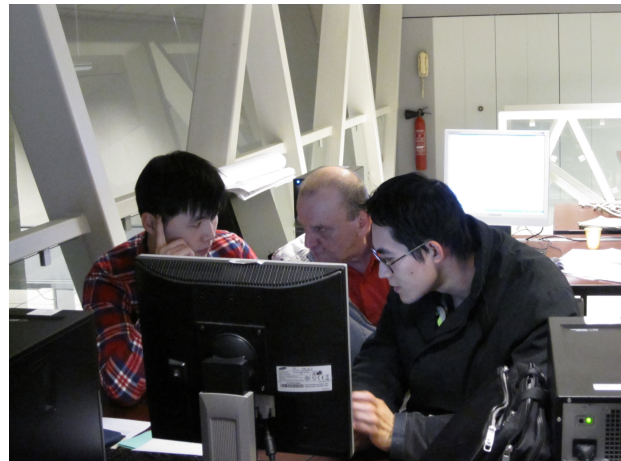


Figure A.13: FUMTRAIC 2013 - Students performing remote discharges from Cadarache and analyzing GOLEM tokamak data.





Figure A.14: a) Map of GOMTRAIC 2012 participants, b) Prague Museum Night 2013

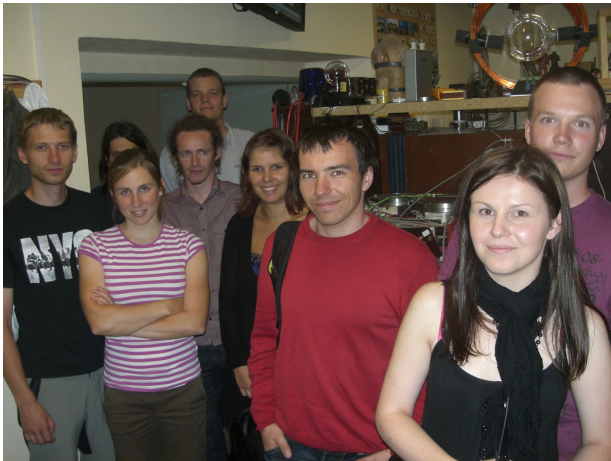


Figure A.15: Excursions: two examples from at least 70 excursions during 2009-2013







# Appendix B

## Press coverage

### B.1 12/10 Launch of the world's first global tokamak experiment. ITER news



the way to new energy

china eu india japan korea russia usa

Home Construction Transport The Machine The Science The Organization The Project Glossary Contact ITER

search:

**ITER Newsline**  
 Latest Issue  
 Newsline Archive  
 Subscribe to Newsline

**News in Brief**

38th International Conference on Plasma Science (ICOPS) - Second Announcement

15th International Conference on Fusion Reactor Materials (ICFRM-15).

**Links**

"InterFaces"

"Worldwide Fusion Links"

"ITER on Facebook"

"ITER on YouTube"

**Conferences**

02 Dec - 06 Dec, 2012  
 6th ITER International School  
 Ahmedabad, India

18 Mar - 21 Mar, 2013  
 6th Int'l Workshop on Stochasticity in Fusion Plasmas  
 Jülich, Germany

29 Jul - 02 Aug, 2013  
 International Conference on Nuclear Engineering (ICONE)  
 Chengdu, China

16 Sep - 20 Sep, 2013  
 Int'l Symposium on Fusion Nuclear Technology (ISFNT)  
 Barcelona, Spain

## iter newsline

**03 Dec, 2010 - #156**  
[view printable version](#)  
[<< return to Newsline #156](#)  
 Fusion World

### Launch of the world's first global tokamak experiment

Culham Centre for Fusion Energy (CCFE) PhD student Billy Huang has set up a website for the world's first global tokamak experiment, which began today. The project allows anyone in the world with a physics background and internet access to apply to have a go at running shots on the GOLEM tokamak in Prague, a machine that has been made remotely operable by Tokamak Engineer Dr Vojtech Svoboda and his team.

"The Tokamak Global Experiment is an innovative project that gives participants the opportunity to change real parameters on a real machine, from anywhere in the world," said Billy Huang (pictured right). "Our goal with this project is to get people participating and interested in fusion research around the globe."

GOLEM is one of the oldest tokamaks in the world, originating from Russia. Although not nearly as large as JET, GOLEM still produces small amounts of fusion energy and is used as an educational device.

Promotion of this initiative, which is run in conjunction with the Institute of Plasma Physics of the Czech Republic and the Czech Technical University, is mainly targeted at university level physics students, but anyone with a physics background is welcome to register to run an experiment (see <http://tokamakglobal.com/>). On its debut day, the experiment was a success and received 37 applications from ten countries. The organisers plan to run more sessions in the future.

Delighted with this response to the project, Billy Huang said:  
 "It's been a real challenge setting up the website, but to have so many people from countries across the world already participating in real live fusion experiments is great."

Read more about the Culham Centre for Fusion Energy (CCFE) [here](#).

2 people like this. [Sign Up](#) to see what your friends like.


[<< return to Newsline #156](#)



© 2012, ITER Organization

Comments & questions should be addressed to [webmaster@iter.org](mailto:webmaster@iter.org).

## B.2 03/12 Students command 100 plasma pulses, remotely. ITER news



the way to new energy

[china](#) [eu](#) [india](#) [japan](#) [korea](#) [russia](#) [usa](#)

[Home](#)
[Construction](#)
[Transport](#)
[The Machine](#)
[The Science](#)
[The Organization](#)
[The Project](#)
[Glossary](#)
[Contact ITER](#)

**ITER Newsline**  
 Latest Issue  
 Newsline Archive  
 Subscribe to Newsline

**News in Brief**  
[New worksite videos](#)  
[F4E Newsletter March 2012](#)

**Links**  
["InterFaces"](#)  
["Worldwide Fusion Links"](#)  
["ITER on Facebook"](#)  
["ITER on YouTube"](#)

**Conferences**  
**02 Dec - 06 Dec, 2012**  
**6th ITER International School**  
**Ahmedabad, India**  
**18 Mar - 21 Mar, 2013**  
**6th Int'l Workshop on**  
**Stochasticity in Fusion Plasmas**  
**Jülich, Germany**  
**29 Jul - 02 Aug, 2013**  
**International Conference on**  
**Nuclear Engineering (ICONE)**  
**Chengdu, China**  
**16 Sep - 20 Sep, 2013**  
**Int'l Symposium on Fusion**  
**Nuclear Technology (ISFNT)**  
**Barcelona, Spain**

# iter newsline

## Students command 100 plasma pulses, remotely

-Remy Guirlet, CEA

Participants in the French Master's in Fusion Science program have been hard at work since early February at the nearby IRFM (l'Institut de Recherche sur la Fusion Magnétique), participating in hands-on workshops and attending specialized lectures on magnetic fusion (see Newsline [208](#)).


For the 2012 edition of this annual intensive program a new hands-on project was proposed: taking control—remotely—of the Czech tokamak [GOLEM](#).

The GOLEM Tokamak, formerly CASTOR, was re-installed in 2009 at the Czech Technical University (CTU) in Prague by Dr. V. Svoboda and his students. The Czech team has implemented a reliable and user-friendly interface with the tokamak control and data acquisition systems, allowing graduate and post-graduate students to become acquainted with the operation of a small tokamak and to propose and perform experiments.

Under the supervision of Dr. Svoboda, GOLEM was (almost) exclusively in the students' hands for one week. More than 100 plasma pulses were performed. By groups of two or three, students studied plasma parameters' roles on performance and worked to optimize parameters to achieve the longest plasma. They also investigated conditioning techniques, ion mass number effects, and energy confinement time. Following data analysis and questioning, students presented the scientific results of their experiments at the end of their hands-on session.

The [Master des Sciences de la Fusion](#) is a collaborative training program sponsored by major French institutions of higher education (Aix-Marseille, Bordeaux, Nancy and Paris-Sud Universities, Ecole Polytechnique and CEA-INSTN). Next year's February gathering is expected to draw 40 students, including students from the pan-European [Erasmus Mundus Master](#) program.

**08 Mar, 2012 - #213**  
[view printable version](#)  
[<< return to Newsline #213](#)  
**Fusion World**



Putting theoretical knowledge to the test and "driving" a real machine.

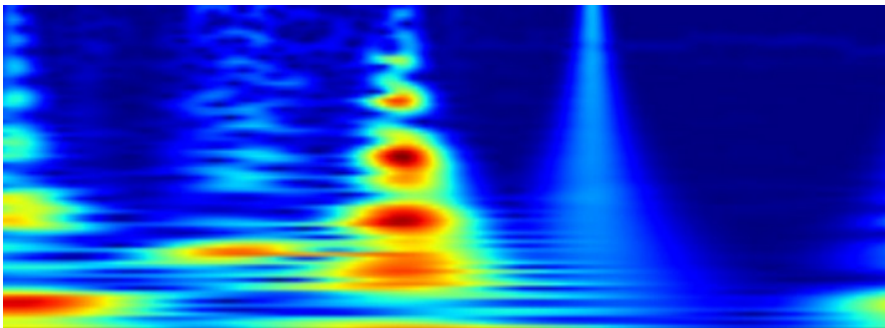
[Sign Up to see what your friends like.](#)

[<< return to Newsline #213](#)

© 2012, ITER Organization

Comments & questions should be addressed to [webmaster@iter.org](mailto:webmaster@iter.org).

### B.3 05/12 A global fusion experiment, EFDA website, picture of the week



A student spectrogram from the Golem tokamak, showing high frequency noise in the kilohertz range during a 20 millisecond long pulse.

## A global fusion experiment

Posted May 14th 2012 in [EFDA](http://www.efda.org/category/efda/) [<http://www.efda.org/category/efda/>], [Picture of the week](http://www.efda.org/category/picture-of-the-week/) [<http://www.efda.org/category/picture-of-the-week/>]

The JET project represents all of Europe, ITER represents over half of the world's population, but the Golem project in the Czech Republic goes even further. It is a fusion experiment for everyone in the world! Golem is a training tokamak in the Czech Technical University that has been set up to allow students to learn how to run a fusion experiment from anywhere in the world, over the internet.

[The Golem Tokamak experiment](https://sites.google.com/site/gomtraic/) [<https://sites.google.com/site/gomtraic/>]

Golem, which was formerly a research tokamak known as Castor, is only 80 centimetres across, and has a plasma minor radius of 8.5 centimetres. It has been set up to be remote controlled, so anyone with an internet connection can set up and run experiments and watch the results unfold in their browser via a data and video feed. Although it has a maximum plasma current nearly a thousand times less than JET's, it is still an authentic fusion experiment and gives real results, such as the spectrogram pictured above.

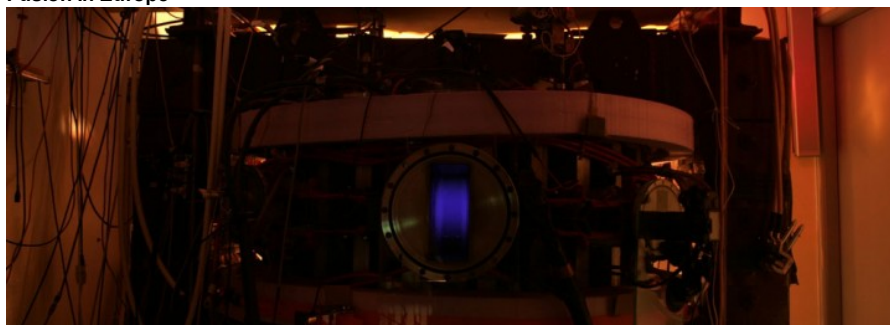
So far, students from twenty countries, as far afield as Mexico, 9000 km to the west and Korea, 8500 km to the east, have taken part. In the course they work through a program that includes breakdown studies, generating runaway electrons, magnetohydrodynamic activity observations, spectroscopic studies and video processing and analysis.

Not only does Golem training program allow students from anywhere to join in, it all takes place in less than three months – nothing compared with the years of training and experience you would need to acquire before being allowed to run JET or ITER!

- [Click to print this page](#)

## B.4 06/12 The tokamak experiment near you, EFDA newsletters

### Fusion In Europe



GOLEM tokamak with its plasma that can be also created from afar: (Picture: Bara Drtinova, Czech Technical University)

## The tokamak experiment near you

Posted June 28th 2012

With its remotely operated tokamak Golem Czech Technical University in Prague makes experimental fusion possible for students that do not have direct access to a fusion machine.

### “For many, fusion is far, far away”

Czech scientist Milan Ripa once said to underline that the only fusion machines in entire eastern Europe are located in Prague. Worldwide, around 50 tokamak experiments are up and running and not all students fascinated by fusion energy happen to live near one. But now they can enrol in the GOMTRAIC project and – within an international team of fellow students and under the guidance of a scientist – operate a tokamak from home.

GOMTRAIC stands for GOLEm reMote TRAIning Course and is offered by the Faculty of Nuclear Sciences and Physical Engineering, at the Czech Technical University in Prague. The faculty's small tokamak Golem can be fully operated remotely via the internet. It has been used for many face-to-face experimental fusion summer schools over the past years, and now the faculty is using this experience to pioneer a remote training course. GOMTRAIC aims at Masters and PhD students with an interest in experimental tokamak physics. All they need is a recommendation from their tutor and internet access. Within three months, they learn how to conduct tokamak experiments and how to operate the diagnostic systems that measure the plasma.

### Global participation

The first course started in March 2012 and was advertised through personal contacts and through FUSENET, a European fusion education network. Almost fifty participants registered from all over

## B.5 07/13 Tokamak Golem in Prague remotely operated during the lecture Introduction to Plasma Physics. Ruhr-Universität Bochum News

### Tokamak Golem in Prague remotely operated during the lecture Introduction to Plasma Physics

An old legend tells that Rabbi Löwe ([http://en.wikipedia.org/wiki/Judah\\_Loew\\_ben\\_Bezalel](http://en.wikipedia.org/wiki/Judah_Loew_ben_Bezalel)), an important Talmudic scholar, Jewish mystic, and philosopher in the 16th century Prague, created an animate being fashioned from clay: The Golem of Prague (<http://en.wikipedia.org/wiki/Golem>). This creature was unnaturally strong and followed blindly the orders of its master, whether they were good or not. And even if the intention of its master was good, it was very difficult to control Golem's powers.

The researchers from the Czech Technical University in Prague (CTU, <http://www.cvut.cz/en>) have, therefore, selected the name Golem for their experimental Tokamak reactor, where the first experience with magnetized plasmas for nuclear fusion and power generation can be made. In parallel to the legend of Golem, also the nuclear fusion can be utilized in a hydrogen bomb (as "successfully" demonstrated several times during the cold war) or for generation of fusion energy in a fusion power plant. This latter application is however quite difficult due to inherent instability of the hot fusion plasma and still large and more advanced devices has to be built to achieve an ultimate goal of save and environmental friendly power generation. Well known is currently running construction of the International Thermonuclear Experimental Reactor (ITER), a € 15 billion machine with the main diameter of 12.4 m.

The Golem Tokamak is, in contrast, with its main diameter of 0.8 m one of the smallest Tokamaks in the world. And also the oldest still functioning one. It was built in former Soviet Union as TM1-MH Tokamak at the beginning of sixties. It moved then to Institute of Plasma Physics in Prague in 1977 (being called CASTOR there) and is now for the last six years operated with name Golem at CTU. It has become an educational device for domestic as well as for foreign students. It is offered to the FUSENET (the 7th FWP European Fusion Education Network) as a remote practica experiment, since its operation can be fully maintained through an internet browser (<http://golem.fifi.cvut.cz/>).

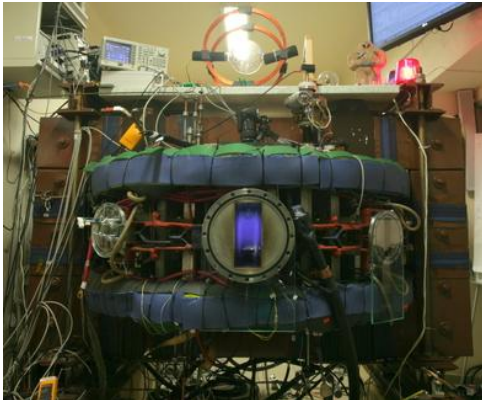


Fig. 1: Golem Tokamak in action. Photo: courtesy...

Additionally, the measurements of many experimental parameters are processed and analyzed automatically and are available online several seconds after the plasma operation, allowing very quickly to have a closer look to the plasma performance or even to perform a further analysis.

Ruhr-University Bochum is a well-known plasma center in Germany and in the world, where both low- and high-temperature (fusion) plasmas are discussed in the bachelor and master study courses and close cooperation exist with the Research Centrum Jülich, with its TEXTOR Tokamak (main diameter 3.5 m).

The participants of the "Introduction to Plasma Physics" in this summer semester had now the possibility to operate the GOLEM Tokamak remotely during the lecture and got familiar with its operation principle. The effect of different plasma parameters such as pressure, magnetic field and pre-conditioning of the reactor chamber were tested.



*Fig. 2: Participants of the "Introduction to Plasma Physics" lecture during the introduction to the reactor. 08.07.2013, Photo: courtesy Hendrik Bahre.*

Thanks to the GOLEM team, lead by Dr. Vojtěch Svoboda, the physic students at RUB will have now the opportunity to control the Tokamak also in the following years. Moreover, the organization of a remote practica, Bachelor theses or even short training visits in Prague is now being prepared.





## Appendix C

**An example of instruction material and student's report (BME Budapest University, Hungary 14.1.2010)**

# Instructions for student measurements on the GOLEM tokamak

Dr. Gergo Pokol<sup>(1)</sup>, Laszlo Horvath<sup>(1)</sup>, Csaba Buday<sup>(1)</sup>, Daniel Imre Refy<sup>(1)</sup>

<sup>(1)</sup> Department of Nuclear Techniques, Budapest University of Technology and Economics, Association EURATOM, Műegyetem rkp. 3-9., H-1111 Budapest, Hungary

Last update: September 17, 2012

## Abstract

The instructions present a 6 hour long measurement program making use of the remote measurement potential of the GOLEM tokamak located at the Faculty of Physical and Nuclear Engineering of the Czech Technical University (CTU). The purpose of the measurement is to demonstrate the very basics of tokamak operation, and to get the students acquainted with basic properties and operational limits.

## 1 Introduction

Participants of the present student measurement are strongly encouraged to read chapters 1 and 3 of John Wesson's The science of JET [1] to be downloaded from <http://www.iop.org/Jet/fulltext/JETR99013.pdf>.

This reading gives an introduction to the basic concept of thermonuclear fusion and magnetic confinement.

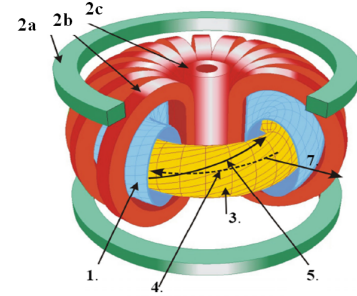


Figure 1: Structure of a tokamak: (1) vacuum chamber, (2a) poloidal field coil / vertical field coil, (2b) toroidal field coil, (2c) transformer coil, (3) plasma, (4) plasma current, (5) magnetic field line, (7) radial direction ( $r$ ).

Basic build up of a tokamak can be seen on Figure 1. The confining magnetic field structure is the result of the superposition of the toroidal magnetic field ( $B_t$ ) generated by external coils and the poloidal magnetic field ( $B_p$ ) generated by a strong toroidal plasma current ( $I_p$ ) induced by the transformer coil.

In the resulting magnetic geometry, field lines are winding helically around a torus surface, which is called the magnetic surface. The tokamak magnetic field consists of such nested magnetic surfaces. The helical structure at each magnetic surface is described by the safety factor ( $q$ ). It gives the number of toroidal turns necessary for the magnetic field line at the given magnetic surface to reach its original position poloidally. On large aspect ratio circular tokamaks (like GOLEM), where the major radius ( $R$ ) is much larger than the minor radius ( $r_0$ ), it can be approximated by:

$$q(r, t) = \frac{r}{R} \frac{B_t(t)}{B_p(r, t)}, \quad (1)$$

where  $R$  is the major radius of the magnetic axis. An illustration for the meaning of the safety factor can be seen on Figure 2.

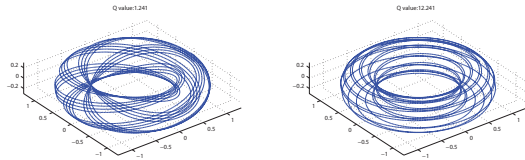


Figure 2: Magnetic field lines in a tokamak for different safety factors.

An important concept regarding the energy balance of the tokamak fusion reactor is the energy confinement time ( $\tau_E$ ). It is the characteristic time of energy loss:

$$P_{loss} = \frac{W_{pl}}{\tau_E}, \quad (2)$$

where  $P_{loss}$  is the power lost and  $W_{pl}$  is the total plasma energy. The energy confinement time is a global parameter of the confined plasma, and reaching higher values is of central interest of tokamak research.

The Lawson criterion is a simple threshold for self-sustained thermonuclear fusion plasma burn at optimum temperature, and it also includes the energy confinement time along with plasma density ( $n$ ):

$$n\tau_E > 10^{20} \text{ s m}^{-3}. \quad (3)$$

More general information on fusion power production and the tokamak concept can be found at the following sites: <http://www.magfuzio.hu>, <http://www.iter.org>, <http://www.jet.efda.org/>

### 1.1 GOLEM

The GOLEM tokamak is a tokamak with full remote control capability and educational purpose. It is a small sized tokamak device equipped with basic controls and diagnostics having dimensions:

- Major radius at the magnetic axis:  $R_0 = 0.4$  m.
- Minor radius:  $r_0 = 0.1$  m.
- Radial position of the limiter:  $a = 0.085$  m.

The device was originally called TM1. Designed and constructed in Kurchatov Institute of Nuclear Research (Soviet Union), it was one of the first operational tokamaks in the world. The original concept of the device did not include poloidal field coils of stabilization however, it was believed that integrating one more layer of vacuum into the chamber would help to achieve better stability of plasma column. The capacitor battery for toroidal field coils and transformer filled several rooms.

Some time later, there was a microwave heating system integrated and the device was renamed to TM1-MH. The microwave heating, in addition to ohmic heating had to heat the plasma further.

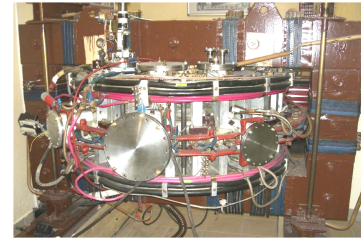


Figure 3: Photo of the GOLEM tokamak

After the device was moved to Institute of Plasma Physics, Czech Academy of Sciences (IPP CAS) in September 1977, thanks to cooperation between the Kurchatov Institute and IPP, some changes in the engineering took place. The microwave heating system was left in Russia, alongside with the most of the oil capacitors of the toroidal field generation, since there was not enough room in the new tokamak hall. A few years later, the device went under major reconstruction. The vacuum vessel was replaced for a new one, the layer of vacuum between the liner and coating were fully removed and a feedback stabilization system was integrated instead. The power supply was substituted by a stronger one, and the ignition was replaced by a glow discharge. Between the years 1977 and 2007 there were several small changes over the device, such as the use of new diagnostics sensors.

In the end of 2007 the device was transferred to the Faculty of Physical and Nuclear Engineering of the Czech Technical University (CTU). Work on the reoperation started on the 14th of July 2008 with limited capabilities, and improvements are still underway. Further upgrade of GOLEM is envisaged in a near future - an increase of  $B_t$ ,  $I_p$  and the discharge duration. Dynamic plasma position stabilization is under present consideration and investigation. Basic diagnostics will be enriched with the plasma density measurement (microwave interferometer),  $H_\alpha$  and X-ray radiation measurement will be installed in a near future. Investigation of plasma edge physics with the help of the various probe measurements is planned, as the previous version of the GOLEM tokamak, the CASTOR had a very good inspiring tradition in this field of interest.

More information can be reached via the home site of the GOLEM tokamak:

<http://golem.fjfi.cvut.cz>

Detailed experimental arrangement can be seen at the following link (This should be studied in detail before the measurement!):

<http://golem.fjfi.cvut.cz/?p=tokamak>

### The parameters to be set remotely:

- Toroidal magnetic field ( $B_t$ ) through the voltage of the toroidal field capacitor bank ( $U_B = U_{C-Bt}$ ), range: 400 – 1400 V.

- Toroidal electric field ( $E_t$ ) through the capacitor bank for the current drive ( $U_E = U_{CD}$ ), range: 100 – 600 V.
- The time delay between the triggers of the toroidal magnetic field and the current drive ( $T_{CD} = \tau_{OH}$ ), range: 0 – 20000  $\mu$ s.
- Hydrogen gas pressure ( $p_{H2}$ ), range: 0 – 100 mPa.
- Preionization ON/OFF

Figure 4 shows the effect of time delay parameter.

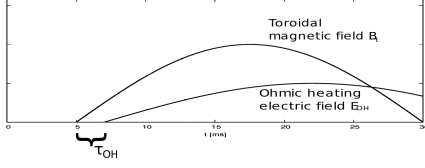


Figure 4: Time delay parameters.

The diagnostics used during the session to be accessed online:

- Time resolved measurement of loop voltage ( $U_l$ ).
- Time resolved measurement of total toroidal current by Rogowski coil ( $I_t$ ).
- Time resolved toroidal magnetic field by coil measurement ( $B_t$ ).
- Time resolved measurement of plasma radiation by photodiode.
- Vacuum chamber pressure ( $p_{ch}$ ).
- The temperature of the vacuum chamber ( $T_{ch}$ ).

## 2 Measurement procedure

This section summarizes the technical procedures necessary for the remote control of the GOLEM tokamak.

### 2.1 Communication with local support

Primary real time communication to the local support (Dr. Vojtech Svoboda) is through Skype instant messaging. For this purpose a user (name: nti.hallgato, passwd: vendeg0 or name: nti.hallgato2, passwd: vendeg1) has been created. Before starting the experiment an instant messaging conference is to be started including users nti-hallgato, gergo\_pokol (Dr. Gergo Pokol, Hungarian supervisor) and tokamak.golem (Dr. Vojtech Svoboda, Czech support). After the session the conversation log should be saved and appended to the measurement log.

5

### 2.2 Remote control

Measurements are to be set up and shots initiated using the web interface of GOLEM tokamak, which can be seen on figure 5. The exact url address of it is provided by Dr. Vojtech Svoboda just at the beginning of the session.

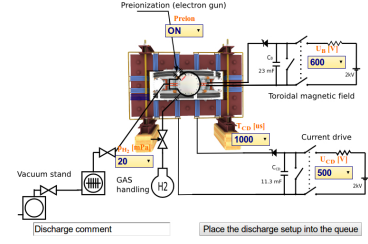


Figure 5: Remote control interface of GOLEM tokamak.

### 2.3 Remote data access

All the recorded data and the settings for each shot are available at the GOLEM website. The root directory for the files is:

<http://golem.fjfi.cvut.cz/operation/shots/<shotnumber>/>

Basic data of the present shot series are collected at a page to be reached at:

<http://golem.fjfi.cvut.cz/operation/currentsession/>

during the session and later archived at:

<http://golem.fjfi.cvut.cz/operation/tasks/Practica/BudapestBME-NTI/>

In order to facilitate the procedure of data analysis, a MATLAB package is available for basic data processing. (This package is also compatible with the OCTAVE freeware software.) The task is to build a proper work flow using these building blocks. It should be noted that these routines do not cover the whole procedure, some additional programs are supposed to be written by the students. The routines are listed in the Table below:

6

File name	Input parameters	Description
GOLEM_get_data.m	shot_nr	Loads raw data from database into the MATLAB workspace
GOLEM_plot_rawdata.m	shot_nr	Makes plots of the time varying raw data
GOLEM_offset_correction.m	raw_signal, time_vector, t1,t2	Makes offset correction for raw data
GOLEM_cut_data.m	raw_signal, time_vector, t1,t2	Crop the given signal
GOLEM_integrate.m	time_vec, signal	Integrates the given signal
GOLEM_chamber_current.m	time_vec,	Calculates chamber current
	$I_t, U_l, R_{ch}, L_{ch}$	integrating equation (7)
GOLEM_diff.m	$x, y$	Calculates $dx/dy$

**GOLEM\_get\_data.m** The return value of GOLEM\_get\_data.m contains the following variables:

- **nr:** shotnumber
- **timedata:** structure, contains  $U_l, dB_t/dt, dI_{tot}/dt$ , photodiode signal
- **N:** number of data points
- **samplerate:** samplerate of the measurements in [Hz]
- **pressure:** pressure of vacuum chamber in [mPa]
- **T\_ch:** temperature of the chamber in [K]
- **trigger:** time delay between starting diagnostics and toroidal magnetic in [s]
- **time\_delay:** time delay between toroidal field and inductive current drive in [s]
- **Bt\_calibration:** calibration factor of toroidal magnetic field diagnostic in [T/Vs]
- **Rogowski\_calibration:** calibration factor of plasma current diagnostics in [A/Vs]
- **U\_loop\_calibration:** calibration factor of loop voltage diagnostic [V/V]

## 3 Measurement tasks, method of evaluation

The sampling rate of the time resolved measurements is returned by GOLEM\_get\_data.m. The measurement loop of the loop voltage is connected to a voltage divider, therefore the signal must be multiplied by a calibration factor (U\_loop\_calibration). The toroidal magnetic field ( $B_t$ ) and the total current ( $I_t$ ) signals, besides multiplying by calibration factors (Bt\_calibration and Rogowski\_calibration), must be integrated. The reason for this is that the voltage measured is induced in these diagnostic loops and coils by the changing of the toroidal and poloidal magnetic field respectively.

Integrated magnetic measurements are very sensitive to the DC bias of the measurement circuit, which needs to be corrected for. If the sampling rate is 1 MHz, and the shot starts at 5 ms, we have

7

5000 samples from the background noise. This is important, because these samples measure the bias, and we can correct the integrated values with this factor. Exact parameters should be optimized for each set of parameters!

The Rogowski coil measurement, for example, has a large negative bias needing correction. The algorithm is the following: we average the data points from the first 4,5 ms ( $\langle DC \rangle$ ), and subtract it from the measured value ( $D(t)$ ):

$$\langle DC \rangle = \frac{1}{4500} \sum_{i=0}^{4500} D(i); \quad (4)$$

$$I_{total} = C_{I_{tot}} \int_0^t D(t') dt' - \langle DC \rangle t' = C_{I_{tot}} \left( \int_0^t D(t') dt' - \langle DC \rangle t \right) \quad (5)$$

$$I_{total} \approx C_{I_{tot}} \sum_{i=0}^{t/\Delta t} D(i) \Delta t - \langle DC \rangle t, \quad (6)$$

where  $\Delta t$  is the sampling time. A higher order integration scheme can also be used instead of (6) to improve accuracy. This bias correction has to be calculated separately in each shot.

Switching the toroidal magnetic field on causes an offset in the toroidal current measurement, which has to be corrected by subtracting the average value measured in the  $\tau_{OH}$  long interval before switching on the toroidal electrical field.

### 3.1 Determination of vacuum chamber parameters

In GOLEM, part of the toroidal current always flows in the vacuum vessel, which has to be taken into account during the interpretation of experimental results. In a vacuum shot, when no plasma is formed, it is possible to determine the resistance of the vacuum vessel: all the current measured by the Rogowski-coil flows in the vessel. This is an important parameter for further evaluations.

Let us denote the loop voltage with  $U_l$ , the resistance of the chamber by  $R_{ch}$ , the total current (which is the chamber current ( $I_{ch}$ ) in this case) with  $I_{tot}$  and the inductance of the chamber by  $L_{ch}$ .

The circuit equation is then

$$U_l(t) = R_{ch} \cdot I_{tot}(t) + L_{ch} \frac{dI_{tot}}{dt}. \quad (7)$$

Using the loop voltage measurement and the Rogowski-coil, we have both  $U_l$ ,  $I_{tot}$  and  $dI_{tot}/dt$  measured, so  $R_{ch}$  and  $L_{ch}$  can be determined.

A simple method is the following: Just after switching on the toroidal electric field, the toroidal current is still close to zero ( $I_{tot} \approx 0$ ), so  $U_l \approx L_{ch} dI_{tot}/dt$ , so  $L_{ch}$  can be determined. On the other hand, at the flat top of the current curve ( $dI_{tot}/dt \approx 0$ ) equation (7) simplifies to  $U_l \approx R_{ch} \cdot I_{tot}$ , so  $R_{ch}$  can be estimated.

A more sophisticated method is a 2D least squares linear fit making use of all data points ( $U_l, I_{tot}, dI_{tot}/dt$ ). Since we have only two independent parameters  $R_{ch}$  and  $L_{ch}$ , the fitted plane has to pass through the origin. If we divide equation (7) by  $I_{tot}$ , we can simplify the task to a 1D least squares linear fit, which can be easily implemented in MATLAB (OCTAVE), using *polyfit* function.

Values of  $R_{ch}$  and  $L_{ch}$  should be calculated for about 5 discharges having different parameters, and the results should be compiled to a single best estimate for both parameters. Estimation should be performed by both methods described above, and the results of the method giving the more precise estimates should be used in the further steps.

8

### 3.2 Plasma breakdown

After measuring the vacuum chamber properties, we can make the next step towards creating a tokamak plasma: we can let  $H_2$  gas into the chamber before initiation of the toroidal electric field. The  $p_{H_2}$  value, which can be set as a discharge parameter, is a control parameter for the inlet valve. The actual value of the pre-discharge gas pressure is measured by a vacuummeter  $p_{ch}$ .

As we will see, letting  $H_2$  gas into the chamber is not always sufficient to produce a plasma. The toroidal electric field must also reach a critical value for mass ionization, in other words plasma breakdown.

The task is to plot the  $p_{ch}$  against the maximum of the loop voltage spikes in the beginning of the discharge for several discharges, and indicate the plasma breakdown by the shape of the symbols. Shots should be concentrated around the critical line separating breakdown and non-breakdown shots. Detailed scan should be performed for a given magnetic field and the effect of the magnetic field should be studied with a few discharges. During this exercise the pre-ionization should be turned on to produce more reproducible results, but the effect of turning it off could also be studied. About a total of **30** discharges are available for this exercise.

### 3.3 Estimation of main plasma parameters

If plasma breakdown occurs, plasma parameters can be determined - with different accuracy - from the measured parameters. The aim of this task is to investigate the effect of different parameters on the performance of the discharge, and reach discharges with the highest central temperature, plasma energy or energy confinement time. This task should result in about **25** discharges.

#### 3.3.1 Plasma current

A simple electrical model for the inductive current drive is a time-varying voltage source ( $U_i(t)$ ) connected to the plasma and the vacuum chamber in parallel can be seen on Figure 6. Both the vacuum chamber and the plasma are modeled by LR circuits. The main difference is, that while the internal inductance and resistance of the chamber are constant, and thus they can be measured separately, the parameters of the plasma differ in each discharge.

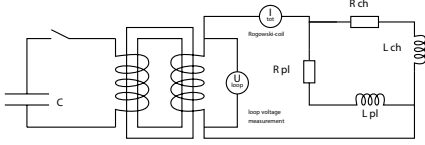


Figure 6: Model of the inductive current drive circuit

9

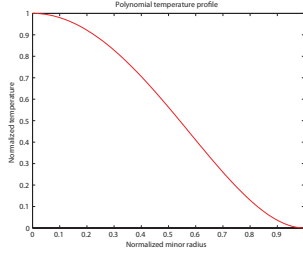


Figure 7: Equilibrium temperature profile used in the estimation of central plasma temperature

The central electron temperature ( $T_{e0}$ ) is then calculated from equation (3.20) of [3], which itself is based on Spitzer's resistivity formula:

$$T_{e0}(t) = \left( \frac{R_0}{a^2} \frac{8Z_{eff}}{1544} \frac{1}{R_{pl}(t)} \right)^{2/3}, \quad (13)$$

where  $R_{pl}(t)$  is in Ohms, distances are in meters and we get  $T_{e0}(t)$  in electronvolts.

It has to be noted that plasma in the GOLEM tokamak is only fully ionized in the central region,  $Z_{eff}$  can be estimated with large uncertainty and even the  $a$  plasma small radius might change in an unmonitored way due to the lack of plasma stabilization. All these factors make the estimation of the central electron temperature quite uncertain.

Nevertheless, central electron temperature has to be calculated for all discharges with plasma and the maximum value has to be included in the shot summary table.

#### 3.3.4 Electron density

In its current state, the GOLEM tokamak does not have any density measurements. However, as electron density is needed for further calculations, we estimate its order of magnitude from the state law of ideal gases.

For the average density it is assumed, that it is constant during the discharge, apart from the dissociation of the hydrogen gas. There is a 30 second delay between the gas filling and the actual shot, which is enough for the gas to reach thermal equilibrium with the chamber wall. Chamber temperature is monitored with respect to the room temperature, and the difference is normally be zero, but should be checked. (If chamber temperature is not measured, room temperature can be used instead.) The ideal gas law is used to give an order of magnitude estimate of the electron density (in particle/ $m^3$ ):

$$n_{avr} = \frac{2p_{ch}}{k_B T_{ch}}. \quad (14)$$

We have to note that this is a very rough estimate basically for two reasons:

The basic circuit equations are:

$$U_i(t) = R_{ch} \cdot I_{ch}(t) + L_{ch} \frac{dI_{ch}(t)}{dt} \quad (8)$$

$$U_i(t) = R_{pl}(t) \cdot I_{pl}(t) + L_{pl} \frac{dI_{pl}(t)}{dt} \quad (9)$$

$$I_{tot}(t) = I_{pl}(t) + I_{ch}(t) \quad (10)$$

The chamber parameters have already been determined according to Section 3.1. As a first approximation, we can neglect the inductance of the plasma ( $L_{pl} \approx 0$  H), and we can integrate the (8) circuit equation using the initial condition  $I_{tot}(t=0) = I_{ch}(t=0)$  to arrive to  $I_{ch}(t)$ . This can then be used to determine the plasma current, as  $I_{pl}(t) = I_{tot}(t) - I_{ch}(t)$ . Plasma resistivity can be determined in turn from equation (9).

*This task needs some programming that should be done parallel to the task described in Section 3.2!*

It can be attempted to investigate the effect of the  $L_{pl} \approx 0$  H approximation by a more careful integration of choosing  $L_{pl} \approx L_{ch}$  in the time region with plasma. If significant differences are found, this latter approximation has to be implemented for all further data processing.

Plasma current has to be calculated for all discharges with plasma and the maximum value has to be included in the shot summary table.

#### 3.3.2 Plasma heating power

In the GOLEM tokamak the only heating mechanism of the plasma is ohmic heating resulting from current flowing in a conductor with finite resistivity. The ohmic heating power can be calculated as:

$$P_{OH}(t) = R_{pl}(t) \cdot I_{pl}^2(t) \quad (11)$$

Ohmic heating power has to be calculated for all discharges with plasma and the maximum value has to be included in the shot summary table.

#### 3.3.3 Central electron temperature

Specific resistivity of a fully ionized plasma only depends on its electron temperature ( $T_e$ ) and effective charge number ( $Z_{eff}$ ). This dependence is quantified by the Spitzer formula [2]. It has to be noted that the ion temperature can be very much different from electron temperature. The effective charge number is determined by the amount, composition and state of impurities in the  $H_2$  plasma, and we can take value  $Z_{eff} \approx 2.5$  for GOLEM plasmas.

Center of the plasma has higher temperature, and lower resistivity with higher current density, which makes the estimation of the electron temperature ambiguous from an integrated value of resistivity ( $R_{pl}(t)$ ). However, if we use an equilibrium temperature profile (12) (Figure 7), measured in more detailed measurements [3], we can estimate one parameter of the profile, which is in this case the central electron temperature ( $T_{e0}(t)$ ):

$$T_e(r, t) = T_{e0}(t) \left( 1 - \frac{r^2}{a^2} \right)^2 \quad (12)$$

10

1. Plasma in the GOLEM tokamak is not fully ionized, which makes us overestimate the electron density.
2. Due to the plasma-wall interaction, adsorbed gases are released from the surface of plasma facing components during the discharge. These atoms enter the plasma and can be ionized, thus making us underestimate the electron density.

The order of magnitude estimate of the average electron density has to be calculated for all discharges with plasma and included in the shot summary table.

#### 3.3.5 Plasma energy

The total energy content can be simply calculated from the temperature, density and volume ( $V$ ), based on the ideal gas law, taking into account the assumed (12) temperature profile:

$$W_{pl}(t) = V \frac{n_{avr} k_B T_{e0}(t)}{3}. \quad (15)$$

The information that the magnetic field reduces the degrees of freedom of the particles to two has been used to derive this formula.

Uncertainty of this formula is dominated by the uncertainty of our density estimate, which makes it good only for an order of magnitude estimate. Qualitative time trace reflects that of the electron temperature and thus is more reliable.

Nevertheless, plasma energy has to be calculated for all discharges with plasma and the maximum value has to be included in the shot summary table.

#### 3.3.6 Energy confinement time

Having an estimate for the plasma energy, the energy confinement time can be estimated at the point where the plasma energy has its maximum. In tokamaks with more stable plasma, this maximum can be taken for an extended duration of time, and this region is called the flat-top.

During the flat-top, the ohmic heating power equals the losses, allowing us to calculate the energy confinement time:

$$\tau_E(t_{top}) = \frac{W_{pl}(t_{top})}{P_{OH}(t_{top})}. \quad (16)$$

$$\frac{dW_{pl}}{dt}(t_{top}) = 0. \quad (17)$$

Given the uncertainty of the input parameters, this value for the energy confinement time should be taken with care. Nevertheless, it should be included in the shot summary table.

### 3.4 $q = 2$ disruptions

When the plasma current grows so strong that the edge safety factor, defined by (1), reaches the value of 2, a plasma instability resonant to the  $q = 2$  rational surface destabilizes, and a discharge terminating disruption occurs. This limit of operation is to be attempted to be reached in this task using about **5** dedicated shots.

We can calculate the poloidal field at the edge (for large aspect ratio circular tokamaks) using Ampère's law, as the enclosed current is the total plasma current:

$$B_p(a, t) = \frac{\mu_0 I_{pl}(t)}{2\pi a}, \quad (18)$$

12

where  $a$  is the plasma minor radius. Substituting this expression into formula (1), the safety factor at the edge can be estimated as:

$$q(a, t) = \frac{a^2}{R_0} \frac{2B_t(t)\pi}{\mu_0 I_p(t)}. \quad (19)$$

Discharges aiming to reach a low  $q(a, t)$  need as large plasma current as possible. As we have very limited control over the evolution of plasma current in GOLEM, we can also set the  $\tau_{OH}$  time delay to set up a discharge at the declining phase of the toroidal magnetic field, which will constantly decrease the edge safety factor.

In order to monitor the success of our efforts, the evolution of the discharges should be plotted on the Hugill diagram. The Hugill diagram positions a discharge on the plane of two parameters:

- Inverse edge safety factor:  $\frac{1}{q(a, t)}$
- Murakami parameter (normalized density):  $\frac{n_{avg} R_0}{B_t}$

The Hugill diagram serves as an operation envelope for tokamaks. If either the Murakami parameter is too high or the inverse edge safety factor reaches the value of 0.5, the plasma disrupts.

First, the temporal evolution of the dedicated shots aiming  $q = 2$  disruptions should be plotted on the Hugill diagram. Afterwards, all previous shots could be plotted to check that none reach the region  $1/q > 0.5$ .

## 4 Requirements for the measurement logbook

There should be a single measurement log written in English language. The measurement log should include:

- Exact method of executing the measurement.
- Exact method of derivation of final results.
- Results of the measurement tasks.
- Time traces of shot parameters for some characteristic shots.
- Shot summary table indicating all calculated parameters of all shots executed. (Unsuccessful shots also need to be recorded.)
- Skype log as appendix

All comments and proposals regarding the measurements are welcome.

It would be nice, if the participants of the session would write some thankful words to the <http://golem.fjfi.cvut.cz/hodnoceni.html> homepage, and/or send a postcard to the following address: Tokamak GOLEM, Brehova st. 7, Prague 1, Czech Republic. These activities should also be indicated in the logbook.

## References

- [1] John Wesson. The science of JET. In *JET Reports*, pages JET-R(99)13. 1999.
- [2] *NRL plasma formulary*. Naval Research Laboratory, 2009.
- [3] Jana Brotánková. *Study of high temperature plasma in tokamak-like experimental devices*. PhD thesis, Charles University in Prague, 2009.

## Measurement log for the 2010.01.14. GOLEM experiment from BME-NTI

Csaba Buday  
Gergo Pokol  
Daniel Imre Refy

January 28, 2010

- Vessel pressure through the vacuum system ( $P_v$ ). Local!
  - The temperature of the vacuum chamber ( $T_{ch}$ ). Local!
- The diagnostics we would like to use during our session:
- Loop voltage.
  - Total toroidal current by Rogowski coil.
  - Toroidal field measurement coil.
  - Plasma radiation by photodiode.

## Chapter 1

### Introduction

The measurement series presented herein was performed with the aim to explore the possibility of developing a regular student measurement program in the Budapest University of Technology and Economics (BME), Institute of Nuclear Techniques (NTI) making use of the remote measurement potential of the GOLEM tokamak. The student measurement is to be developed for students at the nuclear technology branch of the physics MSc program at BME. The purpose of such measurement would be to demonstrate the very basics of tokamak operation, and to get the students acquainted with basic properties and operational limits.

The experiment was remote controlled by the Hungarian party: Csaba Buday, Daniel Imre Refy and Gergo Pokol, and supervised by the Czech party: Dr. Vojtech Svoboda. Measurements were performed on the 14th January 2010. 9:20-13:45 by controlling the GOLEM tokamak from the Electronics laboratory of BME NTI.

#### 1.1 Measurement conditions

The GOLEM is a small size tokamak device equipped with basic controls and diagnostics having dimensions:

- Major radius at the magnetic axis:  $R_0 = 0.4$  m.
- Minor radius:  $r_0 = 0.1$  m.
- Radial position of the limiter:  $a_0 = 0.085$  m.

The parameters that can be set (most of them remotely) are:

- Toroidal magnetic field ( $B_t$ ) through the voltage of the toroidal field capacitor bank ( $U_B$ ).
- Toroidal electric field ( $E_t$ ) through the capacitor bank for the ohmic heating ( $U_E$ ).
- The time delay between the triggers of the toroidal field and the ohmic heating ( $\tau$ ).
- Hydrogen gas pressure ( $P_{H2}$ ).

1

## Chapter 2

### Measurement evaluation

During the reported session, measurements were set up and shots were initiated using a SSH connection to the *buon.fjfi.cvut.cz* control computer. On the Budapest side the SSH shell was provided by a Putty program running on a Windows system. Shots were programed into a text file named *makefile* by the Hungarian party following the examples found at the beginning of the file. After confirmation from the Czech party, shots were started by the Hungarian party using the `makefile tag` command in the SSH shell, where `tag` is the label of the shot series in the file named *makefile*. The file used is copied into Appendix 4. Communication between the parties was by Skype instant messaging involving three parties. The Skype log of the session is copied into Appendix 5. Using these tools, remote control and communication went smoothly.

After executing the `firsttrial` and `scndtrial` trial shots, the measurement program unfolded as follows.

#### 2.1 Data sources

All the recorded data and the settings for each shot are available at the GOLEM website. The root directory for the files is:

`http://golem.fjfi.cvut.cz/operation/shots/<shotnumber>/`

Basic data of the present shot series is collected at:

`http://golem.fjfi.cvut.cz/operation/tasks/Practica/BudapestBME-NTI/140110_0850/`

During the evaluation not all the files were needed. Used ones are:

- `/basicdiagn/usbscopes` (time-dependent measurements:  $U_{loop}$ ,  $dB_t$ ,  $dI_{total}$ , photodiode signal)
- `/Aktual_PfeifferMerkaVakua` (initial pressure [mPa])
- `/Td_aktual` (time delay between toroidal field and inductive current drive [us])

- `/Aktual_TermoclanekNaKomore` (relative temperature of the chamber (compared to room temperature) [K])

We have a direct measurement for the loop voltage, while the toroidal magnetic field and the total current signals must be integrated and multiplied by a calibration factor.

The sampling rate is 100 kHz, and the shot starts at 5 ms, so we have 500 samples from the background noise. This is important, because using this we can measure the bias, and correct the integrated values with this factor. The Rogowski coil measurement, for example, has a large negative bias needing correction. The algorithm is the following: we average the first 450 data points ( $\langle bkg \rangle$ ), and subtract it from the measured value ( $D(t)$ ):

$$\langle bkg \rangle = \int_0^{4.5 \text{ ms}} D(t') dt' \approx \sum_{i=0}^{450} D(i); \quad (2.1)$$

$$I_{total} = c_1 \left( \int_0^t D(t') dt' - \langle bkg \rangle t \right) \quad (2.2)$$

This bias correction has to be calculated in each shot.

For the evaluation, it is important to know the time of the flat-top window. We simply define the flat-top by taking the maximum of the total current.

## 2.2 Vacuum shot evaluation

In GOLEM, part of the toroidal current always flows in the vacuum vessel, which has to be taken into account during the interpretation of experimental results. In a vacuum shot, when no plasma is formed, it is possible to determine the resistance of the vacuum vessel: all the current measured by the Rogowski-coil flows in the vessel. This is an important parameter for further evaluations.

Let us denote the loop voltage with  $U_l$ , the resistance of the chamber with  $R_{ch}$ , the total current (which is the chamber current ( $I_{ch}$ ) in this case) with  $I_{tot}$  and the inductance of the chamber with  $L_{ch}$ .

The circuit equation is then

$$U_l = R_{ch} \cdot I_{tot} + L_{ch} \frac{dI_{tot}}{dt} \quad (2.3)$$

Using the loop voltage measurement and the Rogowski-coil, we have both  $U_l$  and  $I_{tot}$  measured, so  $R_{ch}$  and  $L_{ch}$  can be determined.

Let us notice, that this is a linear model:

$$\begin{bmatrix} I(0) & dI(0)/dt \\ I(1) & dI(1)/dt \\ \dots & \dots \end{bmatrix} \cdot \begin{bmatrix} R_{ch} \\ L_{ch} \end{bmatrix} = \begin{bmatrix} U_{loop}(0) \\ U_{loop}(1) \\ \dots \end{bmatrix} \quad (2.4)$$

This means, we can use the linear least squares method to approximate the values of the  $\underline{a}$  vector:

$$\underline{\hat{a}} = (\underline{B}^T \underline{B})^{-1} \underline{B}^T \underline{q}$$

Because of the parallel connection, the voltage is the same on both circuits:

$$U_{loop} = R_{ch} \cdot I_{ch} + L_{ch} \frac{dI_{ch}}{dt} \quad (2.5)$$

$$U_{loop} = R_{pl} \cdot I_{pl} + L_{pl} \frac{dI_{pl}}{dt} \quad (2.6)$$

$$I_{pl} + I_{ch} = I_{tot} \quad (2.7)$$

$$\frac{dI_{ch}}{dt} + \frac{dI_{ch}}{dt} = \frac{dI_{tot}}{dt} \quad (2.8)$$

All parameters are known in the (2.5) differential-equation, so it can be solved with the initial conditions: both the current and its time derivative being equal to zero at  $t=0$ . The plasma current is just the difference between the total and the chamber current.

Both the resistance and the internal inductance of the plasma vary in time, so there is no straightforward way to determine them from the (2.6) equation. If we assume that the inductance term is negligible compared to resistance term, plasma resistance ( $R_{pl}$ ) can be calculated.

The Ohmic heating power can be calculated as follows:

$$P_{OH}(t) = U_{loop}(t) \cdot I_{pl}(t). \quad (2.10)$$

The safety factor at the edge can be estimated as:

$$q_{edge} = \frac{a_0^2}{R_0} \frac{2B_t \pi}{\mu_0 I_{pl}}, \quad (2.11)$$

where  $a_0$  is the plasma minor radius.

For the average density we assumed, that it was constant during the discharge, apart from the dissociation of the hydrogen gas. There is a 30 second delay between the gas filling and the actual shot, which was supposed to be enough for the gas to reach thermal equilibrium with the chamber wall. Chamber temperature was monitored with respect to the room temperature, and the difference was found to normally be zero. The room temperature is again assumed to be 300 K. The ideal gas law is used to calculate the density (in particle/ $m^3$ ):

$$n = \frac{p}{k_B T}. \quad (2.12)$$

The central plasma temperature ( $T_{e0}$ ) is calculated from equation (3.20) of [1], which itself is based on Spitzer's resistivity formula, and an assumed temperature profile:

$$T_{e0} = \left( \frac{R_0}{a_0^2} \frac{8Z_{eff}}{1.544 \cdot 10^{-3}} \frac{I_{pl}}{U_{loop}} \right)^{2/3} \quad (2.13)$$

The energy content of the plasma is calculated from the temperature, density and volume, based on the ideal-gas law, taking into account the assumed temperature profile:

$$W_{pl} = \frac{f n k_B T_e(0)}{6}. \quad (2.14)$$

Because we know both the total current and it's time derivative, we know everything on the right hand side of the equation, meaning we can evaluate it.

This way, we determined the internal inductance and the resistance of the chamber, which are:

$$R_{ch} = 9.81 \text{ m}\Omega \quad L_{ch} = 7.5 \cdot 10^{-4} \text{ mH}$$

Experiment was conducted by running the shot series labeled `vacuumseq` (see Chapter 4). Shot numbers of vacuum shots: #1554-1556, #1558-1561 and #1613.

The tokamak has an inductive heating system, mainly for baking the vacuum vessel, but it can also be used to alter the resistance of the chamber. By heating up the chamber with the baking system, and doing vacuum shots, we can measure the chamber resistance at different chamber temperatures. This way, vacuum chamber resistivity calculations can be checked.

#	$t[s]$	$U_l[V]$	$B_t[T]$	$I_{tot}[kA]$	$R_{ch}[m\Omega]$	$L_{ch}[mH]$
1554	0.0060	10.5	0.037	1.03	10.32	0.00107
1555	0.0061	18.9	0.045	2.01	9.20	0.00083
1556	0.0080	14.0	0.112	1.29	8.79	0.00029
1558	0.0061	4.1	0.047	0.53	7.38	0.00047
1559	0.0060	10.5	0.039	0.94	11.31	0.00088
1560	0.0061	18.7	0.043	1.96	9.96	0.00077
1561	0.0061	25.5	0.041	2.45	10.91	0.00088
1613	0.0060	29.5	0.038	2.92	10.61	0.00084
1620	0.0060	20.4	0.038	1.93	10.93	0.00082
1622	0.0059	20.1	0.037	1.76	11.44	0.00114

Table 2.1: Table of resistivity and impedance values from vacuum shots

Experiment was conducted by running the shot series labeled `vacuumheated` (see Chapter 4) after heating the chamber to  $100^\circ \text{ deg C}$  (shot #1620) and  $200^\circ \text{ C}$  (shot #1622) relative to room temperature. The room temperature is assumed to be 300 K. Calculated resistivity and impedance values are summarized in Table 2.1 for all vacuum shots.

It can be concluded that resistivity seems to be higher at higher temperature, which is in good agreement with the expectations, however, resistivity values at room temperature show the large uncertainty of the measurement. Making more measurements at higher temperatures could make this experiment more conclusive, but it is probably not worth the effort to do it remotely, as it inevitably requires manual local control of the vacuum chamber heating.

## 2.3 Plasma shot evaluation

Knowing the resistance ( $R_{ch}$ ) and inductance of the chamber ( $L_{ch}$ ), we can proceed to the plasma current evaluation. A simple electrical model of the tokamak is a time-varying voltage source ( $U_{loop}$ ) which is connected to two parallel LR circuits. One circuit is the chamber, the other one is the plasma.

During the flat-top the ohmic heating power equals to the losses, this way we calculate the energy confinement time:

$$\tau_E = \frac{W_{pl}}{P_{OH}}. \quad (2.15)$$

The experiment was conducted according to plans: shot series labeled `grandloop_n1` (see Appendix 4). Some shots needed to be repeated (`repeatseq`), and the  $U_B$ - $U_E$  grid was refined at areas of special interest (`detailed_loop1`). Finally, runaway electrons were searched for (`runaway_seq`, `runaway_seq2`). Results for each shot are summarized in the Tables 2.2 and 2.3. Table 2.2 shows parameters of shots having no breakdown due to too low  $U_E$  values, and Table 2.3 shows parameters of shots successfully generating plasma.

It can be concluded that all parameters estimated with the above simple methods are in the right order of magnitude therefore a similar evaluation procedure can be suitable to demonstrate the most important parameters of the tokamak plasma. The experiment can be declared to be successful in that sense, despite having some difficulties: some discharges failed and reproducing discharges had some uncertainties. *No runaway electron discharges* were found probably due to the lack of pre-ionization and/or large enough toroidal electrical fields. We speculate that pre-ionization might also improve on the reproducibility of the discharges, and make runaway discharges possible.

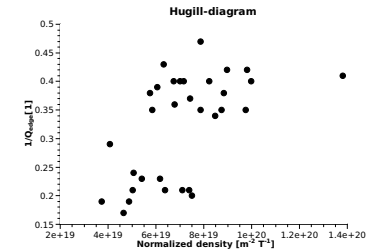


Figure 2.1: Shots with breakdown in the coordinate system of the Hugill diagram

Shots with breakdown were plotted in the coordinate system of the Hugill diagram. The  $1/q$  region is completely consistent with the criterion that  $q_{edge}$  must be greater than 2. The normalized density of  $n_e^{norm} R/B_t$  seems to be little high for GOLEM, so it might needed to check if it is in the right order of magnitude, and if there exists a better way of estimating it.

Figures 2.2 and 2.3 show the temporal evolution of the plasma current and the edge safety factor respectively for shot #1610. This is the discharge shown on the 2.1 Hugill diagram most closely approaching the value of  $q_{edge} = 2$ . In



#	$t[s]$	$U_l[V]$	$B_l[T]$	$I_{tot}[kA]$	$Photo.[a.u.]$
1548	0.008	-30.0	0.108	1.58	0.011
1549	0.008	14.2	0.109	1.37	0.004
1551	0.008	14.0	0.107	1.38	0.006
1553	0.003	-0.1	0.090	0.01	0.011
1554	0.006	10.5	0.037	1.03	0.004
1555	0.006	18.9	0.045	2.01	0.001
1556	0.008	14.0	0.112	1.29	0.008
1558	0.006	4.1	0.047	0.53	0.006
1559	0.006	10.5	0.039	0.94	0.001
1560	0.006	18.7	0.043	1.96	0.011
1561	0.006	25.5	0.041	2.45	0.008
1562	0.007	4.1	0.080	0.65	0.008
1563	0.007	10.2	0.075	1.05	0.008
1565	0.007	23.4	0.083	2.37	0.015
1566	0.007	4.1	0.125	0.30	0.004
1567	0.007	10.9	0.125	1.35	0.001
1570	0.007	4.4	0.140	0.33	0.004
1571	0.011	-0.1	-0.001	0.05	0.004
1574	0.008	4.1	0.091	0.34	0.001
1575	0.007	10.5	0.076	1.15	0.008
1578	0.007	4.1	0.117	0.61	0.006
1579	0.007	10.2	0.106	1.34	0.004
1582	0.007	4.1	0.142	0.82	0.006
1583	0.007	10.9	0.145	1.12	0.008
1586	0.007	4.4	0.073	0.34	0.008
1587	0.007	10.5	0.077	1.23	0.011
1590	0.000	-0.1	0.000	0.00	0.006
1591	0.027	0.1	0.000	0.07	0.004
1594	0.007	4.1	0.159	0.20	0.008
1595	0.007	10.2	0.147	1.22	0.013
1598	0.007	10.2	0.142	0.81	0.004
1599	0.007	4.1	0.116	0.42	0.013
1600	0.007	10.9	0.110	1.02	0.004
1613	0.006	29.5	0.038	2.92	0.011
1614	0.006	28.6	0.038	2.68	0.001
1615	0.006	28.4	0.040	2.85	0.008
1616	0.006	28.6	0.042	2.87	0.008
1617	0.006	28.4	0.040	2.93	0.008
1618	0.006	28.6	0.040	2.78	0.006
1619	0.006	28.6	0.047	2.78	0.013
1620	0.006	20.4	0.038	1.93	0.001
1621	0.005	0.1	0.000	0.01	0.018
1622	0.006	20.1	0.037	1.76	0.013

Table 2.2: Shots without breakdown

#	$t$ [s]	$U_l$ [V]	$B_l$ [T]	$I_{tot}$ [kA]	$Photo.$ [a.u.]	$I_{pl}$ [kA]	$q_{edge}$ [1]	$P_{OH}$ [kW]	$T_{eo}$ [eV]	$\tau_E$ [s]
1550	0.011	9.3	0.156	3.33	0.076	2.39	5.0	22	36	1.010E-4
1552	0.010	8.8	0.160	3.44	0.084	2.52	4.8	22	39	1.100E-4
1557	0.010	9.3	0.162	3.53	0.086	2.59	4.8	24	38	9.600E-5
1564	0.009	12.1	0.128	4.65	0.102	3.40	2.9	41	39	5.000E-5
1568	0.009	11.2	0.197	4.70	0.109	3.57	4.2	40	42	5.500E-5
1569	0.009	17.5	0.189	7.31	0.138	5.52	2.6	97	42	2.500E-5
1572	0.009	12.4	0.244	4.81	0.109	3.57	5.2	44	39	4.300E-5
1573	0.008	17.8	0.230	6.73	0.124	5.00	3.5	89	39	2.100E-5
1576	0.009	12.1	0.134	4.75	0.095	3.51	2.9	42	39	5.500E-5
1577	0.009	19.2	0.139	5.95	0.128	4.19	2.5	81	33	2.400E-5
1580	0.009	11.4	0.197	4.26	0.107	3.08	4.9	35	38	7.100E-5
1581	0.009	18.0	0.185	7.82	0.140	6.07	2.3	109	44	2.500E-5
1584	0.009	10.9	0.264	4.47	0.107	3.32	6.0	36	41	7.200E-5
1585	0.009	16.6	0.246	5.56	0.128	3.86	4.9	64	34	3.500E-5
1588	0.009	12.4	0.133	5.48	0.109	4.21	2.4	52	44	5.800E-5
1589	0.009	18.0	0.134	5.42	0.107	3.57	2.9	64	31	3.300E-5
1592	0.009	10.9	0.210	4.73	0.102	3.63	4.4	40	43	7.500E-5
1593	0.009	16.1	0.192	7.55	0.131	5.84	2.5	94	46	3.300E-5
1596	0.009	11.4	0.263	5.01	0.109	3.87	5.2	44	44	6.700E-5
1597	0.009	16.6	0.238	5.83	0.131	4.15	4.4	69	36	3.500E-5
1601	0.009	13.8	0.139	5.46	0.116	4.06	2.6	56	40	4.600E-5
1602	0.009	16.8	0.133	5.29	0.107	3.60	2.8	60	32	3.300E-5
1603	0.009	20.4	0.122	6.13	0.102	3.92	2.4	80	30	2.200E-5
1604	0.010	15.4	0.152	5.54	0.102	4.20	2.8	65	38	3.200E-5
1605	0.009	15.2	0.147	6.10	0.095	4.48	2.5	68	40	3.200E-5
1606	0.009	18.2	0.151	6.16	0.114	4.25	2.7	77	34	2.600E-5
1607	0.010	14.0	0.172	6.41	0.109	5.12	2.6	72	46	3.500E-5
1608	0.010	15.4	0.180	6.29	0.109	4.85	2.8	75	42	3.100E-5
1609	0.009	18.2	0.164	6.87	0.102	4.97	2.5	90	38	2.500E-5
1610	0.008	24.8	0.099	5.94	0.046	3.49	2.1	86	24	1.100E-5
1611	0.008	23.2	0.091	5.17	0.069	2.77	2.5	64	22	1.600E-5
1612	0.007	24.8	0.072	4.80	-0.015	2.26	2.4	56	18	1.700E-5

Table 2.3: Shots with breakdown

fact, given the uncertainties of the measurements used, it might well even reach  $q_{edge} = 2$ . This later assumption is supported by the fact that the plasma current starts to decay and the discharge terminates shortly after reaching the lowest  $q_{edge}$  value. Even is shot #1610 ended with a  $q_{edge} = 2$  disruption, this was a rare occasion as it required a very steep plasma current rise to overcome the effect of the growing toroidal field on the edge safety factor according to equation (2.11).

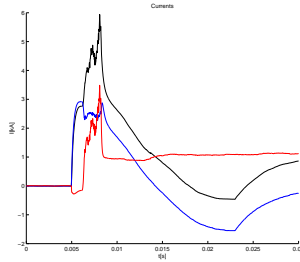


Figure 2.2: Time evolution of the total (black), chamber (blue) and plasma (red) currents for shot #1610

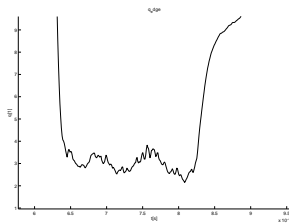


Figure 2.3: Time evolution of edge safety factor for shot #1610

## Chapter 3

## Discussion

Authors of this measurement log have discussed results with colleagues from KFKI-RMKI (Gabor Veres and Gabor Petravich), former operators of the MT-M1 tokamak. Some of the main conclusions are to be summarized in the following:

1. Inductance of the plasma could be estimated instead of neglecting it.
2. Best practice at the MT-M1 tokamak dictates that the  $\tau$  time delay between the inductive current drive and toroidal magnetic field condensers should be set so that the flattop of the toroidal magnetic field is made use of, in order to achieve the best performance discharges.
3. At the very low temperature plasma of GOLEM discharges, ionization is only partial and the Spitzer formula for conductivity should be used with care. In fact, the formula could be applied to the central, higher temperature part of the plasma, but such a calculation requires the knowledge of an estimate of temperature profile. Such a profile could be taken to be the equilibrium profile presented in [1]. In such a way, a rough estimate of the maximum temperature could be calculated from the plasma resistivity.
4. There appears to be no flattop during the discharge, so equilibrium profiles cannot develop and even the  $a_0$  plasma radius changes in time in an unmonitored way. Physical quantities derived using these data have huge uncertainties and can only be used for demonstration purposes.
5. It appears that measurements presented above could conclusively detect only the plasma breakdown operational limit. This could be interesting, however other operational limits of the Hugill diagram could also be attempted to be systematically measured:
  - (a) The low density runaway limit could be attempted to be measured. Toroidal electric field in GOLEM is calculated to be well above the critical electric field for runaway electron generation. The physical mechanism of runaway electron generation requires pre-ionization of the plasma, so such a measurement would require to switch it on. (It was always switched on in MT-M1.) A runaway discharge should be recognizable from the measurements having plasma current but no signal on the photodiode.

- (b) The  $q = 2$  disruption limit could be attempted to be demonstrated by setting the discharge time to the downslope of the toroidal magnetic field. This would cause a rapid decrease in the boundary safety factor.
6. It would be nice to demonstrate the meaning and calculation of the  $\tau_E$  energy confinement time. Having no diamagnetic loop measurement, this requires the calculation of total kinetic plasma energy from the ideal gas law, which requires the density as a parameter. The order of magnitude of the average density can be estimated from pre-discharge chamber pressure. (The influx from the wall is expected to be limited in the GOLEM tokamak due to low edge temperatures.) Taking the equilibrium profile from [1], one can estimate the total kinetic energy, and so the energy confinement time at the "flattop", where total kinetic energy curve has its maximum.

Based on these remarks, a proposal for a GOLEM discharge series will be prepared shortly. Such a measurement series is necessary before writing the instructions for the student measurement.

## Bibliography

- [1] Jana Brotánková. *Study of high temperature plasma in tokamak-like experimental devices*. PhD thesis, Charles University in Prague, 2009.

## Chapter 4

## Appendix: Remote control file

```

firsttrial: #without hydrogen
make -lBs -C velin shot Ue=400 Ub=400 Td=2000 HZfilling=0 pR2=68

scndtrial: #with hydrogen
make -lBs -C velin shot Ue=400 Ub=400 Td=2000 HZfilling=1 pR2=66

H2seq:
make -lBs -C velin shot Ue=400 Ub=400 Td=2000 HZfilling=0 pR2=66 #R2 off
make -lBs -C velin shot Ue=400 Ub=400 Td=2000 HZfilling=1 pR2=66 #approx 30 mPa
make -lBs -C velin shot Ue=400 Ub=400 Td=2000 HZfilling=1 pR2=68 #approx 40 mPa
make -lBs -C velin shot Ue=400 Ub=400 Td=2000 HZfilling=1 pR2=70 #approx 50 mPa
make -lBs -C velin shot Ue=400 Ub=400 Td=2000 HZfilling=1 pR2=75 #approx 70 mPa
make -lBs -C velin shot Ue=400 Ub=400 Td=2000 HZfilling=1 pR2=100 #approx 100 mPa

firstloop:
for Ue in 'seq 300 100 700'; do\
make -lBs -C velin shot Ue=$Ue Ub=400 Td=2000 pR2=68 HZfilling=1;\
done;\

grandloop:
for Td in 'seq 2000 2000 8000'; do\
for pR2 in 68 70 72; do\
for Ub in 'seq 600 300 1200'; do\
for Ue in 'seq 600 300 1200'; do\
make -C velin -lBs shot Ue=$Ue Ub=$Ub Td=$Td pR2=$pR2 HZfilling=1;\
done;\
done;\
done;\
done;\

vacumseq:
for Ue in 'seq 100 200 700'; do\
make -lBs -C velin shot Ue=$Ue Ub=400 Td=0 pR2=66 HZfilling=0;\
done;\

grandloop_wt1:
for pR2 in 66 70 100; do\
for Ub in 'seq 400 200 800'; do\
for Ue in 'seq 100 200 700'; do\
make -C velin -lBs shot Ue=$Ue Ub=$Ub Td=1000 pR2=$pR2 HZfilling=1;\
done;\
done;\
done;\

repeatseq:
make -lBs -C velin shot Ue=300 Ub=800 Td=1000 HZfilling=1 pR2=66

```

```

make -lBs -C velin shot Ue=100 Ub=600 Td=1000 HZfilling=1 pR2=100
make -lBs -C velin shot Ue=300 Ub=600 Td=1000 HZfilling=1 pR2=68

detailed_loop:
for pR2 in 66 ; do\
for Ub in 'seq 400 50 800'; do\
for Ue in 'seq 600 100 800'; do\
make -C velin -lBs shot Ue=$Ue Ub=$Ub Td=1000 pR2=$pR2 HZfilling=1;\
done;\
done;\
done;\

runaway_seq:
for pR2 in 60 62 64 ; do\
make -C velin -lBs shot Ue=800 Ub=400 Td=0 pR2=$pR2 HZfilling=1;\
done;\
make -lBs -C velin shot Ue=800 Ub=400 Td=0 HZfilling=0 pR2=60

runaway_seq2:
for pR2 in 68 59 60; do\
make -C velin -lBs shot Ue=800 Ub=400 Td=0 pR2=$pR2 HZfilling=1;\
done;\

vacumheated:
make -lBs -C velin shot Ue=500 Ub=400 Td=0 HZfilling=0 pR2=68

```

## Appendix: Log of conversation during the experiment

[illegible]

2020.01.14. 13:21:14 svbwnboj: OK, I continue heating, do not make shots ...  
2020.01.14. 13:21:18 Remy Banaal: well done  
2020.01.14. 13:21:21 Remy Banaal: ok  
2020.01.14. 13:22:43 svbwnboj: heating on again ...  
2020.01.14. 13:31:00 Remy Banaal: can i start?  
2020.01.14. 13:31:09 svbwnboj: moment  
2020.01.14. 13:33:12 svbwnboj: go on  
2020.01.14. 13:33:20 Remy Banaal: started  
2020.01.14. 13:34:29 svbwnboj: It went down very quickly, I will go up to 200 once more again  
2020.01.14. 13:40:02 Remy Banaal: ok  
2020.01.14. 13:40:57 svbwnboj: 1621 was bad!  
2020.01.14. 13:41:57 Remy Banaal: yes ...  
2020.01.14. 13:41:53 Remy Banaal: can i start the next shot?  
2020.01.14. 13:42:14 svbwnboj: go  
2020.01.14. 13:44:03 Remy Banaal: well done  
2020.01.14. 13:44:15 svbwnboj: So 72 shots for Budapest, ok, can we finish?  
2020.01.14. 13:44:25 Remy Banaal: yes, thank you!  
2020.01.14. 13:45:45 svbwnboj: Best regards! I am looking forward to you (and postcard). And we are welcome for the next time. You are the very first so heavily working remotely on the GUESS tokamak. Thank you. Vojtech Svoboda  
2020.01.14. 13:46:09 gergo.gubol: Thank you for the important work! Best regards!  
2020.01.14. 13:46:33 Remy Banaal: best regards! have a nice day!  
2020.01.14. 13:46:33 svbwnboj: Remy Banaal: bye

## Appendix D

# GOMTRAIC 2013 reports

Online versions available at following addresses:

- MHD group
- Rake probe group
- Tomography group
- HXR group

# Plasma MHD Activity Observations via Magnetic Diagnostics.

GOMTRAIC 2013

Faculty of Nuclear Sciences and Physical Engineering  
Prague

## Plasma MHD Activity Observations via Magnetic Diagnostics

F.Ostyn\* M.R. Ramos\*\* D.H.Arriaga\*\*\*

10 de mayo de 2013

### Índice

1. Introduction	2
2. Basics of the theory	2
2.1. Plasma & Fusion	2
2.2. Magnetic confinement: Tokamak	4
2.3. GOLEM	5
2.4. Magnetis Islands	7
3. Principles of the measurement	9
4. Measurement setup	11
5. Data processing methods	13
5.1. Fluctuation of raw data analysis (theta-time diagram)	13
5.2. Spectrogram	16
5.3. Cross correlation analysis	18
6. Results	20
7. Discussion	21
8. Appendix	22
8.1. Appendix I	22
8.1.1. Safety Factor	22
8.2. Appendix II	24
8.2.1. Frederyk's Scripts	24
8.3. Appendix III	28
8.3.1. List of	28
9. Bibliography	29

\*UGent

\*\*University of Seville

\*\*\*CICATA-IPN

1

Faculty of Nuclear Sciences and Physical Engineering of the Czech Technical University

... somewhere, in the ancient cellars of Prague, there is hidden indeed **infernal power**. Yet it is the very of **power celestial stars** themselves. Calmly dormant, awaiting mankind to discover **the magic key**, to use this power for their benefit....

## 1. Introduction

In a lot of plasma experiments, the main parameters of the experiment consist of the magnitude of currents and magnetic and electric fields inside and outside the plasma volume.

Reliable measurement of these parameters is basic to performing and understanding the experiments. Moreover, in many cases, measurements of these global quantities can give considerable information about the microscopic properties of the plasma such as temperature, density, and composition. It is therefore logical to begin our consideration of the topic of plasma diagnostic by consideration of magnetic techniques.

The GOMTRAIC 2013 MHD team measured the mode number of magnetic islands appearing in the plasma of GOLEM tokamak using magnetic diagnostics. In this report, basic theory, measurement setup and results are presented.

## 2. Basics of the theory

### 2.1. Plasma & Fusion

It is projected that the global energy demands will have a rise of 40 % between 2009 and 2035 [1] [2]. Furthermore it is very likely that greenhouse gases (e.g. CO<sub>2</sub>), which are a substantial by product in the combustion of fossil fuels, have a climate-changing effect. By the end of the century there may be the need for a technology producing a significant amount of energy in an environmentally friendly and economical way.

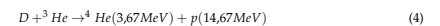
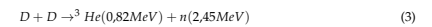
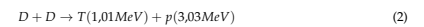
The alternative energy sources: sun, wind, tide and hydro-energy are subject to the local weather conditions. Therefore they cannot be considered as the full substitution for commonly used fossil fuels.

In the 20th century it was discovered a new form of energy, nuclear energy. Nuclear energy is gained in two processes: fission and fusion. The fission energy is gained from the splitting up heavy elements, e.g. uranium or thorium and nowadays there are about 400 fission reactors all over the world.

The fusion of light elements, especially hydrogen isotopes is the way in which the stars obtain their energy. has the potential of providing an essentially unlimited source of energy.

Human beings have been searching a long time for a way to reproduce such a source of energy on Earth. The cross-section for the whole cycle in the stars due to the weak interaction involved in reaction is too low to be reproduced on Earth (the Stars overcome this problem by its huge mass).

The fusion reactions of most practical interest for terrestrial fusion power production [3] [4] [12] are:



To initialize and preserve reactions in thermonuclear reactor the particles need to be heated to high energies, in the range of tens of keV to overcome the repulsive Coulomb force. Under this temperature, matter goes into state of plasma.

There are two categories of plasma (and also plasma physics): hot and cold plasmas. In the cold plasmas only a small fraction of the atoms is ionized, the temperature of gas is low (2 eV). In the hot plasmas full ionization takes place, and the particles are in thermal equilibrium with the temperature 10 - 10 000 eV. When the temperature is high enough ( $T \geq 5\text{keV}$ ), the particles are able to pass Coulomb barrier, so the hot plasma is suitable background for the fusion.

For using fusion as a source of energy (positive energy gain), a relation among plasma parameters, termed the Lawson criterion [5], must be fulfilled:

$$L = n\tau_E T_i > C_{crit} \quad (5)$$

where  $n$  is the plasma density,  $T_i$  is the ion temperature and the definition of  $\tau_E$  depends on the approach to the fusion; roughly it is the time when the thermonuclear reactions can take place. For different reactions  $C_{crit}$  is different, for example for the D-T reaction, the  $C_{crit} \approx 5 \times 10^{21} \text{ s keV m}^{-3}$ . In order to build up a fusion reactor, we are looking for a compromise among density, energy confinement time, and temperature.

Nowadays, two methods of confinement are investigated in fusion research to reach an ignited plasma:

- Lasers (inertial fusion): High density and short confinement time. A solid D-T sphere (pellet) is heated by a laser or a heavy ion beam. Very high  $n$  is achieved by this approach, however only for a very short time  $\tau_E$ .
- Magnetic devices (closed systems - toruses): Low density and long confinement time, use magnetic confinement to improve parameters in Lawson criterion, especially  $\tau_E$  at modest level of  $n$  and  $T_i$ .

## 2.2. Magnetic confinement: Tokamak

On principle, tokamak [4] [12] [13] is a ring-shaped vacuum vessel placed as the secondary circuit of a transformer. Plasma is confined inside by a strong magnetic field (toroidal and poloidal magnetic fields) along the chamber.

The vessel, torus, has two symmetry axes: major and minor to characterize two basic directions: toroidal which is parallel to the minor axis and poloidal which is azimuthal to the minor axis. Another important geometrical parameters are minor radius (shortest distance between the minor axis and the edge of a torus) and major radius (shortest distance between major and minor axis).

Since the plasma is an electrical conductor, it is possible to heat the plasma by inducing a current through it; in fact, the induced current that heats the plasma usually provides most of the poloidal field. The current is induced by slowly increasing the current through an electromagnetic winding linked with the plasma torus: the plasma can be viewed as the secondary winding of a transformer. (figure 1).

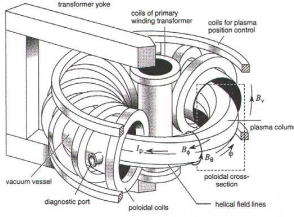


Figura 1: Tokamak configuration scheme.

This plasma current  $I_p$  produces a poloidal magnetic field  $B_p$ . Solenoid coils (toroidal field coils) wound around the torus creates a strong toroidal magnetic field  $B_t$ . The resultant magnetic field is helically shaped and its lines form nested closed magnetic surfaces. Degree of helicity is characterized by dimensionless parameter called safety factor  $q$  [6].

The  $q(r)$  is the number of toroidal turns it takes a magnetic field line to encircle the full poloidal circumference of the torus. For tokamak with a circular cross-section<sup>1</sup> it is defined as

$$q(r) = \frac{r}{R} \frac{B_\phi}{B_\theta} \xrightarrow{\text{Golem}} q(r=a) \approx 90,3 \frac{B_\phi}{I_p} \quad (6)$$

For the stability of plasma column there are quadrupole coils for plasma position control, that create vertical and horizontal magnetic fields.

<sup>1</sup>Appendix I

## 2.3. GOLEM

The GOLEM tokamak [8] [9] [10] [11] is a tokamak with a circular cross section and with full remote control capability and educational purpose. It's a small sized tokamak device equipped with basic controls and diagnostics (table 1 and figure 2).

Cuadro 1: GOLEM: Dimensions and Parameters

Major radius R	0.4 m	Minor radius r	0.1 m
Radial position of the limiter	0.085 m	Toroidal magnetic field $B_\phi$	<0.8 T
Toroidal plasma current $I_p$	<8 kA	Safety Factor at Edge $q(a)$	15
Pulse length t	<13ms	Background Pressure of Vacuum P	10-200 mPa
Central electron temperature $T_e$	<80 eV	Work Gas	$H_2$

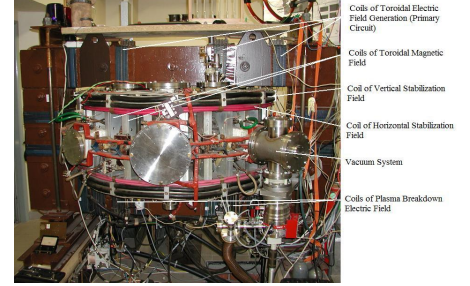


Figura 2: Front view of the GOLEM tokamak.

Before discharge, the vacuum vessel is evacuated down to the work pressure and filled by working gas (hydrogen).

After that, the power supplies are connected to the toroidal magnetic field coils. Since now, the toroidal magnetic field  $B_\phi$  starts increasing. When  $B_\phi$  reaches a certain valor, the primary transformer winding is automatically connected to its power supplies (capacitor banks) and the toroidal electric field  $E_\phi$  is induced within the vacuum vessel. The  $E_\phi = \frac{U_{top}}{2\pi R}$  starts to accelerate free electrons<sup>2</sup>, which are produced by an electron gun placed in the limiter shadow.

<sup>2</sup>Free electrons are always present due to the cosmic radiation, but their amount is not sufficient for a reproducible breakdown (the moment of ignition of the discharge)

After breakdown, the electron density  $n_e$  increases exponentially.

After several ms from breakdown, the working gas is completely ionized. Simultaneously, the plasma current  $I_p$  increases, which is determined by the primary circuit parameters. The slope  $\frac{dI_p}{dt}$  has to be kept relatively low to negate the skin effect, which could drive the current only on the surface of the plasma column and plasma gets unstable and disrupts.

After the plasma current reaches values of  $\approx 5-8$  kA, it tends to remain constant for the next  $\approx 5$  ms. During this quasistationary phase of discharge, the loop voltage is 2-3 V. The quasistationary phase is exploited for physical measurements. After ms, the primary winding of the transformer is set to be short circuited. The plasma current exponentially decays (figure 3).

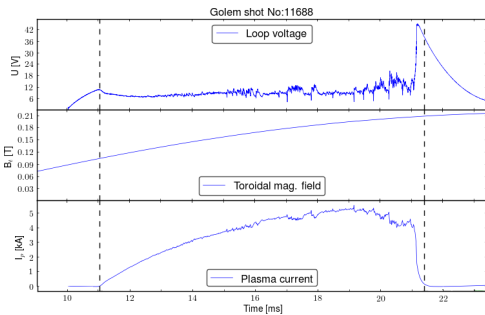


Figure 3: Temporal evolution of a typical GOLEM discharge, with parameters: loop voltage ( $U_{top}$ ) toroidal magnetic field ( $B_\phi$ ) and plasma current ( $I_p$ ). The whole discharge is plotted. Blue vertical lines indicate the beginning and the end of the discharge.

Fusion plasma is a source of many instabilities that deteriorate confinement of particles and energy. There are two main types of instabilities occurring in plasmas:

- Magnetic instabilities: The magnetohydrodynamics (MHD) instabilities occur at the radii where safety factor has rational value  $q(r) = m/n$  and they can even create layers where the magnetic field is fully ergodized, which strongly deteriorates plasma confinement.
- Electrostatic instabilities: Electrostatic turbulence is dominant at the plasma edge and it demonstrates itself by fluctuations of plasma density and potential.

## 2.4. Magnetics Islands

Magnetohydrodynamics (MHD) studies the dynamics of electrically conducting fluids, like plasma. MHD provides a good theoretical framework to describe inhomogeneities such as magnetic islands [4] [7] [17]. They are present where the poloidal magnetic field flux is perturbed. At the top of the figure 4, a cross section was taken of the nested poloidal magnetic flux surfaces.

With long axial plasma column with circular cross section, plasma current is constant only if there is no  $B_z$  gradient, thus no Shafranov shift. After all, poloidal flux surfaces in general are solution of Grad-Shafranov equation, which originates from:

$$\nabla p = j \times B \quad (7)$$

On these surfaces, poloidal magnetic field flux, pressure ( $p$ ), temperature ( $T$ ) and plasma current ( $j$ ) are constant. If inhomogeneities are present, the situation changes to the one present at the bottom of the figure 4. Now  $p, T$  and  $j$  are short circuited where the lines intersect. As this changes plasma behavior, it is important to know where and when this happens.

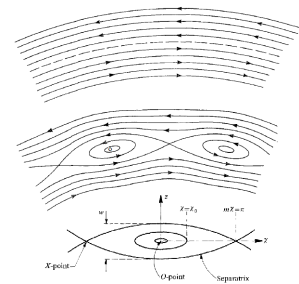


Figure 4: Contour plot of  $m \geq 2$  island in the R-Z plane. The O-point, the X-point and the (full) island width  $w$  are indicated.

These islands manifest at low safety factor  $q$ , a key parameter in MHD. The safety factor is than equal to  $m/n$ , where  $m$  and  $n$  are natural numbers.

As for GOLEM tokamak,  $n$  can be put equal to one, islands will appear if  $q = m$ .

Mode number  $m$  than corresponds to the number of intersections defined above. For example, for  $m = 3$  we get a poloidal cross section of the plasma's poloidal magnetic field lines like the one at figure 5.

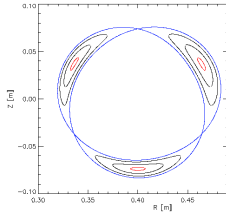


Figura 5: Island flux surfaces

The tokamak is equipped with a basic diagnostic system for measuring key plasma parameters.[8] [9] [10]

- A single loop surrounding the transformer core measures the loop voltage  $U_{loop}$ .
- A Rogowski coil surrounding the tokamak chamber measures the sum of the plasma and chamber current  $I_{(p+ch)}$ .
- A small pick-up coil placed on the tokamak chamber detects the toroidal magnetic field  $B_{tor}$ .
- A photocell which faces a glass port of the tokamak detects the plasma radiation from the emitted visible spectra.

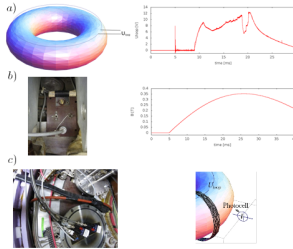


Figura 6: Basic parameter measurements: a)  $U_{loop}$  measurements and result, b)  $B_{tor}$  measurement and result, c)  $I_{(p+ch)}$  and plasma radiation measurement

### 3. Principles of the measurement

Structure of magnetohydrodynamic (MHD) modes has always been a study of interest in tokamak devices. It is well known that Mirnov oscillations with poloidal and toroidal mode numbers  $m$  and  $n$ , respectively, are created by perturbation of current channel on rational magnetic surfaces. The coherent structure of such rotating modes can be obtained by poloidal and toroidal arrays of Mirnov coils.

In GOLEM, array of 16 magnetic probe (Mirnov coils) are installed to detect poloidal magnetic field  $B_\theta$  inside the vacuum vessel [17].



Figura 7: Set of 16 Mirnov coils mounted in a poloidal ring to work like sensors of local magnetic field.

Magnetic coil is used like an inductive sensor for magnetic field measurement based on Maxwell equations [15] [13]. In a region free of charges ( $\rho = 0$ ) and no currents ( $J = 0$ ), such as in a vacuum, Maxwell's equations reduce to:

$$\nabla \cdot \mathbf{E} = 0 \quad \text{Gauss's law} \quad (8)$$

$$\nabla \times \mathbf{E} = -\frac{\partial \mathbf{B}}{\partial t} \quad \text{Maxwell-Faraday law} \quad (9)$$

$$\nabla \cdot \mathbf{B} = 0 \quad \text{Gauss's law for magnetism} \quad (10)$$

$$\nabla \times \mathbf{B} = \mu_0 \mathbf{J} + \frac{1}{c^2} \frac{\partial \mathbf{E}}{\partial t} \quad \text{Ampere's circuital law} \quad (11)$$

where  $c$  is the speed of light in vacuum.

Even though magnetic coil is used as a magnetic field sensor, it measures rate of change of magnetic induction  $B_\theta$  instead of the quantity itself. This is because its principle of operation is based on integral form of Faraday's law.

The Maxwell - Faraday law establish that a time-varying magnetic field is always accompanied by a spatially-varying, non-conservative electric field, and vice-versa.

$$\nabla \times \mathbf{E} = -\frac{\partial \mathbf{B}}{\partial t} \quad (12)$$

where  $\nabla \times$  is the curl operator and again  $\mathbf{E}(r, t)$  is the electric field and  $\mathbf{B}(r, t)$  is the magnetic field.

It can also be written in an integral form by the Stokes theorem

$$\oint_{\partial \Sigma} \mathbf{E} \cdot d\mathbf{l} = - \int_{\Sigma} \frac{\partial \mathbf{B}}{\partial t} \cdot d\mathbf{A} \quad (13)$$

where  $\Sigma$  is a surface bounded by the closed contour  $\partial \Sigma$ ,  $\mathbf{E}$  is the electric field,  $\mathbf{B}$  is the magnetic field,  $d\mathbf{l}$  is an infinitesimal vector element of the contour  $\partial \Sigma$ ,  $d\mathbf{A}$  is an infinitesimal vector element of surface  $\Sigma$ .

The integral on the left-hand side is the electric potential or voltage  $\hat{V}$  in Volts induced at the ends of the wire of coil and is equals the rate of change of  $\Phi = \int \mathbf{B} \cdot d\mathbf{S}$  in Webers per second (product of effective area of coil  $S$  and time-derivation of averaged magnetic field magnitude in the coil  $B$ ), thus mean value of  $B$  can be obtained from equation:

$$\hat{V} = -\frac{d\Phi}{dt} \quad (14)$$

Such a magnetic coil, illustrated in the figure, may be considered the archetype of magnetic measurements. In a uniform magnetic field, varying with time  $B(t)$ , the voltage induced in the coil is

$$\hat{V} = -N A \frac{dB}{dt} = -A_{eff} \frac{dB}{dt} \rightarrow dB = -\frac{1}{A_{eff}} \hat{V} dt \quad (15)$$

where  $\Phi = B(t)NA = B(t)A_{eff}$  is the magnetic flux,  $N$  is the number of turns in the coil of area  $A$  and  $A_{eff}$  is the effective surface of each coils.

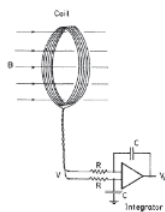


Figura 8: Typical magnetic coil and integrating circuit

As indicated in the figure, because one is interested in  $B$  rather than  $\hat{B}$ , therefore analog integrating circuit, such as the one show, is generally used to obtain a signal proportional to the field.

### 4. Measurement setup

There are currently 16 Mirnov coils placed on a circular rack, put inside of liner. Locations of respective coils are depicted in fig. 9.

Coils are placed on minor radius of 93.5 mm. Although Mirnov coils are used for measurement of poloidal field.

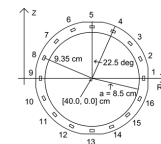


Figura 9: On tokamak GOLEM, Mirnov coils are used for small coils of local poloidal magnetic field measurement, placed inside of liner. The main purpose of Mirnov coils is for plasma MHD activity measurements.

There are three stated requirements that have to be met, for magnetic coil to become a reliable sensor of magnetic field [16]:

- Have minimal perturbing effect on plasma column.
- Sufficient sensitivity to overcome electric noise associated with electronics devices.
- High frequency response to follow rapid magnetics fluctuations.

However, these conditions are in conflict with each other, since in order to rise sensitivity of sensor, effective area of the coil has to rise as well. For better frequency response, this area has to be in configuration of less numerous large loops, rather than large number of small loops. This, however, collides with the requirement of minimal perturbing effect on plasma. The effective area and polarity of all sensitivity of sensor [17] are shown in the table 2.

Cuadro 2: Characterization of Mirnov Coils

Coil #	Polarity	$A_{eff}$ [cm <sup>2</sup> ]	$\theta$ [°]	Coil #	Polarity	$A_{eff}$ [cm <sup>2</sup> ]	$\theta$ [°]
1	-	68.93	0	9	-	67.62	180
2	-	140.68	22.5	10	+	142.80	202.5
3	+	138.83	45	11	-	140.43	225
4	+	140.43	67.5	12	x	x	247.5
5	-	68.59	90	13	x	x	270
6	+	134.47	112.5	14	x	x	292.5
7	-	134.28	135	15	-	139.82	315
8	+	142.46	157.5	16	-	139.33	337.5



In a uniform magnetic field, varying with time  $B(t)$ , the voltage induced in each coil is

$$\hat{V} = -NA \frac{dB}{dt} = -A_{eff} \frac{dB}{dt} \quad (16)$$

Experimentally  $\hat{V} : \hat{V}(i)$  is a discrete signal and that voltage  $\hat{V}$  obtained by the sensor will have to be integrated in order to obtain measured quantity of B.

$$B(t) \approx -\frac{\Delta t}{A_{eff}} \sum_i \hat{V}(i) \quad (17)$$

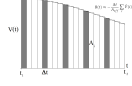


Figure 10: Numerical integration consists of finding numerical approximations for the value  $A_i$

where  $\Delta t$  is the sampling time. Integrated magnetic measurements are very sensitive to the DC bias of the measurement circuit [14], which needs to be corrected. If the sampling rate is 1 MHz, and the shot starts at 5 ms, we have 5000 samples from the background noise.

$$\hat{V}(i) = V_{measured}(i) - \frac{1}{5000} \sum_{i=1}^{5000} V_{measured}(i) \quad (18)$$

The poloidal magnetic field perturbation can be obtained by the elimination of the smooth signal from the original signal of the magnetic field.

$$B_{per}(t) = B(t) - \text{smooth}(B(t)) \quad (19)$$

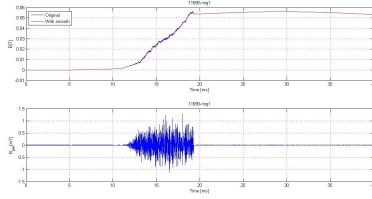


Figure 11: Temporal evolution of the original magnetic field (blue, top panel), smooth magnetic field (red, top panel) and the magnetic field perturbation for ring 1 obtain subtracting to the original magnetic field signal the smooth signal for the discharge # 11688.

12

For this shot and the ring 1 (magnetic sensor at  $\theta = 0^\circ$ ) obtained:

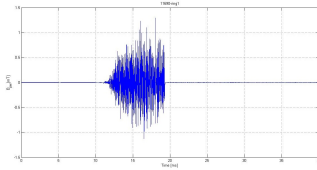


Figure 13: Poloidal magnetic field perturbation obtain by numerical integration of the Mirnov Signal of the ring 1 for the shot # 11688. There are similar signals for all poloidal sensors at the poloidal ring.

For time-space domain, the most common format is a graph with two geometric dimensions: the horizontal axis represents time, the vertical axis the poloidal position of the Mirnov coils; a third dimension indicating the amplitude of perturbed magnetic field at a particular time is represented by the intensity or colour of each point in the image.

Applying this to the oscillation of poloidal magnetic field, one could estimate the mode number of the wave and so determine the mode number of the magnetic island appearing in the plasma projected to poloidal plane. Figure illustrates a typical ohmic discharge contour, with a edge safety factor  $q(a) = 3.4$  according to the  $I_p$  and  $B_\theta$  at edge.

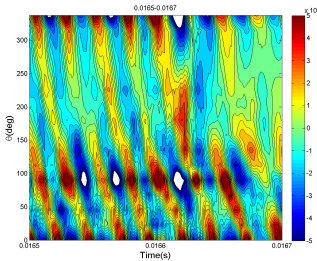


Figure 14: Contour plot of the poloidal magnetic field oscillations in shot # 11688 and with a window time from 0.0165-0.0167 s, where the horizontal and vertical axes correspond to time and poloidal localization of the Mirnov coils. The red and blue region represent the oscillations positive and negative respectively. The color bar on the right side represents intensity of the poloidal magnetic field perturbation in T.

14

## 5. Data processing methods

The data are acquired at fast sampling rate in order to follow the rotating modes. The Mirnov signals are oscillating time series from which the overall structure is extracted.

A look at the time traces of Mirnov coil signals may sometimes be sufficient to determine the mode number, particularly when only a single mode is present.

### 5.1. Fluctuation of raw data analysis (theta-time diagram)

We are trying to identify the mode number (m) and the frequency (f) from data because the analysis of temporal and spatial domain of Mirnov signal sensors can help us of the identification of these quantities.

We have chosen shot # 11688 to explain the analysis of MHD modes using the set of Mirnov coils. Out of 16 probes, 13 probes were operational and were used for the analysis because other 3 probes connections were inoperative.

Loop voltage, plasma current (in the unit of kA) and toroidal magnetic field measured by differents diagnostics can be seen in figure 12 .

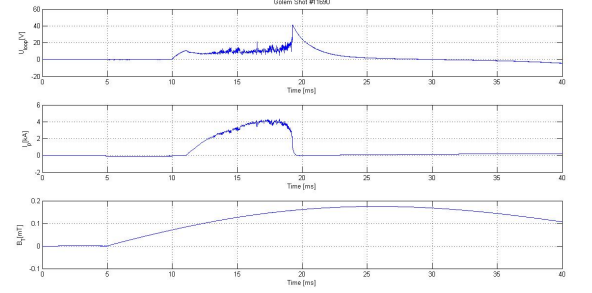


Figure 12: Temporal evolution of whole discharge # 11688, with parameters: loop voltage ( $U_{loop}$ ), plasma current ( $I_p$ ) and toroidal magnetic field ( $B_{tor}$ ).

13

The method for the identification of f and m is count the number of oscillation maxima for one period time given time.

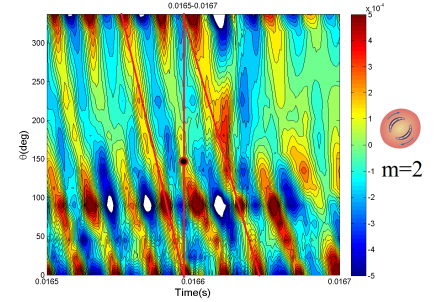


Figure 15: Contour plot of the poloidal magnetic field oscillations in shot #11688 and with a window time from 0.0165-0.0167 s. To determinate m mode, search for a periodicity of a field line (red) and draw a vertical line and count how many maxima are "inside". The number mode m is equal to the number of maxima (minima) inside 1, in this case  $m=2$ . The big black dot mark one cut of the vertical line with a maximum inside. At the right we can see a drawing of the  $m=2$  rotating island.

15



## 5.2. Spectrogram

Fourier analysis [19] is useful to study the spatial and time behavior of a system in wave number and frequency domain. There are several common conventions for defining the Fourier transform  $\hat{f}$  of an integrable function  $f: \mathbb{R} \rightarrow \mathbb{C}$ , for example:

$$\hat{f}(\xi) = \int_{-\infty}^{\infty} f(x) e^{-2\pi i x \xi} dx \quad \text{for every real number } \xi. \quad (20)$$

When the independent variable  $x$  represents time (with SI unit of seconds), the transform variable  $\xi$  represents frequency (in hertz).

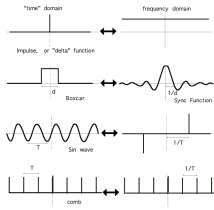


**Figure 16:** The Fourier transform relates the function's time domain, shown at right, to the function's frequency domain, shown at left. A spike in time is a constant in frequency, a switch on and off in time is a squiggly Bessel function in frequency, a sinusoidal wave in time is a spike in frequency, and a comb of spikes in time is a comb of spikes in frequency. This is true because waves of different frequency add.

Applying this to the oscillation of poloidal magnetic field in a poloidal cross section, one could estimate the mode number of the wave and so determine the MHD mode number appearing in the plasma.

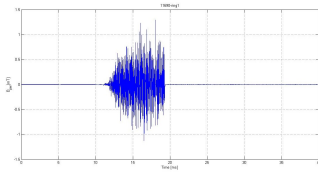


**Figure 17:** Poloidal magnetic field perturbation obtain by numerical integration of the Mirnov Signal of the ring 1 for the shot # 11688. There are similar signals for all poloidal sensors at the poloidal ring.

16

However, as only 13 magnetic Mirnov coils were operational, not enough data points are available to do proper Fourier analysis.

The oscillation in time of the poloidal magnetic field at a certain poloidal angle can be studied. This way it is possible to see whether an island is present or not<sup>3</sup>. As it comes with sinusoidal variation in time of the poloidal magnetic field, one should look for peaks in the frequency spectrum, and this for different time windows. If peaks appear at a certain time span, further investigation of the data at that time is done

For frequency domain, the most common format is a graph with two geometric dimensions: the horizontal axis represents time, the vertical axis is frequency; a third dimension indicating the amplitude of a particular frequency at a particular time is represented by the intensity or colour of each point in the image. This special graph is called spectrogram and is a visual representation of the spectrum of frequencies of the magnetic perturbation.

Here is an example of such a spectrogram. The dark red areas are peaks. The corresponding time intervals have to be further investigated to see if magnetic islands appear.

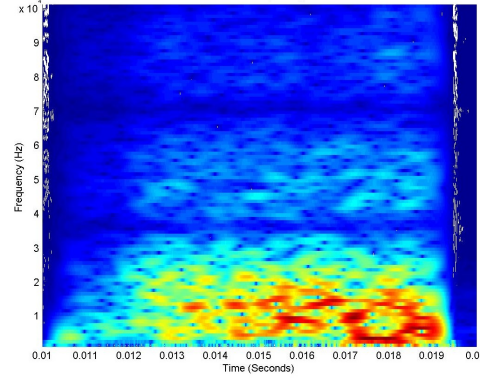


**Figure 18:**  $B_y$  spectrogram of shot n° 11767

<sup>3</sup>This is not necessarily an island not MHD wave, there are a lot of phenomena can appear in the plasma.  $|FFT|^2$  gives the spectral distribution of the power of the fluctuation.

17

## 5.3. Cross correlation analysis

These analysis is useful in data processing as FFT.

Cross correlation [18] [20] is a standard method of estimating the degree to which two series are correlated. Consider two series  $x(i)$  and  $y(i)$  where  $i=1,2,3...N$ . The cross correlation  $P$  at delay  $Lag$  is defined as

$$P_{xy}(Lag) = \frac{\sum_{k=1}^{N-Lag} (x_k - \bar{x}) \cdot (y_{k+Lag} - \bar{y})}{\sqrt{\left[ \sum_{k=1}^N (x_k - \bar{x})^2 \right] \cdot \left[ \sum_{k=1}^N (y_k - \bar{y})^2 \right]}} \quad \text{for } Lag < 0 \quad (21)$$

$$P_{xy}(Lag) = \frac{\sum_{k=1}^{N-Lag} (x_k - \bar{x}) \cdot (y_{k+Lag} - \bar{y})}{\sqrt{\left[ \sum_{k=1}^N (x_k - \bar{x})^2 \right] \cdot \left[ \sum_{k=1}^N (y_k - \bar{y})^2 \right]}} \quad \text{for } Lag > 0 \quad (22)$$

If the above is computed for all delays  $Lag=1,2,3...N$  then it results in a cross correlation series of twice the length as the original series.

- $x$  and  $y$  represent signals with  $N$  data points.  $Lag$  has dimension of data point index  $t_L = \frac{Lag}{f_{sample}}$ . Barred  $x$  and  $y$  represent averages. Therefore, denominator is geometrical average of signal variances – this causes that  $P$  is from  $(-1,1)$

There is the issue of what to do when the index into the series is less than 0 or greater than or equal to the number of points. ( $i - Lag < 0$  or  $i - Lag \geq N$ ) The most common approaches are to either ignore these points or assuming the series  $x$  and  $y$  are zero for  $i < 0$  and  $i \geq N$ . The Cross-correlation data processing is excellent for island tracking – normalizes the signals, inhibits fluctuations and brings forward its periodical character.

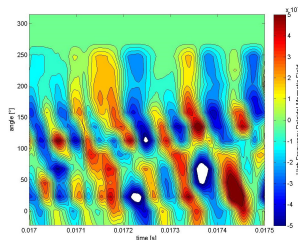


**Figure 19:** Cross-correlation analysis. A detail of perturbation of shot n° 11767

18

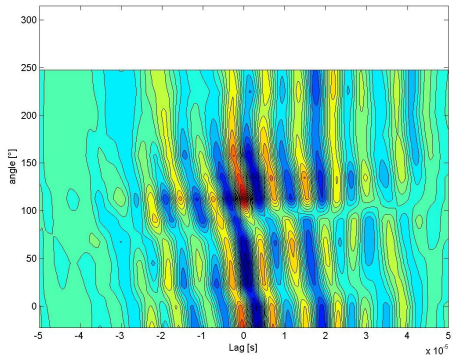


**Figure 20:** Cross-correlation profile of MHD activity in shot n° 1176. Begin at 0.017 s and end at 0.0175 s.

19

## 6. Results

The mode number of a magnetic island has been directly obtained using  $\theta$ -time diagram for all discharges and the result are shown<sup>4</sup> in table 3 .

Cuadro 3: Determination of  $m$  mode in the shots from the Kick-off week session

Shot #	Island Index	Time <sub>d</sub> [ms]	Time <sub>e</sub> [ms]	Mode number $m$
11686	1	14.7	14.9	2
11687	1	15.1	15.3	2
11688	1	16.4	16.6	2
11689	1	14.8	15.0	2
11690	1	16.1	16.3	2
11691	1	24.1	24.3	2
11691	2	25.8	26	2 or $i_3$ ?
11692	1	25.3	25.5	2
11701	1	14	14.2	2
11702	1	15	15.2	2
11703	1	16.7	16.9	2
11759	1	17.6	17.8	2
11762	1	17.6	17.8	2
11762	2	18.0	18.2	2
11762	3	19.4	19.6	2
11765	1	13.8	14.0	2
11767	1	14.7	14.9	2

It's proven that magnetic island informations are visible from the contour plot of poloidal magnetic field oscillations profile. It's proven that the  $\theta$ -time diagram is a useful tool for the measurement of magnetic islands .

<sup>4</sup>Same color in discharges indicated the same parameters in the control room

## 8. Appendix

### 8.1. Appendix I

#### 8.1.1. Safety Factor

Magnetic field in tokamak has a helical shape. The geometry of the magnetic field lines can be described by the safety factor

$$q = \frac{\Delta\Phi}{2\pi} \quad (23)$$

A magnetic field line does not come into the same poloidal position after one toroidal turn, but after several of them, after it covers a toroidal angle  $\Delta\Phi$ .

The safety factor depends on the geometry of the machine and it varies along the minor radius. For large aspect ratio tokamaks ( $\epsilon = \frac{R}{a}$ ) with circular poloidal cross-section (as in the case of GOLEM),  $q$  can be written as:

$$q(r) = \frac{d\chi}{d\psi} = \frac{2\pi r dr B_\Phi}{2\pi R dr B_\theta(r)} = \frac{r}{R} \frac{B_\Phi}{B_\theta(r)} \quad (24)$$

where  $r$  and  $R$  are the minor and major radii, while  $B_\Phi$  and  $B_\theta$  are the toroidal and poloidal magnetic fields.

If we suppose a density current profile like:

$$j(r) = j_0 \left[ 1 - \frac{r^2}{a^2} \right]^p \quad (25)$$

The poloidal magnetic field generated by the plasma currents  $B_\theta$  can be expressed as (using

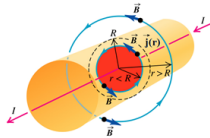


Figura 21

Biot-Savart law, see fig 19):

$$\nabla \wedge \mathbf{B} = \mu_0 \mathbf{j} \rightarrow \oint_{2\pi R B_\theta(r)} \mathbf{B}_\theta(r) \cdot d\mathbf{l} = \mu_0 I = \mu_0 \int \int_{\Sigma} j(r) dS = \mu_0 \int_0^{2\pi} \int_0^r j(r') r' dr' d\theta = \quad (26)$$

$$= \frac{\mu_0 j_0}{2\pi r} \int_0^{2\pi} \int_0^r \left[ 1 - \frac{r'^2}{a^2} \right]^p r' dr' d\theta = \frac{\mu_0 j_0}{r} \int_0^r \left[ 1 - \frac{r'^2}{a^2} \right]^p r' dr' = -\frac{a \mu_0 j_0}{r(p+1)} \left( \left[ 1 - \frac{r'^2}{a^2} \right]^{p+1} - 1 \right) \quad (27)$$

## 7. Discussion

Energy has played a major role in the development of human civilization. Energy is a vital component to sustain the industrial countries as well as to improve the economic condition of less developed nations. To maintain the balance between the increase of energy supply and the decrease of pollution level, fusion energy has been proposed as a promising candidate for the existing energy options. It has many attractive features in terms of safety, abundance of fuel, and minimal impact on nature.

GOLEM Tokamak is designed to generate plasma using several heating and to confine it by a combination of external and self - induced magnetic fields. A tokamak is a donut-shaped device that uses magnetic fields to confine the plasma. A central solenoid is used to drive the toroidal plasma current. The plasma torus is regarded as a single secondary winding of a transformer.

Tokamak GOLEM is equipped with a set of diagnostic instruments for measuring specific plasma parameters during the discharge. It is desirable to measure these parameters with high precision.

The information on these fluctuations has been retrieved mainly from the measurement of oscillating magnetic fields detected with coils situated inside the plasma for Tokamak GOLEM. MHD instabilities have been successfully observed in Tokamak GOLEM. The detection and interpretation of the MHD fluctuations occurring in tokamak plasma is a challenging task for plasma diagnostics.

The magnetic oscillations, are fluctuations in the magnetic field of the discharge current (particularly the current near plasma boundary) which can be detected outside the plasma ring. A concept which has proved to be of great significance for the stability of plasma in the toroidal magnetic field is that of resonance oscillations. These are oscillations where the helix of the perturbation exactly matches the helix of the confining magnetic field.

The perturbed helix is described by the poloidal and toroidal mode numbers  $m$  and  $n$ . MHD instabilities in tokamaks may simultaneously occur at different rational surfaces and rotate at either the same or different angular frequencies. Plasma diagnostics (Mirnov coils ring) collect the spatial and temporal information of MHD perturbations. In Tokamak GOLEM MHD studies is by 16 Mirnov coils mounted in a poloidal ring at the same time low values for safety factor are ideal to observe magnetic island as show in the present report, Mode number 2 was observed a lot of times.

Therefore, the first step for an accurate interpretation of the output signals of plasma diagnostics is to choose proper data processing techniques. Fourier transform is considered the universal method for time to frequency domain conversion. The spectrograms show the magnitude of the signal in frequency state for each coil of poloidal arrangement.

and we can express the poloidal magnetic field by:

$$B_\theta(r) = \frac{\mu_0 I_p(r)}{2\pi r} = \frac{\mu_0 I_p(a)}{2\pi r} \left[ 1 - \left( 1 - \frac{r^2}{a^2} \right)^{p+1} \right] \quad (28)$$

where  $I_p(r=a) = \frac{2\pi j_0}{p+1}$  is the plasma current which is driven within the radius  $r=a$ .

The safety factor  $q(r)$  can be written as

$$q(r) = q(a) \frac{\frac{r^2}{a^2}}{\left[ 1 - \left( 1 - \frac{r^2}{a^2} \right)^{p+1} \right]} \quad (29)$$

where  $q(a)$  is the edge safety factor at edge:

$$q(a) = \frac{2\pi a^2}{\mu_0 R} \frac{B_\Phi}{I_p(a)} \quad (30)$$

For the edge of GOLEM tokamak ( $a = 85$  mm), we can write

$$q(a) \approx 90.3 \frac{B_\Phi(T)}{I_p(a)(kA)} \quad (31)$$

This is true in an ideal case when the plasma column is centralized with the poloidal circumference  $a = 85$  mm.

## 8.2. Appendix II

### 8.2.1. Frederyk's Scripts

#### ■ dataProc.m

```
1 function out = dataProc(v,AEff,pol)
2 step = 1e-6; %time step in sec
3 %Eliminate offset.
4 av = mean(v(1:5000)); %Look for average value over 5ms
5 vNoOffset = v-av; %Data - offset
6 %Integrate
7 b = zeros(length(v),1);
8 b(1) = vNoOffset(1)*step/AEff/pol;
9 for i = 2:length(v)
10     b(i) = b(i-1)+step*vNoOffset(i)/AEff/pol;
11 end
12 %Subtract moving average to have high freq only
13 out = smooth(b-smooth(b,250),30); %band pass filter
14 end
```

#### ■ getMirnovData.m

```
1 function finalTransp = getMirnovData(numberShot)
2 AEff = [68.93e-4, 140.68e-4, 138.83e-4, 140.43e-4, 68.59e-4, 134.47
3         e-4,134.28e-4, 142.46e-4, 67.62e-4, 142.80e-4, 140.43e-4, 138.02
4         e-4, 76.32e-4, 142.18e-4, 139.82e-4, 139.33e-4]; %in m^2
5 pol = [-1,-1,1,1,-1,1,-1,1,-1,1,-1,-1,-1,-1,-1,-1]; %polarity
6 final = zeros(40000,16);
7 for ring = 1:11
8     [t,v] = golem_data(numberShot,['ring_' num2str(ring)]);
9     final(:,ring+2) = dataProc(v,AEff(ring),pol(ring));
10 end
11 for ring = 15:16
12     [t,v] = golem_data(numberShot,['ring_' num2str(ring)]);
13     final(:,ring-14) = dataProc(v,AEff(ring),pol(ring));
14 end
15 finalTransp = final';
```

24

```
20 fftWindow = fft(window);
21 for amb = t:(t+step-1)
22     spec(:,amb) = fftWindow;
23 end
24 end
25 %Post processing
26 spec = abs(spec);
27 fRange = (1:(windowSize/2+1))/windowSize*1e6;
28 fRangeOfInterest = fRange(1:find(fRange>maxFreqOfInterest,1)); %
29 %Getting the interesting part
30 specOfInterest = spec(1:find(fRange>maxFreqOfInterest,1),1:(length(
31 tRange)));
32 [T,F] = meshgrid(tRange,fRangeOfInterest);
33 surf(T,F,specOfInterest.^((1/3),'edgecolor','none');
34 axis tight;
35 view(0,90);
36 xlabel('Time (Seconds)'); ylabel('Frequency (Hz)');
37 title(['Shot' num2str(numberShot) 'Coil' num2str(numberCoil) '
38 Spectrogram'], 'Fontweight', 'bold');
39 end
```

#### ■ makeThetaTime.m

```
1 function [] = makeThetaTime(numberShot,timeWindow)
2 data = getMirnovData(numberShot);
3 [X,Y] = meshgrid(22.5*(-1:14)',timeWindow);
4 levels=linspace(-5e-4,5e-4,20);
5 figure; contourf(Y',X',data(:,round(1e6*timeWindow)),levels);
6 xlabel('time [s]');
7 ylabel('angle [deg]');
8 t = colorbar('peer','gca');
9 set(get(t,'ylabel'),'String','High Frequency Poloidal Magnetic
10 Field');
11 title(['Shot' num2str(numberShot) ': Theta - lag diagram'],'
12 Fontweight','bold');
13 saveas(gcf,['Shot' num2str(numberShot) '_ThetaTime.jpg']);
14 end
```

#### ■ spectrograms.m

```
1 clc;
2 clear all;
3 close all;
4 shotnumbers = [11762 11765 11767 11768 11769 11770]; %Put the
5 numbers of shots here
6 coils = [5]; %Put the coils you're interested in here
7 begin = 0.010; %Begin of time window you want to investigate in
8 seconds, should be begin of plasma discharge
9 final = 0.027; %End of time window you want to investigate in
10 seconds, should be end of plasma discharge
```

26

#### ■ makeCrossCorAlt.m

```
1 function [] = makeCrossCorAlt(shotNumber,timeWindow)
2 initial = getMirnovData(shotNumber);
3 [rn,cn] = size(initial);
4 twi = round(timeWindow*1e6);
5 tws = length(twi);
6 final = zeros(rn,2*tws-1);
7 %Choose reference at coil 5
8 ref = initial(7,twi);
9 for i = 1:rn
10     final(i,:) = xcorr(initial(i,twi),ref,'coeff');
11 end
12 [X,Y] = meshgrid(22.5*(-1:14)',(-tws+1):(tws-1)/10e6);
13 levels = linspace(-1.0,1.0,25);
14 figure; contourf(Y',X',final,levels);
15 xlabel('Lag [s]');
16 ylabel('angle [deg]');
17 title(['Shot' num2str(shotNumber) ' begin ' num2str(timeWindow(1))
18 's end ' num2str(timeWindow(length(timeWindow))) 's: Cross -
19 correlation diagram'],'Fontweight','bold');
20 saveas(gcf,['Shot' num2str(shotNumber) '_Begin' num2str(timeWindow
21 (1)) 's_End' num2str(timeWindow(length(timeWindow))) '_CrossCor.
22 jpg']);
23 end
```

#### ■ makeSpectrogramAlt.m

```
1 function [] = makeSpectrogramAlt(numberShot,numberCoil,begin,final)
2 close all;
3 %Parameters
4 windowSize = 1000; %Size of windows (number represents indices of
5 input vector)
6 step = 1; %Next window at 'step' away from last one.
7 maxFreqOfInterest =100000; %Maximum frequency of interest in Hz
8 %Getting data
9 tRange = begin:1e-6:final;
10 X = getMirnovDataCoil(numberShot,numberCoil);
11 XCut = X(round(1e6*begin):(round(1e6*final)+windowSize)));
12 hanning = hann(windowSize);
13 spec = zeros(windowSize,length(tRange)+windowSize);
14 %Fast Fourier Transform
15 for t = 1:step:(length(tRange))
16     window = XCut(t:t+windowSize-1); %window of interest
17     window = window-mean(window); %Eliminating off set
18     for w = 1:windowSize
19         window(w) = window(w)+hanning(w); %Multiplying with
20         Hanning function to make sure boudaries are zero
21     end
22 end
```

25

```
8
9 for i = 1:length(shotnumbers)
10     for j = 1:length(coils)
11         makeSpectrogramAlt(shotnumbers(i),coils(j),begin,final)
12         saveas(gcf,['Shot' num2str(shotnumbers(i)) 'Coil' num2str(
13 coils(j)) 'Spectrogram.jpg']);
14     end
15 end
16 display('Done!')
```



Figura 22

27

### 8.3. Appendix III

#### 8.3.1. List of

- Figure I: From Plasma confinement in tokamaks. J. Stockel Institute of Plasma Physics, Academy of Association EURATOM / IPPCR, Czech Republic
- Figure II: From <http://golem.fjfi.cvut.cz/?p=tokamak>
- Figure IV: From Wesson. Tokamaks. Oxford University Press, Clarendon Press, Oxford, 2004.
- Figure VI: From <http://golem.fjfi.cvut.cz/?p=uvod>
- Figure VII: From <http://golem.fjfi.cvut.cz/?p=uvod>
- Figure VIII: From I. H. Hutchinson, Principles of Plasma Diagnostics, Cambridge University Press, Cambridge, 2002
- Figure XVI: From [http://brokensymmetry.typepad.com/broken\\_symmetry/2008/06/cost-accounting.html](http://brokensymmetry.typepad.com/broken_symmetry/2008/06/cost-accounting.html)
- Figure XXII: From [http://www.physics.sjsu.edu/beckler/physics51/mag\\_field.htm](http://www.physics.sjsu.edu/beckler/physics51/mag_field.htm)

### 9. Bibliography

#### Referencias

- [1] World energy outlook 2011, IEA, International Energy Agency OECD, Paris, 2011.
- [2] Climate change 2007 : synthesis report, IPCC, Geneva, Switzerland, 2008.
- [3] F. Francis Chen, Introduction fo Plasma Physics, Plenum Press, New York (1974).
- [4] Wesson. Tokamaks. Oxford University Press, Clarendon Press, Oxford, 2004.
- [5] J. D. Lawson, "Some Criteria for a Power Producing Thermonuclear Reactor", Proceedings of the Physical Society B, Volume 70 (1957), p. 6.
- [6] García Muñoz, Manuel (2006): Fast Response Scintillator Based Detector for MHD Induced Energetic Ion Losses in ASDEX Upgrade. Dissertation, LMU München: Faculty of Physics.
- [7] <http://scitation.aip.org/pop/announcements/Fitzpatrickaps2008.pdf>.
- [8] Former tokamak CASTOR becomes remotely controllable GOLEM at the Czech Technical University in Prague,V. Svoboda,G. Pokol, D. I. Réfy, J. Stöckel, G. Vondrášek,37th EPS Conference on Plasma Physics P2.111.
- [9] Recent results from GOLEM tokamak. Indeed, you can teach an old dog some new tricks.Ī. Duran, S. El-Ahmar, O. Grover, M. Gryaznevich, J. Jankowski, J. Kocman, K.Kovarik, T. Marković, M. A. Martínez-Fuentes, M. Odstrčil, T. Odstrčil, M. Oszwaldowski, T. Růžicková, J. Stöckel, V. Svoboda, G. Vondrášek, 39th EPS Conference & 16th Int. Congress on Plasma Physics P2.059.
- [10] The GOLEM Tokamak for Fusion Education,E. Bromová, I.Duran, O. Grover, J. Kocman, T. Marković, M. Odstrčil, T. Odstrčil,O. Pluhar, J. Stöckel, V. Svoboda, A. Šindlery, G. Vondrášek, J. Zara., 38th EPS Conference on Plasma Physics (2011) P1.021.
- [11] Golem: <http://golem.fjfi.cvut.cz/?p=tokamak>.
- [12] The Science of JET, John Wesson,JET-R(99)13
- [13] IPP Summer University for Plasma Physics,Max-Planck-Institut fur plasmaphysik.
- [14] Instructions for student measurements on the GOLEM tokamak. Dr. Gergo Pokol, Laszlo Horvath, Csaba Buday, Daniel Imre Refy
- [15] I. H. Hutchinson, Principles of Plasma Diagnostics, Cambridge University Press, Cambridge, 2002.
- [16] Fluktuace magnetickeho pole na tokamaku Castor, Ivan Duran, Praha, listopad 2003
- [17] Plasma MHD Activity Observations via Magnetic Diagnostics,Magnetic islands, statistical methods, magnetic diagnostics, tokamak operation.Tomáš Markovič,2013
- [18] Cross Correlation: AutoCorrelation – 2D Pattern Identification, Written by Paul Bourke, August 1996 .
- [19] Wikipedia: [http://en.wikipedia.org/wiki/Fourier\\_analysis](http://en.wikipedia.org/wiki/Fourier_analysis).
- [20] Wikipedia: <http://en.wikipedia.org/wiki/Cross-correlation>.

# Electrostatics Probes

## Gomtraic 2013 final report – Remote part

by Marco Martínez<sup>1</sup>, and Miguel Gomez<sup>2</sup>

<sup>1</sup>Universidad Nacional Autónoma de México (UNAM), Mexico City, Mexico  
<sup>2</sup>Instituto Superior Técnico, Lisbon, Portugal

### Experimental Set-up

In order to study the temporal and spatial evolution of the floating potential ( $U_n$ ) of the plasma in the tokamak GOLEM, we used a rake probe with 12 tips, which are made of Molybdenum wire of the diameter 0.7 mm, spaced by 2.5 mm and length of individual tips is about 2 mm. The rake probe is inserted in the tokamak vessel from bottom, as schematically shown in Figure 1.

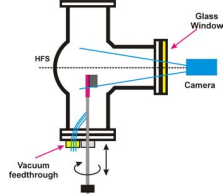


Figure 1. Lay-out of the experiment.

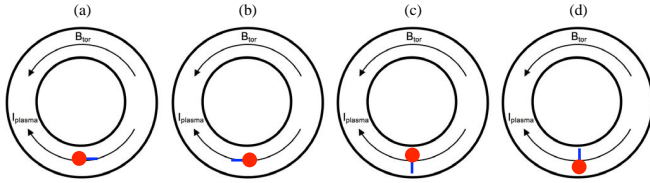


Figure 2. Orientations of the rake probe with respect to the toroidal magnetic field direction as seen from the top of the GOLEM. (a) Downstream orientation, (b) Upstream orientation, (c) Low-Field side (LFS) orientation, (d) High-Field side (HFS) orientation.

## Results

The shots #11754, #11749, #11743, and #11748 (downstream, upstream, LFS and HFS, respectively), are shown in following figures. Figure 4 shows the floating potential in each direction, Figure 5 shows 3D plot and its contour of the floating potential, Figure 6 shows smoothing of floating potential with a degree of 100, Figure 7 shows the floating potential integrated over different intervals of time, Figure 8 shows the fluctuations of the floating potential, Figure 9 shows 3D plot and its contour of the smoothing of FFT, Figure 10 shows the cross correlations for the probe 6, Figure 11 shows 3D plot and its contour of the cross correlations for the probe 6, Figure 12 radial velocity between probes, and Figure 13 skewness and kurtosis for the four position of the rake.

Figure 4 shows raw data of the floating potential of individual tips. For further analysis, it is important to check the raw data out as there may be errors in electronics, arcing in the case of ion saturation regime and other defects. Figure 5 puts the data to 3D plots. In both the figures, we can observe that the floating potential is higher in downstream direction, then the LFS direction, after the HFS direction and finally upstream direction. Also, the value of floating potential is bigger in the probe No.1 and this value decreases for the other probes.

There are two main ways to characterize the plasma from the probe measurements: the mean values and the fluctuations. First, we will focus on the mean values. The signal is smoothed in a suitable time window of 1 ms, as shown in figure 6. The most practical way is usually the radial profile of the measured parameter, as shown in Figure 7, which shows how the floating potential is changing, over different intervals of time and between probes.

The fluctuation analysis is shown in following figures. Figure 8 shows the raw data fluctuations, e.g. the raw signal (Figure 4) subscribed from the smoothed signal (Figure 6). We can see that the fluctuations are bigger in LFS direction and upstream direction than HFS direction, and it is lower for downstream direction. But, from Figure 9 it can be seen that FFT is bigger in downstream direction, then the LFS direction, after the HFS direction and finally upstream direction. Also, Figure 9 shows that there are dominant frequencies between 3 kHz and 5 kHz and 8 kHz and 10 kHz.

Cross-correlation analysis can help us to get an idea about structures in the investigated region and to estimate the radial velocity from the fluctuations. First, we need to calculate the cross-correlations of the adjacent probes as shown in Figure 10. Figures 10 and 11 show that the cross correlation (from 9ms to 21ms) between probe 6 and the other probes is lower for HFS direction, then increase for downstream direction, then for LFS direction and finally for upstream direction. For HFS, downstream and LFS directions the cross correlation between probes 6-5 and 6-7 is higher than 0.5, while the cross correlation in upstream direction between probes 6-4, 6-5, 6-7, 6-8 and 6-9 is higher than 0.5. The peak in correlation around the probe 6 suggest that there is a big structure sitting in this area. The velocity can be estimated from the lag of the cross-correlation maxima. This lag shows how fast the structures moved from one tip to another. Thus, the radial velocity is the ratio of the time lag to the distance of the probes. The resulting radial velocities between probes (in three time windows: 9ms to 10ms, 14ms to 15ms and 20ms to 21ms) are in the Figure 12.

For statistical analysis, the most important moments are the first four: mean value  $\mu$ , variance  $\sigma^2$ , skewness  $S$  and kurtosis  $K$ . Where  $\sigma^2$  (it's square root is the standard deviation) indicates the variability of the distribution. Skewness shows the dominating part of the data: the negative value of skewness indicates that the left tail of respective PDF (probability distribution function) is longer than

The first tip of the rake probe was placed at the radius position  $r = 60$  mm from the centre of the tokamak chamber. The rake probe is installed on the rotatable shaft; therefore, it was possible to change orientation of the tips with respect to the direction of the toroidal magnetic field and the plasma current as depicted in Figure 2.

Measurements were performed for two different series of shots by charging voltage of the capacitor bank for the toroidal magnetic field  $U_B = 600$  V, and changing voltage of the capacitor bank for the primary winding of the GOLEM transformer  $U_{CD} = 400$  V and  $U_{CD} = 350$  V. The time delay between triggers of these capacitor banks are  $T_{CD} = 2000$   $\mu$ s and  $T_{CD} = 10000$   $\mu$ s, respectively for each value of  $U_{CD}$ . The pressure of the working gas (Hydrogen) is  $P_{H_2} = 10$  mPa, and pre-ionization was switched ON. All the parameters are shown in the Table 1 and Figure 3 shows the basic parameters.

# Shot	Orientation	$U_B$ [V]	$U_{CD}$ [V]	$T_{CD}$ [ $\mu$ s]	$P_{H_2}$ [mPa]	Pre-ionization	Plasma [s]
11754	Downstream	600	350	2000	10	on	0.01226
11749	Upstream	600	350	2000	10	on	0.01202
11743	LFS	600	350	2000	10	on	0.01238
11748	HFS	600	350	2000	10	on	0.01226
11781	Downstream	600	400	10000	10	on	0.01222
11784	Upstream	600	400	10000	10	on	0.01178
11788	LFS	600	400	10000	10	on	0.01198
11790	HFS	600	400	10000	10	on	0.01118

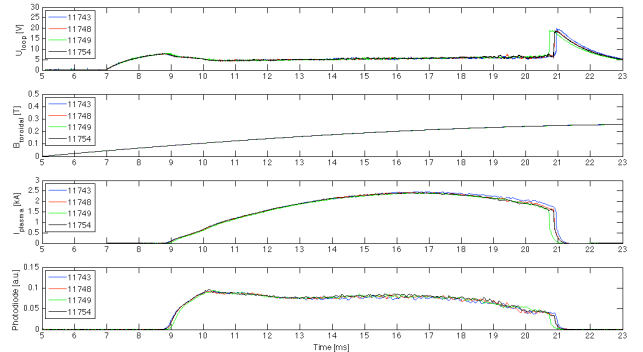


Figure 3. Basic parameters

the right one. The skewness for a normal distribution is equal to zero. Kurtosis indicates how "peaked" the distribution is, "peaked" distributions have positive kurtosis while "flat" ones have negative values of kurtosis.

In this work the skewness and the kurtosis were calculated for each position (downstream, upstream, LFS and HFS), with a time window of 2 ms, see Figure 13. This analysis shows the following results:

- For downstream position: the skewness shows predominant negative values, which it means that left tail of its respective PDF is longer than the right one. On the other hand, the behaviour of kurtosis is predominant positive, which means that PDF is peaked, and this behaviour is more remarkable between 16ms and 20ms.
- For upstream position: the skewness shows negative values like downstream position, but between 16 ms and 20 ms the skewness becomes positive, which means that right tail of its respective PDF is longer than the left one. On the other hand, the behaviour of kurtosis is predominant positive, which means that PDF is peaked, but it is less positive than in downstream position.
- For LFS position: the skewness shows predominant negative values, like in downstream position, but it is less negative. The behaviour of kurtosis is predominant positive like downstream position, but there is not a remarkable behaviour between 16ms and 20ms.

For HFS position: the skewness shows the same behaviour as upstream position. And the behaviour of kurtosis is the same as upstream position.



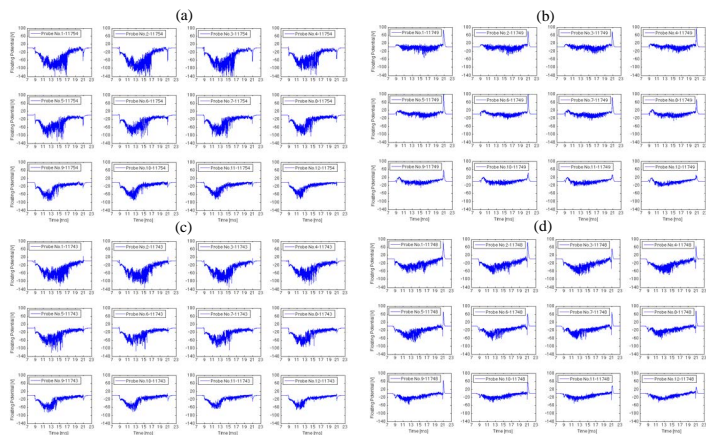


Figure 4. Floating potential in each direction: (a) downstream, (b) upstream, (c) LFS and (d) HFS.

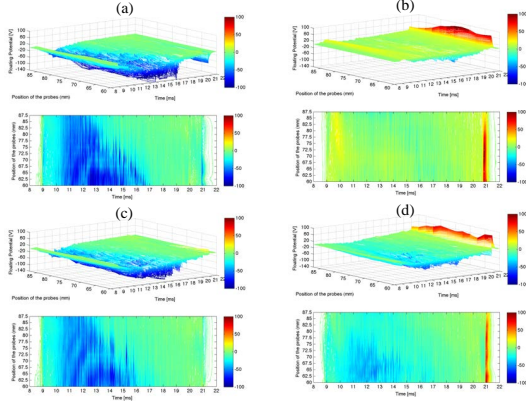


Figure 5. Floating potential. (a) downstream, (b) upstream, (c) LFS and (d) HFS.

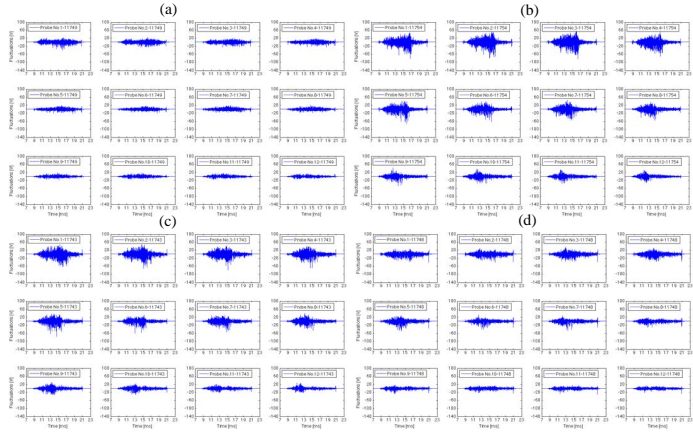


Figure 8. Fluctuations of the floating potential. (a) downstream, (b) , (c) LFS and (d) HFS.

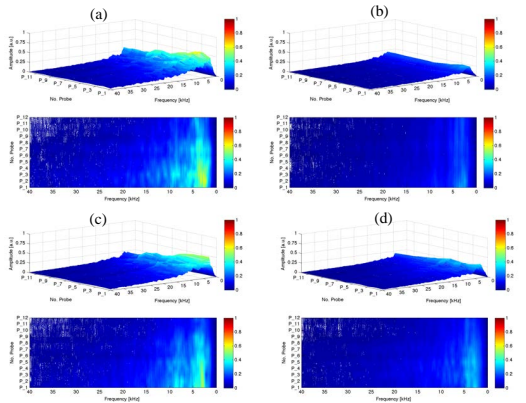


Figure 9. 3D plot and its contour of the smoothing of FFT. (a) downstream, (b) upstream, (c) LFS and (d) HFS.

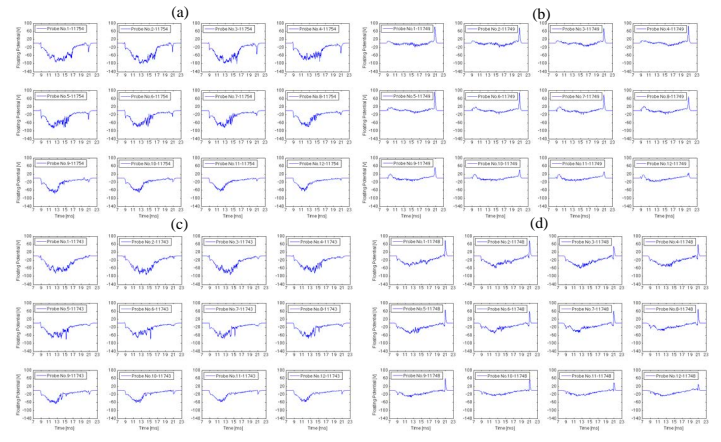


Figure 6. Smoothing of floating potential with a degree of 100. (a) downstream, (b) upstream, (c) LFS and (d) HFS.

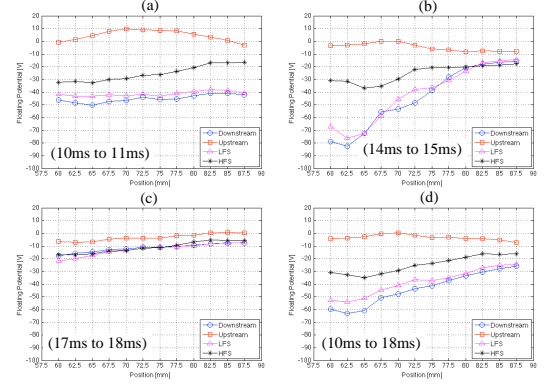


Figure 7. Floating potential integrated, for all orientations of the rake: downstream, upstream, LFS and HFS. Intervals of integration (a) from 10ms to 11ms, (b) from 14ms to 15ms, (c) from 17ms to 18ms, (d) from 10ms to 18ms

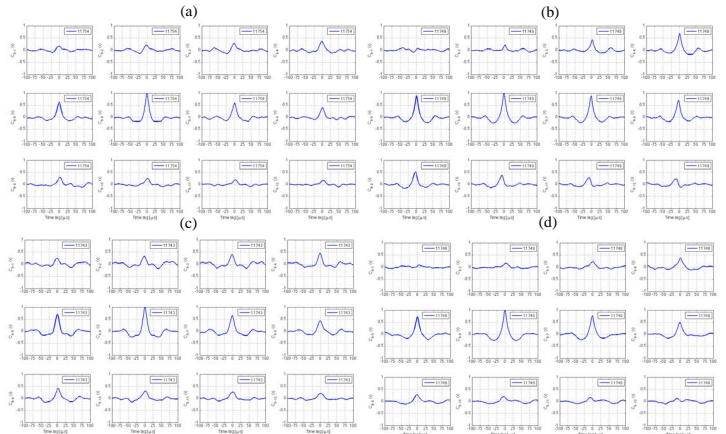


Figure 10. Cross correlations for the probe 6. (a) downstream, (b) upstream, (c) LFS and (d) HFS.

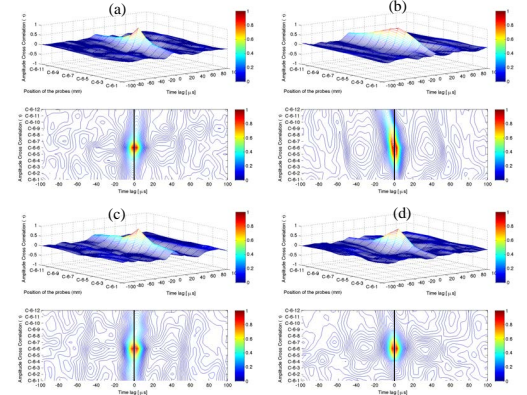


Figure 11. 3D plot and its contour of the cross correlations for the probe 6. (a) downstream, (b) upstream, (c) LFS and (d) HFS.

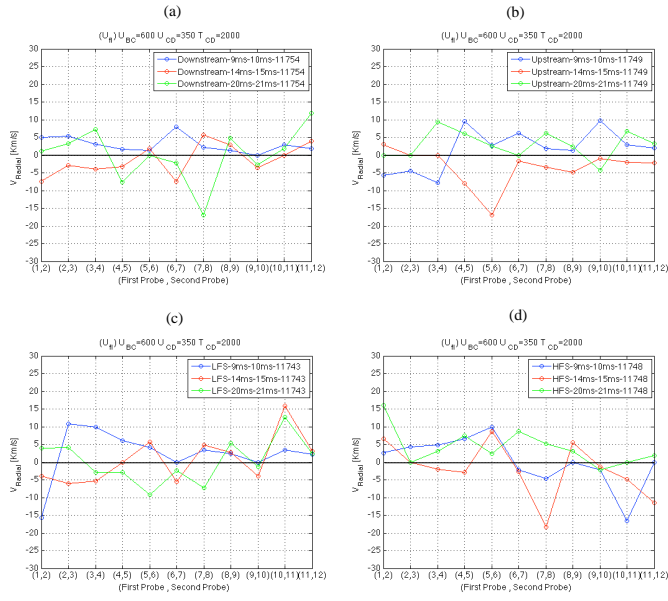


Figure 12. Radial velocity between probes in three time windows: 9ms to 10ms, 14ms to 15ms and 20ms to 21ms. (a) downstream, (b) upstream, (c) LFS and (d) HFS.

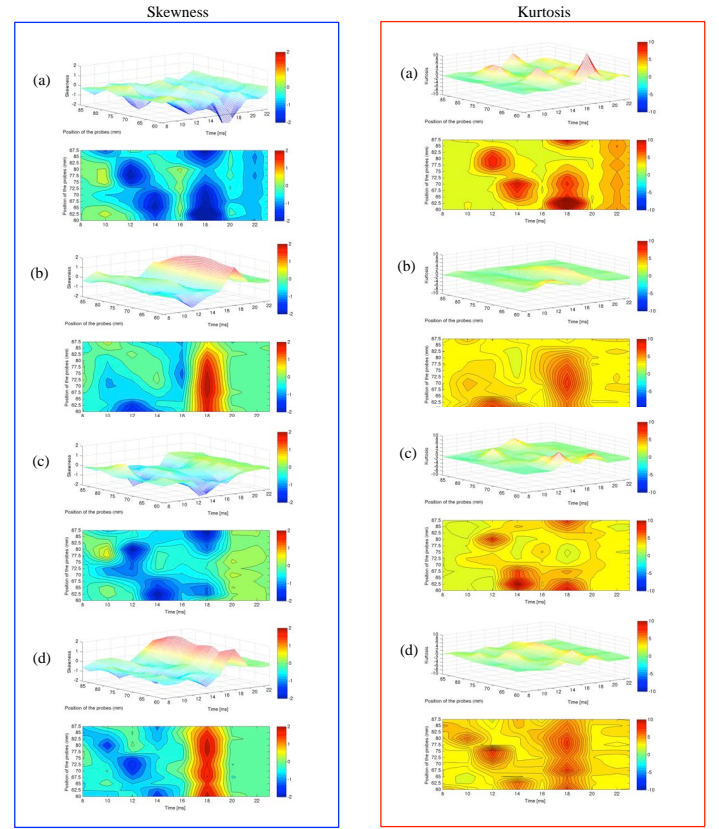


Figure 13. (Left column) Skewness for (a) downstream, (b) upstream, (c) LFS and (d) HFS. (right column) Kurtosis for (a) downstream, (b) upstream, (c) LFS and (d) HFS.

# Report on Tomography

## 1 Experiment and objective

### 1.1 Goal and basic apparatus

The aim of tomography is to be able to have a 2D reconstruction of the plasma cross section and its evolution in time. For this we use two Casio EX-F1 cameras. The cameras are equipped with a variable objective with an anti-reflexive coating. Entrance pupil size is 4.5 cm, the viewing angle is variable from 9.2° to 88° with the corresponding maximal numerical aperture from 0.11 to 0.18. The cameras contain a 1/1.8" CMOS imaging chip IMX017CGE with a maximum 6.2 Mpix resolution and 2.5µm square pixels with a minimal sensitivity of 4200e<sup>-</sup> at color 3200 K. The flux is of 700 cd/m<sup>2</sup> with an exposure of 1/50 and an F-number of 5.6.

- Operation regimes: High speed video mode - 336 × 96@1200 fps, 432 × 192@600 fps, 512 × 384@300 fps
- Shutter speed: up to 1/40000 s
- Sensitivity: ISO 100 - 1600

### 1.2 Experimental setting

Two cameras are placed on perpendicular diagnostic ports as it is shown in figure 1. Orientation of the cameras is set so that the horizontal rows of the CMOS chip were rotated perpendicularly to the toroidal magnetic field direction in order to allow exploitation of the rolling shutter effect.

## 2 Data processing

First cameras give us the images in Figure 2, if everything worked correctly otherwise we have a blurry mess, after some processing (removal of background and reflections) :

To have synchronized data we are using the data from the photodiode and we try to match the data from cameras and photodiodes. As seen in figure 3 we have a pretty good synchronization for shot 11691 which allows us to study it further with some relevance.

1

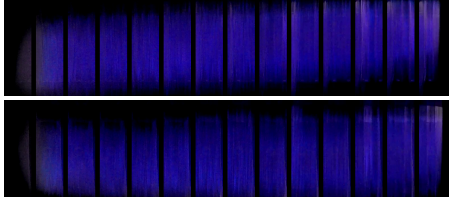


Figure 2: Top: Corrected images of the side camera; bottom: corrected images of the top camera

tomography and magnetic diagnostics is around 2 cm. In the following graphs we see the discrepancy between magnetic and camera diagnostics but it is important to notice that magnetic diagnostic is unreliable at the start of the discharge. Figure 4 gives us comparison between the two diagnostics for a larger number of shots.

In the figure 5, we can see that according to the cameras image the plasma shifts to the top and the right at the end of the discharge.

We did a fast check over more shots to see if the trend seen for shot 11691 was a global or local trend. However, there is a limited number of shots with available camera signal and reliable magnetic position estimation. Therefore, the magnetic data are rather poor.

### 2.2 Tomography

The goal of this course is to reach a polished tomography reconstruction as seen in the video in ogv or in avi

In the previous video we see that the plasma goes from the bottom left (High Field Side or HFS) of the vessel to the top right (Left Field Side or LFS) of the vessel. We can also see magnetic islands but barely because the plasma is moving. Though magnetic islands can be confirmed by magnetic diagnostics. The following video is for the same shot but using a first SVD mode subtraction which means that we remove the temporal mean of each pixel in the video. The issue being that the plasma is moving so it doesn't give a nice video: in ogv or in avi.

3

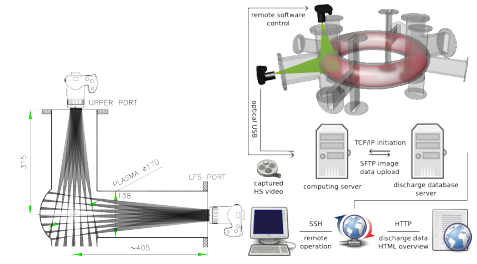


Figure 1: Experimental setting for tomographic reconstruction

Michal Odstril gave me the preprocessed data from the cameras which I was then exploiting to try to reconstruct an image of the plasma. We decided to focus on shot 11691 because it's a nice shot with a long plasma life and more particularly, with both cameras working and well aligned. The images from the camera and tomography automatically done by Michal Odstril's scripts are visible here. For the reconstruction I used a minimal Fisher regularization which consists in solving the following equation :

$$(Ts' * fs)x - TT - \lambda H = 0$$

which is of the form  $ax + b = 0$  and whose solution is :

$$x = (TT + \lambda H) / (Ts' * fs)$$

with  $\lambda$  a constant and  $H$  a smoothing matrix.  $\lambda$  was chosen at  $10^9$  because there was no real difference with higher values and the calculation time wasn't important. We then reshape the pixels in a 50\*50 pixels image and apply some filtering and smoothing to have a nicer image. We then plot the 30 frames you can see in this video.

### 2.1 Position

The white point is the center of mass of the plasma, calculated by taking only pixels with a high enough recorded emissivity. The cameras diagnostic see the center of mass slightly more during a discharge, especially at start but the change seen by magnetics diagnostics isn't as high. The discrepancy between

2

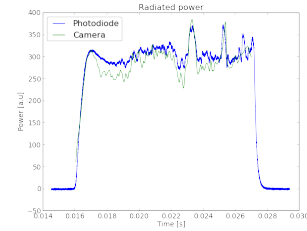


Figure 3: Synchronization

### 2.3 Dependencies

In figure 8 we see fitting of the vertical (Z) and radial (R) position. It is important to notice that the fitting is mainly on the linear part, we remove the start and the end because it isn't very reliable. A reliability under 200 is a correct reliability but not a very good one. In figure 9 we have four subplots. The top right shows the loop voltage dependence on the plasma life time. The three following show the dependence of plasma displacement in regard to (respectively) chamber current, loop voltage and plasma life time. As we can see, the higher the mean chamber current or the voltage, the faster the plasma displacement (keep in mind the values are negative) and the higher the plasma displacement the lower the plasma life time, which is coherent to the fact that the plasma will hit a wall faster.

### 2.4 Comparison with magnetics

When we multiply the vertical magnetic field per current in the center with the mean chamber current we obtain the mean vertical magnetic field in the center, which is 0.48 mT. We then did the ratio between the mean vertical magnetic field and the mean toroidal magnetic field (204 mT) and we obtained 0.002 which is 0.2%. We have  $f = j \times B_z$  (the plasma current being in the toroidal direction, only the vertical component of the magnetic field has an influence on the horizontal force. The ratio of the vertical component of the magnetic field compared to the toroidal component of the magnetic field shows that the toroidal magnetic field is an important source and that the vertical field is weak but it still seems to be an important source of stray magnetic field. The effects of the iron core transformer and the effects of the metallic chamber are neglected

4



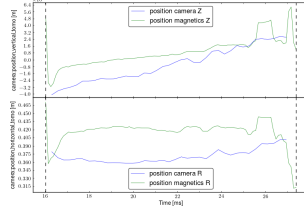


Figure 4: Comparison between magnetic and camera diagnostics for shot 11691

due to their complexity.

### 3 Discussion

The first remarkable thing is that the plasma position given by cameras is close to the position given by magnetics but magnetics isn't so precise for plasma position, especially at the start and the end of the discharge. We also see that the plasma, and especially the center of mass go from the bottom HFS to the top LFS.

### 4 Residuuum vs Smoothness graph

In order to find the optimum value of  $\lambda$ , a Residuuum vs Smoothness graph is useful. Residuuum is defined as  $\sqrt{(f - T * g)/L^2}$  (where L is the number of detectors) and smoothness as  $g' * H * g$ .

There is a competition between smoothness and residuuum (good-fitting) and the optimum value of  $\lambda$  may be identified in a Residuuum vs Smoothness graph localizing the 'corner' in the L-curve (see figure 11) for which the error is acceptable. The greater  $\lambda$  is the smoothed emissivity is obtained, although the greater the error becomes. In other words, the optimum value of  $\lambda$  is a compromise between good-fitting and smoothing.

Figures 12 and 13 show two different tomographic reconstructions for different values of  $\lambda$ . Figure 11 corresponds to the tomographic reconstruction for the optimum value of  $\lambda$  given in figure 11 (which is  $10^4$ ). This has to be compared with figure 11 (or video) in which a higher  $\lambda$  value is used.

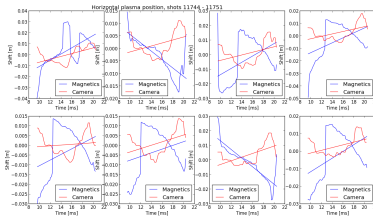


Figure 6: Comparison between magnetic and camera diagnostics for horizontal position on 8 shots

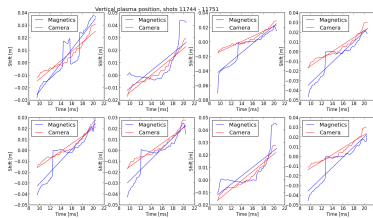


Figure 7: Comparison between magnetic and camera diagnostics for vertical position on 8 shots

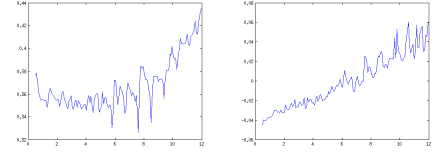


Figure 5: Top: plasma position seen by horizontal camera for shot 11691; bottom: plasma position seen by vertical camera for shot 11691

### 5 Cross validation

In order to select the best value of  $\lambda$  we employed Cross Validation (CV). The idea is to make a reconstruction with k detectors out and then measure the mean square error of the missing detectors. If n is the number of detectors, then the CV made by choosing k = n-1 is called Leave Out One CV (LOOCV), otherwise the method is called K-fold CV. Clearly, LOOCV demands more computational time.

We used K-fold CV and LOOCV. Figures 14 and 15 show the results for both types of CV. In both cases the mean square error reach a minimum at  $\lambda = 10^5$ . This is not far from the previous result, computed by means of the L-curve, where  $\lambda = 10^4$  seemed better.

### 6 Matlab scripts

Matlab script for tomography  
Matlab script for the plasma position

### 7 References

- Odstrcil, T., Odstrcil, M., Grover, O., Svoboda, V., Duran, I., & Mlynr, J. (2012). Low cost alternative of high speed visible light camera for tokamak experiments. Review of Scientific Instruments, 83(10), 10E505-10E505.
- Odstrcil, M., Mlynar, J., Odstrcil, T., Alper, B., & Murari, A. (2012). Modern numerical methods for plasma tomography optimisation. Nuclear Instruments and Methods in Physics Research Section A: Accelerators, Spectrometers, Detectors and Associated Equipment.

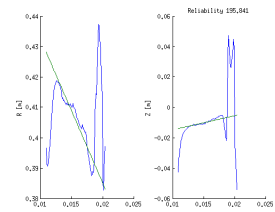


Figure 8: Fitting of vertical and radial position from magnetic diagnostic (data from cameras were not available for most of the shots)

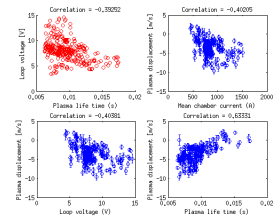


Figure 9: Dependence of the plasma displacement on different parameters

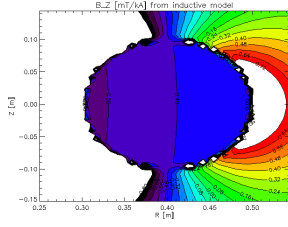


Figure 10: Magnetic field poloidal cross section (thanks to Tomas Markovic)

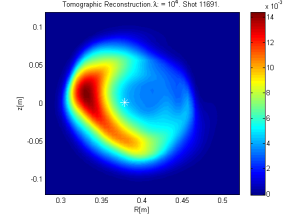


Figure 12: Tomographic Reconstruction  $\lambda = 10^4$ .

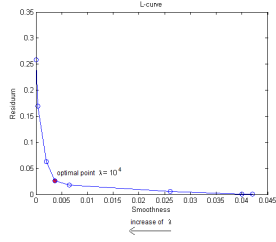


Figure 11: Residuum vs Smoothness graph

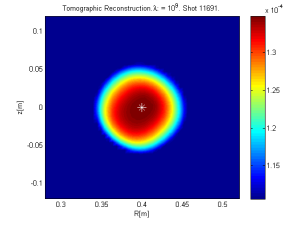


Figure 13: Tomographic Reconstruction  $\lambda = 10^9$ .

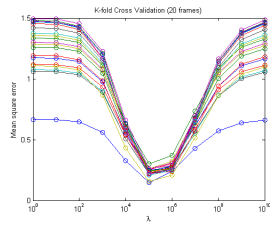


Figure 14: K-fold Cross Validation.

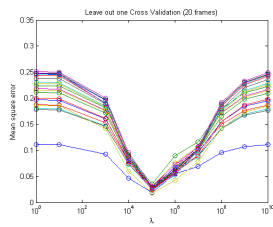


Figure 15: Leave Out One Cross Validation.

## Contents

<b>HXR measurement on GOLEM tokamak – dependence on pressure II</b>	<b>1</b>
Description	1
Measured data	3
Conclusion	3
<b>HXR measurement on the GOLEM tokamak – Spatial distribution of HXR radiation.</b>	<b>4</b>
Description	4
Experimental setup	4
Measured data	5
Conclusion	6

## HXR measurement on GOLEM tokamak – dependence on pressure II

Date: 11.4.2013  
Shots: 11799-11822

Goal: The goal of this measurement was to further investigate how HXR count depends on pressure.

### Description

Similar measurement was already conducted, however its results were quite puzzling, because the HXR count was highly influenced by strange tokamak behaviour (see report for details). Our goal now was to try to avoid the strange

1

was made just before the glow discharge. The HXR count dependence on pressure is plotted in Fig. 1.

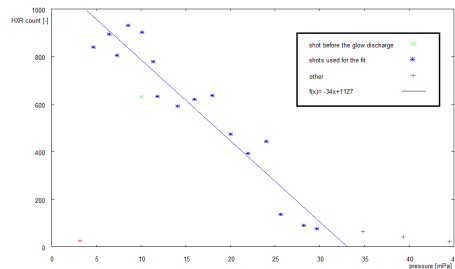


Figure 2: Fig. 1: HXR dependence on pressure

There are several things that should be noted. Firstly, the sudden drop in loop voltage that was troubling during the previous measurement was not observed. It is possible that the glow discharge performed before the measurement contributed to this. Secondly, plasma was achieved for much higher pressures than usually. The plasma was observed even for pressure above 40 mPa, which is something that does not happen very often. The glow discharge can again be the reason. The data now clearly show the trend, and there is no need to do any alternations to see it. Except for very low and very high pressures, the HXR count shows approximately linear decrease with pressure, which is exactly what was expected.

### Conclusion

Due to the fact that the phenomenon observed during previous measurement was avoided, this measurement was more successful and the results more conclusive. The HXR count decreases linearly with pressure, as predicted by theory. The rate at which the runaway electrons are slowed is proportional to density, which is proportional to pressure. The linear behaviour apparently fades for high pressures, where the decrease is slower. However, it should be noted that pressures as high as observed in this session are not seen very often, usually plasma does not appear at all. The fact that it appeared this time may be attributed to the fact that there was a glow discharge prior to the measurement. Even at these pressures, some runaways are produced.

3

phenomenon observed at the time, so that the results are more reliable. There was a glow discharge before shot 11802 (i.e. before the actual measurement commenced). A proposal was made that the discharge could prevent the issue from occurring, and it was also needed to check whether anything else changes. The settings of the tokamak parameters were not changed during the session (apart from pressure) and are noted below.

Preionisation ON  $C_{BT}=1000$  V triggered at 5.0 ms  $C_{CD}=500$  V triggered at 8.0 ms  $C_{BD}$  and  $C_{ST}$  were not charged.

The experimental setup was similar as it was in the previous measurement. An HXR scintillator detector was placed in proximity of the tokamak. The measured data were processed the same way as before, the same MATLAB script was used to count number of peaks in the signal.

### Measured data

Shot #	p [mPa]	HxR [-]	Shot #	p [mPa]	HxR [-]
11801	10,08	631	11812	20,04	473
11802	10,12	903	11813	21,97	392
11803	8,58	930	11814	24	443
11804	6,46	895	11815	25,62	137
11805	4,68	839	11816	28,2	91
11806	3,2	26	11817	29,64	75
11807	7,33	804	11818	34,83	63
11808	11,35	778	11819	39,38	42
11809	14,13	592	11820	44,52	23
11810	15,98	620	11821	11,84	633
11811	18	637			

Figure 1:

Tab. 1 lists all relevant shots performed during the session. First shot (11801)

2

The presence of the glow discharge prior to the session clearly puts the tokamak in some sort of unusual state, although it is unclear what exactly happens (there is likely less impurities on the walls, but other effects may arise). This state appears to prevent the sudden drop in  $U_{loop}$  that was observed previously. It may also enable the plasma to exist for higher pressures than without the discharge. These statements however may not be true – more research would have to be done in order to test whether the glow discharge really has the above mentioned effects.

## HXR measurement on the GOLEM tokamak – Spatial distribution of HXR radiation.

Date: 20.6.2013  
Shots: 12611-12629

Goal: The main goal of the measurement was to examine the spatial distribution of HXR emission, namely to scan the dependence of HXR emission on the vertical position of the detector.

### Description

The measurement required that significant amount of HXR photons is present. With respect to this requirement, the machine parameters were set as follows (see shot 12611 to see the settings):

Preionisation ON  
 $C_{BT}=600$  V triggered at 5.0 ms  
 $C_{CD}=500$  V triggered at 5.5 ms  
 $C_{BD}$  and  $C_{ST}$  were not charged.  
Requested pressure  $p=12$  mPa

These parameters were kept constant during the whole session, and the vertical position of the detector was changed. Glow discharge was performed in the tokamak after shot 12622.

### Experimental setup

HXR radiation was directly measured by a NaI crystal scintillator detector mounted on the tokamak in a way that allowed shifting in the vertical direction. The analog signal was collected and digitized by the Niturbo data acquisition system. By plotting the raw signal in time, Fig. 1, stand-alone peaks can be observed, each corresponding to an incident photon. A simple MATLAB script was written to identify and therefore count the number of peaks in each shot. This script was used to post-process all shots within the session.

4

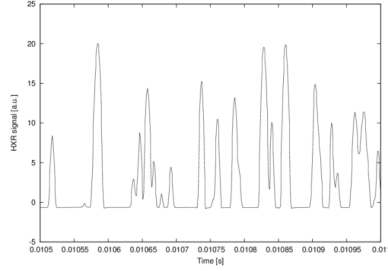


Figure 3: Fig. 1: An example of raw HXR signal from the detector plotted against time.

5

the random variance of the points. One also has to realize that increasing the vertical distance also increases the total distance from the source, and even if the radiation is isotropic, the number of detected photons will slowly decrease due to geometry (the correction was not done).

The measured data from batches 1 (pre glow discharge) and 2 (post glow discharge) and their linear fits are visible in Fig. 2.

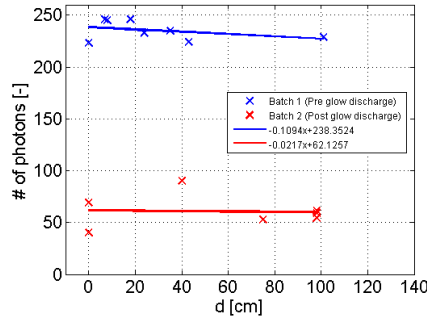


Figure 5: Fig. 2: Dependence of the number of detected photons on the vertical position of the detector.

## Conclusion

HXR emission does not seem to depend (or the dependence is very hard to notice) on the vertical position of the detector. A few reasons for this behaviour can be suggested: - The HXR radiation does not follow the direction of the runaways, but instead it is significantly scattered when passing through the chamber wall. The information about the direction of the runaways is therefore mostly lost after the radiation exits the tokamak.

- The runaways themselves are scattered and rapidly change direction while producing the radiation.

7

## Measured data

Tab. 1 lists all shots performed during the session with available HXR data. HXR data from shots 12613 to 12616 were unavailable due to technical problems with the DAS.

#	d (cm)	HXR photons (-)	#	d (cm)	HXR photons (-)
12611	0	223	12623	98	59
12612	7	246	12624	0	69
12617	24	233	12625	40	90
12618	18	246	12626	75	53
12619	8	245	12627	0	40
12620	35	235	12628	98	54
12621	43	224	12629	98	61
12622	101	229			

Figure 4:

Tab. 2: All shots with available HXR data. The quantity d denotes the vertical distance of the detector from the horizontal plane defined by the torus.

It is very important to note that between shots 12622 and 12623, glow discharge was performed in the tokamak, decreasing the number of detected photons from several hundreds to several dozens. Pre and post glow discharge shots thus have to be treated as distinct batches.

It is qualitatively expected that the number of incident photons would fall with increasing vertical distance. Runaway electrons orbit the chamber and gain more energy until the centrifugal force increases their orbit enough to make them collide with the wall. They should therefore strike in the horizontal plane and their velocity should not have vertical component. The bremsstrahlung produced should have about the same direction as the electron that caused it.

In reality, the number of detected photons does not seem to change significantly with the vertical distance, at least not for the range that has been scanned (0-98 cm). Although the count shows small decrease, it is not significant considering

6

- The range on which the dependence was measured (0-98 cm) was too narrow. The scope was restricted by the hardware used to mount the detector on the tokamak. It was expected that the decrease will be much faster, hence the range had been considered sufficient when the measurement was prepared. Measuring further is possible, but it requires to carefully consider geometry of the situation.
- The number of shots was too low. If the dependence is light, it can be obscured by random variance of each shot. If more shots were performed, the dependence may become visible.

Apart from this inconclusive measurement of spacial distribution an interesting observation was made. By performing glow discharge in the tokamak, and thus lowering the level of impurities, HXR emission is significantly suppressed. It could be illuminating to try measuring the dependence of HXR emission on  $Z_{eff}$ . Mitigation of damage to the first wall caused by runaway electrons is a principal issue for the ITER design.

8



## Appendix E

# Slide repository for oral presentations

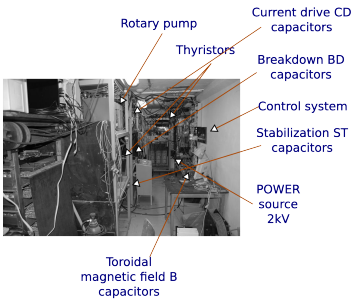
Online versions available at following addresses:

- The GOLEM tour
- The GOLEM experimental setup
- The GOLEM diagnostics
- The GOLEM data access
- The GOLEM physical quantities
- The MHD activity I
- The MHD activity II





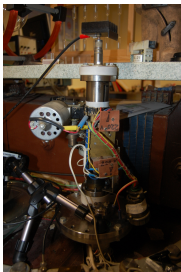
Infrastructure room



Content

- 1 Introduction
- 2 Overviews
- 3 Ports
- 4 Data acquisition system
- 5 Vacuum management system
- 6 Gas management system
- 7 Preionization
- 8 Energetics infrastructure
- 9 Control system
- 10 Others
- 11 Conclusion

SouthEast-Upper port - glow discharge/biasing electrode



Glow Discharge

Glow discharge/Biasing electrode - chamber view

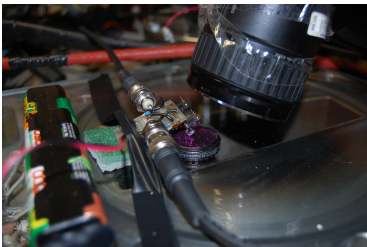


South-Upper port: Fast camera CASIO FX1 II



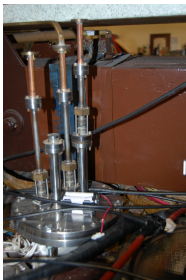
Manual, Discharge sequence

South-Upper port: Photodiodes (I-w/o filter, II-H $\alpha$  filter)



Manual, H $\alpha$  Spectral sensitivity

SouthWest-Upper port: Interferometry - input

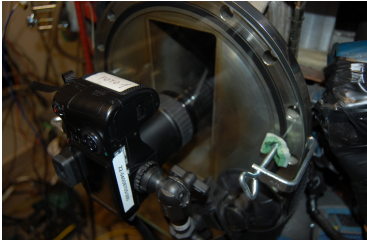


SouthEast-Middle port - IP camera viewing chamber



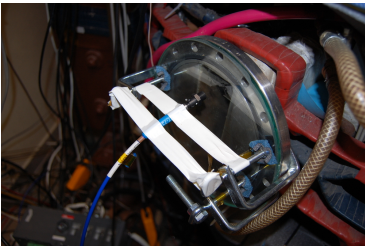
Manual, Tokamak Discharge, Glow Discharge

South-Middle port: Fast camera CASIO FX1 I



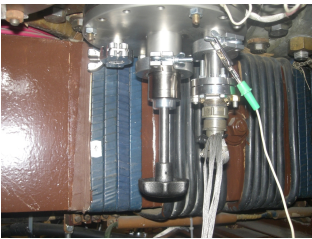
Manual, Discharge sequence

SouthEast-Middle port: Spectroscopy fiber connecting spectrometer HR2000+ES



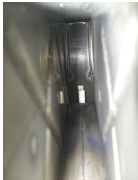
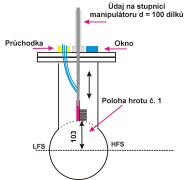
He spectrum No:7163

SouthEast-Bottom: Rake probe

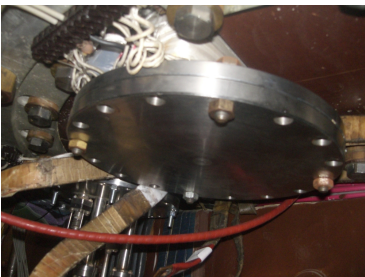


Description, Discharge sequence

Rake probe (2012)



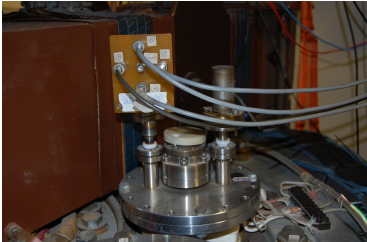
South-Bottom: vacant



SouthWest-Bottom port: Interferometry - output



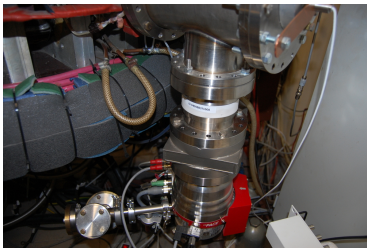
NorthEast-Upper: Mirnov coils



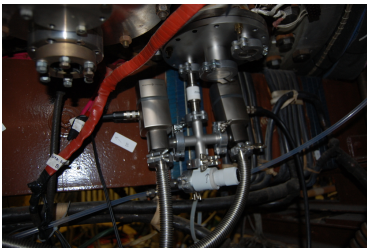
Description



NorthEast-Middle: Vacuum Stand

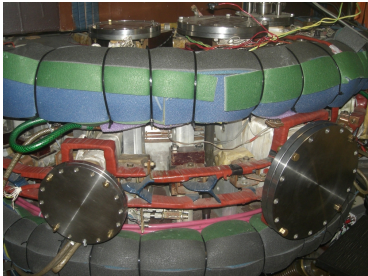


NorthEast - Bottom: Gas injection system - H<sub>2</sub>, Air, He

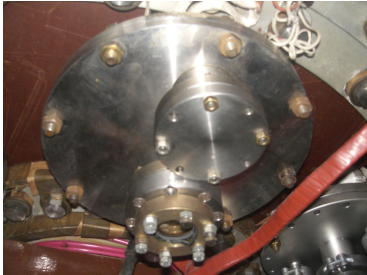


Gas pressure evolution

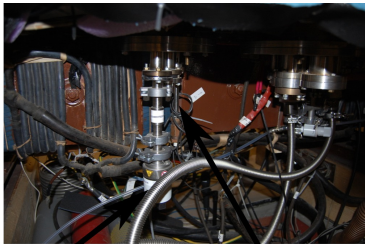
NorthWest and North - Top and Middle: vacant



North - Bottom: vacant



NorthWest - Bottom: Vacuum Gauge & Preionization Gun



Vacuum gauge Preionization gun

Content

- 1 Introduction
- 2 Overviews
- 3 Ports
- 4 Data acquisition system
- 5 Vacuum management system
- 6 Gas management system
- 7 Preionization
- 8 Energetics infrastructure
- 9 Control system
- 10 Others
- 11 Conclusion

Data acquisition system I - basic



NI PXI-1031, NI PXI-8195, NI PXI-6251

Data acquisition system II - turbo



NI PXIe-1062Q, NI PXIe-8108, NI PXIe-6358

Data acquisition system III - papouchSt

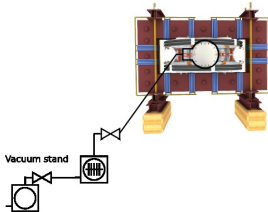


Papouch DAS1210

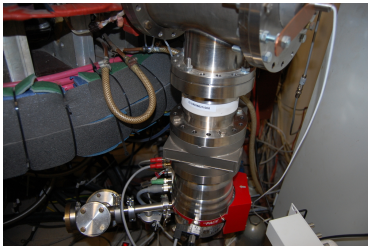
Content

- 1 Introduction
- 2 Overviews
- 3 Ports
- 4 Data acquisition system
- 5 Vacuum management system
- 6 Gas management system
- 7 Preionization
- 8 Energetics infrastructure
- 9 Control system
- 10 Others
- 11 Conclusion

Vacuum management

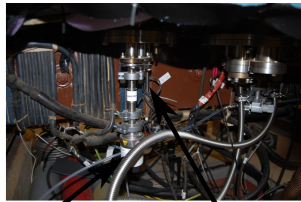


Vacuum Stand - Turbomolecular pump, Ultravacuum gauge, Galvanic insulation



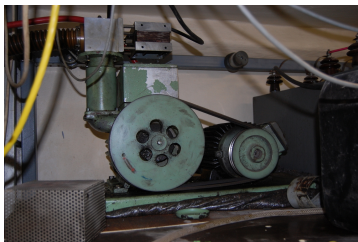
TMP manual, Controller manual

Vacuum Gauge



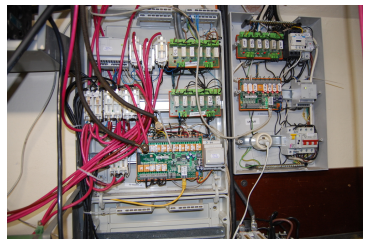
Vacuum gauge Preionization gun

Rotary Pump with valve



Rotary Pump

Control system for capacitor charging and vacuum management

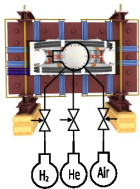


Manual

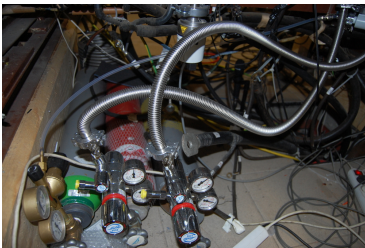
Content

- 1 Introduction
- 2 Overviews
- 3 Ports
- 4 Data acquisition system
- 5 Vacuum management system
- 6 Gas management system
- 7 Preionization
- 8 Energetics infrastructure
- 9 Control system
- 10 Others
- 11 Conclusion

Gas management

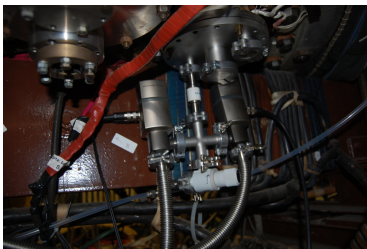


Gas reservoirs - Air, H<sub>2</sub>, He



Comparison of discharges in H and He

Gas injection system - H<sub>2</sub>, Air, He

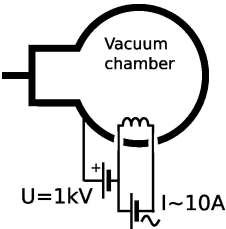


Manual

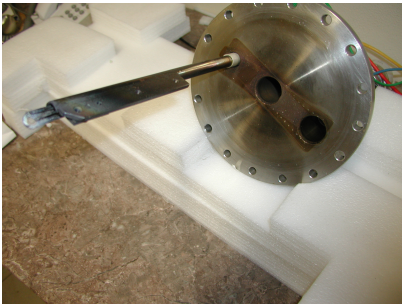
Content

- 1 Introduction
- 2 Overviews
- 3 Ports
- 4 Data acquisition system
- 5 Vacuum management system
- 6 Gas management system
- 7 Preionization
- 8 Energetics infrastructure
- 9 Control system
- 10 Others
- 11 Conclusion

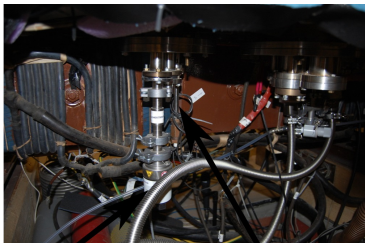
Preionization - scheme



Preionization Gun

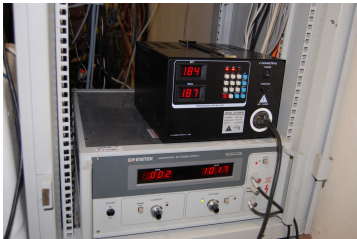


NorthWest - Bottom: Vacuum Gauge & Preionization Gun



Vacuum gauge    Preionization gun

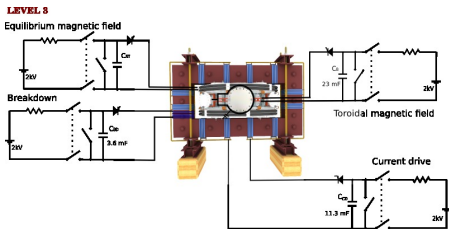
Preionization - power sources



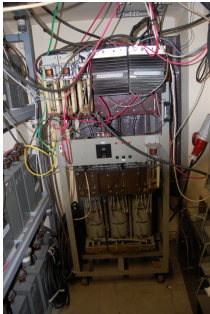
Content

- 1 Introduction
- 2 Overviews
- 3 Ports
- 4 Data acquisition system
- 5 Vacuum management system
- 6 Gas management system
- 7 Preionization
- 8 Energetics infrastructure
- 9 Control system
- 10 Others
- 11 Conclusion

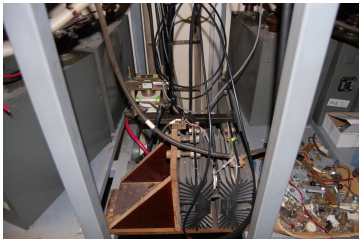
Energetics infrastructure - setup



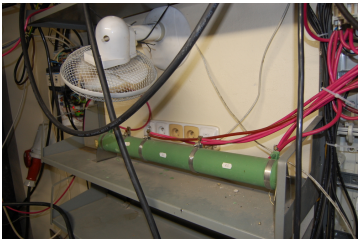
2kV power source, short circuit system and thyristors for breakdown and plasma stabilization



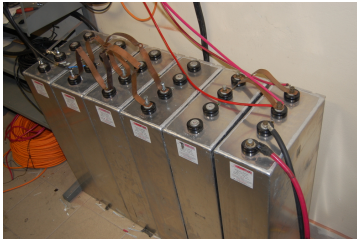
Thyristors for magnetic field and current drive



Charging resistor (common for all 4 circuits)



Capacitor bank for toroidal magnetic field



13500 fd, 1300 Volt, 11500 Joule Oil-Filled Energy Storage Capacitor



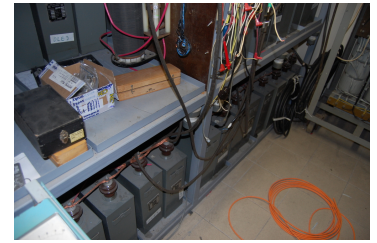
## Capacitor bank for current drive



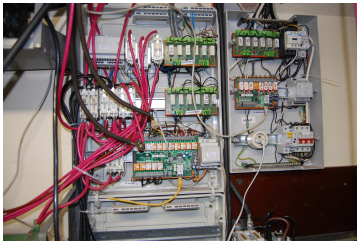
## Capacitor bank for breakdown



## Capacitor bank for plasma stabilization



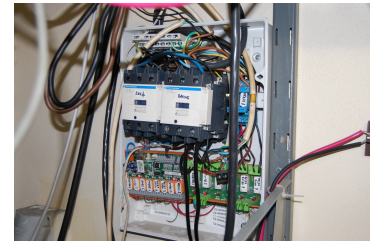
## Control system for capacitor charging and vacuum management



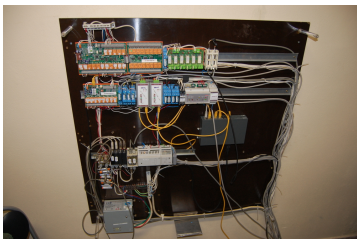
## Content

- 1 Introduction
- 2 Overviews
- 3 Ports
- 4 Data acquisition system
- 5 Vacuum management system
- 6 Gas management system
- 7 Preionization
- 8 Energetics infrastructure
- 9 **Control system**
- 10 Others
- 11 Conclusion

## Control system for Global Power source



## Basic control /including triggering system



## Content

- 1 Introduction
- 2 Overviews
- 3 Ports
- 4 Data acquisition system
- 5 Vacuum management system
- 6 Gas management system
- 7 Preionization
- 8 Energetics infrastructure
- 9 Control system
- 10 **Others**
- 11 Conclusion

## Looking into chamber with the help of glow discharge



## High Temperature Superconductor in cryostat



2 x 6 turns of the 2nd generation HTS (Re)BCO tape

## VIP wall. Do you know somebody?



## Original TM1 chamber



## Content

- 1 Introduction
- 2 Overviews
- 3 Ports
- 4 Data acquisition system
- 5 Vacuum management system
- 6 Gas management system
- 7 Preionization
- 8 Energetics infrastructure
- 9 Control system
- 10 Others
- 11 **Conclusion**

## Acknowledgement

The financial support by FUSENET, MSM 6840770039, MSM 6840770014 and A1581 is acknowledged.

### GOLEM team (students, teachers, technicians)

Edita Bromova, Zdenek Cespiro, Ivan Duran, Vladimir Fuchs, Ondrej Grover, Pavel Hacek, Billy Huang, Igor Jex, Michal Kazda, Jindrich Kocman, Martin Kubic, Ondrej Kudlacek, Petr Liska, Tomas Markovic, Jan Mlynar, Michal Odstrcil, Tomas Odstrcil, Ondrej Pluhar, Gergo Pokol, Ondrej Sebek, Adam Sindlery, Michal Smid, Jan Stöckel, Gabriel Vondrasek, Ondrej Vrba, Frantisek Zacek, and Jiri Zara.

Special thanks: 


## Final


Thank you for your attention



<http://gomtraic.fjfi.cvut.cz>,  
you are welcome.

 G. Van Oost, M. Berta, J. Brotankova, R. Dejarnac, E. Del Bosco, E. Dufkova, I. Duran, M. P. Gryaznevich, J. Horacek, M. Hron, A. Malaquias, G. Mank, P. Peleman, J. Sentkerestiova, J. Stoeckel, V. Weinzett, S. Zoletnik, B. Tal, J. Ferrera, A. Fonseca, H. Hegazy, Y. Kuznetsov, A. Ossyannikov, A. Singh, M. Sokholov, and A. Talebitaher. Joint experiments on small tokamaks: edge plasma studies on CASTOR. *NUCLEAR FUSION*, 47(5):378–386, MAY 2007.

 V. Svoboda, J. Mlynář, G. Pokol, D. Réfy, J. Stöckel, and G. Vondrášek. Former Tokamak CASTOR becomes remotely controllable GOLEM at the Czech Technical University in Prague . In *Europhysics Conference Abstracts. 37th EPS Conference on Plasma Physics* (online: <http://ocs.ciemat.es/EPS2010PAP/pdf/P2.111.pdf>), volume 34A, 2010.

 Brotankova, J. Study of high temperature plasma in tokamak-like experimental devices. PhD. thesis 2009.

 Tokamak GOLEM at the Czech Technical University in Prague. <http://golem.fjfi.cvut.cz>, 2007.

 V. Svoboda, B. Huang, J. Mlynar, G.I. Pokol, J. Stockel, and G Vondrasek. Multi-mode Remote Participation on the GOLEM Tokamak. *Fusion Engineering and Design*, 86(6-8):1310–1314, 2011.

The GOLEM experimental setup

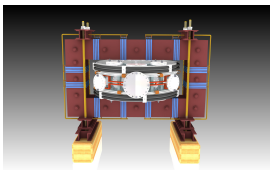
Vojtěch Svoboda & the GOLEM team

September 26, 2012

- 1 Introduction
- 2 Experimental setup
- 3 Golem discharge
- 4 (Remote) operation of the GOLEM tokamak
- 5 Conclusion

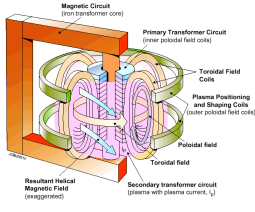
- 1 Introduction
- 2 Experimental setup
- 3 Golem discharge
- 4 (Remote) operation of the GOLEM tokamak
- 5 Conclusion

Tokamak GOLEM - basic parameters:



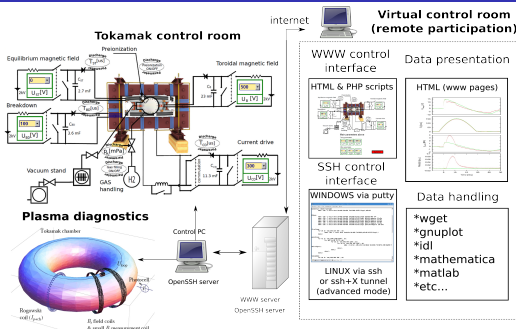
- major radius  $R = 0.4$
- plasma current  $I_{pl} < 10$  kA
- toroidal magnetic field  $B_{tor} < 1$  T
- electron temperature  $T_e(0) < 200$  eV
- minor radius  $a = 0.085$  m
- pulse length  $t < 20$  ms
- plasma density  $n_e = 0.2 - 3.0 \times 10^{19} / m^3$
- ion temperature  $T_i(0) < 100$  eV

Plasma in Tokamak (GOLEM) - the least to do



- Evacuate the chamber.
- Fill in the working gas.
- Toroidal magnetic field to confine plasma.
- Toroidal electric field to breakdown neutral gas into plasma.
- Toroidal electric field to heat the plasma.
- Plasma positioning.
- Diagnostics.

Unique remote operation capability

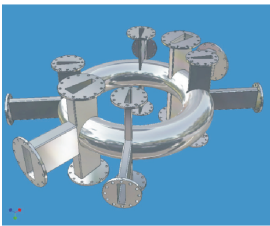
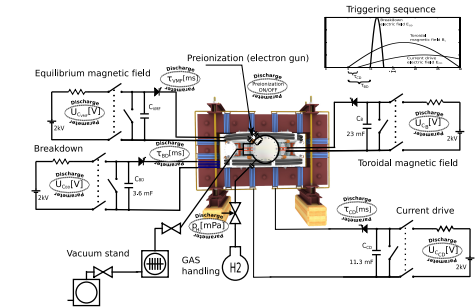


Content

Engineering scheme of the GOLEM tokamak

The GOLEM chamber

- 1 Introduction
- 2 Experimental setup
- 3 Golem discharge
- 4 (Remote) operation of the GOLEM tokamak
- 5 Conclusion

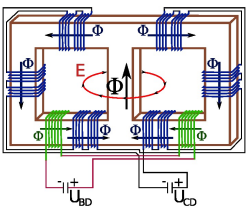


- The plasma cross section is circular.
- The vacuum vessel is made of stainless steel.
- It is /on request/ baked with a series of cycles at 200°C before an experiment.

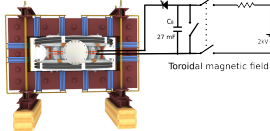
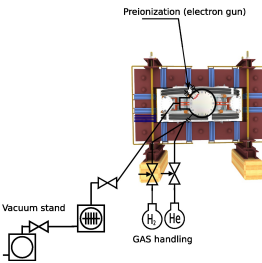
Golem transformer

Preionization, Vacuum and Gas management

Toroidal magnetic field  $B_{tor}$  circuit



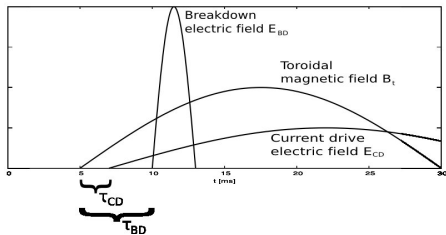
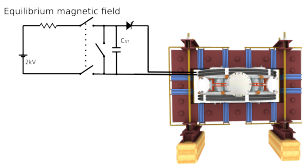
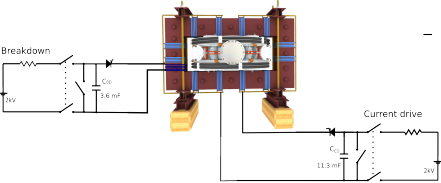
Iron transformer core.



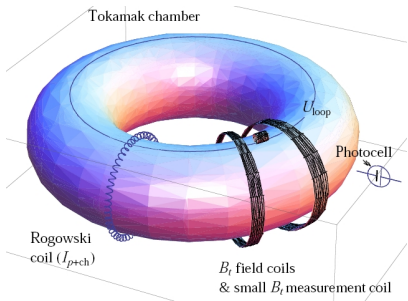
Toroidal electric field  $E_{tor}$  circuit

Vertical magnetic (stabilization) field  $B_{ST}$  circuit

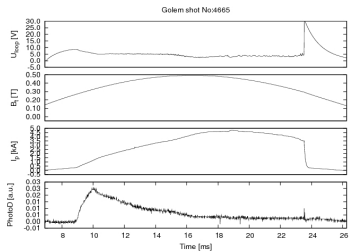
Trigger sequence



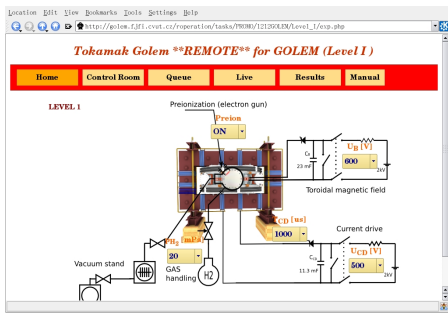
Basic plasma diagnostics on tokamak GOLEM



Golem discharge



The GOLEM tokamak real Control Room



Data access

All the recorded data and the settings for each shot are available at the GOLEM website. The root directory for the files is:

<http://golem.fjfi.cvut.cz/operation/shots/<shotnumber>/>

Basic data of the shot series are collected at a page to be reached at:

<http://golem.fjfi.cvut.cz/operation/tasks/<session>/>

Actual discharge has the web page:

<http://golem.fjfi.cvut.cz/operation/currentshot.>

Actual session has the web page:

<http://golem.fjfi.cvut.cz/operation/currentsession.>

Final

Thank you for your attention

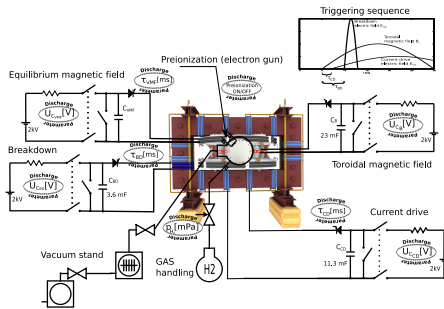


<http://gomtraic.fjfi.cvut.cz.>  
you are welcome.

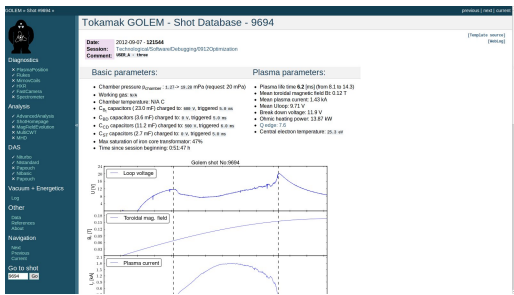
Content

- 1 Introduction
- 2 Experimental setup
- 3 Golem discharge
- 4 (Remote) operation of the GOLEM tokamak
- 5 Conclusion

Engineering scheme of the GOLEM tokamak



The result webpage



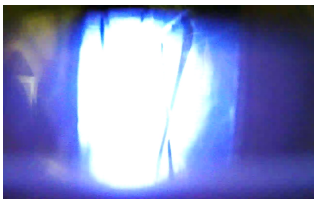
Content

- 1 Introduction
- 2 Experimental setup
- 3 Golem discharge
- 4 (Remote) operation of the GOLEM tokamak
- 5 Conclusion

References I

G. Van Oost, M. Berta, J. Brotankova, R. Dejarnac, E. Del Bosco, E. Dufkova, I. Duran, M. P. Gryaznevich, J. Horacek, M. Hron, A. Malaquias, G. Mank, P. Peleman, J. Sentkerstiova, J. Stoeckel, V. Weinzett, S. Zoletnik, B. Tal, J. Ferrera, A. Fonseca, H. Hegazy, Y. Kuznetsov, A. Ossyannikov, A. Singh, M. Sokholov, and A. Talebitaher. Joint experiments on small tokamaks: edge plasma studies on CASTOR. NUCLEAR FUSION, 47(5):378–386, MAY 2007.

The plasma generation



Content

- 1 Introduction
- 2 Experimental setup
- 3 Golem discharge
- 4 (Remote) operation of the GOLEM tokamak
- 5 Conclusion

Operational parameters and their limits

- The parameters to be set remotely:
- Toroidal magnetic field ( $B_z$ ) through the voltage of the toroidal field capacitor bank  $U_B$ , range: 400 – 1300 V.
  - Toroidal electric field ( $E_{CD}$ ) through the capacitor bank for the current drive  $U_{CD}$ , range: 200 – 600 V.
  - Toroidal electric field ( $E_{BD}$ ) through the capacitor bank for the breakdown  $U_{BD}$ , range: 100 – 200 V.
  - The time delay between the triggers of the toroidal magnetic field and the current drive  $T_{CD}$ , range: 0 – 20000  $\mu$ s.
  - The time delay between the triggers of the toroidal magnetic field and the breakdown  $T_{BD}$ , range: 0 – 20000  $\mu$ s.
  - Hydrogen or Helium gas pressure  $p_{WG}$ , range: 0 – 100 mPa.
  - Status of preionization (ON/OFF).
  - Requested working gas (H2/He).

Acknowledgement

The financial support by FUSENET, MSM 6840770039, MSM 6840770014 and A1581 is acknowledged.

GOLEM team (students, teachers, technicians)

Edita Bromova, Zdenek Cespiro, Ivan Duran, Vladimir Fuchs, Ondrej Grover, Pavel Hacek, Billy Huang, Igor Jex, Michal Kazda, Jindrich Kocman, Martin Kubic, Ondrej Kudlacek, Petr Liska, Tomas Markovic, Jan Mlynar, Michal Odstrcil, Tomas Odstrcil, Ondrej Pluhar, Gergo Pokol, Ondrej Sebek, Adam Sindler, Michal Smid, Jan Stöckel, Gabriel Vondrasek, Ondrej Vrba, Frantisek Zacek, and Jiri Zara.

Special thanks: NATIONAL INSTRUMENTS

References II

V. Svoboda, J. Mlynář, G. Pokol, D. Réfy, J. Stöckel, and G. Vondrášek. Former Tokamak CASTOR becomes remotely controllable GOLEM at the Czech Technical University in Prague. In Europhysics Conference Abstracts. 37th EPS Conference on Plasma Physics (online: <http://ocs.ciemat.es/EPS2010PAP/pdf/P2.111.pdf>), volume 34A, 2010.

Brotankova, J. Study of high temperature plasma in tokamak-like experimental devices. PhD. thesis 2009.

-  Tokamak GOLEM at the Czech Technical University in Prague.  
<http://golem.fjfi.cvut.cz>, 2007.
-  V. Svoboda, B. Huang, J. Mlynar, G.I. Pokol, J. Stockel, and G Vondrasek.  
Multi-mode Remote Participation on the GOLEM Tokamak.  
*Fusion Engineering and Design*, 86(6-8):1310–1314, 2011.



The GOLEM diagnostics

Vojtěch Svoboda & GOLEM team

March 12, 2012

- 1 Data acquisition system
- 2 Radiation
  - Photodiodes
  - Fast cameras
  - Spectra
  - HXR
- 3 Magnetic diagnostics
  - Loop voltage
  - Toroidal magnetic field
  - Current through the chamber and plasma
  - Mirnov coils - plasma position
- 4 Particle Flux
  - Rake probe
- 5 Basic diagnostics
- 6 Conclusion

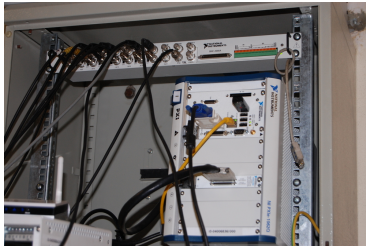
- 1 Data acquisition system
- 2 Radiation
  - Photodiodes
  - Fast cameras
  - Spectra
  - HXR
- 3 Magnetic diagnostics
  - Loop voltage
  - Toroidal magnetic field
  - Current through the chamber and plasma
  - Mirnov coils - plasma position
- 4 Particle Flux
  - Rake probe
- 5 Basic diagnostics
- 6 Conclusion

Data acquisition system I - basic



NI PXI-1031

Data acquisition system II - turbo



NI PXIe-1062Q

Data acquisition system III - papouchSt



Papouch DAS1210

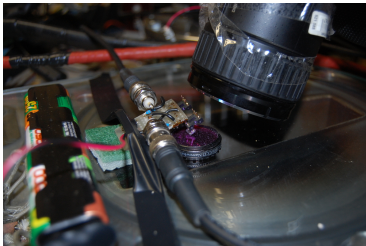
Content

- 1 Data acquisition system
- 2 Radiation
  - Photodiodes
  - Fast cameras
  - Spectra
  - HXR
- 3 Magnetic diagnostics
  - Loop voltage
  - Toroidal magnetic field
  - Current through the chamber and plasma
  - Mirnov coils - plasma position
- 4 Particle Flux
  - Rake probe
- 5 Basic diagnostics
- 6 Conclusion

Outline

- 1 Data acquisition system
- 2 Radiation
  - Photodiodes
  - Fast cameras
  - Spectra
  - HXR
- 3 Magnetic diagnostics
  - Loop voltage
  - Toroidal magnetic field
  - Current through the chamber and plasma
  - Mirnov coils - plasma position
- 4 Particle Flux
  - Rake probe
- 5 Basic diagnostics
- 6 Conclusion

South-Upper port: Photodiodes (I-w/o filter, II-H<sub>α</sub> filter)

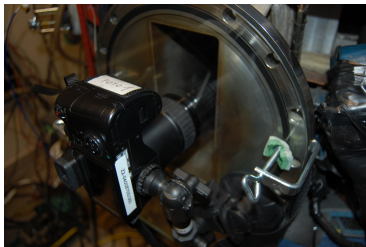


Manual, Spectral sensitivity

Outline

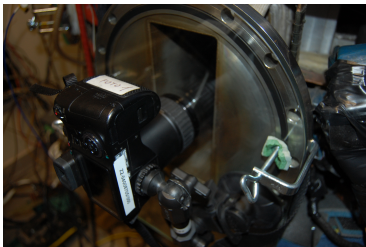
- 1 Data acquisition system
- 2 Radiation
  - Photodiodes
  - Fast cameras
  - Spectra
  - HXR
- 3 Magnetic diagnostics
  - Loop voltage
  - Toroidal magnetic field
  - Current through the chamber and plasma
  - Mirnov coils - plasma position
- 4 Particle Flux
  - Rake probe
- 5 Basic diagnostics
- 6 Conclusion

South-Middle port: Fast camera CASIO FX1 I



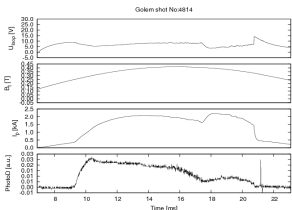
Manual, Graph

South-Upper port: Fast camera CASIO FX1 II



Manual, Graph

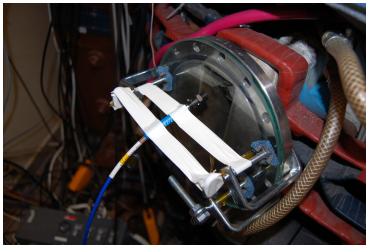
Fast camera CASIO FX1 - results



Outline

- 1 Data acquisition system
- 2 Radiation
  - Photodiodes
  - Fast cameras
  - Spectra
  - HXR
- 3 Magnetic diagnostics
  - Loop voltage
  - Toroidal magnetic field
  - Current through the chamber and plasma
  - Mirnov coils - plasma position
- 4 Particle Flux
  - Rake probe
- 5 Basic diagnostics
- 6 Conclusion

Fiber connecting spectrometer HR2000+



He spectrum No:7163



Spectrometer HR2000+ES

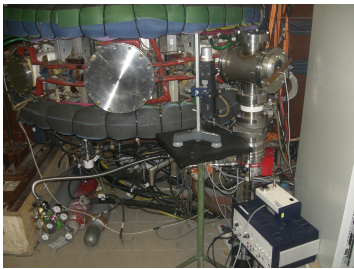


He spectrum No:7163

Outline

- 1 Data acquisition system
- 2 Radiation
  - Photodiodes
  - Fast cameras
  - Spectra
  - HXR
- 3 Magnetic diagnostics
  - Loop voltage
  - Toroidal magnetic field
  - Current through the chamber and plasma
  - Mirnov coils - plasma position
- 4 Particle Flux
  - Rake probe
- 5 Basic diagnostics
- 6 Conclusion

HXR

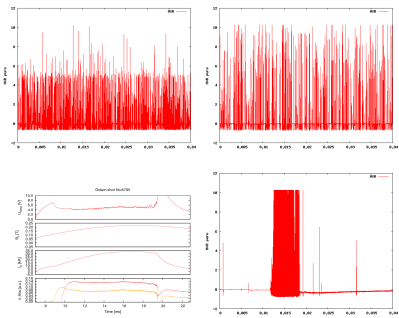


Gamma detector Phywe



Manual

HXR



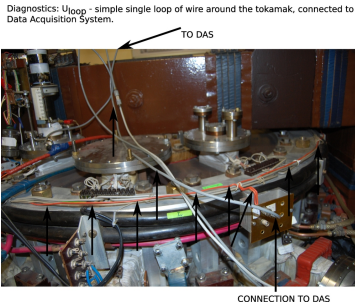
Content

- 1 Data acquisition system
- 2 Radiation
  - Photodiodes
  - Fast cameras
  - Spectra
  - HXR
- 3 Magnetic diagnostics
  - Loop voltage
  - Toroidal magnetic field
  - Current through the chamber and plasma
  - Mirnov coils - plasma position
- 4 Particle Flux
  - Rake probe
- 5 Basic diagnostics
- 6 Conclusion

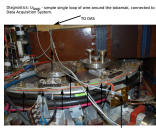
Outline

- 1 Data acquisition system
- 2 Radiation
  - Photodiodes
  - Fast cameras
  - Spectra
  - HXR
- 3 Magnetic diagnostics
  - Loop voltage
  - Toroidal magnetic field
  - Current through the chamber and plasma
  - Mirnov coils - plasma position
- 4 Particle Flux
  - Rake probe
- 5 Basic diagnostics
- 6 Conclusion

Loop Voltage



Basic diagnostic - Loop Voltage



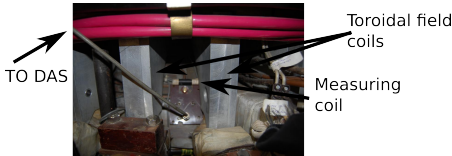
Is deduced from ...

- bla

Outline

- 1 Data acquisition system
- 2 Radiation
  - Photodiodes
  - Fast cameras
  - Spectra
  - HXR
- 3 Magnetic diagnostics
  - Loop voltage
  - Toroidal magnetic field
  - Current through the chamber and plasma
  - Mirnov coils - plasma position
- 4 Particle Flux
  - Rake probe
- 5 Basic diagnostics
- 6 Conclusion

Bt



Basic diagnostic - toroidal magnetic filed  $B_t$



Is deduced from small coil measurements with three operations:

- offset identification from first 4500 data rows).
- time integration (it is a magnetic diagnostic, where  $U_{acquired} \sim \frac{dB_t}{dt}$ )
- multiplication of calibration factor  $C_{Bt}$

$$\langle U_{offset}^{Bt} \rangle = \frac{1}{4500} \sum_{i=0}^{4500} U_i^{Bt}; B_t \approx C_{Bt} \left( \sum_{i=0}^{40000} U_i^{Bt} \Delta t - \langle U_{offset}^{Bt} \rangle t \right).$$

Outline

- 1 Data acquisition system
- 2 Radiation
  - Photodiodes
  - Fast cameras
  - Spectra
  - HXR
- 3 Magnetic diagnostics
  - Loop voltage
  - Toroidal magnetic field
  - Current through the chamber and plasma
  - Mirnov coils - plasma position
- 4 Particle Flux
  - Rake probe
- 5 Basic diagnostics
- 6 Conclusion

Basic diagnostic - total current  $I_{total}$ ,  $I_{pl+ch}$  respectively



Is deduced from Rogowski coil measurements with three operations:

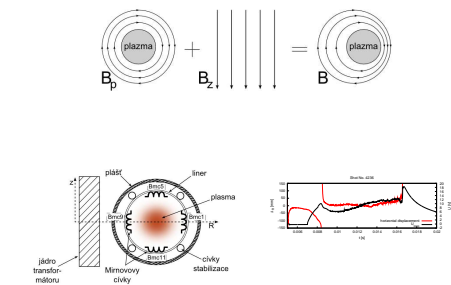
- offset identification from first 4500 data rows).
- time integration (it is a magnetic diagnostic, where  $U_{acquired} \sim \frac{dI_{total}}{dt}$ )
- multiplication of calibration factor  $C_{rog}$

$$\langle U_{offset}^{rog} \rangle = \frac{1}{4500} \sum_{i=0}^{4500} U_i^{rog}; I_{total} \approx C_{rog} \left( \sum_{i=0}^{40000} U_i^{rog} \Delta t - \langle U_{offset}^{rog} \rangle t \right).$$

Outline

- 1 Data acquisition system
- 2 Radiation
  - Photodiodes
  - Fast cameras
  - Spectra
  - HXR
- 3 Magnetic diagnostics
  - Loop voltage
  - Toroidal magnetic field
  - Current through the chamber and plasma
  - Mirnov coils - plasma position
- 4 Particle Flux
  - Rake probe
- 5 Basic diagnostics
- 6 Conclusion

Plasma Position using Mirnov Coils

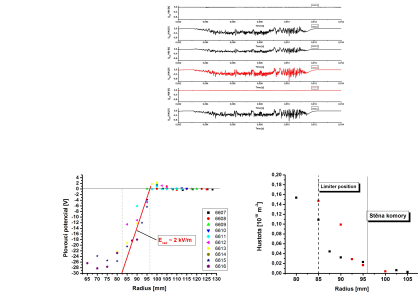


SouthEast-Bottom: Rake probe

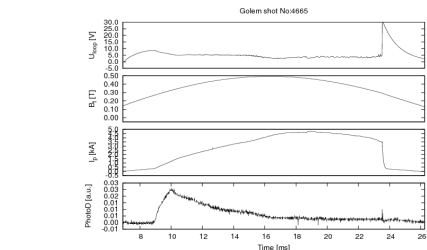


Description, Discharge sequence

Rake probe (2012) - results




Golem discharge



Final

Thank you for your attention

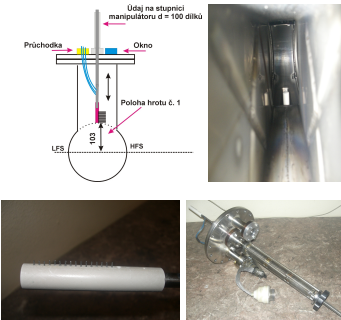


<http://gomtraic.fjfi.cvut.cz>,  
you are welcome.

Content

- 1 Data acquisition system
- 2 Radiation
  - Photodiodes
  - Fast cameras
  - Spectra
  - HXR
- 3 Magnetic diagnostics
  - Loop voltage
  - Toroidal magnetic field
  - Current through the chamber and plasma
  - Mirnov coils - plasma position
- 4 Particle Flux
  - Rake probe
- 5 Basic diagnostics
- 6 Conclusion

Rake probe (2012)



Content

- 1 Data acquisition system
- 2 Radiation
  - Photodiodes
  - Fast cameras
  - Spectra
  - HXR
- 3 Magnetic diagnostics
  - Loop voltage
  - Toroidal magnetic field
  - Current through the chamber and plasma
  - Mirnov coils - plasma position
- 4 Particle Flux
  - Rake probe
- 5 Basic diagnostics
- 6 Conclusion

Content

- 1 Data acquisition system
- 2 Radiation
  - Photodiodes
  - Fast cameras
  - Spectra
  - HXR
- 3 Magnetic diagnostics
  - Loop voltage
  - Toroidal magnetic field
  - Current through the chamber and plasma
  - Mirnov coils - plasma position
- 4 Particle Flux
  - Rake probe
- 5 Basic diagnostics
- 6 Conclusion

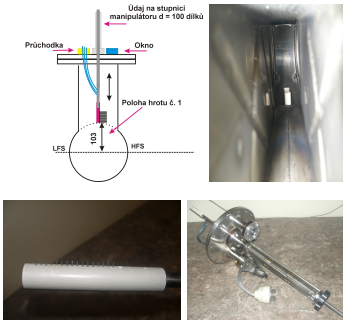
References I

G. Van Oost, M. Berta, J. Brotankova, R. Dejarnac, E. Del Bosco, E. Dufkova, I. Duran, M. P. Gryaznevich, J. Horacek, M. Hron, A. Malaquias, G. Mank, P. Peleman, J. Sentkerstiova, J. Stoeckel, V. Weinzett, S. Zolentnik, B. Tal, J. Ferrera, A. Fonseca, H. Hegazy, Y. Kuznetsov, A. Ossyannikov, A. Singh, M. Sokholov, and A. Talebitaher. Joint experiments on small tokamaks: edge plasma studies on CASTOR. *NUCLEAR FUSION*, 47(5):378–386, MAY 2007.

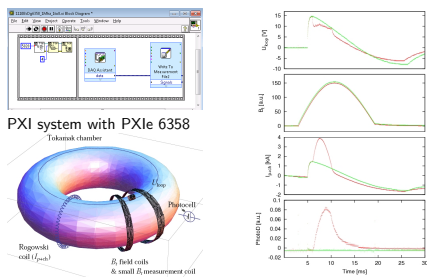
Outline

- 1 Data acquisition system
- 2 Radiation
  - Photodiodes
  - Fast cameras
  - Spectra
  - HXR
- 3 Magnetic diagnostics
  - Loop voltage
  - Toroidal magnetic field
  - Current through the chamber and plasma
  - Mirnov coils - plasma position
- 4 Particle Flux
  - Rake probe
- 5 Basic diagnostics
- 6 Conclusion

Rake probe (2012)



Basic plasma diagnostics in tokamak GOLEM



Data Acquisition System based on: NATIONAL INSTRUMENTS

Acknowledgement

The financial support by FUSENET, MSM 6840770039, MSM 6840770014 and A1581 is acknowledged.

GOLEM team (students, teachers, technicians)

Edita Bromova, Zdenek Cespiro, Ivan Duran, Vladimir Fuchs, Ondrej Grover, Pavel Hacek, Billy Huang, Igor Jex, Michal Kazda, Jindrich Kocman, Martin Kubic, Ondrej Kudlacek, Petr Liska, Tomas Markovic, Jan Mlynar, Michal Odstrcil, Tomas Odstrcil, Ondrej Pluhar, Gergo Pokol, Ondrej Sebek, Adam Sindler, Michal Smid, Jan Stöckel, Gabriel Vondrasek, Ondrej Vrba, Frantisek Zacek, and Jiri Zara.

Special thanks: NATIONAL INSTRUMENTS

References II

V. Svoboda, J. Mlynář, G. Pokol, D. Réfy, J. Stöckel, and G. Vondrášek. Former Tokamak CASTOR becomes remotely controllable GOLEM at the Czech Technical University in Prague. In *Europhysics Conference Abstracts. 37th EPS Conference on Plasma Physics* (online: <http://ocs.ciemat.es/EPS2010PAP/pdf/P2.111.pdf>), volume 34A, 2010.

Brotankova, J. Study of high temperature plasma in tokamak-like experimental devices. PhD. thesis 2009.

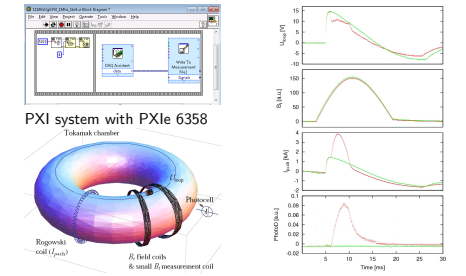
-  Tokamak GOLEM at the Czech Technical University in Prague.  
<http://golem.fjfi.cvut.cz>, 2007.
-  V. Svoboda, B. Huang, J. Mlynar, G.I. Pokol, J. Stockel, and G Vondrasek.  
Multi-mode Remote Participation on the GOLEM Tokamak.  
*Fusion Engineering and Design*, 86(6-8):1310–1314, 2011.

The GOLEM data access

Vojtěch Svoboda & the GOLEM team

March 27, 2012

Basic plasma diagnostics in tokamak GOLEM

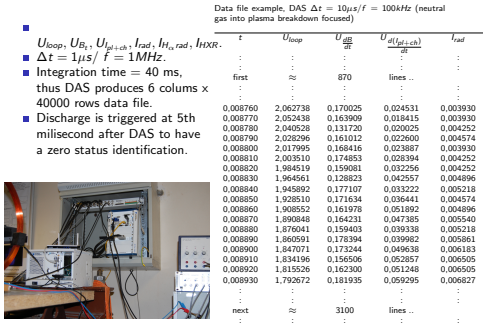


Data Acquisition System based on: NATIONAL INSTRUMENTS

Outline of the talk

- 1 Introduction
- 2 GNU Wget
- 3 Data access
  - Basic parameters
  - Session parameters
  - Discharge setup
  - Basic diagnostics
- 4 GOLEM data import in various graphing utilities
  - Matlab
  - Octave
  - Gnuplot
  - Python
  - Mathematica
  - IDL
  - Excel
- 5 Usefull scripts
- 6 Conclusion

GOLEM basic Data Acquisition System (DAS)



GNU Wget

GNU Wget is a free software package for retrieving files using HTTP, HTTPS and FTP, the most widely-used Internet protocols. It is a non-interactive commandline tool, so it may easily be called from scripts, cron jobs, terminals without X-Windows support, etc.

- Runs on most UNIX-like operating systems as well as Microsoft Windows.
- Homepage: <http://www.gnu.org/software/wget/>
- Basic usage:
  - To get Uloop: `wget http://golem.fjfi.cvut.cz/operation/shots/4665/basicdiag/Uloop_dp.csv`
  - To get whole shot: `wget -r -nH -cut-dirs=3 -no-parent -I2 -Pshot http://golem.fjfi.cvut.cz/operation/shots/4665`

Content

- 1 Introduction
- 2 GNU Wget
- 3 Data access
  - Basic parameters
  - Session parameters
  - Discharge setup
  - Basic diagnostics
- 4 GOLEM data import in various graphing utilities
  - Matlab
  - Octave
  - Gnuplot
  - Python
  - Mathematica
  - IDL
  - Excel
- 5 Usefull scripts
- 6 Conclusion

Data access

All the recorded data and the settings for each shot are available at the GOLEM website. The root directory for the files is:

<http://golem.fjfi.cvut.cz/operation/shots/<shotnumber>/>

Basic data of the shot series are collected at a page to be reached at:

<http://golem.fjfi.cvut.cz/operation/tasks/<session>/>

Actual discharge has the web page:

<http://golem.fjfi.cvut.cz/operation/currentshot.>

Actual session has the web page:

<http://golem.fjfi.cvut.cz/operation/currentsession.>

Session parameters

link: <http://golem.fjfi.cvut.cz/operation/tasks/<sessionname>/Komora/<Parameter>>

where <Parameter> is

- StartTime: session start time.
- AktualPfeifferMerkaVakua: actual pressure in the chamber.
- AktualTermoclanekNaKomora: actual chamber temperature.
- TimeAll: session log.
- graph.jpg: session visual log.

Outline

- 1 Introduction
- 2 GNU Wget
- 3 Data access
  - Basic parameters
  - Session parameters
  - Discharge setup
  - Basic diagnostics
- 4 GOLEM data import in various graphing utilities
  - Matlab
  - Octave
  - Gnuplot
  - Python
  - Mathematica
  - IDL
  - Excel
- 5 Usefull scripts
- 6 Conclusion

Content

- 1 Introduction
- 2 GNU Wget
- 3 Data access
  - Basic parameters
  - Session parameters
  - Discharge setup
  - Basic diagnostics
- 4 GOLEM data import in various graphing utilities
  - Matlab
  - Octave
  - Gnuplot
  - Python
  - Mathematica
  - IDL
  - Excel
- 5 Usefull scripts
- 6 Conclusion

Content

- 1 Introduction
- 2 GNU Wget
- 3 Data access
  - Basic parameters
  - Session parameters
  - Discharge setup
  - Basic diagnostics
- 4 GOLEM data import in various graphing utilities
  - Matlab
  - Octave
  - Gnuplot
  - Python
  - Mathematica
  - IDL
  - Excel
- 5 Usefull scripts
- 6 Conclusion

Outline

- 1 Introduction
- 2 GNU Wget
- 3 Data access
  - Basic parameters
  - Session parameters
  - Discharge setup
  - Basic diagnostics
- 4 GOLEM data import in various graphing utilities
  - Matlab
  - Octave
  - Gnuplot
  - Python
  - Mathematica
  - IDL
  - Excel
- 5 Usefull scripts
- 6 Conclusion

Outline

- 1 Introduction
- 2 GNU Wget
- 3 Data access
  - Basic parameters
  - Session parameters
  - Discharge setup
  - Basic diagnostics
- 4 GOLEM data import in various graphing utilities
  - Matlab
  - Octave
  - Gnuplot
  - Python
  - Mathematica
  - IDL
  - Excel
- 5 Usefull scripts
- 6 Conclusion

Basic parameters

link: <http://golem.fjfi.cvut.cz/operation/shots/<shotnumber>/<Parameter>>

where <Parameter> is

- ShotNo: the discharge number.
- wwwcomment: the discharge comment.
- starttime: the /Central European Time/ time of the discharge.
- SessionNameDate: the full session address.
- SessionName: the short session address.
- date: the date of the session.

Vacuum and gas management

link: <http://golem.fjfi.cvut.cz/operation/shots/<shotnumber>/<Parameter>>

where <Parameter> is

Initial\_PfeifferMerkaVakua: pressure in the chamber before the discharge preparation (vacuum level).

Aktual\_PfeifferMerkaVakua: pressure in the chamber just before the discharge (working gas /H<sub>2</sub> or He/ pressure).

pressure\_setting.mPa: desired working gas pressure.

Aktual\_TermoclanekNaKomore: the chamber temperature before the discharge.

Prelonization: preionization switch ON/OFF ~ 1/0.

H2filling: working gas filling switch ON/OFF ~ 1/0.

Outline

- 1 Introduction
- 2 GNU Wget
- 3 Data access
  - Basic parameters
  - Session parameters
  - Discharge setup
  - Basic diagnostics
- 4 GOLEM data import in various graphing utilities
  - Matlab
  - Octave
  - Gnuplot
  - Python
  - Mathematica
  - IDL
  - Excel
- 5 Usefull scripts
- 6 Conclusion

Discharge appearance

link: <http://golem.fjfi.cvut.cz/operation/shots/<shotnumber>/basicdiagn/<Parameter>>

where <Parameter> is

Plasma: Plasma appearance YES/NO  $\approx$  1/0.

PlasmaStart: Plasma start time.

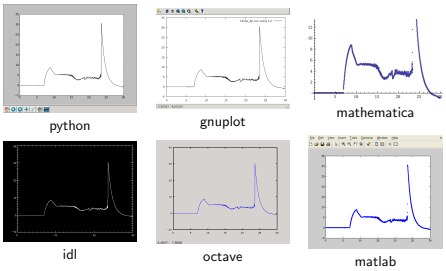
PlasmaEnd: Plasma end time.

PlasmaTimeLength: Plasma duration.

PlasmaStartRow: Plasma start row in data series.

PlasmaEndRow: Plasma end row in data series.

Plot 4665  $U_{loop}$  graph



Outline

- 1 Introduction
- 2 GNU Wget
- 3 Data access
  - Basic parameters
  - Session parameters
  - Discharge setup
  - Basic diagnostics
- 4 GOLEM data import in various graphing utilities
  - Matlab
  - Octave
  - Gnuplot
  - Python
  - Mathematica
  - IDL
  - Excel
- 5 Usefull scripts
- 6 Conclusion

Electromagnetic configuration of the discharge setup

link: <http://golem.fjfi.cvut.cz/operation/shots/<shotnumber>/nabijeni/<Parameter>>

where <Parameter> is

Ub\_limit: desired capacitor voltage  $U_B$  driving toroidal magnetic field  $B_{tor}$ .

Ucd\_limit: desired capacitor voltage  $U_{CD}$  driving toroidal electric field  $E_{CD}$  for current drive.

Ubd\_limit: desired capacitor voltage  $U_{BD}$  driving toroidal electric field  $E_{BD}$  for plasma breakdown.

Ust\_limit: desired capacitor voltage  $U_{ST}$  driving vertical magnetic field  $E_{ST}$  for plasma stabilization.

Discharge basic diagnostics

link: <http://golem.fjfi.cvut.cz/operation/shots/<shotnumber>/basicdiagn/<Parameter>>

where <Parameter> is

usbscopes (tabs & decimal point format): raw voltage data from Data Acquisition System (Uloop,Bt,lp+ch,UPhotoC,UPhotoCHalpha).

usbscopes\_dc (tabs & decimal comma format): raw voltage data from Data Acquisition System (Uloop,Bt,lp+ch,UPhotoC,UPhotoCHalpha).

Discharge physical quantities measured from plasma start to plasma end

link: <http://golem.fjfi.cvut.cz/operation/shots/<shotnumber>/basicdiagn/<Parameter>>

where <Parameter> is

ElectronTemperature: central electron temperature (from Spitzer conductivity).

OhmicHeatingPower: ohmic heating power.

PlasmaTotalCharge: total charge.

MeanBt: mean  $B_{tor}$ .

MeanPlasmaCurrent: mean  $I_p$ .

MeanUloop: mean  $U_{loop}$ ;

Qedge: mean  $Q_{edge}$ .

Outline

- 1 Introduction
- 2 GNU Wget
- 3 Data access
  - Basic parameters
  - Session parameters
  - Discharge setup
  - Basic diagnostics
- 4 GOLEM data import in various graphing utilities
  - Matlab
  - Octave
  - Gnuplot
  - Python
  - Mathematica
  - IDL
  - Excel
- 5 Usefull scripts
- 6 Conclusion

Octave

ShotNo=4665;

baseURL='http://golem.fjfi.cvut.cz/operation/shots/';

diagnPATH='/basicdiagn/Uloop-dp.csv';

%Create a path to data

dataURL=strcat(baseURL,int2str(ShotNo),diagnPATH);

% Write data from GOLEM server to a local file

urlwrite(dataURL,'Uloop-dp.csv');

% Load data

data = dlmread('Uloop-dp.csv',';');

% Plot the graph

plot(data(:,1), data(:,2));

%exit;

% command line execution:

% octave —persist Uloop.m

Triggering configuration of the discharge setup

link: <http://golem.fjfi.cvut.cz/operation/shots/<shotnumber>/<Parameter>>

where <Parameter> is

Tcd\_aktual: time delay for current drive electric field  $E_{CD}$  with respect to toroidal magnetic field  $B_{tor}$ .

Tbd\_aktual: time delay for breakdown electric field  $E_{BD}$  with respect to toroidal magnetic field  $B_{tor}$ .

Tst\_aktual: time delay for stabilising magnetic field  $B_{ST}$  with respect to toroidal magnetic field  $B_{tor}$ .

Discharge basic diagnostics - extracts

link: <http://golem.fjfi.cvut.cz/operation/shots/<shotnumber>/basicdiagn/<Parameter>>

where <Parameter> (decimal point/comma point format) is

Uloop\_dp.csv/Uloop\_cp.csv: Loop voltage:  $<t, U_{loop}>$ .

Btoroidal\_dp.csv/Btoroidal\_cp.csv:  $B_{tor}$  coil:  $<t, B_{tor}>$ .

Irogowski\_dp.csv/Irogowski\_cp.csv: Rogowski coil:  $<t, I_{ch+p}>$ .

lplasma\_dp.csv/lplasma\_cp.csv: Rogowski coil:  $<t, I_p>$ .

Photod\_dp.csv/Photod\_cp.csv: Photocell:  $<t, I_{ad}>$ .

PhotodHalfa\_dp.csv/PhotodHalfa\_cp.csv: Photocell:  $<t, I_{adH\alpha}>$ .

Content

- 1 Introduction
- 2 GNU Wget
- 3 Data access
  - Basic parameters
  - Session parameters
  - Discharge setup
  - Basic diagnostics
- 4 GOLEM data import in various graphing utilities
  - Matlab
  - Octave
  - Gnuplot
  - Python
  - Mathematica
  - IDL
  - Excel
- 5 Usefull scripts
- 6 Conclusion

Matlab

ShotNo=4665;

baseURL='http://golem.fjfi.cvut.cz/operation/shots/';

diagnPATH='/basicdiagn/Uloop-dp.csv';

%Create a path to data

dataURL=strcat(baseURL,int2str(ShotNo),diagnPATH);

% Write data from GOLEM server to a local file

urlwrite(dataURL,'Uloop-dp.csv');

% Load data

data = load('Uloop-dp.csv');

% Plot the graph

plot(data(:,1), data(:,2), 'b');

%exit;

% command line execution:

% matlab —nosplash —nodesktop —r Uloop

Outline

- 1 Introduction
- 2 GNU Wget
- 3 Data access
  - Basic parameters
  - Session parameters
  - Discharge setup
  - Basic diagnostics
- 4 GOLEM data import in various graphing utilities
  - Matlab
  - Octave
  - Gnuplot
  - Python
  - Mathematica
  - IDL
  - Excel
- 5 Usefull scripts
- 6 Conclusion

Gnuplot

```
set macros;
ShotNo = "4665";
baseURL = "http://golem.fjfi.cvut.cz/operation/shots/";
diagnPATH = "/basicdiagn/Uloop_dp.csv";
#Create a path to data
DataURL= "@baseURL@ShotNo@diagnPATH";
#Write data from GOLEM server to a local file
!wget -q @DataURL;
#Plot the graph from a local file
set datafile separator ";";
plotstyle = "with_lines,linestyle_1"
plot 'Uloop_dp.csv' using 1:2 @plotstyle;
exit;

# command line execution:
# gnuplot Uloop_gp -persist
```

Outline

- 1 Introduction
- 2 GNU Wget
- 3 Data access
  - Basic parameters
  - Session parameters
  - Discharge setup
  - Basic diagnostics
- 4 GOLEM data import in various graphing utilities
  - Matlab
  - Octave
  - Gnuplot
  - Python
  - Mathematica
  - IDL
  - Excel
- 5 Usefull scripts
- 6 Conclusion

IDL

```
ShotNo=4665;
baseURL='golem.fjfi.cvut.cz/operation/shots/';
diagnPATH='/basicdiagn/Uloop_dp.csv';
;Create a path to data
dataURL=baseURL+STRTRIM(string(ShotNo,1)+diagnPath;
;Write data from GOLEM server to a local file
oUrl = OBJNEW('IDLnetUrl')
oUrl->SetProperty, URL_HOST = dataURL
fn = oUrl->Get(FILENAME='Uloop_dp.csv')
;Load data
data= read_ascii('Uloop_dp.csv',delimiter = ';')
;Plot the graph
plot, data, field1(0,*),data, field1(1,*)
;exit

;command line execution:
;idl Uloop.pro
```

Content

- 1 Introduction
- 2 GNU Wget
- 3 Data access
  - Basic parameters
  - Session parameters
  - Discharge setup
  - Basic diagnostics
- 4 GOLEM data import in various graphing utilities
  - Matlab
  - Octave
  - Gnuplot
  - Python
  - Mathematica
  - IDL
  - Excel
- 5 Usefull scripts
- 6 Conclusion

The call

Author will highly appreciate any comments, suggestions to the material presented. Especially we are looking forward to enrich the list of possible scripts in graphing systems (e.g. maple, origin, science, root, ...). Thank you in advance. Vojtech Svoboda, [mailto:svoboda@fjfi.cvut.cz](mailto:mailto:svoboda@fjfi.cvut.cz)

Outline

- 1 Introduction
- 2 GNU Wget
- 3 Data access
  - Basic parameters
  - Session parameters
  - Discharge setup
  - Basic diagnostics
- 4 GOLEM data import in various graphing utilities
  - Matlab
  - Octave
  - Gnuplot
  - Python
  - Mathematica
  - IDL
  - Excel
- 5 Usefull scripts
- 6 Conclusion

Mathematica

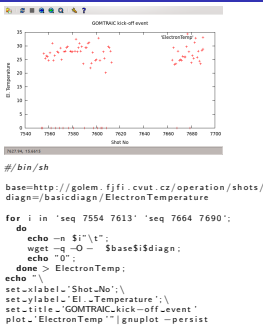
```
baseURL = "http://golem.fjfi.cvut.cz/operation/shots/";
ShotNo = 4665;
diagnPATH = "/basicdiagn/Uloop_dp.csv";
dataURL = baseURL <> ToString[ShotNo] <> diagnPATH;
dataimp=StringSplit[Import[dataURL, "List"], ";", "All"]
data = ToExpression[dataimp];
graf=ListPlot[data]
Export["graf.png",graf]

(* command line execution: *)
(* mathematica Uloop.ma *)
```

Outline

- 1 Introduction
- 2 GNU Wget
- 3 Data access
  - Basic parameters
  - Session parameters
  - Discharge setup
  - Basic diagnostics
- 4 GOLEM data import in various graphing utilities
  - Matlab
  - Octave
  - Gnuplot
  - Python
  - Mathematica
  - IDL
  - Excel
- 5 Usefull scripts
- 6 Conclusion

Linux bash + Gnuplot



Acknowledgement

The financial support by FUSENET, MSM 6840770039, MSM 6840770014 and A1581 is acknowledged.

GOLEM team (students, teachers, technicians)

Edita Bromova, Zdenek Cespiro, Ivan Duran, Vladimir Fuchs, Ondrej Grover, Pavel Hacek, Billy Huang, Igor Jex, Michal Kazda, Jindrich Kocman, Martin Kubic, Ondrej Kudlacek, Petr Liska, Tomas Markovic, Jan Mlynar, Michal Odstrcil, Tomas Odstrcil, Ondrej Pluhar, Gergo Pokol, Ondrej Sebek, Adam Sindlery, Michal Smid, Jan Stöckel, Gabriel Vondrasek, Ondrej Vrba, Frantisek Zacek, and Jiri Zara.

Python

```
import matplotlib.pyplot as plt
from numpy import loadtxt
from urllib import urlopen

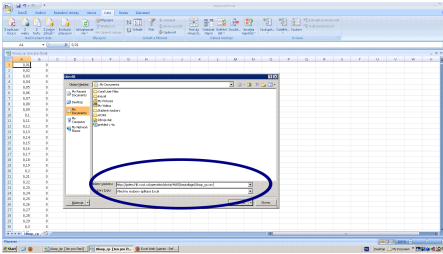
baseURL = "http://golem.fjfi.cvut.cz/shots/"
ShotNo = 4665
diagnPATH = "/basicdiagn/Uloop_dp.csv"
#Create a path to data
dataURL = urlopen(baseURL+ str(ShotNo) + diagnPATH)
#Load data from GOLEM server
data=loadtxt(dataURL, delimiter=';')
#Plot the graph
plt.plot(data[:,0], data[:,1], 'k-')
plt.show()

# command line execution:
# python Uloop.py
```

Outline

- 1 Introduction
- 2 GNU Wget
- 3 Data access
  - Basic parameters
  - Session parameters
  - Discharge setup
  - Basic diagnostics
- 4 GOLEM data import in various graphing utilities
  - Matlab
  - Octave
  - Gnuplot
  - Python
  - Mathematica
  - IDL
  - Excel
- 5 Usefull scripts
- 6 Conclusion

Excel



File→Open→ [http://golem.fjfi.cvut.cz/shots/4665/basicdiagn/Uloop\\_dp.csv](http://golem.fjfi.cvut.cz/shots/4665/basicdiagn/Uloop_dp.csv)

Content


- 1 Introduction
- 2 GNU Wget
- 3 Data access
  - Basic parameters
  - Session parameters
  - Discharge setup
  - Basic diagnostics
- 4 GOLEM data import in various graphing utilities
  - Matlab
  - Octave
  - Gnuplot
  - Python
  - Mathematica
  - IDL
  - Excel
- 5 Usefull scripts
- 6 Conclusion


Final


Thank you for your attention




<http://gomtraic.fjfi.cvut.cz>,  
you are welcome.

 V. Svoboda, B. Huang, J. Mlynar, G.I. Pokol, J. Stockel, and G Vondrasek.  
Multi-mode Remote Participation on the GOLEM Tokamak.  
*Fusion Engineering and Design*, 86(6-8):1310–1314, 2011.

 V. Svoboda, J. Mlynář, G. Pokol, D. Réfy, J. Stöckel, and G. Vondrášek.  
Former Tokamak CASTOR becomes remotely controllable GOLEM at the Czech Technical University in Prague .  
In *Europhysics Conference Abstracts. 37th EPS Conference on Plasma Physics* (online:  
<http://ocs.ciemat.es/EPS2010PAP/pdf/P2.111.pdf>), volume 34A, 2010.

 Brotankova, J.  
Study of high temperature plasma in tokamak-like experimental devices.  
PhD. thesis 2009.

 E. Bromova, I. Duran, O. Grover, J. Kocman, T. Markovic, M. Odstrcil, T. Odstrcil, O. Pluhar, J. Stockel, V. Svoboda, A. Sindlery, G. Vondrasek, and J. Zara.  
The GOLEM Tokamak for Fusion Education .  
In *Europhysics Conference Abstracts. 38th EPS Conference on Plasma Physics*  
(online:<http://ocs.ciemat.es/EPS2011PAP/pdf/P1.021.pdf>), volume 35G, 2011.



# Basic Tokamak Operation Physical Quantities

GOLEM team

July 12, 2012

## 1 Physical Quantities

## 1 Physical Quantities

## Plasma heating power

- In the GOLEM tokamak the only heating mechanism of the plasma is **ohmic heating**.
- This is resulting from current flowing in a conductor with finite resistivity.
- The ohmic heating power can be calculated as:

$$P_{OH}(t) = R_{pl}(t) \cdot I_{pl}^2(t) \quad (1)$$

where  $R_{pl}$  is the resistance of the plasma and  $I_{pl}$  is the current flowing in the plasma.

## Central electron temperature estimation I [3]

Specific resistivity of a fully ionized plasma only depends on:

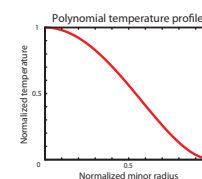
- electron temperature ( $T_e$ )
- effective charge number ( $Z_{eff}$ )

This dependence is quantified by the Spitzer formula [?] and the **effective charge number** is assumed as  $Z_{eff} = 2.5$ .

Making estimation of the electron temperature from integrated value of resistivity ( $R_{pl}(t)$ ) is ambiguous, because center of the plasma has

- Higher temperature
- Lower resistivity
- Higher current density

## Central electron temperature estimation II [3]



However, if we use an equilibrium temperature profile (2) (Figure 6), measured in more detailed measurements [3], we can estimate one parameter of the profile, which is in this case the **central electron temperature** ( $T_{e0}(t)$ ):

$$T_e(r, t) = T_{e0}(t) \left(1 - \frac{r^2}{a^2}\right)^2 \quad (2)$$

## Central electron temperature estimation III [3]

The central electron temperature ( $T_{e0}$ ) is then calculated using Spitzer's resistivity formula. The current density of plasma is

$$j = E \cdot \sigma \quad (3)$$

where  $\sigma$  is the specific conductivity of plasma given by

$$\sigma(r) = 1.544 \cdot 10^3 \cdot \frac{T_e(r, t)^{3/2}}{Z_{eff}}, \quad [\Omega^{-1} \text{m}^{-1}, \text{eV}] \quad (4)$$

and the electric field  $E$  is assumed constant in the poloidal cross-section:

$$E = \frac{U_{loop}}{2\pi R} \quad (5)$$

Plasma current is obtained by integrating current density over the plasma column:

$$I_{pl} = \int_0^a E \cdot \sigma(r) 2\pi r dr. \quad (6)$$

## Central electron temperature estimation IV [3]

Substituting (4) and (5) in (6) gives us the formula for the central electron temperature

$$T_e(0) = \left( \frac{R}{a^2} \cdot \frac{8 \cdot Z_{eff}}{1.544 \cdot 10^3} \right)^{2/3} \cdot \left( \frac{I_{pl}}{U_{loop}} \right)^{2/3} \quad (7)$$

For the CASTOR/GOLEM tokamak geometry with  $a = 78 \text{ mm}$ :

$$T_e(0) = 89.8 \cdot \left( \frac{I_{pl} [\text{kA}]}{U_{loop}} \right)^{2/3} \approx 230 \text{ eV}. \quad (8)$$

## Electron density

The ideal gas law is used to give an order of magnitude estimate of the **electron density** (in particle/ $\text{m}^3$ ):

$$n_{avr} = \frac{2p_{ch}}{k_B T_{ch}} \quad (9)$$

where  $p_{ch}$  is the pressure of the chamber and  $T_{ch}$  is the chamber temperature, which is normally corresponding with the room temperature.

This is a very rough estimate basically for two reasons:

- Plasma is not fully ionized, which makes us overestimate the electron density.
- Adsorbed gases are released from the surface of plasma facing components during the discharge. These atoms enter the plasma and can be ionized, thus making us underestimate the electron density.

## Plasma energy

The **total energy** content can be simply calculated from the temperature, density and volume ( $V$ ), based on the ideal gas law, taking into account the assumed (2) temperature profile:

$$W_{pl}(t) = V \frac{n_{avr} k_B T_{e0}(t)}{3} \quad (10)$$

The information that the magnetic field reduces the degrees of freedom of the particles to two has been used to derive this formula. Uncertainty of this formula is dominated by the uncertainty of our density estimate (9), which makes it good for only an order of magnitude estimate.

## Energy confinement time

An important concept regarding the energy balance of the tokamak fusion reactor is the **energy confinement time** ( $\tau_E$ ). It is the characteristic time of energy loss:

$$P_{loss} = \frac{W_{pl}}{\tau_E} \quad (11)$$

where  $P_{loss}$  is the power lost and  $W_{pl}$  is the total plasma energy.

Having an estimate for the plasma energy (10), the energy confinement time can be estimated at the point where the plasma energy has its maximum:

$$\tau_E(t_{top}) = \frac{W_{pl}(t_{top})}{P_{OH}(t_{top})} \quad (12)$$

$$\frac{dW_{pl}}{dt}(t_{top}) = 0. \quad (13)$$

## Safety factor

- The tokamak magnetic field consists of nested magnetic surfaces.
- Safety factor** ( $q$ ) gives the number of toroidal turns necessary for the magnetic field line at the given magnetic surface to reach its original position poloidally.
- On large aspect ratio circular tokamaks (like GOLEM), it can be approximated by:

$$q(r, t) = \frac{r}{R} \frac{B_t(t)}{B_p(r, t)}, \quad (14)$$

- where  $R$  is the major radius, ( $r_0$ ) is the minor radius,  $B_t(t)$  is the toroidal and  $B_p(r, t)$  is the poloidal magnetic field.

## Safety factor - Illustration I

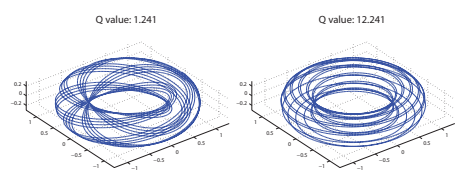


Figure: Magnetic field lines in a tokamak for different safety factors.

## Safety factor - Illustration II

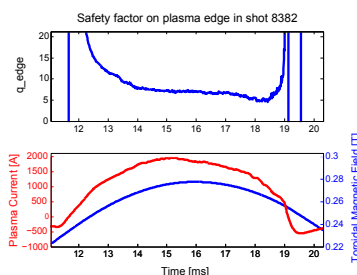




Figure: The time evolution of the safety factor on plasma edge.

## References I

- G. Van Oost, M. Berta, J. Brotankova, R. Dejarnac, E. Del Bosco, E. Dufkova, I. Duran, M. P. Gryaznevich, J. Horacek, M. Hron, A. Malaquias, G. Mank, P. Peleman, J. Sentkerestiova, J. Stoeckel, V. Weinzett, S. Zolotnik, B. Tal, J. Ferrera, A. Fonseca, H. Hegazy, Y. Kuznetsov, A. Ossyannikov, A. Singh, M. Sokholov, and A. Talebitaher. Joint experiments on small tokamaks: edge plasma studies on CASTOR. *NUCLEAR FUSION*, 47(5):378–386, MAY 2007.



 V. Svoboda, J. Mlynář, G. Pokol, D. Réfy, J. Stöckel, and G. Vondrášek.  
Former Tokamak CASTOR becomes remotely controllable GOLEM at the Czech Technical University in Prague .  
In *Europhysics Conference Abstracts. 37th EPS Conference on Plasma Physics* (online:  
<http://ocs.ciemat.es/EPS2010PAP/pdf/P2.111.pdf>), volume 34A, 2010.

 Brotankova, J.  
Study of high temperature plasma in tokamak-like experimental devices.  
*PhD. thesis* 2009.

 Tokamak GOLEM at the Czech Technical University in Prague.  
<http://golem.fjfi.cvut.cz>, 2007.

 V. Svoboda, B. Huang, J. Mlynar, G.I. Pokol, J. Stockel, and G Vondrasek.  
Multi-mode Remote Participation on the GOLEM Tokamak.  
*Fusion Engineering and Design*, 86(6-8):1310–1314, 2011.

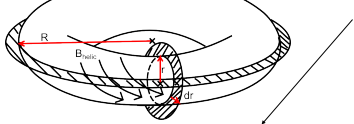
# Plasma MHD Activity Observations via Magnetic Diagnostics

Magnetic islands, statistical methods, magnetic diagnostics, tokamak operation

## Safety factor

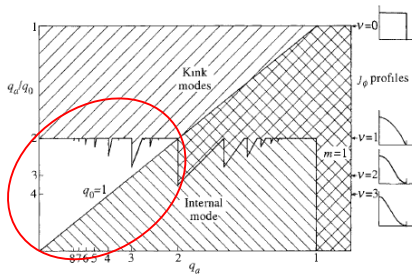
- Critical plasma parameter

- Calculated as:  $q = \frac{d\chi}{d\psi}$

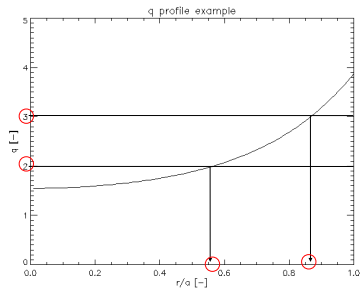


$$q(r) = \frac{2\pi r dr B_T}{2\pi R dr B_\theta(r)} = \frac{r}{R} \frac{B_T}{B_\theta(r)}$$

## Plasma stability as f-tion of q



## Locations where islands will emerge



- Sheared poloidal field in vicinity of resonant surface – approximated by first-order Taylor

$$B_\theta^* = - \left( B_\theta \frac{q'}{q} \right)_{r_s} (r - r_s)$$

$$B_r(r, \chi) = \widehat{B}_r(r) \sin(m\chi)$$

- Cause of flux surface perturbation
- 3-4 orders of magnitude below toroidal field

## Outline

- Safety factor profile calculation
- Perturbation of nested flux surfaces and context with q profile
- Simple magnetic island model
- Signature of magnetic island in poloidal magnetic field
- Principle of detection of this signature
- Tasks within magnetic diagnostics group
- Summary

## Safety factor

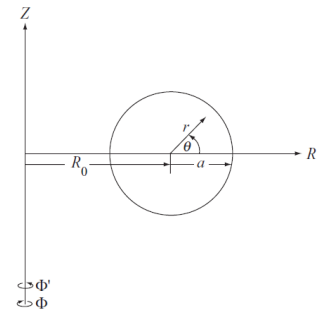
- If plasma current density:  $j(r) = j_0(1 - (r/a)^2)^\nu$

$$j_0 = \frac{\nu + 1}{\pi a^2} I_p$$

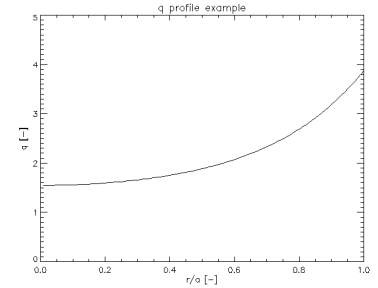
- Then:  $B_\theta(r, \nu) = \frac{\mu_0 j_0}{r} \int_0^r \rho \left(1 - \frac{\rho^2}{a^2}\right)^\nu d\rho$

- And:  $q(r, \nu) = \frac{2\pi B_T}{R\mu_0 I_p} \frac{r^2}{1 - (1 - \frac{r^2}{a^2})^{\nu+1}}$

## Used coordinate system

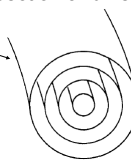


$$q(r, \nu) = \frac{2\pi B_T}{R\mu_0 I_p} \frac{r^2}{1 - (1 - \frac{r^2}{a^2})^{\nu+1}}$$



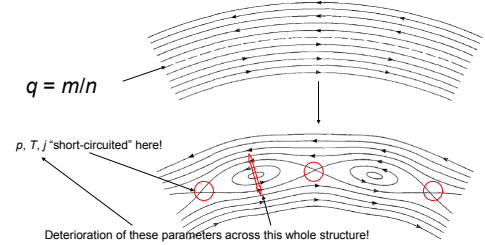
## Nested flux surfaces

- Plasma in equilibrium – set of nested poloidal flux  $\Psi$  surfaces of constant magnitude
- In the case of circular cross-section and zero Shafranov shift
- Each surface:
  - $\Psi = \text{const}$
  - $p = \text{const}$
  - $T = \text{const}$
  - $j_{\text{plasma}} = \text{const}$



## Perturbations of flux surfaces

- Where  $q = m/n$ , where both  $m$  and  $n$  are low natural numbers → flux surfaces perturbed



Deterioration of these parameters across this whole structure!

## Detection of magnetic island

- Let there be magnetic island in GOLEM plasma where  $q_s = \frac{m}{n}$
- Islands affect  $p$ ,  $T$  and  $j$
- On GOLEM,  $p$  and  $T$  measurements are not optimized
- However,  $j$  affects magnetic field, whose measurements are more reliable
- Question: How EXACTLY does island affect magnetic field from plasma? What are we looking for in data?

$$\begin{aligned} \text{Therefore: } \frac{dr}{r_s d\chi} &= \frac{B_r}{B_\theta^*} \\ -B_\theta \frac{q'}{q} (r - r_s) dr &= r_s \widehat{B}_r \sin(m\chi) d\chi \\ -\int_{r_s}^r (r' - r_s) dr' &= \frac{r_s \widehat{B}_r q}{q' B_\theta} \int_{\chi_0}^{\chi} \sin(m\chi) d\chi' \\ z^2 &= \frac{w^2}{8} (\cos(m\chi) - \cos(m\chi_0)) \end{aligned}$$

## Simple model of magnetic island

- Transform:  $\chi = \theta - \frac{n}{m} \phi$
- Island structure obtained from magnetic field line trajectory:

$$\frac{dr}{r_s d\chi} = \frac{B_r}{B_\theta^*}$$

Unknown quantities

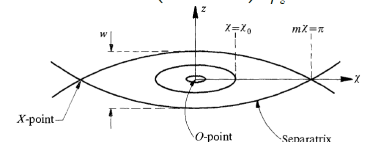
$$B_\theta^* = B_\theta \left(1 - \frac{n}{m} q(r)\right)$$

User-defined coordinates

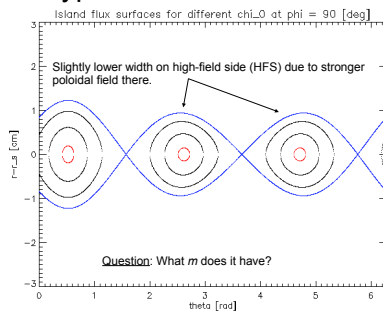
- Island field line equation:

$$z^2 = \frac{w^2}{8} (\cos(m\chi) - \cos(m\chi_0))$$

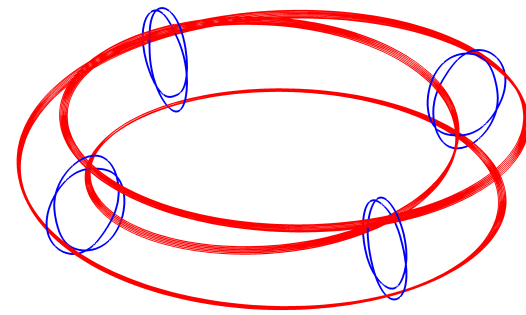
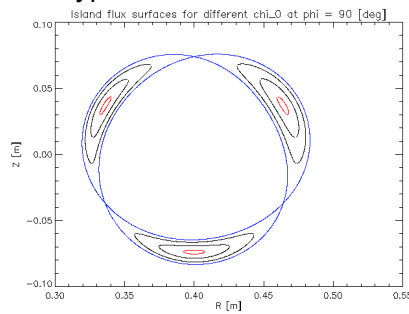
- Where:  $w = 4 \left( \frac{r_s \widehat{B}_r q}{m q' B_\theta} \right)_{r_s}^{1/2}$   $z = r - r_s$



## Typical GOLEM island



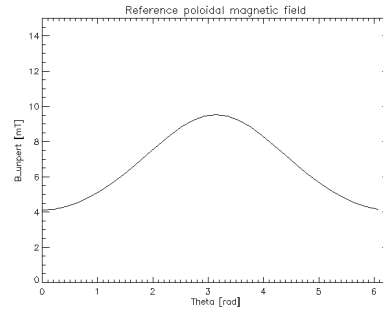
## Typical GOLEM island



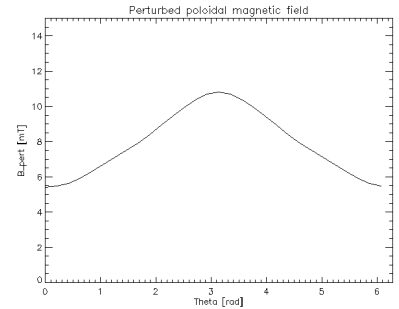
## Island signature in magnetic field

- Poloidal magnetic field – generated by plasma alone (let us forget about poloidal coils for now)
- What is magnitude of this field across the poloidal coordinate and outside of plasma?

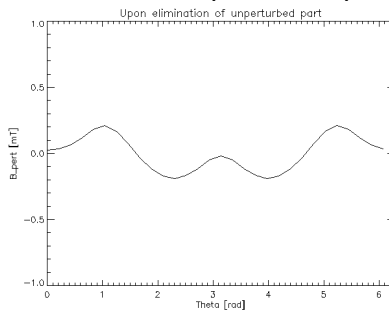
## Unperturbed current density



## Perturbed current density



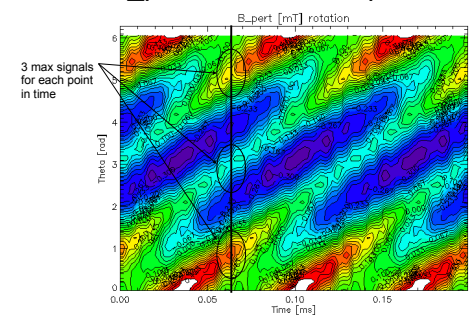
## Elimination of unperturbed part



## Poloidal rotation of island

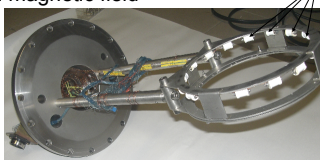
- Plasma and islands exhibit significant intrinsic rotation
- Let plasma be rotating with 5 kHz frequency in poloidal direction
- How will then poloidal field perturbation across poloidal angle change with time?

## B\_pert in time and space



## Detection of magnetic island

- Previous slide → magnetic island identified by detection of plasma magnetic field temporal evolution along poloidal angle
- Optimal detection device – set of many sensors of local magnetic field

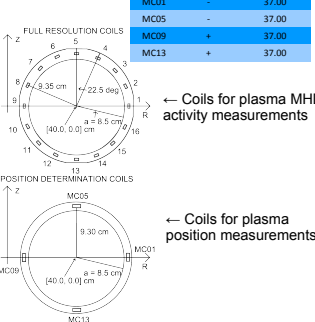


## B\_0 measurement coils

Coil # [ ]	Polarity [ ]	A_eff [cm^2]
MC01	-	37.00
MC05	-	37.00
MC09	+	37.00
MC13	+	37.00

Coil # [ ]	Polarity [ ]	A_eff [cm^2]
1	-	68.93
2	-	140.68
3	+	138.83
4	+	140.43
5	-	68.59
6	+	134.47
7	-	134.28
8	+	142.46
9	-	67.62
10	+	142.80
11	-	140.43
12	x	x
13	x	x
14	x	x
15	-	139.82
16	-	139.33



## Plans within magnetics task group

- Get familiar with operation of tokamak GOLEM
  - $q(r)$  strongly depends on global discharge parameters
  - Operate tokamak in such a way, that nice magnetic island is present at the edge of plasma
- Identify islands as  $B_p$  field fluctuations across time and space
- Apply special statistical methods (FFT, cross-corr, SVD) to get basic island parameters
- Discuss observation vs. calculations from global parameters

## Summary

- In tokamak plasma, magnetic islands emerge on rational  $q$  surfaces
- These cause deterioration in plasma parameters and endanger plasma confinement stability
- Island model based on magnetic field line trajectory and assumption of short-circuiting of  $j(r)$  due to island presence
  - Then, island identified as space-time fluctuations of plasma magnetic field

## Summary

- These fluctuations can be detected by set of local magnetic field sensors
- Application of statistical methods will identify basic island parameters

## Thank you for your attention

- Contact: markovic@ipp.cas.cz



# Plasma MHD Activity Observations via Magnetic Diagnostics

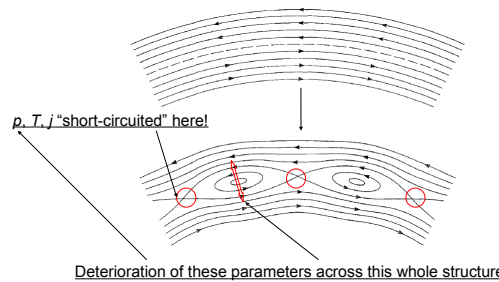
Magnetic islands, statistical methods, magnetic diagnostics, tokamak operation

## Safety factor

- Radial profile:

$$q(r, \nu) = \frac{2\pi B_T}{R\mu_0 I_p} \frac{r^2}{1 - \left(1 - \frac{r^2}{a^2}\right)^{\nu+1}}$$

- On  $r$  where  $q = m/n$  a perturbation of nested poloidal flux surfaces will emerge
  - On flux surface –  $p, j, T$  are constant



## Magnetic island model

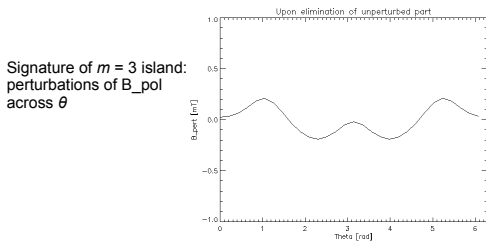
- From perturbed field line trajectory:

$$z^2 = \frac{w^2}{8} (\cos(m\chi) - \cos(m\chi_0))$$

- With  $\chi = \theta - \frac{n}{m}\phi$   $z = r - r_s$

$$w = 4 \left( \frac{r_s \widehat{B}_r q}{mq' B_\theta} \right)^{1/2}_{r_s}$$

- Short-circuited  $j(r)$  profile by island
  - Poloidal magnetic field generated by plasma is slightly perturbed across poloidal angle  $\theta$
  - This depends on  $m$ -mode number of island



## Fast Fourier Transform (FFT)

- FFT – discrete Fourier transform by character
- However, full Fourier transform:

$$B(\nu) = \frac{1}{\sqrt{2\pi}} \int_{-\infty}^{\infty} B(t) e^{-i2\pi\nu t} dt$$

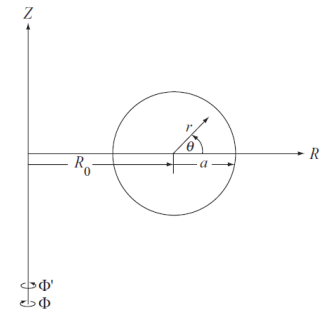
Just how is one supposed to represent infinity by finite interval of measurement?

- Solution – analyzed part of signal is assumed to periodically repeat from infinity to infinity

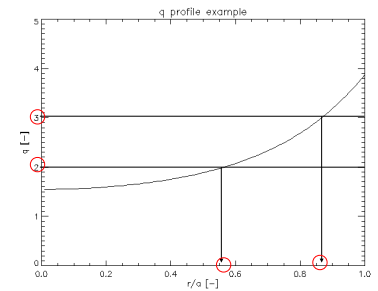
## Outline

- Summarization of island model and theory
- Application of statistical methods
  - FFT and spectrogram
  - Cross-correlation
- Summary of statistical methods

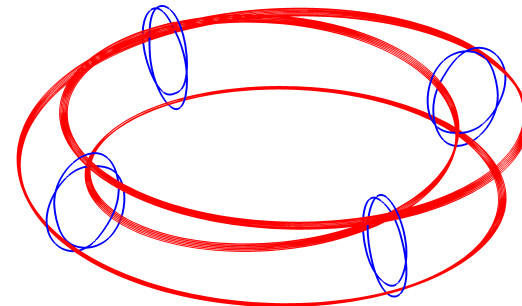
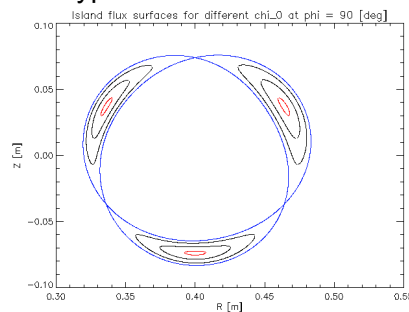
## Used coordinate system



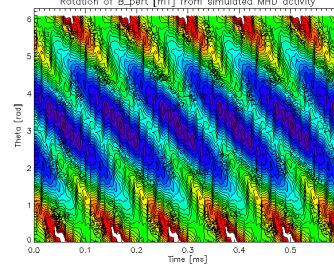
## Locations where islands will emerge



## Typical GOLEM island



- Plasma and island rotates –  $B_{pol}(\theta)$  changes with time
- Example of  $m = 3$  island signal across  $(\theta, t)$  space at 3 kHz poloidal rotation (by model):



## Application of statistical methods

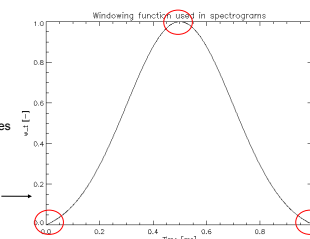
- Up until now – model
  - Known  $m$  and  $f$  of rotation
- Our task – opposite character
  - We are trying to identify  $m$  and  $f$  from data
- Analysis of temporal and spatial domain of signal – identification of  $f$  and  $m$  respectively
- To understand how is output of statistical methods of analysis connected to these quantities – application to known data from model

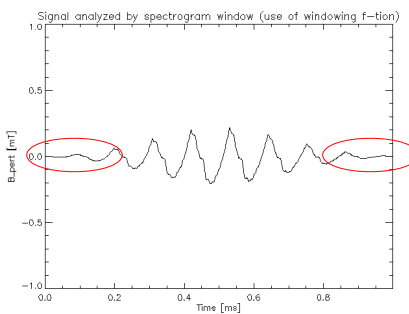
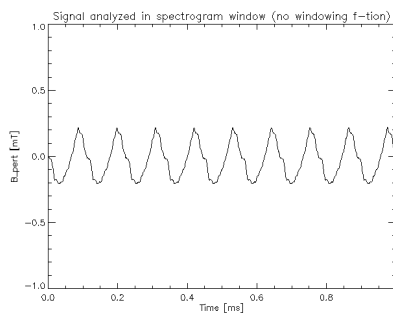
## Windowing method

- Multiplication of signal by an appropriate function
- Most common:
  - Hamming,
  - Gaussian, ...

All have 1 in center and 0 at edges

This is my favorite one →





## FFT algorithm

- Finally, it is safe to apply FFT
- It's IDL implementation:

$$F(\nu) = \frac{1}{N} \sum_{x=0}^{N-1} f(x) e^{-i2\pi\nu x/N}$$

- Most commonly used in temporal domain of signal – to obtain frequencies of signal
  - However, application of FFT on spatial domain may yield  $m$  mode number of island

## Output of FFT (IDL)

- Input – array of time evolution of signal
- Output:
  - Array of same size as input
  - Complex numbers representing Fourier coefficients
  - Each coefficient – “strength” of given frequency in signal
  - Frequencies go from  $-f_{\text{sample}}/2$  to  $+f_{\text{sample}}/2$
  - First half of output array – positive frequencies, second half – negative frequencies
  - Both halves are the same in absolute values

## How to process FFT output

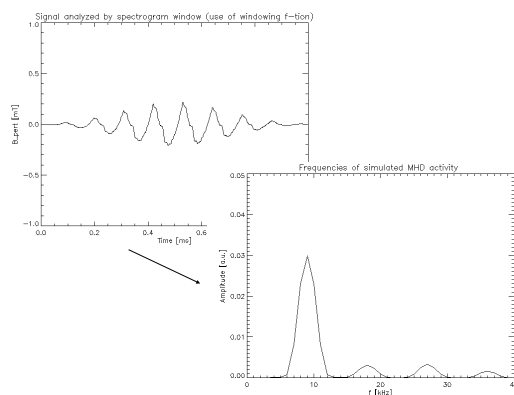
1. Take absolute value of output (the one from complex analysis) to obtain magnitude
  - In the case of interest – Daniel sent you paper when phase is used instead of magnitude
2. Take only first half of signal – the second is the same as the first
3. Calculate which magnitude data point represents which frequency:

$$f(i) = \frac{f_{\text{sample}}}{2} \frac{i}{N_{\text{win}}}$$

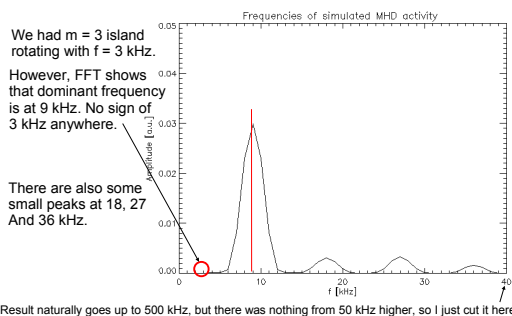
## Frequencies in FFT

$$f(i) = \frac{f_{\text{sample}}}{2} \frac{i}{N_{\text{win}}}$$

- $i$  – index of output data point,  $N_{\text{win}}$  – number of data points in window
- $f_{\text{sample}}/2$  also called Nyquist frequency
  - If you want detection of higher frequencies – you need to increase sampling frequency
- If you want good frequency resolution – you need wider signal window
  - With stationary phenomena – just measure longer
  - In plasma difficult – phenomena last only some limited time – we cannot do much about it

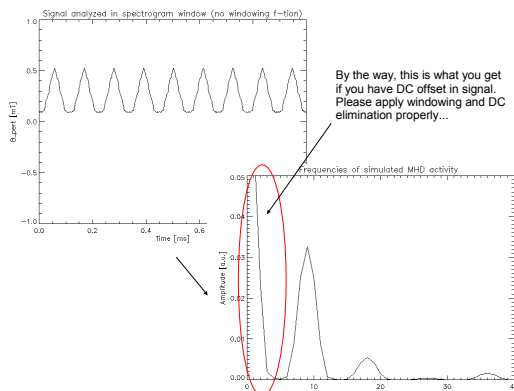


## Interpretation of FFT



## Interpretation of FFT

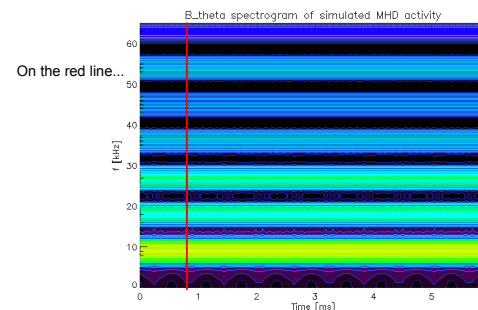
- 18, 27 and 36 kHz part of result are just higher harmonics of main result of 9 kHz
- Why is there 9 kHz instead of 3 kHz?
  - Because  $m=3$ , there are 3 same structures rotating at the same time
  - Therefore it seems that rotation is 3 times faster than it actually is
  - Thus, in order to successfully identify frequency of island rotation, it is necessary to know  $m$  first!



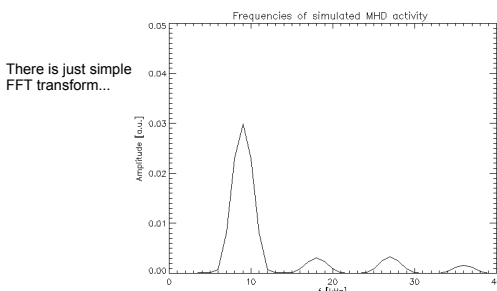
## Spectrograms

- Dividing signal into many time windows and doing FFT in each of them separately
- This way – each time window represents different time interval in data
- Useful to monitor how frequencies in signal change over time
  - To identify time of island existence

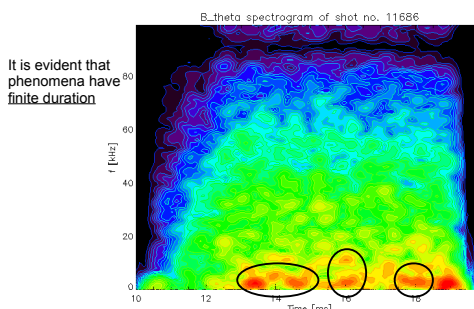
## Model – constant frequency in time



## Model – constant frequency in time



## Application to experimental data



## Spectrogram dilemma

- To capture phenomena of short existence in spectrogram, small windows for FFT are necessary
- However, frequency resolution is given by:

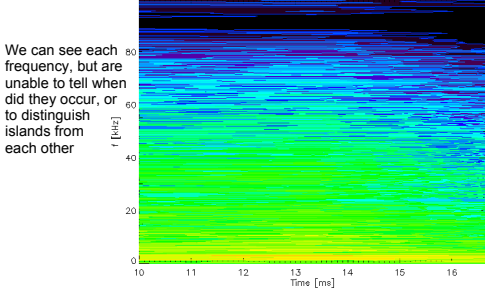
$$f(i) = \frac{f_{\text{sample}}}{2} \frac{i}{N_{\text{win}}}$$

- Narrow window – bad frequency resolution
- Good spectrogram – trade-off between good time resolution and good frequency resolution
- Making windows overlap helps a lot



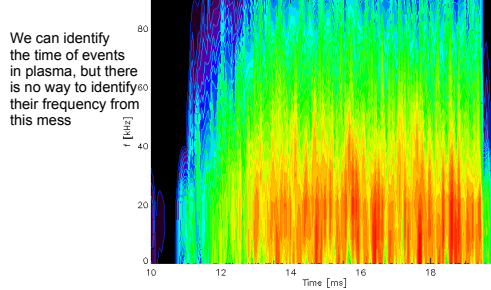
## When window is too wide

B\_theta spectrogram of shot no. 11686



## When window is too narrow

B\_theta spectrogram of shot no. 11686



## Correlation analysis

- As useful in data processing as FFT
- Commonly used in both temporal and spatial domain
- Many interpretations on actual meaning of result
  - So we will only discuss the basic algorithm and what it does to known data provided by island simulation

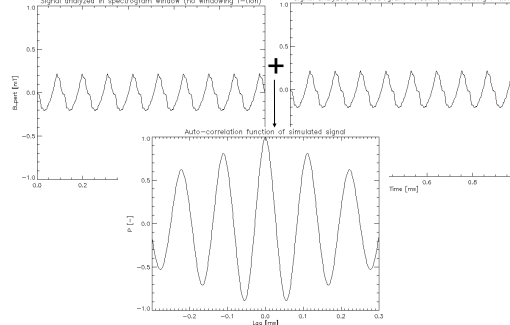
## C\_correlate (IDL implementation)

$$P_{xy}(L) = \frac{\sum_{k=0}^{N-|L|-1} (x_{k+|L|} - \bar{x}) \cdot (y_k - \bar{y})}{\sqrt{\left[ \sum_{k=0}^{N-1} (x_k - \bar{x})^2 \right] \cdot \left[ \sum_{k=0}^{N-1} (y_k - \bar{y})^2 \right]}} \text{ for } L < 0$$

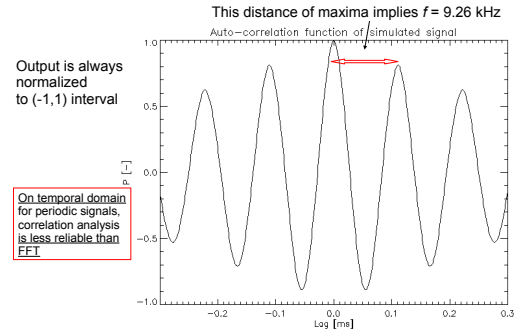
$$P_{xy}(L) = \frac{\sum_{k=0}^{N-|L|-1} (x_k - \bar{x}) \cdot (y_{k+|L|} - \bar{y})}{\sqrt{\left[ \sum_{k=0}^{N-1} (x_k - \bar{x})^2 \right] \cdot \left[ \sum_{k=0}^{N-1} (y_k - \bar{y})^2 \right]}} \text{ for } L > 0$$

- $x$  and  $y$  represent signals with  $N$  data points
- $L$  has dimension of data point index and  $t_L = \frac{L}{f_{\text{sample}}}$
- Barred  $x$  and  $y$  represent averages
- Therefore, denominator is geometrical average of signal variances – this causes that  $P$  is from  $(-1,1)$

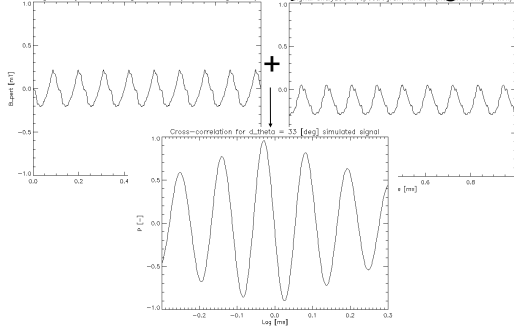
## Auto-correlation of periodical signal



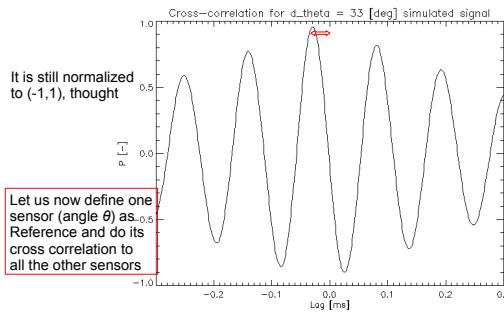
This is how periodic signal "interacts" with itself



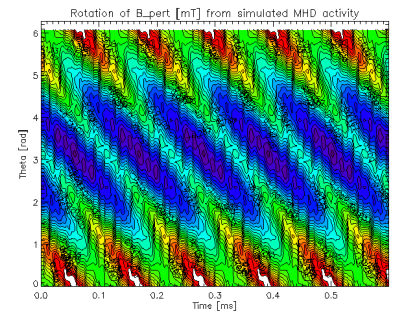
## Cross-correlation of periodical signal



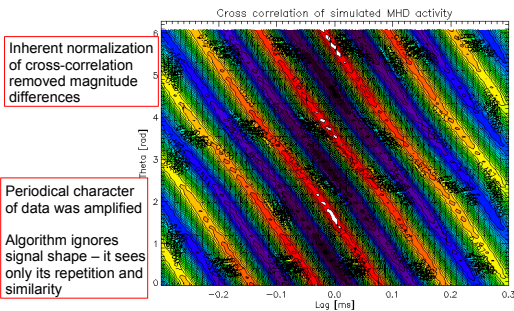
Due to phase shift of signals, maximum of cross correlation is not at lag = 0



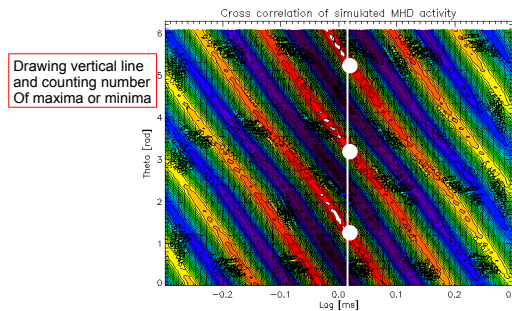
## Original time-space signal:



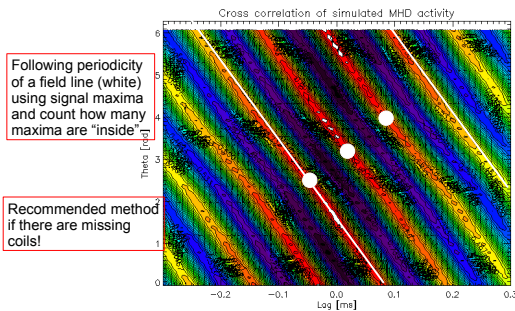
## Upon cross-correlation:



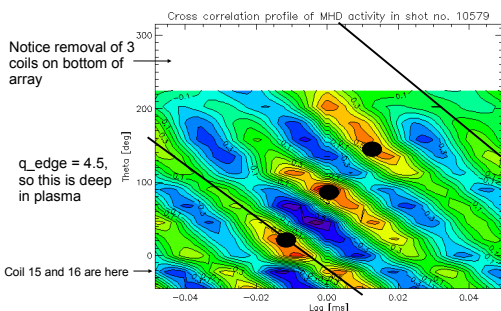
## Identification of $m$ mode number



## Identification of $m$ mode number



## Application to experimental data



## Summary

- Both FFT and  $c_{\text{corr}}$  can be used on temporal and spatial domains to extract island frequency and structure
- FFT
  - Necessary to slightly modify the signal before use
  - Better for time domain, especially to detect changes of frequencies with time
  - To be used on spatial domain, it would be necessary to have more coils or to do reliable interpolation
  - You are encouraged to try this

## Summary

- Cross-correlation
  - Excellent for island tracking – normalizes the signals, inhibits fluctuations and brings forward its periodical character
  - Most reliable method for  $m$  extraction from data
  - However it is not as reliable on temporal domain as FFT





## Appendix F

# Acknowledgement

**Grant Agencies** The financial support by FUSENET, MSM 6840770039, MSM 6840770014 and A1581, SGS SGS11/131/OHK4/2T/14 is acknowledged.

**Special thanks to the GOLEM team (students, teachers, technicians)**

Edita Bromova, Zdenek Cespiro, Ivan Duran, Vladimir Fuchs, Ondrej Grover, Pavel Hacek, Billy Huang, Igor Jex, Michal Kazda, Jindrich Kocman, Martin Kubic, Ondrej Kudlacek, Petr Liska, Tomas Markovic, Jan Mlynar, Michal Odstrcil, Tomas Odstrcil, Ondrej Pluhar, Gergo Pokol, Laszlo Horvath, Csaba Buday, Daniel Imre Refy, Attila Bencze, Jan Stockel, Adam Sindlery, Michal Smid, Gabriel Vondrasek, Frantisek Zacek, and Jiri Zara.

**Special tribute to following persons, contributing personally to the project**

Ondrej Grover, Tomas Markovic, Michal Odstrcil, Jan Stockel and Gabriel Vondrasek.

**Institutional:** Dep. of Physics, Faculty of Nuclear Sciences and Physical Engineering, Czech Technical University - RVO68407700.

**Companies:** National Instruments, Pfeiffer Vacuum.



Prague, September 2013

*V. Svoboda*

Vojtěch Svoboda and tokamak GOLEM



# Bibliography

- [1] Tokamak GOLEM at the Czech Technical University in Prague. <http://golem.fjfi.cvut.cz>, 2007.
- [2] *NRL plasma formulary*. Naval Research Laboratory, 2009.
- [3] E. Bromova, I. Duran, O. Grover, J. Kocman, T. Markovic, M. Odstrcil, T. Odstrcil, O. Pluhar, J. Stockel, V. Svoboda, A. Sindlery, G. Vondrasek, and J. Zara. The GOLEM Tokamak for Fusion Education . In *Europhysics Conference Abstracts. 38th EPS Conference on Plasma Physics (online: <http://ocs.ciemat.es/EPS2011PAP/pdf/P1.021.pdf>)*, volume 35G, 2011.
- [4] Brotankova, J. Study of high temperature plasma in tokamak-like experimental devices. PhD. thesis 2009.
- [5] D. Hernandez-Arriaga, J. Brotankova, O. Grover, J. Kocman, T. Markovic, M. Odstrcil, T. Odstrcil, T. Ruzickova, J. Stockel, V. Svoboda, and G. Vondrasek. Tokamak GOLEM for fusion education - chapter 4 . In *Europhysics Conference Abstracts. 40th EPS Conference on Plasma Physics (online: <http://ocs.ciemat.es/EPS2013PAP/pdf/P2.410.pdf>)*, volume , 2013.
- [6] L. Horvath. *Log-book of GOLEM visit 8 to 12 May 2012*, May 2012.
- [7] ITER news. Launch of the world’s first global tokamak experiment. <http://www.iter.org/newsline/156/512>, 2010.
- [8] G. Papp, G. Pokol, G. Por, S. Zoletnik, and W7-AS Team. Investigation of transient MHD modes of Wendelstein 7-Advanced Stellarator. In *Proceedings of the International Youth Conference on Energetics, (31 May - 2 June 2007, Budapest, Hungary)*, page 109, 2007.
- [9] V. Svoboda, I. Duran, O. Grover, M. Gryaznevich, J. Kocman, K. Kovarik, T. Markovic, M Odstrcil, T. Odstrcil, and J. Stockel. Recent results from GOLEM tokamak. 'Indeed, you can teach an old dog some new tricks. . In *Europhysics Conference Abstracts. 39th EPS Conference on Plasma Physics (online: <http://ocs.ciemat.es/epsicpp2012pap/pdf/P2.059.pdf>)*, volume 36F, 2012.
- [10] V. Svoboda, B. Huang, J. Mlynar, G.I. Pokol, J. Stockel, and G Vondrasek. Multi-mode Remote Participation on the GOLEM Tokamak. *Fusion Engineering and Design*, 86(6-8):1310–1314, 2011.
- [11] V. Svoboda, J. Mlynář, G. Pokol, D. Réfy, J. Stöckel, and G. Vondrášek. Former Tokamak CASTOR becomes remotely controllable GOLEM at the Czech Technical University in Prague . In *Europhysics Conference Abstracts. 37th EPS Conference on Plasma Physics (online: <http://ocs.ciemat.es/EPS2010PAP/pdf/P2.111.pdf>)*, volume 34A, 2010.
- [12] V. Svoboda and J. Stöckel. Tokamak GOLEM Remotely for Worldwide Fusion Education. In *Proceedings: SEFI - PTEE 2011*, pages –, Mannheim, 2011. Hochschule Mannheim - University Of Applied Sciences.